รายงานวิจัยฉบับสมบูรณ์

โครงการ: สรีรวิทยาทางไฟฟ้าและพยาธิสรีรวิทยาของหัวใจ

Electrophysiology and Pathophysiology of the Heart

โดย

ศาสตราจารย์ ดร. นายแพทย์นิพนธ์ ฉัตรทิพากร

ศูนย์วิจัยและฝึกอบรมสาขาโรคทางไฟฟ้าของหัวใจ

ภาควิชาสรีรวิทยา คณะแพทยศาสตร์ มหาวิทยาลัยเชียงใหม่

(หัวหน้าโครงการวิจัยผู้รับทุน)

สิงหาคม 2555

รายงานวิจัยฉบับสมบูรณ์

โครงการ: สรีรวิทยาทางไฟฟ้าและพยาธิสรีรวิทยาของหัวใจ

Electrophysiology and Pathophysiology of the Heart

ผู้วิจัย

หัวหน้าโครงการวิจัยผู้รับทุน

ศ. ดร. นพ. นิพนธ์ ฉัตรทิพากร ศูนย์วิจัยและฝึกอบรม สาขาโรคทางไฟฟ้าของหัวใจ ภาควิชาสรีรวิทยา คณะแพทยศาสตร์ มช.

ผู้ร่วมโครงการวิจัย

ศ. นพ. สุทัศน์ ฟู่เจริญ สถาบันวิจัยและพัฒนาวิทยาศาสตร์และเทคโนโลยี มหาวิทยาลัยมหิดล

รศ. ดร. ทพญ. สิริพร ฉัตรทิพากร ภาควิชาชีววิทยาช่องปากและวิทยาการวินิจฉัยโรค-ช่องปาก คณะทันตแพทยศาสตร์ มช.

รศ. ดร. ปรัชญา คงทวีเลิศ ภาควิชาชีวเคมี คณะแพทยศาสตร์ มช.

รศ. ดร. สมเดช ศรีชัยรัตนกุล ภาควิชาชีวเคมี คณะแพทยศาสตร์ มช.

ผศ. ดร. อัญชลี พงศ์ชัยเดชา ภาควิชาสรีรวิทยา คณะแพทยศาสตร์ มช.

อ. พญ. อรินทยา พรหมินธิกุล ภาควิชาอายุรศาสตร์ คณะแพทยศาสตร์ มช.

อ. พญ. วรรณวรางค์ วงศ์เจริญ ภาควิชาอายุรศาสตร์ คณะแพทยศาสตร์ มช.

อ. ดร. สุวิทย์ แซ่โค้ว ภาควิชารังสีเทคนิค คณะเทคนิคการแพทย์ มช.

อ. ดร. พัฒทรา สวัสดี ภาควิชาเคมี คณะวิทยาศาสตร์ จุฬาลงกรณ์ มหาวิทยาลัย

สนับสุนนโดย สำนักงานกองทุนสนับสนุนการวิจัย

คำนำ

การเสียชีวิตโดยเฉียบพลันจากหัวใจ เป็นสาเหตุหลักของการเสียชีวิตในผู้ป่วยโรคหัวใจที่เกิดจากหลอดเลือดที่ไปเลี้ยงกล้ามเนื้อหัวใจอุดตัน โดยการเสียชีวิตโดยเฉียบพลันนี้ ส่วนใหญ่มาจากการที่เกิดภาวะหัวใจเต้นผิดจังหวะชนิดร้ายแรง ซึ่งจะทำให้เสียชีวิตภายในเวลาไม่กี่นาที หากไม่ได้รับการรักษาอย่างทันท่วงที นอกจากนั้นแล้วหากผู้ป่วยสามารถรอดชีวิตจากภาวะนี้มาได้ ปัญหาที่ตามมาภายหลัง จะเกิดจากการที่กล้ามเนื้อหัวใจตายบางส่วน จากการที่ขาดเลือดไปเลี้ยง ดังนั้นการค้นคว้าวิจัยในปัจจุบัน จึงพยายามหาวิธีการเพิ่มประสิทธิภาพ การรักษาภาวะ heart attack นี้โดยการที่จะพยายามจะลดการตายของกล้ามเนื้อหัวใจลงให้ได้มากที่สุดและเพิ่มประสิทธิภาพการรักษาภาวะหัวใจเต้นผิดจังหวะชนิดร้ายแรง ซึ่งต้องใช้การปล่อยกระแสไฟฟ้าแรงสูงเข้าไปช็อคหัวใจโดยตรง เพื่อหยุดภาวะหัวใจเต้นผิดจังหวะชนิดร้ายแรงนี้

ในรายงานการวิจัยฉบับนี้ ได้รวบรวมเนื้อหางานวิจัยที่ได้มีการใช้ยาหลายชนิด รวมถึงยาต้านเบาหวานเพื่อพัฒนาวิธีการรักษาภาวะกล้ามเนื้อหัวใจขาดเลือดให้ได้ประสิทธิภาพสูงสุด คณะผู้วิจัยหวังเป็นอย่างยิ่งว่าผลงานค้นคว้าวิจัยในรายงานฉบับนี้จะเป็นประโยชน์อย่างยิ่งต่อนักวิจัยและแพทย์ที่สนใจ เพื่อนำไปต่อยอดเพื่อให้เกิดประโยชน์สูงสุด คือ แก่ผู้ป่วย และประชาชนทั่วไป ในอนาคตอันใกล้

สำหรับงานวิจัยในครั้งนี้ ผู้วิจัยขอขอบคุณ สำนักงานกองทุนสนับสนุนการวิจัย (สกว.) (RTA5280003) และคณะแพทยศาสตร์ มหาวิทยาลัยเชียงใหม่ ที่ให้การสนับสนุนงานวิจัยในครั้งนี้เป็นอย่างดี ทำให้งานวิจัยสำเร็จลุล่วงได้โดยตลอด

ศาสตราจารย์ ดร. นพ. นิพนธ์ ฉัตรทิพากร

สิงหาคม 2555

สารบัญ

บทคัดย่อ (ภาษาอังกฤษ)

Heart diseases have been responsible for high morbidity and mortality in most countries worldwide. Acute myocardial infarction is a condition in which coronary artery cannot provide blood supply to myocardium due to the occlusion of this vessel. This can lead to fatal cardiac arrhythmia, i.e. ventricular fibrillation, which can kill the patient in a few minutes if immediate treatment by defibrillation is not provided. Although myocardial reperfusion has been a successful therapy for acute myocardial infarction, reperfusion itself is also known to cause myocardial damage, and is known as reperfusion injury. Since the infarct size has been shown as a good predictor of cardiac function and mortality after acute myocardial infarction, interventions that can reduce the infarct size as well as decrease fatal arrhythmia incidence during ischemia-reperfusion can be useful therapeutic strategies. Currently, several drugs have been shown to provide cardioprotective effects. These drugs include granulocyte-colony stimulating factor (G-CSF), antidiabetic drugs rosiglitazone and vildagliptin, and p38 inhibitor. Nevertheless, the effects of these drugs on the ischemia-reperfused hearts have never been tested.

In the present study, we found that G-CSF, vildagliptin and p38 inhibitor could decrease the infarct size as well as stabilized cardiac electrophysiology by preventing cardiac arrhythmias. However, rosiglitazone provided dual effects, i.e. beneficial and harmful, to the heart. During ischemia-reperfusion, rosiglitazone could decrease the infarct size, but increase the ventricular fibrillation incidence. At the mitochondria level, G-CSF, vildagliptin and p38 inhibitor could improve cardiac mitochondrial dysfunction caused by ischemia-reperfusion injury, and may explain their effects on infarct size reduction. Recent clinical study investigated the role of incretins in acute myocardial infarction patients supported our preclinical studies. In contrast, rosiglitazone did not improved cardiac mitochondrial dysfunction even though the infarct size was decreased. Our finding indicated that the anti-apoptotic effect of rosiglitazone might be via the mitochondrial independent pathway.

Regarding thalassemic heart, we have demonstrated **for the first time that** T-type calcium channel could be mainly responsible for iron uptake into cardiomyocytes of thalassemic mice. Normally, T-type calcium channel is not expressed in normal adult heart except at the electrical conducting pathway inside the heart. However, in some pathological condition such as myocardial infarction and heart failure it can re-expressed. We demonstrated that thalassemic hearts also expressed T-type calcium channel ad played an important role in iron entry into cardiac cells. We also demonstrated that heart

rate variability (HRV) obtained from 24-hour holter monitoring might be used to detect cardiac autonomic balance in thalassemic mice and thalassemia patients at the early state when no cardiac dysfunction was found. These finding could lead to the new strategies for prevention and treatment in thalassemia to prevent iron overload cardiomyopathy, which is responsible for many deaths in this group of patients.

In summary, the output of this research project includes 34 articles listed in PubMed, 42 abstract presentation at national and international scientific meeting, PhD graduates, 11 MSc graduates, 7 current PhD students, and 13 international and national research awards. Furthermore, the entire career research support from the Thailand Research Fund in the past ten years also plays a major role in the Outstanding Scientist Award that this principal investigator received this year.

บทคัดย่อ (ภาษาไทย)

โรคหัวใจเป็นสาเหตุสำคัญของการเสียชีวิตในประเทศต่างๆ ทั่วโลก ภาวะกล้ามเนื้อหัวใจตายเฉียบพลันเป็นภาวะที่เกิดจากการที่หลอดเลือดแดงที่ไปเลี้ยงกล้ามเนื้อหัวใจเกิดจากอุดตันทำให้ไม่มีเลือดไปเลี้ยง ภาวะนี้จะสามารถก่อให้เกิดการเต้นผิดจังหวะของหัวใจห้องล่างชนิดร้ายแรงที่เรียกว่า ฟิบริลเลชั่น ซึ่งเมื่อเกิดขึ้นแล้วสามารถคร่าชีวิตผู้ป่วยได้ในเวลาไม่กี่นาที หากไม่ได้รับการรักษาอย่างทันท่วงที โดยการทำดีฟิบริลเลชั่น ถึงแม้ว่าการรักษาโดยการสวนหัวใจ เพื่อไปเปิดเส้นเลือดที่อุดตันจะช่วยให้กล้ามเนื้อหัวใจได้รับเลือดกลับไปเลี้ยงเหมือนเดิม แต่การรักษาแบบนี้เป็นที่ทราบกันดีว่า สามารถทำให้เกิดการเสียหายต่อกล้ามเนื้อหัวใจได้ และรู้จักกันในชื่อของความเสียหายต่อหัวใจจากการมีเลือดกลับมาเลี้ยงหัวใจได้ ในปัจจุบันขนาดของกล้ามเนื้อหัวใจที่ตาย เชื่อว่าเป็นตัวพยากรณ์ถึงการทำงานของหัวใจในอนาคต รวมถึงการเสียชีวิตในผู้ป่วยกลุ่มนี้ได้ด้วย ดังนั้นการรักษาที่สามารถลดขนาดของกล้ามเนื้อหัวใจที่ตายลง และรวมถึงการรักษาที่สามารถลดอัตราการเกิดภาวะหัวใจเต้นผิดจังหวะชนิดร้ายแรง จึงน่าจะเป็นวิธีการรักษาที่เหมาะสม ปัจจุบันนี้ มียาหลายตัวที่มีรายงานว่าผลในการป้องกันหัวใจ ยาเหล่านี้ ได้แก่ G-CSF, ยารักษาเบาหวาน Rosiglitazone และ Vildagliptin รวมถึงยาใหม่ที่ยับยั้งการทำงานของ p38 อย่างไรก็ตาม ผลของยาเหล่านี้ต่อการป้องกันหัวใจในขณะที่เกิดความเสียหายจากภาวะกล้ามเนื้อหัวใจขาดเลือด และมีเลือดกลับไปเลี้ยงยังไม่มีการศึกษาวิจัย

ในโครงการวิจัยนี้ เราพบว่ายา G-CSF, Vildagliptin และยายับยั้ง p38 สามารถลดขนาดของกล้ามเนื้อที่ตายและยังช่วยป้องกันการเกิดภาวะหัวใจเต้นผิดจังหวะได้อีกด้วย อย่างไรก็ตามยา rosiglitazone ให้ทั้งผลดีและผลเสีย กล่าวคือ สามารถลดขนาดของกล้ามเนื้อที่ตายลงได้ แต่กลับเพิ่มโอกาสของการเกิดภาวะหัวใจเต้นผิดจังหวะชนิดร้ายแรง ในการศึกษาวิจัยระดับไมโตคอนเดรียของหัวใจ เราพบว่า G -CSF, Vildagliptin และยายับยั้ง p38 ช่วยป้องกันความเสียหายต่อไมโตคอนเดรียของหัวใจ ที่เกิดความเสียหายจากการที่กล้ามเนื้อหัวใจขาดเลือดและมีเลือดกลับมาเลี้ยงได้ จึงน่าจะเป็นสาเหตุที่ทำให้ขนาดของกล้ามเนื้อหัวใจตายมีขนาดลดลงได้

สำหรับในหัวใจในโรคธาลัสซีเมีย **<u>เราค้นพบเป็นครั้งแรกว่า</u>** ทีไทพ์แคลเซียมแชนแนล อาจเป็นช่องทางที่นำเหล็กเข้าหัวใจในโรคธาลัสซีเมียได้ ตามปรกติแล้วช่องทางชนิดนี้จะไม่พบในหัวใจของคนปรกติ แต่จะสามารถพบได้ในหัวใจที่มีพยาธิสภาพ ได้แก่ ในโรคกล้ามเนื้อหัวใจตาย และหัวใจล้มเหลว เราพบเป็นครั้งแรกว่าในหัวใจของหนูธาลัสซีเมีย จะมีการแสดงออกของช่องทางนี้ขึ้นในเซลล์กล้ามเนื้อหัวใจ และมีบทบาทสำคัญต่อการนำเข้าของเหล็กเข้าสู่เซลล์กล้ามเนื้อหัวใจ นอกจากนั้นเรายังได้ค้นพบว่า ค่าความแปรปรวนของหัวใจ (HRV) สามารถใช้ในการบ่งบอกค่าความผิดปรกติของการควบคุมระบบประสาทอัตโนมัติในหัวใจของโรคธาลัสซีเมียได้ ตั้งแต่ระยะต้นของโรค ก่อนที่จะตรวจพบการทำงานที่ผิดปรกติของหัวใจ การค้นพบนี้อาจนำไปสู่การพัฒนาวิธีป้องกันและการรักษาใหม่ๆ ในโรคธาลัสซีเมียที่เกิดภาวะหัวใจล้มเหลว จากการที่มีเหล็กสะสมในหัวใจมากเกินไป และเป็นสาเหตุการเสียชีวิตหลักในผู้ป่วยกลุ่มนี้

กล่าวโดยสรุป ผลลัพธ์จากโครงการวิจัยนี้ประกอบไปด้วย ผลงานวิจัยที่ตีพิมพ์ในวารสารระดับนานาชาติ ที่อยู่ในฐานข้อมูล Pubmed จำนวน 34 เรื่อง, ได้มีการนำเสนอผลงานประชุมในงานประชุมระดับนานาชาติ และระดับชาติจำนวน 42 เรื่อง, ผลิตบัณฑิตระดับปริญญาเอกได้ 11 คน และปริญญาโท 7 คน, มีนักศึกษาระดับปริญญาเอกที่เกี่ยวข้องกับทุนวิจัยนี้ 2 คน, และได้รับรางวัลงานวิจัยระดับชาติและนานาชาติจำนวน 13 รางวัล นอกจากนั้นแล้ว ผู้รับทุนส่งเสริมกลุ่มวิจัยยังได้รับรางวัลนักวิทยาศาสตร์ดีเด่น ประจำปี 2555 จากมูลนิธิส่งเสริมวิทยาศาสตร์และเทคโนโลยีในพระบรมราชูปถัมภ์อีกด้วย

Executive Summary

In this research project, two main aims including the pharmacological intervention to attenuate the severity of cardiac ischemia-reperfusion injury and the mechanism of iron entry in thalassemic hearts for iron-overload cardiomyopathy prevention have been extensively investigated. We found that several drugs including the granulocyte-colony stimulating factor (G-CSF), anti-diabetic drug vildagliptin, and a new compound SB203580 that inhibits the action of p38 MAPK could decrease the infarct size as well as stabilized cardiac electrophysiology by preventing cardiac arrhythmias caused by ischemia-reperfusion injury. However, anti-diabetic drug rosiglitazone provided both beneficial and harmful effects to the heart, by decreasing the infarct size, but increasing the ventricular fibrillation incidence. The beneficial effects of G-CSF, vildagliptin and p38 inhibitor could be due to their protection on cardiac mitochondrial function.

Regarding thalassemic heart, we have demonstrated **for the first time** that T-type calcium channel could be mainly responsible for iron uptake into cardiomyocytes of thalassemic mice. Normally, T-type calcium channel is not expressed in an adult heart except at the electrical conducting pathway inside the heart. However, in some pathological condition such as myocardial infarction and heart failure it can re-expressed. We demonstrated that thalassemic hearts also expressed T-type calcium channel ad played an important role in iron entry into cardiac cells. We also demonstrated that heart rate variability (HRV) obtained from 24-hour holter monitoring might be used to detect cardiac autonomic balance in thalassemic mice and thalassemia patients at the early state when no cardiac dysfunction was found. These finding could lead to the new strategies for prevention and treatment in thalassemia to prevent iron overload cardiomyopathy, which is responsible for many deaths in this group of patients.

In summary, the output of this research project includes 34 articles listed in PubMed, 42 abstract presentation at national and international scientific meeting, PhD graduates, 11 MSc graduates, 7 current PhD students, and 13 international and national research awards. Furthermore, the entire career research support from the Thailand Research Fund in the past ten years also plays a major role in the Outstanding Scientist Award that this principal investigator received this year.

เนื้อหางานวิจัย

1. งานวิจัยในโครงการนี้สามารถแบ่งเนื้อหางานวิจัยออกได้เป็น 2 เรื่องใหญ่ ได้แก่ การศึกษาวิจัยในภาวะกล้ามเนื้อหัวใจขาดเลือดเฉียบพลัน และในหัวใจที่มีปริมาณเหล็กสะสมมากเกินในโรคธาลัสซีเมีย ดังนี้

ใน ischemic hearts

1.1 ได้ทำการศึกษาถึงผลของ G-CSF ต่อ cardiac electrophysiology ในสุกรที่เกิดภาวะกล้ามเนื้อหัวใจขาดเลือด สาระสำคัญของงานวิจัยมีดังนี้

Effects of granulocyte colony-stimulating factor (G-CSF) on cardiac electrophysiology during ischemic/reperfusion (I/R) period are unclear. We hypothesized that G-CSF stabilizes cardiac electrophysiology during I/R injury by prolonging the effective refractory period (ERP), increasing the ventricular fibrillation threshold (VFT) and decreasing the defibrillation threshold (DFT). In this study, 30 pigs were used. In intact heart protocol, pigs were infused with either G-CSF or vehicle (n=7 each group) without I/R induction. In I/R protocol, pigs were infused with G-CSF (0.33*u*g/kg/min) or vehicle (n=8 each group) for 30 minutes prior to a 45-minute left anterior descending artery occlusion and at reperfusion. Diastolic pacing threshold (DPT), ERP, VFT and DFT were determined in all pigs before and during I/R period.

We found that neither G-CSF nor vehicle altered any parameter in intact-heart pigs. During ischemic period, G-CSF significantly increased the DPT, ERP and VFT without altering the DFT. In the vehicle group, only the DPT was increased during ischemia. During reperfusion, G-CSF continued to increase the DPT without altering other parameters. Systolic and diastolic pressures were significantly decreased from the baseline in both groups during I/R period. Although the area at risk was not different between the two groups, the infarct size was significantly decreased in the G-CSF group, compared to the vehicle.

All of these findings indicate that G-CSF increases the DPT, ERP and VFT and reduces the infarct size, which may help stabilizing the myocardial electrophysiology, thus preventing fatal arrhythmia in ischemic myocardium. However, G-CSF does not improve defibrillation efficacy during I/R injury.

งานวิจัยเรื่องนี้และที่เกี่ยวข้องได้รับการตีพิมพ์ในวารสารงานวิจัยระดับนานาชาติแล้ว

1.2 ได้ทำการศึกษาถึง ผลของ G-CSF ต่อการป้องกัน mitochondrial damage จาก H_2O_2-induced oxidative stress ใน isolated cardiac mitochondria ของหนูและกลไกการออกฤทธิ์ของ G-CSF บน cardiac mitochondria สาระสำคัญของงานวิจัยมีดังนี้

Ischemic heart disease is one of the major causes of death in most nations. Ischemic heart disease/myocardial infarction causes the increase of reactive oxygen species (ROS), leading to oxidative stress in cardiomyocytes. In the heart, it is known that mitochondria are the principal source of ROS production. Previous studies suggested that ischemic heart disease could cause mitochondrial dysfunction, leading to increased oxidative stress. Recently, granulocyte-colony stimulating factor (G-CSF) has been reported that it has a protective effect on cardiomyocytes following ischemic heart disease. G-CSF was demonstrated to improve doxorubicin-induced mitochondrial damage in cultured cardiomyocytes. However, the effects of G-CSF in isolated cardiac mitochondria have never been investigated.

In the present study, we determined whether G-CSF can improve mitochondrial damage in hydrogen peroxide (H_2O_2)-induced oxidative stress in isolated cardiac mitochondria. In the present study, isolated mitochondria from rat hearts were randomly assigned into eight treatment groups: H_2O_2 (2mM), 50 or 200 ng/ml G-CSF, H_2O_2 pre-treated with G-CSF (25, 50, 100 or 200 ng/ml) and control (n=6 each). All isolated mitochondria were measured for mitochondrial swelling, mitochondrial membrane potential changes ($\Delta\Psi$m) and ROS production.

Our results demonstrated that in H_2O_2 pre-treated with G-CSF groups, G-CSF significantly reduced mitochondrial swelling, $\Delta\Psi$m and ROS production under H_2O_2-induced oxidative stress condition in isolated cardiac mitochondria. However, the dose-dependent effect was not observed in this study. G-CSF alone did not cause any changes in isolated cardiac mitochondria. In conclusion, G-CSF can directly protect mitochondrial damage under H_2O_2-induced oxidative stress condition in isolated cardiac mitochondria.

งานวิจัยเรื่องนี้และที่เกี่ยวข้องได้รับการตีพิมพ์ในวารสารงานวิจัยระดับนานาชาติแล้ว

1.3 ได้ทำการศึกษาถึงผลของยารักษาเบาหวาน Rosiglitazone ต่อการทำงานทางไฟฟ้าในหัวใจ เนื่องจากมีรายงานว่ายาตัวนี้มีผลในทางที่ไม่ดีต่อหัวใจ การศึกษานี้จะทำการศึกษาในสุกรที่ถูกเหนี่ยวนำให้เกิดภาวะกล้ามเนื้อหัวใจขาดเลือดเฉียบพลัน สาระสำคัญของงานวิจัยมีดังนี้

Rosiglitazone, a peroxisome proliferator-activated receptor gamma agonist has been used to treat type II diabetes. Despite debates regarding its cardioprotection, the effects of rosiglitazone on cardiac electrophysiology are still unclear. Our study determined the effect of rosiglitazone on ventricular fibrillation (VF) incidence, VF threshold (VFT), defibrillation threshold (DFT), and mitochondrial function during ischemia and reperfusion. Twenty-six pigs were used. In each pig, either rosiglitazone (1 mg/kg) or normal saline solution was administered intravenously within 60 minutes. Then, the left anterior descending coronary artery was ligated for 60 minutes and released to promote reperfusion for 120 minutes. The cardiac electrophysiologic parameters were determined at the beginning of the study and during ischemia and reperfusion period. The heart was removed then the area at risk and the infarct size in each heart were determined. Cardiac mitochondria were isolated for determination of mitochondrial function. Rosiglitazone did not improve the DFT and VFT during ischemia – reperfusion periods. In rosiglitazone group, VF incidence was increased (58 vs. 10 %) and time to the first occurrence of VF was decreased (3 ± 2 vs. 19 ± 1 min), as compared to the vehicle group ($P<0.05$). However, the infarct size related to the area at risk in the rosiglitazone group was significantly decreased ($P<0.05$). In the cardiac mitochondria, rosiglitazone did not alter the level of reactive oxygen species production and could not prevent mitochondrial membrane potential changes. Rosiglitazone increased the propensity for VF, and could neither increase defibrillation efficacy nor improve cardiac mitochondrial function.

งานวิจัยเรื่องนี้และที่เกี่ยวข้องได้รับการตีพิมพ์ในวารสารงานวิจัยระดับนานาชาติแล้ว

1.4 ได้ทำการศึกษาถึงผลของยารักษาเบาหวานตัวใหม่ คือยาในกลุ่ม Dipeptidyl peptidase 4 inhibitor ซึ่งพบว่ามี cardioprotective effect ในสภาวะที่เกิด acute myocardial infarction สาระสำคัญของงานวิจัยมีดังนี้

Dipeptidyl peptidase-4 (DPP-4) inhibitor is a new antidiabetic drug for type-2 diabetes mellitus patients. Despite its benefits on glycemic control, the effects of DPP-4 inhibitor on the heart during ischemia-reperfusion (I/R) periods are not known. We investigated the effect of DPP-4 inhibitor on cardiac electrophysiology and infarct size in a clinically relevant I/R model in swine and its underlying

cardioprotective mechanism. Fourteen pigs were randomized to receive either DPP-4 inhibitor (vildagliptin) 50 mg or normal saline intravenously prior to a 90-min left anterior descending artery occlusion, followed by a 120-min reperfusion period. The hemodynamic, cardiac electrophysiological and arrhythmic parameters, and the infarct size were determined before and during I/R. Rat cardiac mitochondria were used to study the protective effects of DPP-4 inhibitor on cardiac mitochondrial dysfunction caused by severe oxidative stress induced by H_2O_2 to mimic the I/R condition. Compared to the saline group, DPP-4 inhibitor attenuated the shortening of the effective refractory period (ERP), decreased the number of PVCs, increased the ventricular fibrillation threshold (VFT) during the ischemic period, and also decreased the infarct size. In cardiac mitochondria, DPP-4 inhibitor decreased the reactive oxygen species (ROS) production and prevented cardiac mitochondrial depolarization caused by severe oxidative stress. During I/R, DPP-4 inhibitor stabilized the cardiac electrophysiology by preventing the ERP shortening, decreasing the number of PVCs, increasing the VFT, and decreasing the infarct size. This cardioprotective effect could be due to its prevention of cardiac mitochondrial dysfunction caused by severe oxidative stress during I/R.

งานวิจัยเรื่องนี้และที่เกี่ยวข้องได้รับการตีพิมพ์ในวารสารงานวิจัยระดับนานาชาติแล้ว

1.5 ได้ทำการศึกษาถึงผลของสารเคมีซึ่งมีฤทธิ์ยับยั้งการทำงานของ p38 ซึ่งเป็น intracellular signaling molecule ในเซลล์กล้ามเนื้อหัวใจ ซึ่งมีหลักฐานรายงานว่าอาจจะมี cardioprotective effect ได้ แต่ผลของยาต่อหัวใจในสภาวะที่เกิด acute myocardial infarction ยังขาดความชัดเจนอยู่มาก โดยเฉพาะอย่างยิ่งฤทธิ์ของสารตัวนี้ในระยะเวลาการให้สารในช่วงเวลาต่าง ๆ ขณะที่กล้ามเนื้อหัวใจขาดเลือด สาระสำคัญของงานวิจัยมีดังนี้

p38 mitogen-activated protein kinase (p38) has been shown to play an important role in facilitating myocardial infarction process in ischemia/reperfusion (I/R) injury. Inhibition of p38 prior to ischemia has been shown as cardioprotective. However, the benefit of inhibition of p38 after ischemia or during reperfusion is unknown. We tested the hypothesis that inhibition of p38 at different times during I/R can attenuate ventricular fibrillation (VF) incidence and reduce the infarct size.

Adult Wistar rats were subject to 30-min left anterior descending coronary artery (LAD) occlusion, followed by 120-min reperfusion. A p38 inhibitor, SB203580, was given intravenously (2-mg/kg) either at 15 minutes before ischemia (pretreatment group), 15 minutes after LAD occlusion (ischemia group),

or at onset of reperfusion. Saline was used as a vehicle in each group. Electrocardiogram was recorded and the arrhythmia score was analyzed based on the frequency and duration of arrhythmias detected (1 is lowest and 5 was highest arrhythmia incidence). The infarct size was determined in each heart.

SB203580 given before LAD occlusion and during ischemia significantly decreased the overall arrhythmia score and the incidence of VT/VF, compared with the vehicle-treated group (Figure). However, SB203580 given at onset of reperfusion did not show this benefit. The time to VT/VF onset was not changed for SB203580 treated at any time, compared to the vehicle. Unlike arrhythmia incidence, the infarct size was markedly decreased in SB203580-treated rats in all groups. In summary, Although SB203580 could markedly decrease the infarct size when administered before or after LAD occlusion, as well as during reperfusion, it could only effectively attenuate the fatal arrhythmias when given only prior to LAD occlusion and during ischemia. These findings indicate the crucial role of the timing of p38 inhibition in preventing fatal arrhythmia in an I/R model.

งานวิจัยเรื่องนี้และที่เกี่ยวข้อง ได้รับการตีพิมพ์ในวารสารงานวิจัยระดับนานาชาติแล้ว

1.6 ได้ทำการศึกษาถึงผลของ KP extract ต่อ nitric oxide signaling pathway ในหัวใจของหนูขาวในระดับหนึ่งแล้ว KP extract มี positive effect ต่อ nitric oxide signaling pathway และมีผลต่อการเพิ่มขึ้นของระดับ cGMP ในหัวใจของหนู รวมทั้งมีผลในการออกฤทธิ์ใกล้เคียงกับ sildenafil citrate สาระสำคัญของงานวิจัยมีดังนี้

The rhizomes of Krachai-dam (*Kaempferia parviflora*, KP) is one of the Thai traditional medicine that has been used for rejuvenation in elderly people, relieving digestive disorders, gastric ulcer, diuresis, and has been used as anti-allergy and tonic. The macerated KP rhizome in alcoholic drinking or KP tea are believed to improve erectile dysfunction. However, this effect of KP has not been elucidated by scientific research. Recently, the ethanolic extract of KP has been shown to increase the endothelial nitric oxide (NO) synthase (eNOS) mRNA and protein expression in primary cell culture of human umbilical vein endothelial cells. Moreover, the effect of KP extract has shown to vasodilate rat aortic rings in an *in vitro* study and decreased mean arterial pressure in an *in vivo* model. This vasorelaxation mechanism of KP has been found to regulate via the positive effect on NO signaling pathway. Despite that, the effect of KP extract on NO signaling in the heart has never been investigated.

In the heart, NO signaling has been shown to play an important role in regulating the cellular ionic concentration, especially Ca^{2+}. It has been shown that NO can modulate the function of L-type Ca^{2+} channel by the indirect mechanism via the production of cGMP and phosphorylation of protein kinase G (PKG). Moreover, NO also increase the Ca^{2+} reuptake rate into sarcoplasmic reticulum via the increased the phosphorylation of phospholamban.

In traditional medicine, KP is believed to improve erectile dysfunction (ED) similar to the effect of sildenafil citrate, the phosphodiesterase type 5 (PDE-5) inhibitor. However, there is no scientific study to support this statement. Since KP has been shown to have positive effect on the NO signaling, which may resulting in the increased of intracellular cGMP level similar to that of sildenafil citrate, we further investigated effect of KP extract on PDE-5 in the heart.

We found that KP extract increased cGMP level in the rat hearts, but failed to increase eNOS and neuronal NOS. In swine study, KP extract at high concentration significantly decreased defibrillation efficacy and increased vulnerability to arrhythmia similar to that of the supratherapeutic concentration of sildenafil citrate. These findings suggest that KP extract could have the PDE-5 inhibitory effect similar to that of sildenafil citrate. Future studies are needed to clarify the mechanism by which KP extract has an effect on the NO signaling pathway in addition to the PDE-5 inhibitory effect.

งานวิจัยเรื่องนี้และที่เกี่ยวข้อง ได้รับการตีพิมพ์ในวารสารงานวิจัยระดับนานาชาติแล้ว

ใน thalassemic hearts

1.7 ได้ทำการศึกษาถึงกลไกในการนำเหล็กเข้าเซลล์ของ cultured cardiomyocytes ที่ได้จากหัวใจของหนูที่เป็น thalassemia โดยอาศัยการใช้ blockers ต่อ L-type calcium channels, Transferin Receptor และ DMT-1 เพื่อศึกษาการเปลี่ยนแปลงการนำเหล็กเข้าสู่เซลล์และในระหว่างนี้อยู่ระหว่างรอการทดสอบเพิ่มเติม โดยการใช้ T-type calcium channel blocker ทั้งนี้พบว่า T-type calcium channel blocker สามารถป้องกันการนำเข้าของเหล็ก ใน thalassemic cardiomyocytes ได้ งานวิจัยนี้ทำให้มีการรายงานเป็นครั้งแรกถึงบทบาทของ T-type calcium channel ต่อการนำเข้าของเหล็กเข้าสู่ cardiac cells ซึ่งอาจนำไปสู่การพัฒนาการรักษาที่ดีและมีประสิทธิภาพสูงขึ้นในอนาคต
สาระสำคัญของงานวิจัยมีดังนี้

Iron-overload condition can be found in beta-thalassemic patients with regular blood transfusion, leading to iron deposition in various organs including the heart. Elevated cardiac iron causes iron-overload cardiomyopathy, a condition

which provokes mortality due to heart failure in thalassemic patients. Previous studies demonstrated that myocardial iron uptake may occur via L-type calcium channels (LTCCs). However, direct evidence regarding the claimed pathway in thalassemic cardiomyocytes has never been investigated. Hearts from genetic-altered beta-thalassemic mice and adult wild-type mice were used for cultured ventricular cardiomyocytes. Blockers for LTCC, T-type calcium channel (TTCC), transferin receptor1 (TfR1) and divalent metal transporter1 (DMT1) were used and quantification of cellular iron uptake under various iron loading conditions was performed by Calcein-AM fluorescence assay. Microarray analysis was performed to investigate gene expressions in the hearts of these mice. This study demonstrated that iron uptake under iron-overload conditions in the cultured ventricular myocytes of thalassemic mice was greater than that of wild type cells ($p < 0.01$). TTCC blocker, efonidipine, and an iron chelator, deferoxamine, could prevent iron uptake into cultured cardiomyocytes, whereas blockers of TfR1, DMT1, and LTCC could not. Microarray analysis from thalassemic hearts demonstrated highly up-regulated genes of TTCC, zinc transporter and transferrin receptor2. Our findings indicated that iron uptake mechanisms in cultured thalassemic cardiomyocytes are mainly mediated by TTCC, suggesting that TTCC is the important pathway for iron uptake in this cultured thalassemic cardiomyocyte model.

งานวิจัยเรื่องนี้ และที่เกี่ยวข้องได้รับการตีพิมพ์ในวารสารงานวิจัยระดับนานาชาติแล้ว

1.8 ได้ทำการศึกษาผลของการให้เหล็กในขนาดต่าง ๆ ผสมในอาหารให้กับหนูธาลัสซีเมียและหนูปกติเป็นเวลา 2 เดือน เพื่อตรวจวัดระดับของเหล็ก NTBI ในเลือดรวมถึงการเปลี่ยนแปลงทางไฟฟ้าและการทำงานของหัวใจ เพื่อที่จะศึกษาถึงการตอบสนองของการให้เหล็กต่อระดับเหล็กในอวัยวะต่าง ๆ ระหว่างหนูที่เป็นธาลัสซีเมียกับหนูปกติ และได้ทำการศึกษาถึงผลของ blocker ชนิดต่างๆ รวมถึง T-type calcium channel blocker ต่อการป้องกันการสะสมของเหล็ก NTBI ในหัวใจและอวัยวะต่าง ๆ รวมถึงการศึกษาถึงการเปลี่ยนแปลงทางไฟฟ้าในหัวใจของหนูที่เป็นธาลัสซีเมียและหนูปกติเพื่อศึกษาดูว่ายาชนิดต่างๆ ที่ให้เข้าไปสามารถป้องกันการสะสมของเหล็กในหัวใจและช่วยป้องกันการเปลี่ยนแปลงสมดุลของระบบประสาทอัตโนมัติในหัวใจได้หรือไม่ โดยที่การศึกษานี้จะเป็นการยืนยันว่าผลการศึกษาที่ได้จาก cell culture สามารถนำไปใช้ได้ในตัวสัตว์ทดลองได้หรือไม่ สาระสำคัญของงานวิจัยมีดังนี้

Excess plasma iron can lead to iron deposition in many organs including the heart. In thalassemia, excess cardiac iron deposition can cause cardiac dysfunction and depressed heart rate variability (HRV). Recently, T-type calcium channel (TTCC) has been shown as a possible gateway for iron entry in thalassemic cardiomyocytes. However, the role of TTCC in "in vivo" with iron overload has never been investigated. We tested the hypothesis that TTCC blocker can improve impaired cardiac function and attenuate the depressed HRV, leading to decreased mortality in iron-overloaded mice. C57/BL6 adult mice were fed with either normal diet (control group) or diet supplemented with dicyclopentadienyl iron (FE group) for 90 days to induce iron overload condition. Then, mice in each group were divided into subgroups being treated with L-type calcium channel (LTCC) blocker, verapamil and nifedipine; TTCC blocker, efonidipine; or iron chelator deferoxamine (DFO) for 30 days. Pressure-volume (P-V) conductance catheter system was used for cardiac function assessment. HRV was determined at baseline and at the end of treatment in all mice. Iron-overloaded mice demonstrated impaired cardiac function as shown by decreased stroke volume (SV), cardiac output (CO), ejection fraction (EF), impaired HRV as indicated by increased LF/HF ratio, with high mortality rate (Figure). Efonidipine effectively improved cardiac function impairment, whereas LTCC blockers and DFO did not. Efonidipine and DFO also significantly improved HRV parameter, whereas LTCC blockers could improve it at a lower extent. Both efonidipine and DFO markedly decreased mortality, while LTCC blocker did not, in these mice with iron overload. Impaired cardiac function and depressed HRV caused by iron overload were improved by efonidipine, but not by verapamil and nifedipine, suggesting that TTCC but not LTCC, plays an important role for iron uptake in the heart of iron-overloaded mice.

งานวิจัยเรื่องนี้และที่เกี่ยวข้อง ได้รับการตีพิมพ์ในวารสารงานวิจัยระดับนานาชาติแล้ว

2. **<u>การผลิตนักศึกษาบัณฑิต</u>**

ขณะนี้มีนักศึกษาปริญญาโท ที่ทำงานวิจัยในโครงการนี้ จำนวน 7 คน จบการศึกษาแล้ว จำนวน 4 คน ที่กำลังจะสอบป้องกันวิทยานิพนธ์ภายในเดือนตุลาคม พ.ศ. 2555 นี้ จำนวน 3 คน และมีนักศึกษาปริญญาเอก ที่ทำงานวิจัยในโครงการนี้ จำนวน 11 คน ซึ่งจบการศึกษาไปแล้ว จำนวน 2 คน และส่งได้ส่งไปฝึกปฏิบัติงานด้านงานวิจัย ณ ต่างประเทศอีกจำนวน 2 คน

3. **ผลงานที่เกิดจากทุนส่งเสริมวิจัยนี้**

<u>3.1. ผลงานตีพิมพ์ในวารสารวิชาการนานาชาติ จำนวน 34 เรื่อง</u>

1. Apaijai N, Pintana H, Chattipakorn SC, **Chattipakorn N**. Effects of metformin and vildagliptin on cardiac and mitochondrial function in high-fat diet-induced insulin resistant rats. *Endocrinology* 2012 (in press) (Impact Factor = 4.99)

2. Wongcharoen W, Jai-aue S, Phrommintikul A, Nawarawong W, Woragidpoonpol S, Tepsuwan T, Sukonthasarn A, Apaijai N, **Chattipakorn N**. Effects of Curcuminoids on Frequency of Acute Myocardial Infarction After Coronary Artery Bypass Grafting. *Am J Cardiol* 2012 (in press) (Impact Factor = 3.680)

3. Yarana C, Sripetchwandee J, Sanit J, Chattipakorn S, **Chattipakorn N**. Calcium-induced cardiac mitochondrial dysfunction is predominantly mediated by cyclosporine A-dependent mitochondrial permeability transition pore, but not mitochondrial calcium uniporter. *Arch Med Res* 2012 (in press) (Impact factor = 1.986)

4. Yarana C, Sanit J, **Chattipakorn N**, Chattipakorn S. Synaptic and nonsynaptic mitochondria demonstrate a different degree of calcium-induced mitochondrial dysfunction. *Life Sci* 2012;90:808-814. (Impact Factor = 2.56)

5. Kumfu S, Chattipakorn S, Chinda K, Fucharoen S, **Chattipakorn N**. T-type calcium channel blockade improves survival and cardiovascular function in thalassemic mice. *Eur J Haematol* 2012;88:535-548. (Impact Factor = 2.785)

6. Chinda K, Palee S, Surinkaew S, Phornphutkul M, Chattipakorn S, **Chattipakorn N**. Cardioprotective effect of dipeptidyl peptidase-4 inhibitor during ischemia–reperfusion injury. *Int J Cardiol* 2012 (in press) (Impact Factor = 6.802)

7. Khumpune S, Chattipakorn S, **Chattipakorn N**. Role of p38 inhibition on cardiac ischemia/reperfusion injury. *Eur J Clin Pharmacol* 2012 (in press) (Impact Factor = 3.088)

8. Suwanchai A, Theerapiboon U, **Chattipakorn N**, Chattipakorn S. $Na_V1.8$, but not $Na_V1.9$, is up-regulated in the inflamed dental pulp tissue of human primary teeth. *Int Endod J* 2012;45(4):372-8. (Impact Factor = 2.383)

9. Chinda K, Chattipakorn S, **Chattipakorn N**. Cardioprotective effects of incretin during ischemia-reperfusion. *Diabetes Vasc Dis Res* 2012 (in press) (Impact factor = 2.468)

10. Weerateerangkul P, Surinkaew S, Chattipakorn S, **Chattipakorn N**. Effects of *Kaempferia parviflora* Wall. Ex. Baker on electrophysiology of the swine hearts. *Indian J Med Res* 2012 (in press) (Impact Factor = 1.826)

11. Pramojanee S, Pratchayasakul W, **Chattipakorn N**, Chattipakorn S. Low dose dental radiation decreases oxidative stress in osteoblastic cells. *Arch Oral Biol* 2012;57(3):252-6. (Impact Factor = 1.463)

12. Pipatpiboon N, Pratchayasakul W, **Chattipakorn N**, Chattipakorn S. PPARγ agonist improves neuronal insulin receptor function in hippocampus and brain mitochondria function in rats with insulin resistance induced by long term high-fat diets. *Endocrinology* 2011;153(1):329-338. (Impact Factor = 4.99)

13. Silvilairat S, Wongsathikun J, Sittiwangkul R, Pongprot Y, **Chattipakorn N**. Heart rate variability and exercise capacity in patients with repaired Tetralogy of Fallot. *Pediatr Cardiol* 2011;32(8):1158-1163. (Impact Factor = 1.151)

14. Suwanchai A, Theerapiboon U, **Chattipakorn N**, Chattipakorn S. Expression of sodium channels in dental pulp. *Asian Biomed* 2011;5(6):735-746. (Impact Factor = 0.333)

15. Pratchayasakul W, **Chattipakorn N**, Chattipakorn S. Effects of estrogen in preventing neuronal insulin resistance in hippocampus of obese rats are different between genders. *Life Sci* 2011;89(19-20):702-707. (Impact Factor = 2.56)

16. Silvilairat S, Wongsathikun J, Sittiwangkul R, Pongprot Y, **Chattipakorn N**. Effects of left ventricular function on the exercise capacity in patients with repaired tetralogy of fallot. *Echocardiography* 2011;28(9):1019-1024. (Impact Factor = 1.444)

17. Chattipakorn S, Ittichaicharoen J, Rangdaeng S, **Chattipakorn N**. Changes in peripheral innervations and nociception in reticular type and erosive type of oral lichen planus. *Indian J Dent Res* 2011;22:678-683. (Impact factor = 0.4)

18. Palee S, Weerateerangkul P, Surinkeaw S, Chattipakorn S, **Chattipakorn N**. Effect of rosiglitazone on cardiac electrophysiology, infarct size and mitochondrial function in ischemia and reperfusion of swine and rat heart. *Exp Physiol* 2011;96(8):778-789. (Impact Factor = 3.333)

19. Thummasorn S, Kumfu S, Chattipakorn S, **Chattipakorn N**. Granulocyte-colony stimulating factor attenuates mitochondrial dysfunction induced by oxidative stress in cardiac mitochondria. *Mitochondrion* 2011;11(3):457-466. (Impact Factor = 4.145)

20. Kanlop N, Thommasorn S, Palee S, Weerateerangkul P, Suwansirikul S, Chattipakorn S, **Chattipakorn N**. G-CSF stabilizes cardiac electrophysiology and decreases infarct size during cardiac ischemic/reperfusion in swine. *Acta Physiol* 2011;202(1):11-20. (Impact Factor = 2.81)

21. Pratchayasakul W, Kerdphoo S, Petsophonsakul P, Pongchaidacha A, **Chattipakorn N**, Chattipakorn S. Effects of high-fat diet on insulin receptor function in rat hippocampus and the level of neuronal corticosterone. *Life Sci* 2011;88(13-14):619-627. (Impact Factor = 2.56)

22. Surinkaew S, Chattipakorn S, **Chattipakorn N**. Roles of mitochondrial benzodiazepine receptor in the heart. *Can J Cardiol* 2011;27:262.e3-262.e13. (Impact Factor = 1.796)

23. Weerateerangkul P, Chattipakorn S, **Chattipakorn N**. Roles of nitric oxide signaling pathway in cardiac ischemic preconditioning against myocardial ischemia-reperfusion injury. *Med Sci Monit* 2011;17(2):RA44-52. (Impact Factor = 1.514)

24. Kanlop N, Chattipakorn S, **Chattipakorn N**. Effects of cilostazol in the heart. *J Cardiovasc Med* 2011;12(2):88-95. (Impact factor = 0.712)

25. Palee S, Chattipakorn S, Phrommintikul A, **Chattipakorn N**. PPARγ gamma activator, rosiglitazone: Is it beneficial or harmful to the cardiovascular system? *World J Cardiol* 2011;3(5):144-152. (Impact Factor = N/A)

26. **Chattipakorn N**, Kumfu S, Fucharoen S, Chattipakorn S. Calcium channels and iron uptake into the heart. *World J Cardiol* 2011;3(7):215-218. (Impact Factor = N/A)

27. Kumfu S, Chattipakorn S, Srichairattanakool S, Settakorn J, Fucharoen S, **Chattipakorn N**. T-type calcium channel as a portal of iron uptake into cardiomyocytes of beta-thalassemic mice. *Eur J Haematol* 2010;86:156-166. (Impact Factor = 2.785)

28. Phrommintikul A, Sivasinprasasn S, Lailerd N, Chattipakorn S, Kuanprasert S, **Chattipakorn N**. Plasma urocortin in acute myocardial infarction patients. *Eur J Clin Invest* 2010;40(10):874-882. (Impact Factor = 2.736)

29. Kanlop N, Shinlapawittayatorn K, Sungnoon R, Weerateerangkul P, Chattipakorn S, **Chattipakorn N**. Cilostazol attenuates ventricular arrhythmia induction and improves defibrillation efficacy in swine. *Can J Physiol Pharmacol* 2010;88:422-428. (Impact Factor = 1.849)

30. Pratchayasakul W, Pongchaidecha A**, Chattipakorn N**, Chattipakorn S. Reversible acetylcholinesterase inhibitory effect of *Tabernaemontana divaricata* extract on synaptic transmission in rat CA1 hippocampus. *Indian J Med Res* 2010;131:411-417. (Impact Factor = 1.826)

31. Rutjanaprom W, Kanlop N, Charoenkwan P, Sittiwangkul R, Srichairattanakool S, Tantiworawit A, Phrommintikul A, Chattipakorn S, Fucharoen S, **Chattipakorn N**. Heart rate variability in beta-thalassemia patients. *Eur J Haematol* 2009;83:483-489. (Impact Factor = 2.785).

32. **Chattipakorn N**, Settakorn J, Petsophonsakul P, Suwannahoi P, Mahakranukraugh P, Srichairattanakool S, Chattipakorn S. Cardiac mortality is associated with low levels of omega-3 and omega-6 fatty acids in the heart of cadavers with history of coronary heart disease. *Nutr Res* 2009;29:696-704. (Impact Factor = 2.092)

33. Pongchaidecha A, Lailerd N, Boonprasert W, **Chattipakorn N**. Effects of curcuminoids supplement on cardiac autonomic status in high-fat-induced obese rats. *Nutrition* 2009;25:870-878. (Impact Factor = 2.726)

34. Pratchayasakul W, Pongruangporn M, **Chattipakorn N**, Chattipakorn S. Roles of curcumin in preventing pathogenesis of Alzheimer's disease. *Curr Top Nutraceut Res* 2009;7:11-26. (Impact Factor = 0.238)

3.2 <u>ความก้าวหน้าในการสร้างทีมวิจัย</u>

ในขณะนี้ได้ทำการสนับสนุนนักวิจัยรุ่นใหม่ ได้ทำวิจัยในสาขาที่เกี่ยวข้องกับโครงการ พร้อมทั้งได้สนับสนุนให้ขอรับทุนวิจัยสำหรับนักวิจัยรุ่นใหม่จาก สกว. ซึ่งขณะนี้มีผู้ที่ได้รับทุนไปแล้ว จำนวน 6 คน โดยได้ทำการศึกษาวิจัยในด้านของโรคหัวใจและกลไกการเกิดโรคเป็นหลัก นอกจากนี้ยังได้ร่วมมือในการทำวิจัยกับหน่วยงานต่าง ๆ ในการให้การฝึกอบรมนักวิจัยในสาขา Cardiac electrophysiology ด้วย นอกจากนั้นยังได้รับนักวิจัยในระดับปริญญาโท เข้ามาฝึกการทำวิจัยเพิ่มอีก 2 คน ภายใต้โครงการนี้

3.3 <u>การนำผลจากโครงการไปใช้ประโยชน์</u>

ได้มีการตีพิมพ์เผยแพร่แล้ว 34 เรื่อง (ดังรายละเอียดข้างต้น) และการบรรยายให้ความรู้ต่อสารธารณชน ดังรายละเอียดในข้อ 3 และข้อ 5.4

4. กิจกรรมอื่น ๆ ที่เกี่ยวข้อง ได้แก่

4.1 ผลงานอื่น ๆ เช่น การไปเสนอผลงาน การได้รับเชิญไปเป็นวิทยากร การได้รับรางวัล

4.1.1 การได้รับเชิญเป็นวิทยากร

ปี พ.ศ. 2555

1) อาจารย์พิเศษบรรยายในหัวข้อ “Vital sign” ทำการสอนนักศึกษาทันตแพทยศาสตร์ กระบวนวิชาพิเคราะห์โรคช่องปาก (DDIA 481) ประจำปีการศึกษา 2555 ณ คณะทันตแพทยศาสตร์
จัดโดย คณะทันตแพทยศาสตร์ มหาวิทยาลัยเชียงใหม่
ในวันที่ 16 กรกฎาคม พ.ศ. 2555 ใช้เวลา 13.00-14.00 น.

2) ประธาน (Chairperson) ในการบรรยายของนักศึกษาโครงการปริญญาเอก กาญจนภิเษก ครั้งที่ 13 (RGJ-Ph.D. Congress XIII) ใน Section S4: Viral infection and immunology ในงานประชุมวิชาการ โครงการปริญญาเอกกาญจนภิเษก ครั้งที่ 13 (RGJ-Ph.D. Congress XIII) ณ โรงแรมจอมเทียน ปาล์ม บีช รีสอร์ท พัทยา จังหวัดชลบุรี
จัดโดย โครงการปริญญาเอกกาญจนภิเษก (คปก.) สำนักงานกองทุนสนับสนุนการวิจัย (สกว.)
ในวันที่ 7 เมษายน พ.ศ. 2555 ใช้เวลา 08.30-10.45 น.

3) วิทยากรรับเชิญ บรรยายในหัวข้อ “การตอบคำถามจาก reviewer ในการส่ง manuscript ตีพิมพ์ในวารสารนานาชาติ” ในโครงการอบรมเรื่อง การตอบคำถามจาก reviewer ในการส่ง manuscript ตีพิมพ์ในวารสารนานาชาติ ณ ห้องประชุมศาสตราจารย์เกียรติคุณ นายแพทย์ชัยโรจน์ แสงอุดม ชั้น 12 อาคาร 12 ชั้น
จัดโดย งานวิจัยและวิเทศสัมพันธ์ คณะเทคนิคการแพทย์ มหาวิทยาลัยเชียงใหม่
ในวันที่ 3 เมษายน พ.ศ. 2555 ใช้เวลา 13.30-15.00 น.

4) วิทยากรรับเชิญ บรรยายในหัวข้อ “Heart rate variability and its significance” ในงานประชุม International conference the oxidative stress in congenital and acquired hemolytic anemia” ณ โรงแรมการ์เด้น คลิฟ รีสอร์ท แอนด์ สปา จ. ชลบุรี
จัดโดย ภาควิชาชีวเคมี คณะแพทยศาสตร์ ศิริราชพยาบาล มหาวิทยาลัยมหิดล
ในวันที่ 22 มีนาคม พ.ศ. 2555 ใช้เวลา 15.05-15.25 น.

5) วิทยากรรับเชิญ บรรยายในหัวข้อ Symposium: Up-to-date in cellular and molecular biology in heart failure" ในงานประชุม The 6th Asian pacific congress of heart failure 2012 (APCHF 2012) ณ โรงแรมเลอเมเรเดียนเชียงใหม่ จ. เชียงใหม่
จัดโดย ชมรมหัวใจล้มเหลวแห่งประเทศไทย ร่วมกับ ASEAN federation of cardiology ร่วมกับ Asian pacific of society of cardiology และ สมาคมแพทย์โรคหัวใจแห่งประเทศไทย
ในวันที่ 5 กุมภาพันธ์ พ.ศ. 2555 ใช้เวลา 08.00-09.00 น.

6) วิทยากรรับเชิญ บรรยายในหัวข้อ "Cardiac Electrophysiology and Biomedical Engineering" ในงานประชุม The Biomedical Engineering International Conference (BME icon) 2012 ณ โรงแรม คันทรีฮิวส์ จ. เชียงใหม่ จัดโดย Thai Biomedical Engineering Society (ThaiBME)
ในวันที่ 29-31 มกราคม พ.ศ. 2555

7) วิทยากรรับเชิญ บรรยายในหัวข้อ "คุณภาพวิทยานิพนธ์/การค้นคว้าอิสระ/แลกเปลี่ยนประสบการณ์จากอาจารย์ที่ปรึกษาวิทยานิพนธ์" ณ โรงแรมเชียงใหม่ฮิลล์ จ. เชียงใหม่ ในงานสัมมนาเรื่อง บทบาทอาจารย์ที่ปรึกษาวิทยานิพนธ์/การค้นคว้าแบบอิสระกับคุณภาพวิทยานิพนธ์/การค้นคว้าแบบอิสระ จัดโดย งานบริหารทั่วไป บัณฑิตวิทยาลัย มหาวิทยาลัยเชียงใหม่
ในวันที่ 25 มกราคม พ.ศ. 2555

<u>ปี พ.ศ. 2554</u>

8) วิทยากรรับเชิญ บรรยายในหัวข้อ "Why Literature review?" ในงานประชุมวิชาการคลินิกวิจัย ครั้งที่ 8 ณ ชั้น 15 อาคารสุจิณโณ คณะแพทยศาสตร์ มหาวิทยาลัยเชียงใหม่ จัดโดย ภาควิชาจักษุวิทยา คณะแพทยศาสตร์ มหาวิทยาลัยเชียงใหม่ ในวันที่ 6 มกราคม พ.ศ. 2554

9) วิทยากรรับเชิญ บรรยายในหัวข้อ "บทบาทหน้าที่ของอาจารย์ที่ปรึกษาวิทยานิพนธ์ที่ดีสำหรับนักศึกษาบัณฑิตศึกษา" ในการอบรม "อาจารย์ที่ปรึกษาวิทยานิพนธ์" ณ คณะสัตวแพทยศาสตร์ มหาวิทยาลัยเชียงใหม่ จัดโดย งานบริการการศึกษา และพัฒนาคุณภาพนักศึกษา คณะสัตวแพทยศาสตร์ มหาวิทยาลัยเชียงใหม่ ในวันที่ 24 มีนาคม พ.ศ. 2554

10) วิทยากรรับเชิญ บรรยายในหัวข้อ “แรงจูงใจในการสร้างสรรค์งานวิจัย” ในการสัมมนาเรื่อง “เสวนาวิชาการกับคณะกรรมการส่งเสริม พัฒนางานวิจัย และดำเนินการเกี่ยวกับงบประมาณโรคเอดส์” ณ ห้องประชุมดอกสัก ชั้น 2 คณะแพทยศาสตร์ มหาวิทยาลัยเชียงใหม่ จัดโดย คณะเทคนิคการแพทย์ มหาวิทยาลัยเชียงใหม่ ในวันที่ 2 มิถุนายน พ.ศ. 2554

11) วิทยากรรับเชิญ บรรยายในหัวข้อ “การตั้งวัตถุประสงค์การเรียนรู้” ในการสัมมนาเรื่อง “ปฐมนิเทศนักศึกษาบัณฑิต” ณ ชั้น 2 อาคารเรียนรวม ราชนครินทร์ คณะแพทยศาสตร์ มหาวิทยาลัยเชียงใหม่ จัดโดย หน่วยบริหารหลักสูตร คณะแพทยศาสตร์ มหาวิทยาลัยเชียงใหม่ ในวันที่ 3 มิถุนายน พ.ศ. 2554

12) วิทยากรรับเชิญ บรรยายในหัวข้อ “กลยุทธ์สร้างแรงบันดาลใจในการทำวิจัย” ในการสัมมนางานวิจัย (Research club) ครั้งที่ 5/2554 ณ ห้องประชุมกรรมการคณะฯ ชั้น 2 อาคาร 7 คณะทันตแพทยศาสตร์ มหาวิทยาลัยเชียงใหม่ จัดโดย งานบริการการศึกษาบริหารงานวิจัยและบริการวิชาการ คณะทันตแพทยศาสตร์ มหาวิทยาลัยเชียงใหม่
ในวันที่ 29 มิถุนายน พ.ศ. 2554

13) วิทยากรรับเชิญ บรรยายในหัวข้อ “ทำอย่างไรให้ประสบความสำเร็จในการทำงานวิจัย” ในการประชุมสัมมนาวิจัย ประจำปี 2554 ณ สวนพฤกษาศาสตร์ทวีชล อ. ดอยสะเก็ด จ. เชียงใหม่ จัดโดย ภาควิชาออร์โทปิดิกส์ คณะแพทยศาสตร์ มหาวิทยาลัยเชียงใหม่ ในวันที่ 10 กรกฎาคม พ.ศ. 2554

14) อาจารย์พิเศษ บรรยายในหัวข้อ “Vital sign” ทำการสอนนักศึกษาทันต-แพทยศาสตร์ กระบวนวิชาพิเคราะห์โรคช่องปาก (DDIA 481) ประจำปีการศึกษา 2554 ณ คณะทันตแพทยศาสตร์ มหาวิทยาลัยเชียงใหม่ จัดโดยคณะทันตแพทยศาสตร์ มหาวิทยาลัยเชียงใหม่
ในวันที่ 13 กรกฎาคม พ.ศ. 2554

15) วิทยากรรับเชิญ บรรยายในหัวข้อ “การเขียนบทความทางวิชาการเพื่อตีพิมพ์” ณ ห้องพุทธชาด ชั้น 3 อาคารเฉลิมพระเกียรติ คณะเภสัชศาสตร์ จัดโดย คณะเภสัชศาสตร์ มหาวิทยาลัยเชียงใหม่ ในวันที่ 29 กรกฎาคม พ.ศ. 2554

16) วิทยากรรับเชิญ บรรยายในหัวข้อ “Overview & Pathophysiology” จัดโดย สถาบันสุขภาพเด็กแห่งชาติมหาราชินี กรมการแพทย์ ณ โรงแรมรามาการ์-เด้น ถนนวิภาวดี กรุงเทพมหานคร ในวันที่ 8 กันยายน พ.ศ. 2554

<u>ปี พ.ศ. 2553</u>

17) วิทยากรรับเชิญบรรยายในหัวข้อ “Translational Research in Thailand” ในงานประชุมวิชาการสรีรวิทยาสมาคมแห่งประเทศไทย ครั้งที่ 39 ณ โรงแรมอมารีออคิดรีสอร์ทแอนด์ทาวเวอร์พัทยา จ. ชลบุรี จัดโดยภาควิชาสรีรวิทยา มหาวิทยาลัยมหิดล ร่วมกับ สรีรวิทยาสมาคมแห่งประเทศไทย ในวันที่ 5 พฤษภาคม พ.ศ. 2553

18) วิทยากรรับเชิญ บรรยายในหัวข้อ “Update in Cardiovascular Research” ในงานกิจกรรม Journal Club ณ คณะสหเวชศาสตร์ มหาวิทยาลัยนเรศวร จ. พิษณุโลก จัดโดย คณะสหเวชศาสตร์ มหาวิทยาลัยนเรศวร จ. พิษณุโลก ในวันที่ 11 มิถุนายน พ.ศ. 2553

19) วิทยากรรับเชิญ บรรยายในหัวข้อ “Cardiac Research Update” ในงานประชุม RGJ seminar series XLVIII: Medical Science: Molecular Medicine: Today and Tomorrow ณ โรงแรมศิรินาถการ์เด้น จัดโดย ภาควิชาชีวเคมี คณะแพทยศาสตร์ มหาวิทยาลัยเชียงใหม่ ร่วมกับโครงการปริญญาเอกกาญจนาภิเษก สำนักงานกองทุนสนับสนุนการวิจัย (สกว.) ในวันที่ 2 กรกฎาคม พ.ศ. 2553

20) อาจารย์พิเศษ บรรยายในหัวข้อ “Vital sign” ทำการสอนนักศึกษาทันตแพทยศาสตร์ กระบวนวิชาพิเคราะห์โรคช่องปาก (DDIA 481) ประจำปีการศึกษา 2553 ณ คณะทันตแพทยศาสตร์ จัดโดย คณะทันตแพทยศาสตร์ มหาวิทยาลัยเชียงใหม่ ในวันที่ 7 กรกฎาคม พ.ศ. 2553

21) อาจารย์พิเศษ บรรยายในหัวข้อ “Cardiology (Arrhythmia)” แก่นักศึกษาสัตวแพทย์ ชั้นปีที่ 5 คณะสัตวแพทย์ศาสตร์ มหาวิทยาลัยเชียงใหม่ กระบวนวิชาโรคของสุนัขและแมว (651531) ประจำปีการศึกษา 2553 ณ คณะสัตวแพทยศาสตร์ มหาวิทยาลัยเชียงใหม่ จัดโดย ภาควิชาสัตว์เล็ก คณะสัตวแพทยศาสตร์ มหาวิทยาลัยเชียงใหม่ ในวันที่ 4 สิงหาคม พ.ศ. 2553

22) วิทยากรรับเชิญ บรรยายในหัวข้อ “Writing result and discussion” และหัวข้อ “Dealing with the Editors and Reviewer’s Commen” ในโครงการอบรมเชิงปฏิบัติการ เรื่อง “การเขียนบทความวิชาการทางการแพทย์” ณ ห้องบอลรูมอัลไพน์กอล์ฟรีสอร์ทเชียงใหม่ จัดโดย งานวิจัยและวิเทศสัมพันธ์ คณะแพทยศาสตร์ มหาวิทยาลัยเชียงใหม่ ในวันที่ 9-10 กันยายน พ.ศ. 2553

ปี พ.ศ. 2552

23) วิทยากรรับเชิญในหัวข้อ “How to perform non-invasive central arterial pressure measurement” ในงานประชุมวิชาการ Chiang Mai Cardiology Conference (CMCC) 11th จัดโดย หน่วยระบบหัวใจและหลอดเลือด ภาควิชาอายุรศาสตร์ คณะแพทยศาสตร์ มหาวิทยาลัยเชียงใหม่ ในวันที่ 12 กันยายน พ.ศ. 2552

24) วิทยากรรับเชิญ บรรยายในหัวข้อ “From mice to men: A translation research from the heart” ในงานประชุมโครงการกาญจนาภิเษกครั้งที่ 74 (RGJ Seminar Series LXXIV) เรื่อง From Basic Biomedical Research to Sustainable Development จัดโดย ภาควิชาปรสิตวิทยา คณะแพทยศาสตร์ มหาวิทยาลัยเชียงใหม่ ร่วมกับโครงการปริญญาเอกกาญจนาภิเษก สำนักงานกองทุนสนับสนุนการวิจัย (สกว.) ในวันที่ 16 กันยายน พ.ศ. 2552

25) วิทยากรรับเชิญ บรรยายในหัวข้อ “เกณฑ์มาตราฐานและตัวชี้วัดคุณภาพงานวิจัยและนักวิจัย: มุมมองของ Review, (Journal), Reader (ตำแหน่งทางวิชาการ) และผู้ให้ทุน” ในงานประชุมวิชาการ “Quest for Excellance” ครบรอบ 50 ปี คณะแพทยศาสตร์ มหาวิทยาลัยเชียงใหม่ จัดโดย คณะแพทยศาสตร์ มหาวิทยาลัยเชียงใหม่ ในวันที่ 3 พฤศจิกายน พ.ศ. 2552

26) วิทยากรรับเชิญ บรรยายในหัวข้อ “Defibrillation Threshold Testing” ในงานประชุมวิชาการ Cardiac Electrophysiology Club Meeting ณ โรงแรมภูแมน จังหวัดกรุงเทพฯ จัดโดยชมรมช่างไฟฟ้าหัวใจ (Cardiac Electrophysiology) ในวันที่ 21 พฤศจิกายน พ.ศ. 2552

27) วิทยากรรับเชิญ บรรยายในหัวข้อ “L-type calcium channel blocker fails to inhibit iron uptake into cardiomyocytes of β–thalassemia mice” ในงานประชุมวิชาการ Asia Pacific Iron Academy Conference 2009 ณ โรงแรมแชงกีล่า จังหวัดเชียงใหม่ จัดโดย Siriraj-Thalassemia Research Program,

Department of Research & Development ในวันที่ 28 พฤศจิกายน พ.ศ. 2552

4.1.2 <u>สรุปรางวัลที่ได้รับตลอดระยะที่ได้รับทุนเมธีวิจัยอาวุโส สกว. ตั้งแต่ พ.ศ. 2552-2555</u>

<u>ประจำปี พ.ศ. 2553</u>

1. นักศึกษาปริญญาโทและปริญญาเอก จากศูนย์วิจัยและฝึกอบรมสาขาโรคทางไฟฟ้าของหัวใจ ภายใต้การเป็นอาจารย์ที่ปรึกษาวิทยานิพนธ์ เข้ารับรางวัลในการนำเสนอผลงานวิจัยของงานประชุมสรีรวิทยาสมาคมแห่งประเทศไทย ครั้งที่ 39 ซึ่งจัดขึ้นในวันที่ 5-7 พ.ค. 2553 ณ โรงแรม อมารีออคิดรีสอร์ท แอนด์ทาวเวอร์ พัทยา จ. ชลบุรี รายละเอียด ดังนี้

1.1 การนำเสนองานวิจัยยอดเยี่ยมระดับปริญญาเอกด้วยวาจา
"รางวัลศาสตราจารย์ นายแพทย์ดิถี จึงเจริญ"
ผู้ได้รับรางวัลที่ 1 คือ อ. วาสนา ปรัชญาสกุล
ผลงานวิจัยเรื่อง "The defect of neuronal function of insulin receptor in rat's hippocampus following 12-week high-fat consumption"
ผู้ได้รับรางวัลที่ 2 คือ อ. ภูเนตร วีรธีรางกูร
ผลงานวิจัยเรื่อง "Effects of Kaempferia parviflora extract on the expression of nitric oxide synthase and cGMP level in rat hearts"

1.2 การนำเสนองานวิจัยยอดเยี่ยมระดับปริญญาเอกด้วยโปสเตอร์
"รางวัลศาสตราจารย์ ดร. เลียงชัย ลิ่มล้อมวงศ์"
ผู้ได้รับรางวัลที่ 1 คือ น.ส. ศิรินาฏ คำฟู
ผลงานวิจัยเรื่อง "Mechanism of iron entry in cultured thalassemic cardiomyocytes"

1.3 การนำเสนองานวิจัยยอดเยี่ยมระดับปริญญาโทด้วยวาจา
รางวัลศาสตราจารย์ นายแพทย์ประสพ รัตนากร"
ผู้ได้รับรางวัลที่ 1 คือ นางสาววสาวิตรี ธรรมสอน
ผลงานวิจัยเรื่อง "Cardioprotective effects of granulocyte-colony stimulating factor against mitochondrial damage under oxidative stress in isolated cardiac mitochondria"

ประจำปี พ.ศ. 2554

2. พญ. ชลธิดา ยาระณะ ตำแหน่งแพทย์ใช้ทุน จากศูนย์วิจัยและฝึกอบรมสาขาโรคทางไฟฟ้าของหัวใจ ภายใต้การเป็นอาจารย์ที่ปรึกษา ได้รับรางวัลทุนนักวิจัยรุ่นใหม่ ประจำปี พ.ศ. 2554 จากโครงการวิจัย เรื่อง “การเปรียบเทียบผลของแคลเซียมต่อ mitochondrial permeability transition และ oxidative stress ใน isolated mitochondria จากหัวใจและสมองหนู”

ประจำปี พ.ศ. 2555

3. นักศึกษาปริญญาปริญญาเอก จากศูนย์วิจัยและฝึกอบรมสาขาโรคทางไฟฟ้าของหัวใจ ภายใต้การเป็นอาจารย์ที่ปรึกษาวิทยานิพนธ์ เข้ารับรางวัลในการนำเสนอผลงานวิจัย ในงานประชุมวิชาการโครงการปริญญาเอกกาญจนภิเษก ครั้งที่ 13 (RGJ-Ph.D. Congress XIII) ซึ่งจัดขึ้นในระหว่างวันที่ 6-8 เมษายน พ.ศ. 2555 ณ โรงแรมจอมเทียน ปาล์ม บีช รีสอร์ท เมืองพัทยา จ. ชลบุรี

ผู้ได้รับรางวัลการนำเสนองานวิจัยยอดเยี่ยมระดับปริญญาเอกด้วยวาจา รายละเอียดดังนี้

3.1 อ. ดร. วาสนา ปรัชญาสกุล
ผลงานวิจัยเรื่อง “Effect of estrogen on neuronal insulin receptor function in long term high fat-fed rats”

3.2 น.ส. ศิริรัตน์ สุรินทร์แก้ว
ผลงานวิจัยเรื่อง “Inhibition of p38 activation during ischemia, but not reperfusion, effectively attenuated fatal arrhythmia incidence in rats with ischemia/reperfusion injury”

3.3 น.ส. ศิรินาฏ คำฟู
ผลงานวิจัยเรื่อง “Effect of calcium channel and divalent metal transporter1 blockers on cardiac functions, iron deposition and mortality of iron-loaded thalassemia”

4. นักศึกษาปริญญาปริญญาเอก จากศูนย์วิจัยและฝึกอบรมสาขาโรคทางไฟฟ้าของหัวใจ ภายใต้การเป็นอาจารย์ที่ปรึกษาร่วมวิทยานิพนธ์ เข้ารับรางวัลในการนำเสนอผลงานวิจัย เข้ารับรางวัลในการนำเสนอผลงานวิจัย ของงานประชุมสรีรวิทยาสมาคมแห่งประเทศไทย ครั้งที่ 41 ซึ่งจัดขึ้นในวันที่ 2-4 พ.ค. 2555 ณ อาคารศรีสวรินทิรา คณะแพทยศาสตร์ศิริราชพยาบาล

ผู้ได้รับรางวัลการนำเสนองานวิจัยยอดเยี่ยมระดับปริญญาเอกด้วยวาจา รายละเอียดดังนี้

4.1 น.ส. นพมาศ พิพัฒน์พิบูลย์

ผลงานวิจัยเรื่อง “DPP-4 inhibitor improves neuronal insulin receptor function and brain mitochondrial function caused by high-fat diet consumption”

ผู้ได้รับรางวัลการนำเสนองานวิจัยยอดเยี่ยมระดับปริญญาเอกด้วยโปสเตอร์ รายละเอียดดังนี้

4.2 ภก. จิรภาส ศรีเพ็ชรวันดี

ผลงานวิจัยเรื่อง “Mitochondrial calcium uniporter blocker effectively prevents brain mitochondrial dysfunction caused by iron overload.”

5. น สพ. เกริกเกียรติ จินดา นักศึกษาปริญญาปริญญาเอก จากศูนย์วิจัยและฝึกอบรมสาขาโรคทางไฟฟ้าของหัวใจ ภายใต้การเป็นอาจารย์ที่ปรึกษาวิทยานิพนธ์ ได้รับรางวัลเป็นรางวัลระดับนานาชาติ รางวัล “Frontier in Cardio Vascular Biology 2012 Travel Grant Award” ในการประชุม Frontier in CardioVascular Biology 2012 Meeting ซึ่งจัดขึ้นที่กรุง London ประเทศอังกฤษ จากผลงานวิจัยเรื่อง“Cardioprotective effect of dipeptidyl peptidase-4 inhibitor during ischemia-reperfusion injury is via prevention of cardiac mitochondrial dysfunction”

6. นักศึกษาระดับปริญญาโท จากศูนย์วิจัยและฝึกอบรมสาขาโรคทางไฟฟ้าของหัวใจ คณะแพทยศาสตร์ มหาวิทยาลัยเชียงใหม่ ภายใต้การเป็นอาจารย์ที่ปรึกษาวิทยานิพนธ์ ได้รับรางวัล Excellent Oral Research Presentation จากการประชุม The 1st ASEAN Plus Three Graduate Research Congress (AGRC 2012) ซึ่งจัดขึ้นระหว่างวันที่ 1-2 มีนาคม พ.ศ. 2555 ณ โรงแรมดิเอ็มเพรสเชียงใหม่

ผู้ได้รับรางวัลการนำเสนองานวิจัยยอดเยี่ยมระดับปริญญาเอกด้วยวาจา รายละเอียดดังนี้

6.1 น.ส. ณัฐยาภรณ์ อภัยใจ

ผลงานวิจัยเรื่อง “Effects of metformin on cardiac function in high-fat diet induced insulin resistant rats”

6.2 น.ส. หิรัญญา ปินตานา

ผลงานวิจัยเรื่อง “Effects of metformin on learning and memory behaviors in high-fat diet-induced insulin resistant rats”

4.1.3 <u>การจัดงานประชุมวิชาการประจำปี</u>

<u>ครั้งที่ 1</u> งานประชุมวิชาการ “เมธีวิจัยอาวุโส สกว. ประจำปี พ.ศ. 2553 ศาสตราจารย์ ดร. นายแพทย์ นิพนธ์ ฉัตรทิพากร” เรื่อง “Focused Update on Cardiac Research: From Cell to Bedside” ในวันศุกร์ ที่ 14 พฤษภาคม พ.ศ. 2553 ณ ห้องประชุม 153 ชั้น 15 อาคารสุจิณโณ คณะแพทยศาสตร์ มหาวิทยาลัยเชียงใหม่

<u>ครั้งที่ 2</u> งานประชุมวิชาการ “เมธีวิจัยอาวุโส สกว. ประจำปี พ.ศ. 2554 ศาสตราจารย์ ดร. นายแพทย์นิพนธ์ ฉัตรทิพากร” เรื่อง “Cardioneural Research Network: Bridging Bench to Bedside Care” ในวันศุกร์ ที่ 17 มิถุนายน พ.ศ. 2554 ณ ห้องประชุมเฮือนภัตต์ สวนพฤกษศาสตร์ทวีชล อ. ดอยสะเก็ด จ. เชียงใหม่

<u>ครั้งที่ 3</u> งานประชุมวิชาการ “เมธีวิจัยอาวุโส สกว. ประจำปี พ.ศ. 2555 ศาสตราจารย์ ดร. นายแพทย์นิพนธ์ ฉัตรทิพากร” เรื่อง “The Emerging Frontier of Neurocardiology: Autonomic Regulation of Cardiovascular Function” ในวันที่ 25-26 มิถุนายน พ.ศ. 2555 ณ รวีวารีรีสอร์ท อ. แม่แตง จ. เชียงใหม่

4.2 <u>กิจกรรมที่เกี่ยวข้องกับการนำผลจากโครงการไปใช้ประโยชน์</u>

การนำความรู้ที่ได้จากงานวิจัยไปบรรยายเผยแพร่ในงานประชุมวิชาการต่าง ๆ

<u>ระดับนานาชาติ</u>

1. Chattipakorn S, Pipatpiboon N, Pintana H, Pratchayasakul W, Chattipakorn N. DDP-4 inhibitor prevents neuronal insulin resistance, brain mitochondrial dysfunction, and impaired learning and memory caused by high-fat diet consumption. Diabetes 2012 (In press, Impact Factor = 8.889)

2. Apaijai N, Chattipakorn S, **Chattipakorn N**. Dipeptidyl peptidase-4 (DPP-4) inhibitor preserves cardiac function and heart rate variability and prevents cardiac mitochondrial dysfunction in high fat-induced insulin resistant rats. *Cardiovasc Res* Cardiovasc Res 2012;93:1 (suppl):S44. (Impact Factor = 6.051)

3. Chinda K, Palee S, Surinkaew S, Phornphutkul M, Chattipakorn S, **Chattipakorn N**. Cardioprotective effect of dipeptidyl peptidase-4 inhibitor during ischemia-reperfusion injury is via prevention of cardiac

mitochondrial dysfunction. *Cardiovasc Res* Cardiovasc Res 2012;93:1 (suppl):S22. (Impact Factor =6.051)

4. Palee S, Chattipakorn S, **Chattipakorn N**. PPAR-gamma agonist rosiglitazone facilitated fatal arrhythmia in ischemic-reperfusion rat hearts by decreased cardiac connexin43 phosphorylation. *Cardiovasc Res* 2012;93:1 (suppl):S28-S29. (Impact Factor = 6.051)

5. Surinkaew S, Kumphune S, Chattipakorn S, **Chattipakorn N**. Selective p38 inhibitor administered during ischemia, but not reperfusion, effectively attenuates fatal arrhythmia in rats with ischemia/reperfusion injury. *Circulation* 2011;123:295.(Impact Factor = 14.429)

6. Kumfu S, Chattipakorn S, Fucharoen S, **Chattipakorn N**. T-type calcium channel inhibitor attenuates cardiac dysfunction, improves cardiac sympathovagal imbalance and decreases mortality in iron-overloaded mice. *Circulation* 2011;123:365. (Impact Factor = 14.429)

7. Chattipakorn S, Thommasorn S, **Chattipakorn N**. Novel effects of phosphodiesterase-3 (PDE3) inhibitor in preventing cardiac mitochondrial dysfunction under severe oxidative stress. *Eur Heart J* 2011;32:364. (Impact Factor = 8.917)

8. Senthong W, Phrommintikul A, Kanjanavanit R, Kuanprasert S, **Chattipakorn** N. Effects of metoprolol tartrate versus carvedilol on central aortic pressure in patients with chronic heart failure. *Eur Heart J* 2011;32:966. (Impact Factor = 8.917)

9. Yarana C, Thommasorn S, Sanit J, **Chattipakorn N**, Chattipakorn S. Cardiac mitochondrial dysfunction caused by calcium overload is not due to CsA-dependent mPTP opening. *Eur Heart J* 2011;32:1098-1099 (Impact Factor = 8.917)

10. Sripetchwandee J, Sanit J, **Chattipakorn N**, Chattipakorn S. Mitochondrial calcium uniporter blocker prevents neuronal mitochondrial dysfunction

caused by iron overload. *Neuroscience* 2011; P94. (Impact Factor = 3.215)

11. Pipatpiboon N, Pratchayasakul W, **Chattipakorn N**, Chattipakorn S. Rosiglitazone improves neuronal insulin resistance and neuronal insulin signaling in obese rats induced with high-fat diets. *Neuroscience* 2011;P62. (Impact Factor = 3.215)

12. Chattipakorn S, Yarana C, Sanit J, **Chattipakorn N**. Synaptosomal mitochondria is more susceptible to calcium overload than nonsynaptosomal mitochondria. *Neuroscience* 2011; P41. (Impact Factor = 3.215)

13. Pratchayasakul W, **Chattipakorn N**, Chattipakorn S. Effect of estrogen administration on insulin receptor function in long term high fat-fed ovariectomized rats. *Neuroscience* 2011; P62. (Impact Factor = 3.215)

14. Palee S, Weerateerangkul P, Surinkaew S, Chattipakorn S, **Chattipakorn N**. Rosiglitazone facilitates the occurrence of ventricular fibrillation and does not prevent mitochondrial dysfunction in ischemic/reperfusion swine hearts. *Eur Heart J* 2011;32: 578. (Impact Factor = 8.917)

15. Chattipakorn S, Thummasorn S, **Chattipakorn N**. Granulocyte-colony stimulating factor prevents oxidative stress-induced cardiac mitochondrial dysfunction. *Circulation Journal* 2011;75:504. (Impact Factor = 2.387)

16. Chattipakorn S, Kumfu S, Srichairattanakool S, Settakorn J, Fucharoen S, **Chattipakorn N**. T-type calcium channel is a main portal for iron entry in thalassemic heart. *Circulation* 2010;122:A11087. (Impact factor =14.816)

17. **Chattipakorn N**, Sivasinprasasn S, Phrommintikul A, Lailerd N, Kuanprasert S. Prognostic significance of plasma urocortins in acute myocardial infarction patients. *Eur Heart J* 2009;30:P4680. (Impact Factor = 3.215)

18. Chattipakorn SC, Kumfu S, Srichairattanakool S, Fucharoen S, **Chattipakorn N**. Is L-type calcium channel a major portal for iron uptake into cardiomyocytes under iron overload condition? An investigation in cardiomyocytes of beta-thalassemic mice. *Europace* 2009;11:622. (Impact Factor = 1.839)

19. Weerateerangkul P, Kanlop N, Rutjanaprom W, **Chattipakorn N**, Chattipakorn SC. Nitric oxide signaling may involve in pro-arrhythmic effects of Kaempferia parviflora. *Europace* 2009;11:119. (Impact Factor = 1.839)

20. Kanlop N, Rutjanaprom W, Weerateerangkul P, **Chattipakorn N**. Granulocyte colony-stimulating factor (G-CSF) markedly increases ventricular fibrillation threshold by reducing vulnerability to arrhythmia in ischemic/reperfusion injury model. *J Am Coll Cardiol.* 2009;49:140A. (Impact Factor = 14.292)

ระดับชาติ

21. Palee S, Chattipakorn S, **Chattipakorn N**. Mechanistic effects of rosiglitazone on its facilitation of ventricular fibrillation in ischemic/reperfusion rat hearts. *J Physiol Biomed Sci* 2012;25(1):47.

22. Chinda K, Palee S, Surinkaew S, Phornphutkul M, Chattipakorn S, **Chattipakorn N**. Dipeptidyl peptidase-4 inhibitor attenuates cardiac ischemia-reperfusion injury and cardiac mitochondrial dysfunction. *J Physiol Biomed Sci* 2012;25(1):48.

23. Pramojanee S, **Chattipakorn N**, Chattipakorn SC. The alteration of osteoblastic insulin receptor signaling in insulin resistant rats induced by 12-week high-fat diet consumption. *J Physiol Biomed Sci* 2012;25(1):39.

24. Pipatpiboon N, Pratchayasakul W, **Chattipakorn N**, Chattipakorn SC. DPP-4 inhibitor improves neuronal insulin receptor function and brain

mitochondrial function caused by high-fat diet consumption. *J Physiol Biomed Sci* 2012;25(1):42.

25. Pintana H, Apaijai N, Pratchayasakul W, **Chattipakorn N**, Chattipakorn SC. Effects of metformin on learning behaviors and brain mitochondrial functions in 12-week high-fat diet-induced insulin resistant rats. *J Physiol Biomed Sci* 2012;25(1):43.

26. Sripetchwandee J, Sanit J, **Chattipakorn N**, Chattipakorn SC. Mitochondrial calcium uniporter blocker effectively prevents brain mitochondrial dysfunction caused by iron overload. *J Physiol Biomed Sci* 2012;25(1):50.

27. Apaijai N, Pintana H, Chattipakorn S, **Chattipakorn N**. Cardioprotective effects of vildagliptin in long-term high-fat diet consumption-induced insulin resistant rats. *J Physiol Biomed Sci* 2012;25(1):54.

28. Kobroob A, **Chattipakorn N**, Wongmekiat O. Amelioration of cadmium-induced kidney mitochondrial injury by caffeic acid phenyl ester. *J Physiol Biomed Sci* 2012;25(1):55.

29. Pratchayasakul W, **Chattipakorn** N, Chattipakorn S. Effect of estrogens on neuronal insulin receptor function in long term high fat-fed rats. *Proceedings to the RGJ-Ph.D. Congress XIII of Thailand annual conference* 2012;184.

30. Kumfu S, Chattipakorn S, Chinda K, Fucharoen S, **Chattipakorn** N. Effect of calcium channels and divalent metal transporter1 blockers on cardiac functions, iron deposition and mortality of iron-loaded thalassemia mice. *Proceedings to the RGJ-Ph.D. Congress XIII of Thailand annual conference* 2012;185.

31. Surinkaew S, Kumphune S, Chattipakorn S**, Chattipakorn** N. Inhibition of p38 activation during ischemia, but not reperfusion, effectively attenuated fatal arrhythmia incidence in rats with ischemia/reperfusion injury.

Proceedings to the RGJ-Ph.D. Congress XIII of Thailand annual conference 2012;186.

32. **Chattipakorn N**. Heart rate variability (HRV): A possible indicator for early cardiac complication in thalassemia. *Proceeding to the International Conference on Oxidative Stress in Congenital and Acquired Hemolytic Anemia* 2012:13.

33. Yanpanitch O, Siritanaratkul N, **Chattipakorn N**, Srichairatanakool S, Fucharoen S, Kalpravidh R. Effects of antioxidant cocktails in beta-thalassemia/HbE patients. *Proceeding to the International Conference on Oxidative Stress in Congenital and Acquired Hemolytic Anemia* 2012:11-12.

34. Apaijai N, Pintana H, Chattipakorn SC, **Chattipakorn N**. Effects of metformin on cardiac function in high-fat diet induced insulin resistant rats. *Proceeding to The First ASEAN Plus Three Graduate Research Congress (AGRC)* 2012:202.

35. Pintana H, Apaijai N, **Chattipakorn N**, Chattipakorn SC. The effects of metformin on learning and memory behaviors in high-fat diet induced insulin resistant rats. *Proceeding to The First ASEAN Plus Three Graduate Research Congress (AGRC)* 2012:169.

36. Lertteerawat P, **Chattipakorn N**, Chattipakorn SC. High-fat diet consumption promotes impairment of neuronal nitric oxide synthase expression in hippocampus of wista rats. *Proceeding to The 21st National Graduate Research Conference* 2011.

37. Suwanchai A, Chattipakorn SC, Theerapiboon U, **Chattipakorn N**. Qantification of Nav1.8 Dental pulp of painful primary teeth in relation to pain sensation: A pilot study. *Proceeding to The 21st National Graduate Research Conference* 2011.

38. **Chattipakorn N.** Translational research in cardiovascular diseases at CERT. *Proceedings to the 39th Physiological Society of Thailand annual conference* 2010;79.

39. Kumfu S, Chattipakorn S, Srichairatanakool S, Fucharoen S, **Chattipakorn N**. Mechanism of iron entry in cultured thalassemic cardiomyocytes. *Proceedings to the 39th Physiological Society of Thailand annual conference* 2010;136.

40. Weerateerangkul P, Chattipakorn S, **Chattipakorn N**. Effects of Kaempferia parviflora extract on the expression of nitric oxide synthase and cGMP level in rat hearts. *Proceedings to the 39th Physiological Society of Thailand annual conference* 2010;102.

41. Thummasorn S, Chattipakorn S, **Chattipakorn N**. Cardioprotective effects of granulocyte-colony stimulating factor against mitochondrial damage under oxidative stress in isolated cardiac mitochondria. *Proceedings to the 39th Physiological Society of Thailand annual conference* 2010;97.

42. Pratchayasakul W, Pongchaidecha A, Petsophonsakul P, Kerdphoo S, **Chattipakorn N**, Chattipakorn S. The defect of neuronal function of insulin receptor in rat's hippocampus following 12-week high-fat consumption. *Proceedings to the 39th Physiological Society of Thailand annual conference* 2010;93.

4.3 <u>การเชื่อมโยงทางวิชาการกับนักวิชาการอื่นๆ ทั้งในและต่างประเทศ</u>

1. Professor Andrew Armour
   Universite De Montreal, Montreal, CANADA
2. Professor Jeffrey L. Ardell
   East Tennessee State University, Johnson City, Tennessee
3. Professor Kenji Sunagawa
   Kyushu University Graduate School of Medical Sciences, Fukuoka, Japan
4. Professor Inder Anand
   University of Minnesota and VA Medical Center, Minneapolis, MN

5. Professor Sanjay Mittal
   Medanta THE MEDICITY, Sector-38, Gurgaon, Haryana-122001, India
6. Professor Bruce H. KenKnight
   The Institute of Technology, University of Minnesota, Minneapolis, MN
7. Professor R. Coronel
   Academic Medical Center, Rm K2-112, Meibergdreef 9, 1105 AZ Amsterdam the Netherlands
8. Professor Ofer Binah
   Ruth & Bruce Rappaport Faculty of Medicine, Technion–Israel Institute of Technology, Israel
9. Professor T-J Chen
   Department of Physiology, College of Medicine, National Taiwan University, Taipei, Taiwan
10. Professor Pamela A. Lucchesi
    Louisiana State University, Department of Pharmacology, 1901 Perdido Street P7-1, New Orleans, LA 70112, USA.
11. Professor Henry Krum
    Head of Clinical Pharmacology Unit, Director, NHMRC Centre of Clinical Research Excellence in Therapeutics, Faculty of Medicine, Monash University, Victoria 3800, Australia
12. Professor Peng-Sheng Chen
    Medtronic Zipes Professor of Cardiology
    Kranert Institute, School of Medicine, Indiana University, Indianapolis, USA.
13. Assoc. Professor Lori L. McMahon
    Director, Neuroscience Graduate Program, Department of Physiology and Biophysics 1918 University Blvd, MCLM 964, Birmingham AL 35294-0005 USA.
14. ศาสตราจารย์ นพ. สุทัศน์ ฟู่เจริญ
    โครงการวิจัยธาลัสซีเมีย สถาบันวิจัยและพัฒนาวิทยาศาสตร์และเทคโนโลยี, มหาวิทยาลัยมหิดล วิทยาเขตศาลายา
15. รศ. พญ. นภาพร ตนานุวัฒน์
    ภาควิชาจักษุวิทยา คณะแพทยศาสตร์ มหาวิทยาลัยเชียงใหม่
16. รศ. ดร. พัชรีวัลย์ ปั่นแหน่งเพ็ชร
    ภาควิชาเภสัชวิทยา คณะแพทยศาสตร์ มหาวิทยาลัยขอนแก่น

17. รศ. ดร. รัชนีกร กัลล์ประวิทธ์
    ภาควิชาชีวเคมี คณะแพทยศาสตร์ ศิริราชพยาบาล มหาวิทยาลัยมหิดล
18. อ. ดร. สราวุธ คำปวน
    คณะสหเวชศาสตร์ มหาวิทยาลัยนเรศวร
19. อ. ดร. ภก. ศุภโชค มั่งมูล
    คณะเภสัชศาสตร์ มหาวิทยาลัยมหิดล
20. อ. ดร. น.สพ. อนุศักดิ์ กิจถาวรรัตน์
    คณะสัตวแพทยศาสตร์ จุฬาลงกรณ์มหาวิทยาลัย
21. อ. ดร. สพ.ญ. สุนทรี เพ็ชรดี
    คณะสัตวแพทยศาสตร์ มหาวิทยาลัยเกษตรศาสตร์
22. อ. ดร. สุคนธา งามประมวญ
    ศูนย์วิจัยประสาทวิทยาศาสตร์, สถาบันวิทยาศาสตร์โมเลกุล
    มหาวิทยาลัยมหิดล
23. อ. ดร. น. สพ. เติมพงศ์ วงศ์ตะวัน
    คณะสัตวแพทยศาสตร์ มหาวิทยาลัยมหิดล

4.4 <u>การได้รับทุนอื่น ๆ จากทั้งในและต่างประเทศ</u>

1. ชื่อโครงการวิจัย: Effects of rosiglitazone on the cardiac mitochondrial function and molecular aspects of the cardioprotective effects in ischemic/reperfusion rat heart model. (PI)
   แหล่งทุน: National Research Council of Thailand
   จำนวนเงิน 879,400 บาท
   ช่วงของวัน เดือน ปี ที่ได้รับทุน: 10/2011-09/2012 รวมเวลา 1 ปี

2. ชื่อโครงการวิจัย: Mitochondrial calcium uniporter blocker prevents isolated brain mitochondrial dysfunctions caused by iron overload. (PI)
   แหล่งทุน: Faculty of Medicine Endowment Fund, Chiang Mai University
   จำนวนเงิน 200,000 บาท
   ช่วงของวัน เดือน ปี ที่ได้รับทุน: 03/2012-09/2013 รวมเวลา 1.6 ปี

3. ชื่อโครงการวิจัย: Effect of left vagal nerve stimulation on cardiac ischemic-reperfusion injury (PI)
   แหล่งทุน: บริษัท Cyberonics ประเทศสหรัฐอเมริกา
   จำนวนเงิน 3,708,750 บาท
   ช่วงของวัน เดือน ปี ที่ได้รับทุน: 10/2011-09/2012 รวมเวลา 1 ปี

4. ชื่อโครงการวิจัย: ผลของยาพีพีเออาร์แกมมาอะโกนิสต์)PPAR-gamma agonist) และเอสโตเจน ต่อภาวะการดื้อต่ออินซูลินของเซลล์สมองต่อการทำงานของไมโตคอนเดรียของเซลล์สมองในหนูที่กินอาหารไขมันสูงเป็นเวลานาน ๆ (Co-PI)
   แหล่งทุน: สำนักงานกองทุนสนับสนุนการวิจัย (สกว.)
   จำนวนเงิน. 1,500,000 บาท
   ช่วงของวัน เดือน ปี ที่ได้รับทุน: 05/2011-05/2014 รวมเวลา 3 ปี

5. ชื่อโครงการวิจัย: Effects of Anti-Diabetic Drugs: Vildagliptin in Rats with Neuronal Insulin Resistance Induced by 12- Week High Fat Diet Consumption. (Co-PI)
   แหล่งทุน: Faculty of Medicine Endowment Fund, Chiang Mai University
   จำนวนเงิน. 200,000 บาท
   ช่วงของวัน เดือน ปี ที่ได้รับทุน: 04/2012-10/2013 รวมเวลา 1 ปี

5. Output

Output:	ปี 2552-2553	ปี 2553-2554	ปี 2554-2555	จำนวนรวมทั้งหมด
1. ด้านงานวิจัย				
1.1 จำนวนผลงานตีพิมพ์ที่ list อยู่ใน pubmed	4	4	26	34
1.2 จำนวนผลงานวิจัยที่นำเสนอในระดับชาติ	5	2	15	22
1.3 จำนวนผลงานวิจัยที่นำเสนอในระดับนานาชาติ	4	2	14	20
1.4 รางวัลด้านการวิจัยที่ได้รับ				
➢ *รางวัลการนำเสนอผลงานวิจัยดีเด่นจากงานประชุมวิชาการประจำปีของสรีรวิทยาสมาคมแห่งประเทศไทย ครั้งที่ 39* ประจำปี พ.ศ. 2553	4			4
➢ *รางวัลการนำเสนอผลงานวิจัยดีเด่นจากงานวันมหิดล คณะแพทยศาสตร์ มหาวิทยาลัยเชียงใหม่ ประจำปี 2554*		1		1
➢ *The Travel Award Fellowship for ESC Working Group on Cardiovascular Pharmacology and Drug Therapy. Meeting of The Frontiers in CardioVascular Biology 2012*			1	1
➢ *รางวัลการนำเสนอผลงานวิจัยดีเด่นจากงานประชุมวิชาการประจำปีของสรีรวิทยาสมาคมแห่งประเทศไทย ครั้งที่ 41* ปี ประจำปี พ.ศ. 2555			2	2
➢ *รางวัลการนำเสนอผลงานวิจัยดีเด่นจากงานประชุมวิชาการ งานประชุมวิชาการโครงการปริญญาเอกกาญจนภิเษก ครั้งที่ 13 (RGJ-Ph.D. Congress XIII) ประจำปี* พ.ศ. 2555			3	3
➢ *รางวัลการนำเสนอผลงานวิจัยดีเด่น จาก*			2	2

งานประชุม The 1st ASEAN Plus Three Graduate Research Congress (AGRC 2012)				
1.5 จำนวนทุนวิจัยที่ได้รับสนับสนุนจากองค์กรอื่น	2	1	3	5
2. ด้านบริการวิชาการและการฝึกอบรม				
2.1 จำนวนการเป็นอาจารย์ที่ปรึกษาหรือผู้ทรงคุณวุฒิที่ปรึกษาด้านการวิจัยทุน สกว.	4	2	1	7
2.2 จำนวนนักวิจัยที่ได้รับการฝึกฝนด้านทักษะการวิจัยระดับสูง (Post-doc)	2	2	2	2
2.3 จำนวนการจัดประชุมวิชาการ / การฝึกอบรม	1	1	1	3
3. *ด้านการเรียนการสอน*				
3.1 จำนวนนักศึกษาระดับบัณฑิตศึกษาที่จบการศึกษา				
- ระดับปริญญาโท	1	1	3	5
- ระดับปริญญาเอก	-	1	1	2
3.2 การเป็นอาจารย์เพื่อวิทยานิพนธ์หลักของนักศึกษาระดับปริญญาโท	2	3	1	6
3.3 การเป็นอาจารย์เพื่อวิทยานิพนธ์หลักของนักศึกษาระดับปริญญาเอก	4	4	2	6

6. ภาคผนวก

ผลงานตีพิมพ์ในวารสารวิชาการนานาชาติ จำนวน 34 เรื่อง

1 Apaijai N, Pintana H, Chattipakorn SC, **Chattipakorn N**. Effects of metformin and vildagliptin on cardiac and mitochondrial function in high-fat diet-induced insulin resistant rats. *Endocrinology* 2012 (in press) (Impact Factor = 4.99)
(เอกสารแนบหมายเลข 1)

2 Wongcharoen W, Jai-aue S, Phrommintikul A, Nawarawong W, Woragidpoonpol S, Tepsuwan T, Sukonthasarn A, Apaijai N, **Chattipakorn N**. Effects of Curcuminoids on Frequency of Acute Myocardial Infarction After Coronary Artery Bypass Grafting. *Am J Cardiol* 2012 (in press) (Impact Factor = 3.680)
(เอกสารแนบหมายเลข 2)

3 Yarana C, Sripetchwandee J, Sanit J, Chattipakorn S, **Chattipakorn N**. Calcium-induced cardiac mitochondrial dysfunction is predominantly mediated by cyclosporine A-dependent mitochondrial permeability transition pore, but not mitochondrial calcium uniporter. *Arch Med Res* 2012 (in press) (Impact factor = 1.986)
(เอกสารแนบหมายเลข 3)

4 Yarana C, Sanit J, **Chattipakorn N**, Chattipakorn S. Synaptic and nonsynaptic mitochondria demonstrate a different degree of calcium-induced mitochondrial dysfunction. *Life Sci* 2012;90:808-814. (Impact Factor = 2.56)
(เอกสารแนบหมายเลข 4)

5 Kumfu S, Chattipakorn S, Chinda K, Fucharoen S, **Chattipakorn N**. T-type calcium channel blockade improves survival and cardiovascular function in thalassemic mice. *Eur J Haematol* 2012;88:535-548. (Impact Factor = 2.785)
(เอกสารแนบหมายเลข 5)

6 Chinda K, Palee S, Surinkaew S, Phornphutkul M, Chattipakorn S, **Chattipakorn N**. Cardioprotective effect of dipeptidyl peptidase-4 inhibitor during ischemia–reperfusion injury. *Int J Cardiol* 2012 (in press) (Impact Factor = 6.802)
(เอกสารแนบหมายเลข 6)

7 Khumpune S, Chattipakorn S, **Chattipakorn N**. Role of p38 inhibition on cardiac ischemia/reperfusion injury. *Eur J Clin Pharmacol* 2012 (in press) (Impact Factor = 3.088)
(เอกสารแนบหมายเลข 7)

8 Suwanchai A, Theerapiboon U, **Chattipakorn N**, Chattipakorn S. $Na_V1.8$, but not $Na_V1.9$, is up-regulated in the inflamed dental pulp tissue of human primary teeth. *Int Endod J* 2012;45(4):372-8. (Impact Factor = 2.383)
(เอกสารแนบหมายเลข 8)

9 Chinda K, Chattipakorn S, **Chattipakorn N**. Cardioprotective effects of incretin during ischemia-reperfusion. *Diabetes Vasc Dis Res* 2012 (in press) (Impact factor = 2.468)
(เอกสารแนบหมายเลข 9)

10 Weerateerangkul P, Surinkaew S, Chattipakorn S, **Chattipakorn N**. Effects of *Kaempferia parviflora* Wall. Ex. Baker on electrophysiology of the swine hearts. *Indian J Med Res* 2012 (in press) (Impact Factor = 1.826)
(เอกสารแนบหมายเลข 10)

11 Pramojanee S, Pratchayasakul W, **Chattipakorn N**, Chattipakorn S. Low dose dental radiation decreases oxidative stress in osteoblastic cells. *Arch Oral Biol* 2012;57(3):252-6. (Impact Factor = 1.463)
(เอกสารแนบหมายเลข 11)

12 Pipatpiboon N, Pratchayasakul W, **Chattipakorn N**, Chattipakorn S. PPARγ agonist improves neuronal insulin receptor function in hippocampus and
brain mitochondria function in rats with insulin resistance induced by long term high-fat diets. *Endocrinology* 2011;153(1):329-338. (Impact Factor = 4.99)
(เอกสารแนบหมายเลข12)

13 Silvilairat S, Wongsathikun J, Sittiwangkul R, Pongprot Y, **Chattipakorn N**. Heart rate variability and exercise capacity in patients with repaired Tetralogy of Fallot. *Pediatr Cardiol* 2011;32(8):1158-1163. (Impact Factor = 1.151)
(เอกสารแนบหมายเลข 13)

14 Suwanchai A, Theerapiboon U, **Chattipakorn N**, Chattipakorn S. Expression of sodium channels in dental pulp. *Asian Biomed* 2011;5(6):735-746. (Impact Factor = 0.333)
(เอกสารแนบหมายเลข 14)

15 Pratchayasakul W, **Chattipakorn N**, Chattipakorn S. Effects of estrogen in preventing neuronal insulin resistance in hippocampus of obese rats are different between genders. *Life Sci* 2011;89(19-20):702-707. (Impact Factor = 2.56)
(เอกสารแนบหมายเลข 15)

16 Silvilairat S, Wongsathikun J, Sittiwangkul R, Pongprot Y, **Chattipakorn N**. Effects of left ventricular function on the exercise capacity in patients with repaired tetralogy of fallot. *Echocardiography* 2011;28(9):1019-1024. (Impact Factor = 1.444)
(เอกสารแนบหมายเลข 16)

17 Chattipakorn S, Ittichaicharoen J, Rangdaeng S, **Chattipakorn N**. Changes in peripheral innervations and nociception in reticular type and erosive type of oral lichen planus. *Indian J Dent Res* 2011;22:678-683. (Impact factor = 0.4)
(เอกสารแนบหมายเลข 17)

18 Palee S, Weerateerangkul P, Surinkeaw S, Chattipakorn S, **Chattipakorn N**. Effect of rosiglitazone on cardiac electrophysiology, infarct size and mitochondrial function in ischemia and reperfusion of swine and rat heart. *Exp Physiol* 2011;96(8):778-789. (Impact Factor = 3.333)
(เอกสารแนบหมายเลข 18)

19 Thummasorn S, Kumfu S, Chattipakorn S, **Chattipakorn N**. Granulocyte-colony stimulating factor attenuates mitochondrial dysfunction induced by oxidative stress in cardiac mitochondria. *Mitochondrion* 2011;11(3):457-466. (Impact Factor = 4.145)
(เอกสารแนบหมายเลข 19)

20 Kanlop N, Thommasorn S, Palee S, Weerateerangkul P, Suwansirikul S, Chattipakorn S, **Chattipakorn N**. G-CSF stabilizes cardiac electrophysiology and

decreases infarct size during cardiac ischemic/reperfusion in swine. *Acta Physiol* 2011;202(1):11-20. (Impact Factor = 2.81)
(เอกสารแนบหมายเลข 20)

21 Pratchayasakul W, Kerdphoo S, Petsophonsakul P, Pongchaidacha A, **Chattipakorn N**, Chattipakorn S. Effects of high-fat diet on insulin receptor function in rat hippocampus and the level of neuronal corticosterone. *Life Sci* 2011;88(13-14):619-627. (Impact Factor = 2.56)
(เอกสารแนบหมายเลข 21)

22 Surinkaew S, Chattipakorn S, **Chattipakorn N**. Roles of mitochondrial benzodiazepine receptor in the heart. *Can J Cardiol* 2011;27:262.e3-262.e13. (Impact Factor = 1.796)
(เอกสารแนบหมายเลข 22)

23 Weerateerangkul P, Chattipakorn S, **Chattipakorn N**. Roles of nitric oxide signaling pathway in cardiac ischemic preconditioning against myocardial ischemia-reperfusion injury. *Med Sci Monit* 2011;17(2):RA44-52. (Impact Factor = 1.514)
(เอกสารแนบหมายเลข 23)

24 Kanlop N, Chattipakorn S, **Chattipakorn N**. Effects of cilostazol in the heart. *J Cardiovasc Med* 2011;12(2):88-95. (Impact factor = 0.712)
(เอกสารแนบหมายเลข 24)

25 Palee S, Chattipakorn S, Phrommintikul A, **Chattipakorn N**. PPARγ gamma activator, rosiglitazone: Is it beneficial or harmful to the cardiovascular system? *World J Cardiol* 2011;3(5):144-152. (Impact Factor = N/A)
(เอกสารแนบหมายเลข 25)

26 **Chattipakorn N**, Kumfu S, Fucharoen S, Chattipakorn S. Calcium channels and iron uptake into the heart. *World J Cardiol* 2011;3(7):215-218. (Impact Factor = N/A)
(เอกสารแนบหมายเลข 26)

27 Kumfu S, Chattipakorn S, Srichairattanakool S, Settakorn J, Fucharoen S, **Chattipakorn N**. T-type calcium channel as a portal of iron uptake into cardiomyocytes of beta-thalassemic mice. *Eur J Haematol* 2010;86:156-166. (Impact Factor = 2.785)
(เอกสารแนบหมายเลข 27)

28 Phrommintikul A, Sivasinprasasn S, Lailerd N, Chattipakorn S, Kuanprasert S, **Chattipakorn N**. Plasma urocortin in acute myocardial infarction patients. *Eur J Clin Invest* 2010;40(10):874-882. (Impact Factor = 2.736)
(เอกสารแนบหมายเลข 28)

29 Kanlop N, Shinlapawittayatorn K, Sungnoon R, Weerateerangkul P, Chattipakorn S, **Chattipakorn N**. Cilostazol attenuates ventricular arrhythmia induction and improves defibrillation efficacy in swine. *Can J Physiol Pharmacol* 2010;88:422-428. (Impact Factor = 1.849)
(เอกสารแนบหมายเลข 29)

30 Pratchayasakul W, Pongchaidecha A**, Chattipakorn N**, Chattipakorn S. Reversible acetylcholinesterase inhibitory effect of *Tabernaemontana divaricata* extract on synaptic transmission in rat CA1 hippocampus. *Indian J Med Res* 2010;131:411-417. (Impact Factor = 1.826)
(เอกสารแนบหมายเลข 30)

31 Rutjanaprom W, Kanlop N, Charoenkwan P, Sittiwangkul R, Srichairattanakool S, Tantiworawit A, Phrommintikul A, Chattipakorn S, Fucharoen S, **Chattipakorn N**. Heart rate variability in beta-thalassemia patients. *Eur J Haematol* 2009;83:483-489. (Impact Factor = 2.785)
(เอกสารแนบหมายเลข 31)

32 **Chattipakorn N**, Settakorn J, Petsophonsakul P, Suwannahoi P, Mahakranukraugh P, Srichairattanakool S, Chattipakorn S. Cardiac mortality is associated with low levels of omega-3 and omega-6 fatty acids in the heart of cadavers with history of coronary heart disease. *Nutr Res* 2009;29:696-704. (Impact Factor = 2.092)
(เอกสารแนบหมายเลข 32)

33 Pongchaidecha A, Lailerd N, Boonprasert W, **Chattipakorn N**. Effects of curcuminoids supplement on cardiac autonomic status in high-fat-induced obese rats. *Nutrition* 2009;25:870-878. (Impact Factor = 2.726)
(เอกสารแนบหมายเลข 33)

34 Pratchayasakul W, Pongruangporn M, **Chattipakorn N**, Chattipakorn S. Roles of curcumin in preventing pathogenesis of Alzheimer's disease. *Curr Top Nutraceut Res* 2009;7:11-26. (Impact Factor = 0.238)
(เอกสารแนบหมายเลข 34)

ข้อมูลและประวัติย่อของผู้ได้รับทุนวิจัยระดับปริญญาโท/เอก จากโครงการ

ระดับปริญญาโท

1. น.ส. สาวิตรี ธรรมสอน	สาขาวิชาสรีรวิทยา (จบการศึกษาปี 2554)
2. น.ส. อนงค์ภรณ์ ขอบรูป	สาขาวิชาสรีรวิทยา (จบการศึกษาปี 2555)
3. น.ส. ณัฐยาภรณ์ อภัยใจ	สาขาวิชาสรีรวิทยา (จบการศึกษาปี 2555)
4. น.ส. หิรัญญา ปินตานา	สาขาวิชาสรีรวิทยา (จบการศึกษาปี 2555)
5. นายฤารัฐ สุภากุล	สาขาวิชาสรีรวิทยา
6. น.ส. เพียงขวัญ สงวนหมู่	สาขาวิชาสรีรวิทยา
7. น.ส. กิตติยา ทุ่นสิริ	สาขาวิศวกรรมชีวการแพทย์

ระดับปริญญาเอก

1. น.ส. วาสนา ปรัชญาสกุล	สาขาวิชาสรีรวิทยา (จบการศึกษาปี 2554)
2. นายภูเนตร วีรธีรางกูร	สาขาวิชาสรีรวิทยา (จบการศึกษาปี 2555)
3. น.ส. ศิรินาฏ คำฟู	สาขาวิชาสรีรวิทยา
4. น.ส. ศิริรัตน์ สุรินทร์แก้ว	สาขาวิชาสรีรวิทยา
5. น.ส. นพมาศ พิพัฒน์พิบูลย์	สาขาวิชาสรีรวิทยา
6. นายศิริพงษ์ ปาลี	สาขาวิชาสรีรวิทยา
7. น. สพ. เกริกเกียรติ จินดา	สาขาวิชาสรีรวิทยา
8. ภก. จิรภาส ศรีเพชรวรรณดี	สาขาวิชาสรีรวิทยา

9. น.สพ. วันพิทักษ์ ป้องกัน สาขาวิชาสรีรวิทยา
10. น.ส. ศิวภรณ์ ศิวศิลป์ประสานต์ สาขาวิชาสรีรวิทยา
11. ทพญ. สการัตห์ ประโมจนีย์ สาขาชีววิทยาช่องปาก

ลงนาม.....
(ศ. ดร. นพ. นิพนธ์ ฉัตรทิพากร)
หัวหน้าโครงการผู้รับทุน

Endocrinology. First published ahead of print May 23, 2012 as doi:10.1210/en.2012-1262

Cardioprotective Effects of Metformin and Vildagliptin in Adult Rats with Insulin Resistance Induced by a High-Fat Diet

Nattayaporn Apaijai, Hiranya Pintana, Siriporn C. Chattipakorn, and Nipon Chattipakorn

Cardiac Electrophysiology Research and Training Center (N.A., H.P., S.C.C., N.C.), Faculty of Medicine; Faculty of Dentistry (S.C.C.); and Biomedical Engineering Center (N.C.), Chiang Mai University, Chiang Mai, 50200, Thailand

Insulin resistance has been shown to be associated with cardiac sympathovagal imbalance, myocardial dysfunction, and cardiac mitochondrial dysfunction. Whereas metformin is a widely used antidiabetic drug to improve insulin resistance, vildagliptin is a novel oral antidiabetic drug in a group of dipeptidyl peptidase-4 inhibitors in which its cardiac effect is unclear. This study aimed to determine the cardiovascular effects of metformin and vildagliptin in rats with insulin resistance induced by high-fat diet. Male Wistar rats were fed with either a normal diet or high-fat diet (n = 24 each) for 12 wk. Rats in each group were divided into three subgroups to receive the vehicle, metformin (30 mg/kg, twice daily), or vildagliptin (3 mg/kg, once daily) for another 21 d. Heart rate variability (HRV), cardiac function, and cardiac mitochondrial function were determined and compared among these treatment groups. Rats exposed to a high-fat diet developed increased body weight, visceral fat, plasma insulin, cholesterol, oxidative stress, depressed HRV, and cardiac mitochondrial dysfunction. Metformin and vildagliptin did not alter body weight and plasma glucose levels but decreased the plasma insulin, total cholesterol, and oxidative stress levels. Although both metformin and vildagliptin attenuated the depressed HRV, cardiac dysfunction, and cardiac mitochondrial dysfunction, vildagliptin was more effective in this prevention. Furthermore, only vildagliptin prevented cardiac mitochondrial membrane depolarization caused by consumption of a high-fat diet. We concluded that vildagliptin is more effective in preventing cardiac sympathovagal imbalance and cardiac dysfunction, as well as cardiac mitochondrial dysfunction, than metformin in rats with insulin resistance induced by high-fat diet. **(*Endocrinology* 153: 0000–0000, 2012)**

Ingestion of food laden with animal fat is the major cause of obesity and can lead to an insulin-resistant condition, a state in which insulin receptor function is impaired, and is characterized by hyperinsulinemia with euglycemia (1–3). It has been shown previously that insulin resistance was associated with impaired cardiac function (4). In rats with insulin resistance induced by a high-fat diet, systolic and diastolic dysfunction (5), as well as cardiac sympathovagal imbalance indicated by depressed heart rate variability (HRV) (6). was also reported. In the past decades, several drugs used to improve insulin sensitivity have been shown to cause serious adverse cardiac effects (7, 8). Therefore, drugs with effective glycemic control and without harmful effects to the heart are needed for use in diabetic patients.

Metformin is an oral antidiabetic drug that has been used for decades to reduce plasma glucose, improve insulin sensitivity, increase peripheral glucose uptake, and inhibit hepatic glucose production (9). Previous studies reported that metformin could improve cardiac performance in diabetic rats (10, 11). Furthermore, metformin also improved cardiac mitochondrial respiration and increased ATP synthesis in a rat model of heart failure (12). Despite these beneficial

ISSN Print 0013-7227 ISSN Online 1945-7170
Printed in U.S.A.

doi: 10.1210/en.2012-1262 Received March 5, 2012. Accepted May 4, 2012.

Abbreviations: ECG, Electrocardiogram; EDP, end diastolic pressure; ESP, end systolic pressure; HF, high frequency; HOMA, Homeostasis Model Assessment; HR, heart rate; HRV, heart rate variation; JC-1, 5,5′,6,6′-tetrachloro-1,1′,3,3′-tetra ethylbenzimidazolcarbocyanine iodide; LF, low frequency; MDA, malondialdehyde; ROS, reactive oxygen species; SV, stroke volume; TBA, thiobarbituric acid.

effects, the cardioprotective effect of metformin in rats with insulin resistance induced by high-fat diet remains unknown.

Vildagliptin is a novel oral antidiabetic drug that inhibits the action of the dipeptidyl peptidase-4 enzyme, resulting in an increased level of glucagon-like peptide 1. Glucagon-like peptide 1 is an incretin hormone released from intestinal L-cells that causes an increased insulin secretion, decreased glucagon secretion, and improved insulin sensitivity and has been shown to exert direct cardiovascular effects in both experimental and clinical studies with or without insulin resistance (13, 14). Although the glycemic control effects of dipeptidyl peptidase-4 inhibitor have been extensively studied, the roles of vildagliptin on the heart are still unclear (15, 16). Furthermore, the effects of vildagliptin on the heart of rats with insulin resistance induced by high-fat diet are unknown.

The present study investigated the effects of metformin and vildagliptin on the heart of rats with insulin resistance induced by a high-fat diet. Because high-fat diet-induced insulin-resistant rats are known to have depressed HRV (6) and mitochondrial and cardiac dysfunction (17), we hypothesized that metformin and vildagliptin can improve the insulin-resistant condition, preserve cardiac sympathovagal balance, improve cardiac function, and prevent cardiac mitochondrial dysfunction in rats with insulin resistance induced by high-fat diet.

Materials and Methods

Animals and diet

All experiments were conducted in accordance with an approved protocol from the Faculty of Medicine, Chiang Mai University Institutional Animal Care and Use Committee, in compliance with National Institutes of Health guidelines. Male Wistar rats weighing 180–200 g. were obtained from the National Animal Center, Salaya Campus, Mahidol University, Thailand. Rats were housed in a temperature control with a 12-h dark, 12-h light cycle. After 7 d of acclimatization, the rats were divided into two groups to receive either a normal diet or a high-fat diet (n = 24/group). In the normal diet group, rats were fed with standard laboratory chow that contained 19.77% energy from fat, whereas rats in the high-fat diet group were fed with a diet containing 59.28% energy from fat for 12 wk (3). Then, rats in each diet group were divided into three treatment groups (n = 8/group). The first group received 15-mg/kg metformin (Glucophage, Merck Serono, Bangkok, Thailand) twice daily (18). The second group received 3 mg/kg vildagliptin (Gulvus, Novartis, Bangkok, Thailand) once daily (19). The third group (*i.e.* control group) received normal saline in an equal volume. All rats were treated by intragastric gavage for 21 d. The body weight was recorded weekly. Blood samples were collected from the tail vein at week zero, wk 12, and at the end of 21-d treatment. The plasma was separated and stored at −85 C until use. Heart rate variability (HRV) analysis was performed at week zero, wk 4, wk 8, wk 12, and at the end of a 21-d treatment. After being treated with either drugs or saline for 21 d, rats were anesthetized, and the cardiac function was determined using the pressure-volume catheter (Scisense, London, Ontario, Canada) (20). At the end of the study, the heart was rapidly removed and myocardial tissues were used to determine the cardiac malondialdehyde (MDA) level and cardiac mitochondrial function.

Plasma glucose, cholesterol, and insulin level determination

Plasma glucose and total cholesterol levels were measured by colorimetric assay using a commercial kit (Biotech, Bangkok, Thailand) (2). Plasma insulin levels were measured by a sandwich ELISA kit (Linco Research, St. Charles, MO) (2, 3). Insulin resistance was assessed by Homeostasis Model Assessment (HOMA) as a mathematical model describing the degree of insulin resistance, calculated from fasting plasma insulin and fasting plasma glucose concentration. A higher HOMA index indicates a higher degree of insulin resistance (2).

Plasma and cardiac MDA level determination

Plasma and cardiac MDA levels were measured using HPLC based assay (21). Cardiac tissue was homogenized in phosphate buffer, pH 2.8. Plasma and cardiac tissue were mixed with H_3PO_4 and thiobarbituric acid (TBA) to create TBA-reactive substances. The plasma and cardiac TBA-reactive substances concentration was determined directly from a standard curve and reported as MDA equivalent concentration (22).

Heart rate variability (HRV) analysis

The electrocardiogram (ECG) lead II was recorded in each rat using a PowerLab (ADInstruments, Sydney, Australia) and a Chart 5.0 program (6). During ECG recording, rats were placed in a restraint and prohibited from movement (6, 23, 24). The high frequency (HF, 0.6–3 Hz) component representing cardiac parasympathetic activity and low frequency (LF, 0.2–0.6 Hz) component representing cardiac sympathetic and parasympathetic activity were determined using a MATLAB program (6). The LF/HF ratio was considered as an indicator of cardiac sympathetic/parasympathetic tone balance (25). Increased LF/HF ratio (*i.e.* depressed HRV) indicates the cardiac sympathovagal imbalance (23).

Cardiac function measurement

Rats were anesthetized with Zoletil (50 mg/kg, Vibbac Laboratories, Carros, France) and Xylazine (0.15 mg/kg, LaboratoriosCalier, S.A., Barcelona, Spain) im injection after which ventral midline incision of the neck was performed for tracheostomy, and rats were ventilated with room air. The right carotid artery was identified, and a pressure-volume loop catheter was inserted into the carotid artery and advanced into the left ventricle. Rats were stabilized for 5 min, after which the pressure-volume (P-V) loop (Scisense, Ontario, Canada) was recorded for 20 min. Cardiac function parameters including heart rate, end-systolic and end-diastolic pressure, maximum and minimum dP/dt, and stroke volume were determined using the analytical software program (Labscribe, Dover, NH).

TABLE 1. Metabolic parameters of normal diet-fed and high-fat diet-fed rats at baseline and wk 12

Metabolic parameters	Baseline		Wk 12	
	ND	HF	ND	HF
Body weight (g)	191 ± 10	192 ± 9	462 ± 6[a]	567 ± 13[a,b]
Food intake (g)	21 ± 1	20 ± 5	27 ± 3	24 ± 1
Plasma insulin (ng/ml)	2.15 ± 0.29	2.14 ± 0.26	2.19 ± 0.19	3.50 ± 0.50[a,b]
Plasma glucose (mg/dl)	131.69 ± 8.79	140.11 ± 7.52	138.00 ± 9.95	139.08 ± 4.46
HOMA index	16.80 ± 2.26	16.76 ± 2.03	17.95 ± 1.56	24.26 ± 4.65[a,b]
Plasma total cholesterol (mg/dl)	82.75 ± 5.63	83.15 ± 7.48	83.07 ± 7.14	132.18 ± 8.72[a,b]
Plasma MDA (μmol/ml)	2.28 ± 0.10	2.13 ± 0.03	2.77 ± 0.19	6.79 ± 0.07[a,b]

ND, Normal diet; HF, high-fat diet.

[a], $P < 0.05$ *vs.* baseline; [b], $P < 0.05$ *vs.* ND wk 12.

Cardiac mitochondrial isolation and mitochondrial function determination

Cardiac mitochondrial isolation was performed as previously described (26). In brief, the heart of each rat was perfused with normal saline solution and removed rapidly after which the heart was minced and homogenized in ice-cold buffer containing sucrose (300 mmol/liter), N-(Tris(hydroxymethyl)methyl)-2-aminoethanesulfonic acid sodium salt (5 mmol/liter), and EGTA (0.2 mmol/liter). Then, the homogenates were centrifuged at 800 × *g* for 5 min, and a supernatant was collected and centrifuged at 8800 × *g* for 5 min. Protein concentration was determined using the bicinchoninic acid assay (26). In the present study, cardiac mitochondrial function was determined by measuring the mitochondrial reactive oxygen species (ROS) production, mitochondrial membrane potential changes, and mitochondrial swelling (26).

To determine cardiac mitochondrial ROS production, cardiac mitochondria were incubated with 2 μM DCFH-DA dye at 25 C for 20 min. ROS production was detected by fluorescent microplate reader with $\lambda_{emission}$ at 485 nm and $\lambda_{excitation}$ at 530 nm (BioTek,Winooski, VT) (26). To determine cardiac mitochondrial membrane potential changes, cardiac mitochondria were incubated with 5 μM 5,5′,6,6′-tetrachloro-1,1′,3,3′-tetra ethylbenzimidazolcarbocyanine iodide (JC-1) dye at 37 C for 30 min. Mitochondrial membrane potential changes were measured by fluorescent microplate reader. JC-1 monomer form (green fluorescent) was detected with $\lambda_{emission}$ at 485 nm and $\lambda_{excitation}$ at 590 nm. JC-1 aggregate form (red fluorescent) was detected with $\lambda_{emission}$ at 485 nm and $\lambda_{excitation}$ at 530 nm. Mitochondrial membrane potential changes were calculated as the red/green fluorescent intensity ratio (26). Decreased red/green fluorescent intensity ratio indicated cardiac mitochondrial membrane depolarization (26).

To determine cardiac mitochondrial swelling, cardiac mitochondria were incubated with 1.5 mM respiration buffer containing 100 mM KCl, 10 mM HEPES, 5 mM KH_2PO_4, and the absorbance was measured using a spectrophotometer. Mitochondrial swelling was indicated when the absorbance of the suspension decreased (26).

Statistical analysis

All data were expressed as mean ± SE. One-way ANOVA followed by LSD *post hoc* test was used to determine the difference between groups. $P < 0.05$ was considered statistically significant.

Results

Effects of high-fat diet consumption, metformin, and vildagliptin on metabolic parameters

At the baseline, the body weight, food intake, plasma glucose, insulin, total cholesterol, and MDA level did not differ between the normal diet and the high-fat diet groups (Table 1). After 12 wk of high-fat diet consumption, rats in this group had increased body weight and plasma cholesterol. High-fat diet-fed rats also developed insulin resistance that was characterized by an increased plasma insulin level without an alteration in the plasma glucose level, and an increase in the HOMA index. The plasma MDA level, which is an index of oxidative stress, was also increased in the high-fat group (Table 1). Unlike the high-fat fed rats, rats fed with a normal diet had no change in those metabolic parameters, except the increased body weight (Table 1).

After 21 d of metformin and vildagliptin treatment in normal diet-fed rats, the metabolic parameters including body weight, food intake, visceral fat, plasma insulin, glucose, cholesterol, MDA, cardiac MDA level, and HOMA index were not different from the vehicle-treated rats (Table 2). In high-fat-fed rats, metformin and vildagliptin could significantly decrease the plasma insulin, HOMA index, plasma cholesterol, plasma MDA, and cardiac MDA levels, compared with the vehicle-treated rats in the high-fat-fed group. Metformin and vildagliptin did not alter the body weight, food intake, visceral fat, and plasma glucose, compared with the vehicle-treated rats in the high-fat diet group (Table 2).

Effects of high-fat diet consumption, metformin, and vildagliptin on HRV

At the baseline, the LF/HF ratio was not different between the normal diet and high-fat diet groups (Fig. 1). High-fat diet consumption caused an increased LF/HF ratio beginning at wk 8 and was markedly different at wk 12 (Fig. 1). After 21 d of treatment with metformin and vilda-

TABLE 2. Effects of metformin and vildagliptin on metabolic parameters in normal diet and high-fat diet rats

Metabolic parameters	NDV	NDM	NDVil	HFV	HFM	HFVil
Body weight (g)	464 ± 8	440 ± 17	448 ± 11	544 ± 14[a]	534 ± 5[a]	564 ± 11[a]
Food intake (g)	22 ± 1	21 ± 2	22 ± 2	22 ± 2	22 ± 2	23 ± 2
Visceral fat (g)	25.86 ± 2.37	21.93 ± 3.46	24.12 ± 2.25	54.12 ± 3.17[a]	49.20 ± 5.28[a]	50.34 ± 4.87[a]
Plasma insulin (ng/ml)	2.73 ± 0.30	2.22 ± 0.58	2.4 ± 0.67	3.87 ± 0.5[a]	2.69 ± 0.57[b]	2.93 ± 0.63[b]
Plasma glucose (mg/dl)	140.83 ± 4.94	137.72 ± 7.52	131.69 ± 8.79	143.11 ± 7.52	138.00 ± 9.95	139.08 ± 4.46
HOMA index	16.17 ± 8.12	13.58 ± 8.1	14.05 ± 5.89	25.82 ± 3.76[a]	16.50 ± 5.67	17.11 ± 2.81
Plasma total cholesterol (mg/dl)	83.41 ± 5.55	83.43 ± 5.47	81.31 ± 6.90	160.86 ± 6.5[a]	105.6 ± 5.60[b]	103.47 ± 3.52[b]
Plasma MDA (μmol/ml)	2.47 ± 0.13	2.62 ± 0.16	2.74 ± 0.06	7.08 ± 0.12[a]	6.48 ± 0.18[a,b]	6.41 ± 0.19[a,b]
Cardiac MDA (μmol/mg protein)	5.39 ± 1.89	5.51 ± 1.22	5.47 ± 2.46	11.44 ± 2.15[a]	7.05 ± 1.27[a,b]	7.80 ± 1.43[a,b]

NDV, Normal diet + vehicle; NDM, normal diet + metformin; NDVil, normal diet + vildagliptin; HFV, high-fat diet + vehicle; HFM, high-fat diet + metformin; and HFVil, high-fat diet + vildagliptin.

[a], $P < 0.05$ *vs*. NDV; [b], $P < 0.05$ *vs*. HFV.

gliptin in the high-fat diet group, a significantly decreased LF/HF ratio could be seen, compared with the vehicle-treated group (Fig. 2). Although both metformin and vildagliptin could decrease the LF/HF ratio, it was vildagliptin that brought the ratio back to the baseline level (Fig. 2).

Effects of high-fat diet consumption, metformin, and vildagliptin on cardiac function

In the normal-diet group, cardiac function parameters, including heart rate (HR), end systolic pressure (ESP), end diastolic pressure (EDP), +dP/dt, −dP/dt, and stroke volume (SV) were not different among the vehicle-, metformin-, and vildagliptin-treated rats (Table 3). In high-fat diet-fed rats treated with the vehicle, heart rate (HR), EDP, and −dP/dt were increased, whereas the ESP, +dP/dt, and SV were decreased, compared with the normal-diet group. In high-fat diet rats treated with metformin and vildagliptin, the EDP and −dP/dt were decreased, whereas the ESP, +dP/dt, and SV were increased, compared with the vehicle-treated rats fed with high-fat diet. However, only vildagliptin could restore EDP, whereas metformin could only partially improve the EDP in these high-fat diet rats. Furthermore, decreased HR was observed only in the vildagliptin-treated rats in the high-fat diet group. Metformin did not decrease the HR in these high-fat fed rats (Table 3).

Effects of high-fat diet consumption, metformin, and vildagliptin on cardiac mitochondrial function

Cardiac mitochondrial ROS production

In normal diet-fed rats treated with metformin and vildagliptin, the levels of ROS production were not different from those of the vehicle-treated rats (Fig. 3). How-

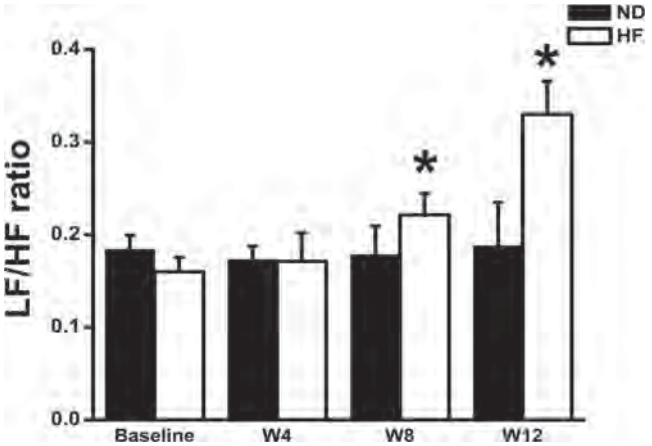

FIG. 1. LF/HF ratio in normal diet fed- and high-fat diet-fed rats. LF/HF ratio significantly increased during wk 8 (W8) of high-fat diet consumption, compared with baseline. *, $P < 0.05$ *vs.* baseline. ND, normal diet; HF, high-fat diet; *black bar*, ND; *white bar*, HF.

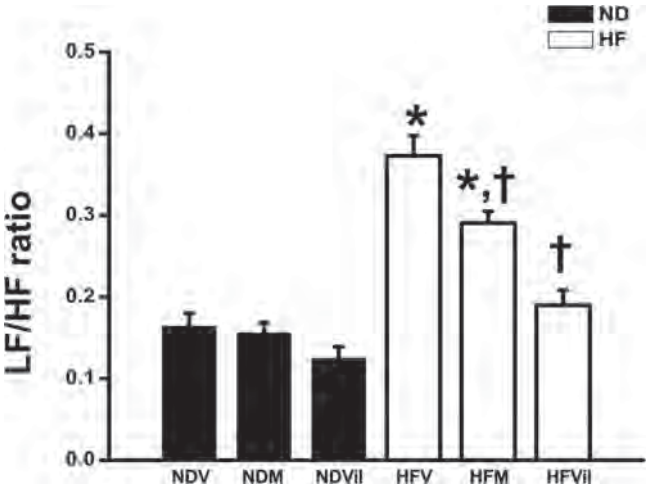

FIG. 2. LF/HF ratio in normal diet and high-fat diet rats treated with vehicle, metformin, and vildagliptin. Vildagliptin completely preserved cardiac sympathovagal imbalance, compared with vehicle. *, $P < 0.05$ *vs.* NDV, †, $P < 0.05$ *vs.* HFV. NDV, normal diet + vehicle; NDM, normal diet + metformin; NDVil, normal diet + Vildagliptin; HFV, high-fat diet + vehicle; HFM, high-fat diet + metformin; and HFVil, high-fat diet + vildagliptin; *black bar*, ND; *white bar*, HF.

TABLE 3. Effects of metformin and vildagliptin on cardiac function in normal diet and high-fat diet rats

Cardiac function	NDV	NDM	NDVil	HFV	HFM	HFVil
HR (beats/min)	327 ± 27	306 ± 24	331 ± 30	416 ± 13[a]	400 ± 18[b]	347 ± 27[c]
SBP (mm Hg)	130 ± 1	130 ± 1	130 ± 2	133 ± 1	132 ± 3	131 ± 2
DBP (mm Hg)	106 ± 1	106 ± 1	107 ± 2	110 ± 1	110 ± 3	108 ± 2
ESP (mm Hg)	131 ± 7	138 ± 7	137 ± 4	117 ± 15[a]	126 ± 3[c]	131 ± 11[c]
EDP (mm Hg)	17 ± 1	16 ± 1	16 ± 1	37 ± 2[a]	24 ± 4[b,c]	21 ± 4[c]
+dP/dt (mm Hg/sec)	8829 ± 401	8622 ± 128	8760 ± 231	6896 ± 277[a]	8077 ± 334[b,c]	8092 ± 282[c,d]
−dP/dt (mm Hg/sec)	−5532 ± 316	−6654 ± 683	−5751 ± 101	−3940 ± 499[a]	−5511 ± 556[b,c]	−5666 ± 858[c]
SV (μl/g)	1.04 ± 0.03	1.04 ± 0.03	1.02 ± 0.07	0.81 ± 0.06[a]	0.96 ± 0.04[c]	0.98 ± 0.05[c]

NDV, Normal diet + vehicle; NDM, normal diet + metformin; NDVil, normal diet + vildagliptin; HFV, high-fat diet + vehicle; HFM, high-fat diet + metformin; and HFVil, high-fat diet + vildagliptin; DBP, diastolic blood pressure; SBP, systolic blood pressure.
[a], $P < 0.05$ *vs.* NDV; [b], $P < 0.05$ *vs.* NDM; [c], $P < 0.05$ *vs.* HFV; [d], $P < 0.05$ *vs.* NDVil.

ever, the ROS level was significantly increased in the high-fat diet-fed rats treated with vehicle. Both metformin and vildagliptin could decrease the ROS level, compared with the vehicle-treated high-fat diet-fed rats. However, ROS reduction in the vildagliptin-treated group was greater than that in the metformin-treated group and was not different from that in the normal-diet group (Fig. 3).

Cardiac mitochondrial membrane potential changes (Δψm)

Similar to the ROS level, the vehicle-treated rats in the high-fat diet group had mitochondrial depolarization as indicated by a decreased red/green fluorescent intensity ratio, compared with the vehicle-treated rats in the normal-diet group (Fig. 4). Both metformin and vildagliptin could attenuate the cardiac mitochondrial depolarization in high-fat diet-fed rats, compared with the vehicle-treated rats of the high-fat diet group. However, only vildagliptin could completely prevent cardiac mitochondrial depolarization in the high-fat diet-fed rats (Fig. 4).

Cardiac mitochondrial swelling

In the normal-diet group, no cardiac mitochondrial swelling was observed in all treated groups (Fig. 5). In high-fat diet-fed rats treated with the vehicle, the absorbance was significantly decreased indicating cardiac mitochondrial swelling. After treatment with metformin or vildagliptin for 21 d, no cardiac mitochondrial swelling was observed in either treatment group (Fig. 5).

Discussion

The major findings of this study are as follows. First, metformin and vildagliptin improved the metabolic parameters of the insulin-resistant condition and oxidative stress

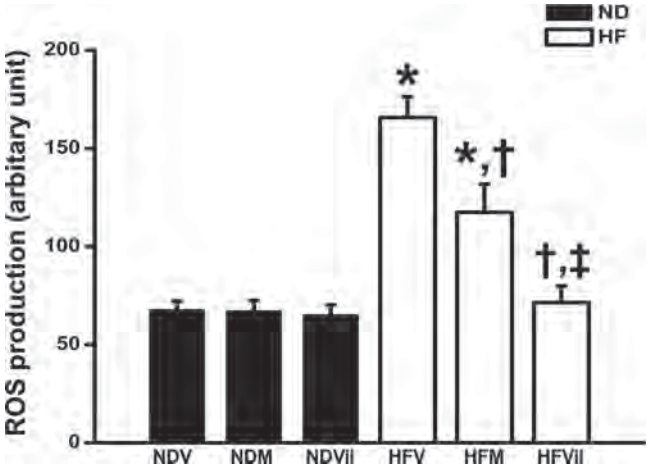

FIG. 3. Cardiac mitochondrial ROS production of normal diet and high-fat diet rats treated with vehicle, metformin, and vildagliptin. Vildagliptin markedly reduced ROS production, compared with vehicle and high-fat diet rats treated with metformin. *, $P < 0.05$ *vs.* NDV; †, $P < 0.05$ *vs.* HFV; ‡, $P < 0.05$ *vs.* HFM. *ROS*= Reactive oxygen species; NDV, Normal diet + vehicle; NDM, normal diet + metformin; NDVil, normal diet + vildagliptin; HFV, high-fat diet + vehicle; HFM, high-fat diet + metformin; and HFVil, high-fat diet + vildagliptin; *black bar*, ND; *white bar*, HF.

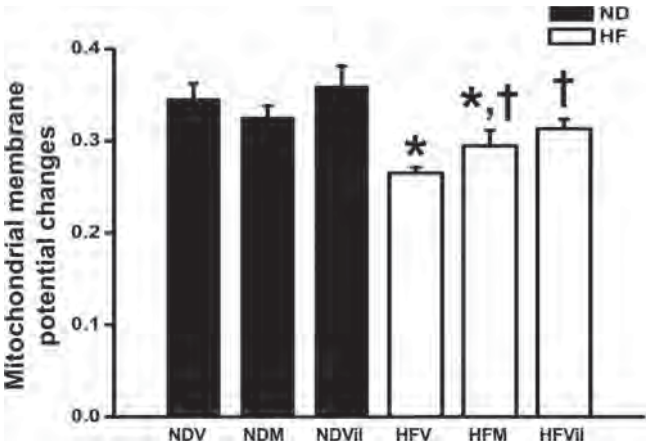

FIG. 4. Cardiac mitochondrial membrane potential changes (Δψm) in normal diet- and high-fat diet-fed rats treated with vehicle, metformin, and vildagliptin. Vildagliptin significantly preserved Δψm, compared with vehicle. *, $P < 0.05$ *vs.* NDV; †, $P < 0.05$ *vs.* HFV. NDV, Normal diet + vehicle; NDM, normal diet + metformin; NDVil, normal diet + vildagliptin; HFV, high-fat diet + vehicle; HFM, high-fat diet + metformin; HFVil, high-fat diet + vildagliptin.

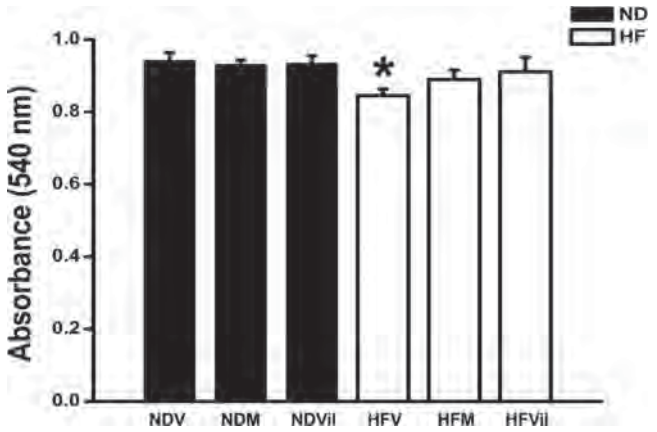

FIG. 5. Cardiac mitochondrial swelling of normal diet-fed and high-fat diet-fed rats treated with vehicle, metformin, and vildagliptin. Metformin and vildagliptin completely prevented cardiac mitochondrial swelling, compared with HFV. *, $P < 0.05$ *vs.* NDV; †, $P < 0.05$ *vs.* HFV. NDV, Normal diet + vehicle; NDM, normal diet + metformin; NDVil, normal diet + vildagliptin; HFV, high-fat diet + vehicle; HFM, high-fat diet + metformin; HFVil, high-fat diet + vildagliptin.

caused by long-term high-fat diet consumption. Second, both metformin and vildagliptin improved cardiac sympathovagal tone imbalance; however, only vildagliptin restored HRV to normal levels. Third, metformin and vildagliptin attenuated cardiac contractile dysfunction. Fourth, metformin and vildagliptin improved cardiac mitochondrial dysfunction caused by consumption of a high-fat diet. However, only vildagliptin completely restored cardiac mitochondrial function.

Long term high-fat diet consumption is known to cause an insulin-resistant condition (3). In this study, rats fed with 12 wk of high-fat diet developed an insulin resistance, characterized by increased insulin and cholesterol levels, but normal plasma glucose levels (2, 3). Previous studies reported that both metformin and vildagliptin have beneficial effects on metabolic parameters in type 2 diabetes patients (27, 28). In this study, metformin and vildagliptin improved the insulin-resistant condition in high-fat diet-fed rats by reducing plasma insulin and cholesterol levels as well as the HOMA index.

Metformin is a widely used antidiabetic drug, which can reduce plasma insulin and cholesterol levels in nonobese insulin-resistant patients (29) and high-fructose diet-induced diabetic rats (30). However, the effect of vildagliptin, a novel antidiabetic drug, on plasma insulin levels is still debated. Although Mari *et al.* (31) reported that vildagliptin reduced plasma insulin levels in patients with type 2 diabetes, Ahren *et al.* (32) found that vildagliptin did not alter plasma insulin levels in these diabetic patients. An experimental study demonstrated that the iv administration of vildagliptin increased the plasma insulin level in conscious dogs (33). In our study, the plasma insulin level in high-fat diet-fed rats was increased, and vildagliptin could reduce plasma insulin as well as plasma cholesterol levels without altering the plasma glucose levels in these insulin-resistant rats. This finding is consistent with a previous clinical study showing that vildagliptin could reduce plasma cholesterol level in diabetic patients (34, 35). The insulin-resistant condition has also been shown to be associated with an increase of oxidative stress levels (36). In this study, we found that plasma and cardiac MDA levels, a marker of oxidative stress, were increased in high-fat diet-fed rats. Treatment with metformin and vildagliptin could attenuate MDA levels in both plasma and heart tissue in insulin-resistant rats, indicating their antioxidative effect.

In past decades, HRV has been used to determine cardiac sympathovagal balance (37). It is well accepted that the LF/HF ratio is the important indicator of cardiac autonomic balance (37, 38) and that an increased LF/HF ratio represents depressed HRV or imbalanced cardiac autonomic tone (23). In this study, depressed HRV was initially observed at wk 8 of high-fat diet-fed rats and markedly depressed in wk 12 after high-fat diet consumption. Previous studies in both human and animal models reported that depressed HRV is associated with the insulin-resistant condition (6, 39). In the present study, metformin and vildagliptin improved not only insulin resistance, but also HRV in insulin-resistant rats. Because insulin resistance and oxidative stress are known to influence the depressed HRV, our findings that the reduction of plasma insulin, as well as reduced plasma and cardiac MDA, could play a crucial role in the protection of the sympathovagal tone imbalance. Although metformin has been shown to improve HRV in type 2 diabetes patients (40), our study demonstrated, for the first time, that vildagliptin had higher efficacy than metformin in preventing the depressed HRV because it could completely prevent cardiac sympathovagal imbalance caused by high-fat diet consumption. One limitation in this HRV study was that the ECG was recorded while the animal was restrained, and this could have affected cardiac autonomic control. However, because all animals were under the same condition during ECG recording, the findings on the effects of high-fat diet consumption as well as the effects of both metformin and vildagliptin on the HRV could still be directly compared.

Previous studies demonstrated that insulin resistance could raise an incidence of coronary artery disease and deteriorate cardiac function (41), and that cardiac systolic dysfunction could be developed after 7 wk of high-fat diet consumption (42). Consistent with those studies, our results showed that both cardiac systolic and diastolic dysfunction were observed in high-fat diet-fed rats treated with the vehicle. Although metformin has been shown pre-

viously to protect cardiac contractile dysfunction in diabetic mice, diabetic rats, and nondiabetic rats (10, 43–45), the cardiac effect of vildagliptin is still unclear. In the present study, we demonstrated that although both metformin and vildagliptin could attenuate the impairment of cardiac function in these obese high-fat diet-induced insulin-resistant rats, only vildagliptin that could restore the EDP and decrease the heart rate in these rats.

Cardiac mitochondria are known as a power house to supply energy for the heart to maintain its daily electrical and mechanical events. Insulin resistance has been shown to be associated with impaired cardiac mitochondrial function, leading to cardiac contractile dysfunction (46). Oxidative stress is known as an important factor to cause cardiac mitochondrial dysfunction. Cardiac mitochondrial dysfunction can be characterized by increased cardiac mitochondrial ROS production, mitochondrial membrane depolarization, and mitochondrial swelling (26, 47, 48). Consistent with a previous report (2), high-fat diet consumption for 12 wk in our study caused cardiac mitochondrial dysfunction. Both metformin and vildagliptin were also effective in attenuating cardiac mitochondrial dysfunction caused by long-term high-fat diet consumption. Although both metformin and vildagliptin could attenuate cardiac mitochondrial ROS production, only vildagliptin that could completely prevent ROS production caused by high-fat diet consumption. Furthermore, despite the fact that both metformin and vildagliptin could attenuate cardiac mitochondrial membrane depolarization, vildagliptin was more effective in preventing mitochondrial depolarization in rats exposed to a high-fat diet. These benefits of vildagliptin in preventing cardiac mitochondrial dysfunction as well as oxidative stress could be responsible for the improved cardiac function and HRV observed in this study.

In summary, our study demonstrates that long-term high-fat diet-fed rats could develop insulin resistance, depressed HRV, cardiac contractile dysfunction, and cardiac mitochondrial dysfunction. Although both metformin and vildagliptin could attenuate these impairments, vildagliptin demonstrated a better efficacy in preventing cardiac dysfunction, depressed HRV, and impaired cardiac mitochondrial function caused by consumption of food containing a high proportion of fat.

Acknowledgments

Address all correspondence and requests for reprints to: Nipon Chattipakorn, M.D., Ph.D., Cardiac Electrophysiology Research and Training Center, Faculty of Medicine, Chiang Mai University, Chiang Mai, 50200, Thailand. E-mail: nchattip@gmail.com.

This work was supported by Thailand Research Fund Grants TRF-RTA 5280006 (to N.C.) and TRF-BRG 5380004 (to S.C.) and the National Research Council of Thailand (to N.C.).

Disclosure Summary: The authors have nothing to disclose.

References

1. **Costa RR, Villela NR, Souza MG, Boa BC, Cyrino FZ, Silva SV, Lisboa PC, Moura EG, Barja-Fidalgo TC, Bouskela E** 2011 High fat diet induces central obesity, insulin resistance and microvascular dysfunction in hamsters. Microvasc Res 82:416–422
2. **Pipatpiboon N, Pratchayasakul W, Chattipakorn N, Chattipakorn SC** 2012 PPARγ agonist improves neuronal insulin receptor function in hippocampus and brain mitochondria function in rats with insulin resistance induced by long term high-fat diets. Endocrinology 153:329–338
3. **Pratchayasakul W, Kerdphoo S, Petsophonsakul P, Pongchaidecha A, Chattipakorn N, Chattipakorn SC** 2011 Effects of high-fat diet on insulin receptor function in rat hippocampus and the level of neuronal corticosterone. Life Sci 88:619–627
4. **Ouwens DM, Diamant M, Fodor M, Habets DD, Pelsers MM, El Hasnaoui M, Dang ZC, van den Brom CE, Vlasblom R, Rietdijk A, Boer C, Coort SL, Glatz JF, Luiken JJ** 2007 Cardiac contractile dysfunction in insulin-resistant rats fed a high-fat diet is associated with elevated CD36-mediated fatty acid uptake and esterification. Diabetologia 50:1938–1948
5. **Raher MJ, Thibault HB, Buys ES, Kuruppu D, Shimizu N, Brownell AL, Blake SL, Rieusset J, Kaneki M, Derumeaux G, Picard MH, Bloch KD, Scherrer-Crosbie M** 2008 A short duration of high-fat diet induces insulin resistance and predisposes to adverse left ventricular remodeling after pressure overload. Am J Physiol Heart Circ Physiol 295:H2495–H2502
6. **Pongchaidecha A, Lailerd N, Boonprasert W, Chattipakorn N** 2009 Effects of curcuminoid supplement on cardiac autonomic status in high-fat-induced obese rats. Nutrition 25:870–878
7. **Eurich DT, McAlister FA, Blackburn DF, Majumdar SR, Tsuyuki RT, Varney J, Johnson JA** 2007 Benefits and harms of antidiabetic agents in patients with diabetes and heart failure: systematic review. BMJ 335:497
8. **Palee S, Chattipakorn S, Phrommintikul A, Chattipakorn N** 2011 PPARγ activator, rosiglitazone: is it beneficial or harmful to the cardiovascular system? World J Cardiol 3:144–152
9. **Khurana R, Malik IS** 2010 Metformin: safety in cardiac patients. Postgrad Med J 86:371–373
10. **Wang XF, Zhang JY, Li L, Zhao XY, Tao HL, Zhang L** 2011 Metformin improves cardiac function in rats via activation of AMP-activated protein kinase. Clin Exp Pharmacol Physiol 38:94–101
11. **Verma S, McNeill JH** 1994 Metformin improves cardiac function in isolated streptozotocin-diabetic rat hearts. Am J Physiol 266:H714–H719
12. **Gundewar S, Calvert JW, Jha S, Toedt-Pingel I, Ji SY, Nunez D, Ramachandran A, Anaya-Cisneros M, Tian R, Lefer DJ** 2009 Activation of AMP-activated protein kinase by metformin improves left ventricular function and survival in heart failure. Circ Res 104:403–411
13. **Zander M, Madsbad S, Madsen JL, Holst JJ** 2002 Effect of 6-week course of glucagon-like peptide 1 on glycaemic control, insulin sensitivity, and β-cell function in type 2 diabetes: a parallel-group study. Lancet 359:824–830
14. **Chinda K, Chattipakorn S, Chattipakorn N** 11 April 2012 Cardioprotective effects of incretin during ischaemia-reperfusion. Diab Vasc Dis Res 10.1177/1479164112440816

15. **Ito M, Abe M, Okada K, Sasaki H, Maruyama N, Tsuchida M, Higuchi T, Kikuchi F, Soma M** 2011 The dipeptidyl peptidase-4 (DPP-4) inhibitor vildagliptin improves glycemic control in type 2 diabetic patients undergoing hemodialysis. Endocr J 58:979–987
16. **Yin M, Silljé HH, Meissner M, van Gilst WH, de Boer RA** 2011 Early and late effects of the DPP-4 inhibitor vildagliptin in a rat model of post-myocardial infarction heart failure. Cardiovasc Diabetol 10:85
17. **Dirkx E, Schwenk RW, Glatz JF, Luiken JJ, van Eys GJ** 2011 High fat diet induced diabetic cardiomyopathy. Prostaglandins Leukot Essent Fatty Acids 85:219–225
18. **Jin HE, Hong SS, Choi MK, Maeng HJ, Kim DD, Chung SJ, Shim CK** 2009 Reduced antidiabetic effect of metformin and down-regulation of hepatic Oct1 in rats with ethynylestradiol-induced cholestasis. Pharm Res 26:549–559
19. **Burkey BF, Li X, Bolognese L, Balkan B, Mone M, Russell M, Hughes TE, Wang PR** 2005 Acute and chronic effects of the incretin enhancer vildagliptin in insulin-resistant rats. J Pharmacol Exp Ther 315:688–695
20. **Ming Z, Legare DJ, Lautt WW** 2011 Absence of meal-induced insulin sensitization (AMIS) in aging rats is associated with cardiac dysfunction that is protected by antioxidants. J Appl Physiol 111: 704–714
21. **Thephinlap C, Phisalaphong C, Lailerd N, Chattipakorn N, Winichagoon P, Vadolus J, Fucharoen S, Porter JB, Srichairatanakool S** 2011 Reversal of cardiac iron loading and dysfunction in thalassemic mice by curcuminoids. Med Chem 7:62–69
22. **Mateos R, Lecumberri E, Ramos S, Goya L, Bravo L** 2005 Determination of malondialdehyde (MDA) by high-performance liquid chromatography in serum and liver as a biomarker for oxidative stress. Application to a rat model for hypercholesterolemia and evaluation of the effect of diets rich in phenolic antioxidants from fruits. J Chromatogr B Analyt Technol Biomed Life Sci 827:76–82
23. **Incharoen T, Thephinlap C, Srichairatanakool S, Chattipakorn S, Winichagoon P, Fucharoen S, Vadolas J, Chattipakorn N** 2007 Heart rate variability in β-thalassemic mice. Int J Cardiol 121:203–204
24. **Kumfu S, Chattipakorn S, Chinda K, Fucharoen S, Chattipakorn N** 2012 T-type calcium channel blockade improves survival and cardiovascular function in thalassemic mice. Eur J Haematol 88:535–548
25. **Ohuchi H, Suzuki H, Yasuda K, Arakaki Y, Echigo S, Kamiya T** 2000 Heart rate recovery after exercise and cardiac autonomic nervous activity in children. Pediatr Res 47:329–335
26. **Thummasorn S, Kumfu S, Chattipakorn S, Chattipakorn N** 2011 Granulocyte-colony stimulating factor attenuates mitochondrial dysfunction induced by oxidative stress in cardiac mitochondria. Mitochondrion 11:457–466
27. **Eriksson A, Attvall S, Bonnier M, Eriksson JW, Rosander B, Karlsson FA** 2007 Short-term effects of metformin in type 2 diabetes. Diabetes Obes Metab 9:330–336
28. **Cai L, Cai Y, Lu ZJ, Zhang Y, Liu P** 22 December 2011 The efficacy and safety of vildagliptin in patients with type 2 diabetes: a meta-analysis of randomized clinical trials. J Clin Pharm Ther 10.1111/j.1365-2710.2011.01323.x
29. **Dorella M, Giusto M, Da Tos V, Campagnolo M, Palatini P, Rossi G, Ceolotto G, Felice M, Semplicini A, Del Prato S** 1996 Improvement of insulin sensitivity by metformin treatment does not lower blood pressure of nonobese insulin-resistant hypertensive patients with normal glucose tolerance. J Clin Endocrinol Metab 81:1568–1574
30. **Anurag P, Anuradha CV** 2002 Metformin improves lipid metabolism and attenuates lipid peroxidation in high fructose-fed rats. Diabetes Obes Metab 4:36–42
31. **Mari A, Sallas WM, He YL, Watson C, Ligueros-Saylan M, Dunning BE, Deacon CF, Holst JJ, Foley JE** 2005 Vildagliptin, a dipeptidyl peptidase-IV inhibitor, improves model-assessed β-cell function in patients with type 2 diabetes. J Clin Endocrinol Metab 90:4888–4894
32. **Ahrén B, Landin-Olsson M, Jansson PA, Svensson M, Holmes D, Schweizer A** 2004 Inhibition of dipeptidyl peptidase-4 reduces glycemia, sustains insulin levels, and reduces glucagon levels in type 2 diabetes. J Clin Endocrinol Metab 89:2078–2084
33. **Edgerton DS, Johnson KM, Neal DW, Scott M, Hobbs CH, Zhang X, Duttaroy A, Cherrington AD** 2009 Inhibition of dipeptidyl peptidase-4 by vildagliptin during glucagon-like peptide 1 infusion increases liver glucose uptake in the conscious dog. Diabetes 58:243–249
34. **Matikainen N, Mäntäri S, Schweizer A, Ulvestad A, Mills D, Dunning BE, Foley JE, Taskinen MR** 2006 Vildagliptin therapy reduces postprandial intestinal triglyceride-rich lipoprotein particles in patients with type 2 diabetes. Diabetologia 49:2049–2057
35. **Rosenstock J, Baron MA, Dejager S, Mills D, Schweizer A** 2007 Comparison of vildagliptin and rosiglitazone monotherapy in patients with type 2 diabetes: a 24-week, double-blind, randomized trial. Diabetes Care 30:217–223
36. **Urakawa H, Katsuki A, Sumida Y, Gabazza EC, Murashima S, Morioka K, Maruyama N, Kitagawa N, Tanaka T, Hori Y, Nakatani K, Yano Y, Adachi Y** 2003 Oxidative stress is associated with adiposity and insulin resistance in men. J Clin Endocrinol Metab 88:4673–4676
37. **Chattipakorn N, Incharoen T, Kanlop N, Chattipakorn S** 2007 Heart rate variability in myocardial infarction and heart failure. Int J Cardiol 120:289–296
38. **Lombardi F, Sandrone G, Pernpruner S, Sala R, Garimoldi M, Cerutti S, Baselli G, Pagani M, Malliani A** 1987 Heart rate variability as an index of sympathovagal interaction after acute myocardial infarction. Am J Cardiol 60:1239–1245
39. **Van De Borne P, Hausberg M, Hoffman RP, Mark AL, Anderson EA** 1999 Hyperinsulinemia produces cardiac vagal withdrawal and nonuniform sympathetic activation in normal subjects. Am J Physiol 276:R178–R183
40. **Manzella D, Grella R, Esposito K, Giugliano D, Barbagallo M, Paolisso G** 2004 Blood pressure and cardiac autonomic nervous system in obese type 2 diabetic patients: effect of metformin administration. Am J Hypertens 17:223–227
41. **Hintz KK, Aberle NS, Ren J** 2003 Insulin resistance induces hyperleptinemia, cardiac contractile dysfunction but not cardiac leptin resistance in ventricular myocytes. Int J Obes Relat Metab Disord 27:1196–1203
42. **Ouwens DM, Boer C, Fodor M, de Galan P, Heine RJ, Maassen JA, Diamant M** 2005 Cardiac dysfunction induced by high-fat diet is associated with altered myocardial insulin signalling in rats. Diabetologia 48:1229–1237
43. **Yin M, van der Horst IC, van Melle JP, Qian C, van Gilst WH, Silljé HH, de Boer RA** 2011 Metformin improves cardiac function in a nondiabetic rat model of post-MI heart failure. Am J Physiol Heart Circ Physiol 301:H459–H468
44. **Xie Z, Lau K, Eby B, Lozano P, He C, Pennington B, Li H, Rathi S, Dong Y, Tian R, Kem D, Zou MH** 2011 Improvement of cardiac functions by chronic metformin treatment is associated with enhanced cardiac autophagy in diabetic OVE26 mice. Diabetes 60: 1770–1778
45. **Kravchuk E, Grineva E, Bairamov A, Galagudza M, Vlasov T** 2011 The effect of metformin on the myocardial tolerance to ischemia-reperfusion injury in the rat model of diabetes mellitus type II. Exp Diabetes Res 2011:907496
46. **Kim JA, Wei Y, Sowers JR** 2008 Role of mitochondrial dysfunction in insulin resistance. Circ Res 102:401–414
47. **Palee S, Weerateerangkul P, Surinkeaw S, Chattipakorn S, Chattipakorn N** 2011 Effect of rosiglitazone on cardiac electrophysiology, infarct size and mitochondrial function in ischaemia and reperfusion of swine and rat heart. Exp Physiol 96:778–789
48. **Chinda K, Palee S, Surinkaew S, Phornphutkul M, Chattipakorn S, Chattipakorn N** 25 January 2012 Cardioprotective effect of dipeptidyl peptidase-4 inhibitor during ischemia-reperfusion injury. Int J Cardiol 10.1016/j.bbamcr.2012.01.014

Effects of Curcuminoids on Frequency of Acute Myocardial Infarction After Coronary Artery Bypass Grafting

Wanwarang Wongcharoen, MD[a,b,*], Sasivimon Jai-aue, MD[d], Arintaya Phrommintikul, MD[a,b], Weerachai Nawarawong, MD[c], Surin Woragidpoonpol, MD[c], Thitipong Tepsuwan, MD[c], Apichard Sukonthasarn, MD[a], Nattayaporn Apaijai, BSc[b], and Nipon Chattipakorn, MD, PhD[b]

It is well established that myocardial infarction (MI) associated with coronary artery bypass grafting (CABG) predicts a poor outcome. Nevertheless, cardioprotective therapies to limit myocardial injury after CABG are lacking. Previous studies have shown that curcuminoids decrease proinflammatory cytokines during cardiopulmonary bypass surgery and decrease the occurrence of cardiomyocytic apoptosis after cardiac ischemia/reperfusion injury in animal models. We aimed to evaluate whether curcuminoids prevent MI after CABG compared to placebo. The 121 consecutive patients undergoing CABG were randomly allocated to receive placebo or curcuminoids 4 g/day beginning 3 days before the scheduled surgery and continued until 5 days after surgery. The primary end point was incidence of in-hospital MI. The secondary end point was the effect of curcuminoids on C-reactive protein, plasma malondialdehyde, and N-terminal pro–B-type natriuretic peptide levels. Baseline characteristics were comparable between the curcuminoid and placebo groups. Mean age was 61 ± 9 years. On-pump CABG procedures were performed in 51.2% of patients. Incidence of in-hospital MI was decreased from 30.0% in the placebo group to 13.1% in the curcuminoid group (adjusted hazard ratio 0.35, 0.13 to 0.95, p = 0.038). Postoperative C-reactive protein, malondialdehyde, and N-terminal pro–B-type natriuretic peptide levels were also lower in the curcuminoid than in the placebo group. In conclusion, we demonstrated that curcuminoids significantly decreased MI associated with CABG. The antioxidant and anti-inflammatory effects of curcuminoids may account for their cardioprotective effects shown in this study. **(Am J Cardiol 2012;xx:xxx)**

Curcuminoids, the polyphenols responsible for the yellow color of the curry spice turmeric, have been used to treat a variety of diseases in traditional Chinese and Indian medicine. The major curcuminoids present in turmeric are curcumin (curcumin I), demethoxycurcumin (curcumin II), and bisdemethoxycurcumin (curcumin III).[1] Modern scientific research has confirmed the good therapeutic effects of the curcuminoid complex and its pharmacologic safety has been well established.[2] A previous study has shown that curcuminoids suppress proinflammatory cytokines during cardiopulmonary bypass surgery and decrease the occurrence of cardiomyocytic apoptosis after cardiac ischemia/reperfusion injury in an animal model.[3] Furthermore, a histopathologic study has demonstrated that curcuminoid treatment decreases the degree of myocardial necrosis in isoproterenol-administered rats.[4] The well-known anti-inflammatory, antioxidant, and membrane-stabilizing effects of curcuminoids may help preserve cellular viability during cardiopulmonary bypass surgery.[5,6] Therefore, curcuminoids may have a potential role in the limitation of myocardial ischemia/reperfusion injury after coronary artery bypass grafting (CABG). The present study evaluated whether curcuminoids prevent myocardial infarction (MI) after CABG compared to placebo.

Methods

The present study was a randomized, prospective, double-blinded, placebo-controlled trial performed at Maharaj Nakorn Chiang Mai Hospital, Chiang Mai University. We prospectively studied 121 consecutive patients undergoing CABG without valve surgery from September 2009 to December 2011. Informed consent was obtained from each patient to participate in the study. Patients were excluded if they had emergency cardiac surgery or any increase in creatine kinase-MB above the upper limit of the normal range at time of randomization. Because curcuminoids are mainly metabolized by the liver, patients with cholesteric jaundice (total bilirubin higher than twofold the upper normal limit) or severe liver disease (aspartate aminotransferase or alanine amino-

[a]Department of Internal Medicine, [b]Cardiac Electrophysiology Research and Training Center, and [c]Department of Surgery, Faculty of Medicine, Chiang Mai University, Chiang Mai, Thailand; [d]Department of Internal Medicine, Chiangrai Prachanukroh Hospital, Chiang Rai, Thailand. Manuscript received January 3, 2012; revised manuscript received and accepted February 28, 2012.

This work was supported by Grants MRG 5380258 (Dr. Wongcharoen), MRG 5280169 (Dr. Phrommintikul), and RTA5280006 (Dr. Chattipakorn) from the Thailand Research Fund, Bangkok, Thailand; The Research and Development Institute, the Government Pharmaceutical Organization, Bangkok, Thailand (Dr. Wongcharoen); and the Faculty of Medicine Endowment Fund for Medical Research, Chiang Mai University, Chang Mai, Thailand (Dr. Wongcharoen, Dr. Phrommintikul, and Dr. Chattipakorn).

*Corresponding author: Tel: 66-53-946713; fax: 66-53-945486.

E-mail address: bwanwarang@yahoo.com (W. Wongcharoen).

0002-9149/12/$ – see front matter
doi:10.1016/j.amjcard.2012.02.043

Table 1
Demographic data and clinical features

Characteristics	Curcuminoid (n = 61)	Placebo (n = 60)	*p* Value
Age (years)	61.0 ± 9.1	61.1 ± 8.2	0.966
Men	34 (55.7%)	35 (58.3%)	0.917
Body mass index (kg/m^2)	24.1 ± 3.4	24.8 ± 4.8	0.290
New York Heart Association class	1.9 ± 0.5	2.0 ± 0.5	0.224
Canadian Cardiovascular Society class	1.9 ± 0.6	2.0 ± 0.5	0.194
Serum creatinine (mg/dl)	1.3 ± 0.4	1.4 ± 0.6	0.380
Preoperative creatine kinase-MB (ng/ml)	4.5 ± 4.1	5.5 ± 6.8	0.308
Preoperative C-reactive protein (mg/dl)	0.4 ± 0.5	0.5 ± 0.9	0.313
Preoperative malondialdehyde (mmol/ml)	7.4 ± 1.4	7.4 ± 1.1	0.908
Preoperative N-terminal pro–B-type natriuretic peptide (pg/ml)*	410.9 ± 577.2	533.4 ± 1,529.7	0.219
Diabetes mellitus	23 (37.7%)	30 (50.0%)	0.238
Hypertension†	55 (90.2%)	54 (90.0%)	1.000
Dyslipidemia‡	55 (90.2%)	52 (86.7%)	0.751
Previous myocardial infarction	17 (27.9%)	15 (25.0%)	0.879
Current smoker	8 (13.1%)	4 (6.7%)	0.378
Heart failure	5 (8.3%)	6 (10.0%)	1.000
Previous coronary angioplasty	4 (6.6%)	1 (1.7%)	0.371
Left ventricular ejection fraction (%)	54.8 ± 14.4	51.6 ± 15.1	0.483
Preoperative medications			
Aspirin or clopidogrel	55 (90.2%)	59 (98.3%)	0.125
β blocker	48 (78.7%)	48 (80.0%)	0.891
Statin	56 (91.8%)	56 (93.3%)	1.000
Angiotensin-converting enzyme inhibitor or angiotensin II receptor blocker	42 (68.9%)	44 (73.3%)	0.732

* Median ± interquartile range.
† Blood pressure ≥140/90 mm Hg or currently treated with antihypertensive drugs.
‡ Low-density lipoprotein cholesterol >100 mg/dl, high-density lipoprotein cholesterol <40 mg/dl, or triglyceride >150 mg/dl.

Table 2
Perioperative features of patients in curcuminoid and placebo groups

Characteristics	Curcuminoid (n = 61)	Placebo (n = 60)	*p* Value
Vessel involvement			
Left main coronary artery stenosis	12 (20.3%)	17 (28.3%)	0.422
3-Vessel disease	45 (76.3%)	49 (81.7%)	0.619
Off-pump coronary artery bypass grafting	32 (52.5%)	27 (45.0%)	0.523
On-pump coronary artery bypass grafting	29 (47.5%)	33 (55.0%)	
On-pump with beating heart	14 (23.3%)	17 (28.3%)	
On-pump with cardioplegic arrest	15 (24.6%)	16 (26.7%)	
Cardiopulmonary bypass duration (minutes)	108.5 ± 48.1	106.6 ± 43.0	0.872
Cross-clamp duration (minutes)	80.0 ± 27.7	71.4 ± 26.3	0.379
Temporary ventricular pacing	24 (39.3%)	19 (31.8%)	0.231
Number of bypass grafts	3.5 ± 1.3	3.7 ± 1.0	0.374
Myocardial infarction after coronary artery bypass grafting	8 (13.1%)	18 (30.0%)	0.028
Non–Q-wave myocardial infarction	8 (13.1%)	15 (25.0%)	
Q-wave myocardial infarction	0 (0%)	3 (5.0%)	

transferase higher than threefold the upper normal limit) were not included in the study.

Curcuminoids and placebo used in the present study were provided in caplet form by the Research and Development Institute, the Government Pharmaceutical Organization, Bangkok, Thailand. One curcuminoid capsule contained curcuminoids 250 mg, which consisted of curcumin, demethoxycurcumin, and bisdemethoxycurcumin, in a ratio of 1.0:0.6:0.3, respectively, confirmed by high-performance liquid chromatography/mass spectrometry.

Enrolled patients were randomly allocated to receive placebo or curcuminoids 4 capsules 4 times/day (4 g/day) in addition to standard therapy beginning 3 days before the scheduled surgery and patients continued to receive the assigned treatment until 5 days after surgery. To assign patients to curcuminoids or placebo, a block randomization sequence was obtained by a statistical consultant who was not involved in the study. Assigned therapy was fully blinded; surgeons and investigators performing postoperative assessment were not aware of the randomization assignment.

All patients undergoing CABG were treated with standard therapy according to their physicians. Three surgeons

performed CABG in the present study. The surgical techniques were determined at the discretion of the individual surgeons. On-pump CABG procedures were performed in 62 patients (51.2%), of whom 31 (25.6%) underwent on-pump CABG with the heart beating and 31 (25.6%) underwent on-pump CABG with conventional cardioplegic arrest. Myocardial protection was done with antegrade and retrograde cold blood cardioplegia. Off-pump CABG was performed in the remaining patients. The conduits used in patients in this study included the internal mammary arteries, radial arteries, and saphenous veins.

Twelve-lead electrocardiograms were recorded before surgery, 24, 48, and 72 hours after surgery, and 30-day follow-up visit. Serial creatine kinase-MB levels were assessed before surgery, at 8, 16, 24, 48, and 72 hours after intensive care unit arrival, and whenever an ischemic event was suspected. N-terminal pro–B-type natriuretic peptide (NT–pro-BNP) level was assessed before surgery and on the 5th postoperative day.

To examine the effects of curcuminoids on inflammatory response and oxidative stress after surgery, C-reactive protein (CRP) level was assessed before surgery and on postoperative days 3 and 5. In addition, plasma malondialdehyde (MDA) level, a marker for oxidative stress, was assessed before surgery and on postoperative day 5 using the high-performance liquid chromatographic method.

The primary end point of the study was to demonstrate that curcuminoids decrease the incidence of in-hospital MI compared to placebo. The secondary end point was to examine the effects of curcuminoids on CRP, MDA, and NT–pro-BNP levels after surgery.

The diagnosis of Q-wave MI was determined by the presence of new pathologic Q waves according to Minnesota Code criteria or new-onset left bundle branch block and creatine kinase-MB increase more than fivefold the upper normal limit of the investigators' local laboratory within 24 hours of CABG. In the absence of the aforementioned electrocardiographic findings, creatine kinase-MB increase >10-fold the upper normal limit within 24 hours of CABG was considered indicative of non–Q-wave MI.[7] If MI was suspected >24 hours after CABG, a creatine kinase-MB increase >2 times the upper normal limit with chest pain or an increase >3 times the upper normal limit was considered indicative of MI.[8]

All analyses were done on an intention-to-treat basis. Demographic and perioperative variables were compared between groups with *t* test for normally distributed values; otherwise the Mann–Whitney *U* test was used. Proportions were compared by chi-square test or Fisher's exact test when appropriate. Continuous variables are presented as mean ±SD or median ± interquartile range when appropriate. Categorical variables are displayed as percentages. Hazard ratios and 95% confidence intervals to assess the risk of the primary end point according to potential confounding variables were determined by logistic regression. Multivariate analyses were performed for variables with a p value <0.1 in univariate analysis using the logistic regression procedure. A p value <0.05 (2-tailed) was considered statistically significant.

Table 3
Multivariable logistic regression for myocardial infarction after coronary artery bypass grafting

Risk Factor	OR (95% CI)	*p* Value
Curcuminoid therapy	0.35 (0.13–0.95)	0.038
On-pump coronary artery bypass grafting	5.23 (1.92–14.28)	0.001

CI = confidence interval; OR = odds ratio.

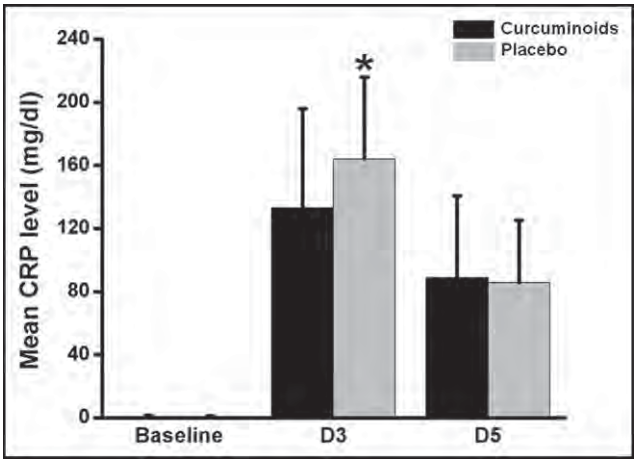

Figure 1. C-reactive protein levels before and after coronary artery bypass grafting in curcuminoid and placebo groups. C-reactive protein level on postoperative day 3 (D3) was significantly lower in the curcuminoid group compared to the placebo group. *p <0.05 versus placebo. D5 = postoperative day 5.

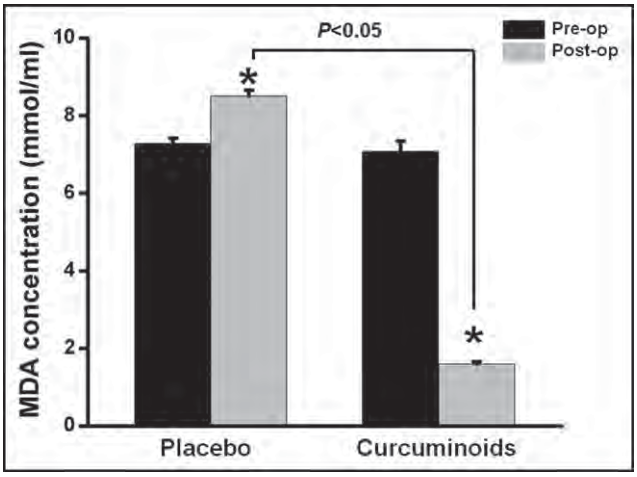

Figure 2. Levels of plasma malondialdehyde before (Pre-op) and after (Post-op) coronary artery bypass grafting in curcuminoid and placebo groups. Plasma malondialdehyde level increased after coronary artery bypass grafting in the placebo group but decreased significantly after coronary artery bypass grafting in the curcuminoid group. *p <0.05 versus preoperatively.

Results

Demographic and perioperative variables are presented in Tables 1 and 2, respectively. From September 2009 to December 2011, 121 consecutive patients who met the inclusion criteria were randomly divided to a curcuminoid group (n = 61) or a control group (n = 60). Baseline characteristics of patients in the 2 treatment groups were

Table 4
Adverse events and study drug discontinuation

Characteristics	Curcuminoid (n = 61)	Placebo (n = 60)	*p* Value
Adverse events			
Nausea	8 (13.1%)	5 (8.3%)	0.559
Diarrhea	2 (3.3%)	2 (3.3%)	1.000
Abdominal pain	3 (4.9%)	1 (1.7%)	0.619
Dizziness	2 (3.3%)	1 (1.7%)	1.000
Sore throat	1 (1.6%)	1 (1.7%)	1.000
Serious adverse events of special interest			
Serum creatinine increase*	4 (6.6%)	2 (3.3%)	0.691
Liver function			
Alanine aminotransferase or aspartate aminotransferase >3× upper limit of normal range	0 (0%)	2 (3.3%)	0.469
Alanine aminotransferase or aspartate aminotransferase >3× upper limit of normal range with concurrent bilirubin >2× upper limit of normal range	0 (0%)	1 (1.7%)	0.993
Inotrope requirement	43 (70.5%)	44 (73.3%)	0.884
Intra-aortic balloon pump usage	0 (0%)	4 (6.7%)	0.057
Severe postoperative hemorrhage required reoperation to stop bleeding	1 (1.6%)	1 (1.7%)	1.000
Stroke/transient ischemic attack	2 (3.3%)	1 (1.7%)	1.000
Death	1 (1.6%)	1 (1.7%)	1.000
Premature study drug discontinuation			
Overall	14 (22.9%)	11 (18.3%)	0.654
Owing to adverse drug events	6 (9.8%)	4 (6.7%)	0.743
By subject's request	7 (11.5%)	6 (10.0%)	1.000
For other reasons	1 (1.6%)	1 (1.7%)	1.000

* Increase in serum creatinine of ≥50%.

comparable including age, gender, co-morbidities, and previous percutaneous coronary revascularization (Table 1). Perioperative features were not different between the curcuminoid and placebo groups (Table 2).

Incidence of the primary outcome (in-hospital MI) was decreased from 30.0% in the placebo group to 13.1% in the curcuminoid group (unadjusted hazard ratio 0.35, 0.14 to 0.89, p = 0.028). Most MI events were non–Q-wave MI (Table 2). Apart from curcuminoid treatment, other predictors of in-hospital MI were identified. We found that on-pump CABG was significantly associated with a higher incidence of MI compared to off-pump surgery (35.5%, 22 of 62, vs 6.8%, 4 of 59, respectively, p <0.001). After multivariate analysis, we found that curcuminoid therapy remained the independent protective factor of in-hospital MI and that on-pump CABG was the independent predictive factor of in-hospital MI (Table 3). Of 121 patients, 57 patients underwent echocardiography 1 month after surgery. Incidence of postoperative left ventricular dysfunction (left ventricular ejection fraction <40%) was significantly higher in the placebo group than in the curcuminoid group (25.9%, 7 of 27, vs 3.3%, 1 of 30, respectively, p = 0.021).

Baseline preoperative CRP, MDA, and NT–pro-BNP levels were not different between the curcuminoid and placebo groups. However, mean increase in CRP level on postoperative day 3 compared to baseline level was significantly greater in the placebo group than in the curcuminoid group (difference +161.8 ± 54.1 vs +128.6 ± 60.5 mg/dl, respectively, p = 0.031; Figure 1). Plasma MDA level was increased after CABG in the placebo group but was decreased significantly after CABG in the curcuminoid group (difference +0.8 ± 1.4 vs −5.7 ± 1.5 mmol/ml, respectively, p <0.001; Figure 2). Furthermore, mean increase in postoperative NT–pro-BNP level compared to preoperative level was greater in the placebo group than in the curcuminoid group (difference +2,542.2 ± 2,631.2 vs +1,822.1 ± 2,102.9 pg/ml, respectively, p = 0.015).

Incidence of drug-related adverse events was not different between the curcuminoid and placebo groups (Table 4). The main drug-related adverse events were gastrointestinal symptoms. Incidences of serious adverse events and drug discontinuation did not differ between the 2 groups.

Discussion

Adequate myocardial protection during CABG is crucial in preventing myocardial injury after surgery.[7,9] Previous studies have shown that an increase of cardiac enzymes after CABG is associated with increased long-term mortality.[10] Nevertheless, some interventions reported to be cardioprotective in experimental models of ischemia/reperfusion injury have failed to translate their protective effects into clinical studies.[11] Until recently, only few clinical studies have shown promising results.[7,12–14] Mangano et al[14] recently examined the efficacy of the adenosine-regulating agent acadesine in patients undergoing CABG. They demonstrated that acadesine improved long-term survival in this group of patients. Furthermore, cariporide, the sodium-hydrogen exchange inhibitor, has been shown to decrease the incidence of MI associated with CABG, although the neurologic complications observed with the high dose preclude its clinical use.[7]

Preclinical data have shown that curcuminoids have cardiovascular protective effects in experimental models of various cardiac conditions.[15] In the present study, we demonstrated that curcuminoids decreased the incidence of in-

hospital MI after CABG significantly. In addition, curcuminoids attenuated postoperative NT–pro-BNP levels and decreased the incidence of postoperative left ventricular dysfunction. Accumulating evidence has suggested that curcuminoids have a diverse range of molecular targets and influence numerous biochemical and molecular cascades.[2] We propose that the beneficial effects of curcuminoids in the decrease of MI may be exerted by several mechanisms. First, it has been suggested that oxidative stress and systemic inflammatory response during cardiopulmonary bypass may account for ischemia/reperfusion injury occurring in patients receiving CABG. Curcuminoids have been shown to possess striking antioxidant and anti-inflammatory properties and to inhibit such mediators of inflammation as nuclear factor-κB, cyclooxygenase-2, lipoxygenase, and inducible nitric oxide synthase.[16] Correspondingly, in the present study, we demonstrated that curcuminoids decreased postoperative CRP and MDA levels significantly. Therefore, the anti-inflammatory and antioxidative effects of curcuminoids may attenuate myocardial injury associated with cardiac surgery. Second, curcuminoids may protect against cardiac injury through a membrane-stabilizing effect.[17–20] Nirmala and Puvanakrishnan[4,21] demonstrated that curcuminoids significantly attenuated increased lysosomal hydrolase activity in serum and myocardial tissue in isoproterenol-induced MI in rats. Histopathologic findings also showed that the curcuminoid treatment decreased the degree of myocardial necrosis in isoproterenol-administered rats.[4] The membrane-stabilizing effect of curcuminoids may protect cells from autolytic and heterolytic damage and may attenuate the tissue damage owing to myocardial ischemia. Third, additional evidence from in vitro studied has shown that curcuminoids inhibit human platelet activation.[21,22] The antiplatelet property of curcuminoids may potentially decrease the occurrence of myocardial ischemia.

Because of the relatively small studied population, our results need to be confirmed in larger studies. Apart from the anti-inflammatory and antioxidant effects of curcuminoids shown in this study, other mechanisms of cardioprotective effects of curcuminoids are not clearly elucidated. Furthermore, the effect of curcuminoids on long-term outcome after CABG is unknown. Future studies are warranted to clarify this issue.

1. Kiuchi F, Goto Y, Sugimoto N, Akao N, Kondo K, Tsuda Y. Nematocidal activity of turmeric: synergistic action of curcuminoids. *Chem Pharm Bull* 1993;41:1640–1643.
2. Goel A, Kunnumakkara AB, Aggarwal BB. Curcumin as "Curecumin": from kitchen to clinic. *Biochem Pharmacol* 2008;75:787–809.
3. Yeh CH, Chen TP, Wu YC, Lin YM, Jing Lin P. Inhibition of NFkappaB activation with curcumin attenuates plasma inflammatory cytokines surge and cardiomyocytic apoptosis following cardiac ischemia/reperfusion. *J Surg Res* 2005;125:109–116.
4. Nirmala C, Puvanakrishnan R. Effect of curcumin on certain lysosomal hydrolases in isoproterenol-induced myocardial infarction in rats. *Biochem Pharmacol* 1996;51:47–51.
5. Srivastava R, Srimal RC. Modification of certain inflammation-induced biochemical changes by curcumin. *Indian J Med Res* 1985;81:215–223.
6. Winter CA. Nonsteroid anti-inflammatory agents. *Annu Rev Pharmacol* 1966;6:157–174.
7. Mentzer RM, Jr., Bartels C, Bolli R, Boyce S, Buckberg GD, Chaitman B, Haverich A, Knight J, Menasché P, Myers ML, Nicolau J, Simoons M, Thulin L, Weisel RD; EXPEDITION Study Investigators. Sodium-hydrogen exchange inhibition by cariporide to reduce the risk of ischemic cardiac events in patients undergoing coronary artery bypass grafting: results of the EXPEDITION study. *Ann Thorac Surg* 2008;85:1261–1270.
8. Thygesen K, Alpert JS, White HD, Jaffe AS, Apple FS, Galvani M, Katus HA, Newby LK, Ravkilde J, Chaitman B, Clemmensen PM, Dellborg M, Hod H, Porela P, Underwood R, Bax JJ, Beller GA, Bonow R, Van der Wall EE, Bassand JP, Wijns W, Ferguson TB, Steg PG, Uretsky BF, Williams DO, Armstrong PW, Antman EM, Fox KA, Hamm CW, Ohman EM, Simoons ML, Poole-Wilson PA, Gurfinkel EP, Lopez-Sendon JL, Pais P, Mendis S, Zhu JR, Wallentin LC, Fernandez-Aviles F, Fox KM, Parkhomenko AN, Priori SG, Tendera M, Voipio-Pulkki LM, Vahanian A, Camm AJ, De Caterina R, Dean V, Dickstein K, Filippatos G, Funck-Brentano C, Hellemans I, Kristensen SD, McGregor K, Sechtem U, Silber S, Widimsky P, Zamorano JL, Morais J, Brener S, Harrington R, Morrow D, Lim M, Martinez-Rios MA, Steinhubl S, Levine GN, Gibler WB, Goff D, Tubaro M, Dudek D, Al-Attar N. Universal definition of myocardial infarction. *Circulation* 2007;116:2634–2653.
9. Onorati F, De Feo M, Mastroroberto P, Cristodoro L, Pezzo F, Renzulli A, Cotrufo M. Determinants and prognosis of myocardial damage after coronary artery bypass grafting. *Ann Thorac Surg* 2005;79:837–845.
10. Domanski MJ, Mahaffey K, Hasselblad V, Brener SJ, Smith PK, Hillis G, Engoren M, Alexander JH, Levy JH, Chaitman BR, Broderick S, Mack MJ, Pieper KS, Farkouh ME. Association of myocardial enzyme elevation and survival following coronary artery bypass graft surgery. *JAMA* 2011;305:585–591.
11. Bolli R, Becker L, Gross G, Mentzer R Jr, Balshaw D, Lathrop DA; NHLBI Working Group on the Translation of Therapies for Protecting the Heart from Ischemia. Myocardial protection at a crossroads: the need for translation into clinical therapy. *Circ Res* 2004;95:125–134.
12. Mentzer RM, Jr., Birjiniuk V, Khuri S, Lowe JE, Rahko PS, Weisel RD, Wellons HA, Barker ML, Lasley RD. Adenosine myocardial protection: preliminary results of a phase II clinical trial. *Ann Surg* 1999;229:643–649.
13. Cohen G, Feder-Elituv R, Iazetta J, Bunting P, Mallidi H, Bozinovski J, Deemar C, Christakis GT, Cohen EA, Wong BI, McLean RD, Myers M, Morgan CD, Mazer CD, Smith TS, Goldman BS, Naylor CD, Fremes SE. Phase 2 studies of adenosine cardioplegia. *Circulation* 1998;98(suppl):II225–II233.
14. Mangano DT, Miao Y, Tudor IC, Dietzel C; Investigators of the Multicenter Study of Perioperative Ischemia (McSPI) Research Group, Ischemia Research and Education Foundation (IREF). Post-reperfusion myocardial infarction: long-term survival improvement using adenosine regulation with acadesine. *J Am Coll Cardiol* 2006;48:206–214.
15. Wongcharoen W, Phrommintikul A. The protective role of curcumin in cardiovascular diseases. *Int J Cardiol* 2009;133:145–151.
16. Bengmark S. Curcumin, an atoxic antioxidant and natural NFkappaB, cyclooxygenase-2, lipoxygenase, and inducible nitric oxide synthase inhibitor: a shield against acute and chronic diseases. *J Parenter Enteral Nutr* 2006;30:45–51.
17. Decker RS, Poole AR, Griffin EE, Dingle JT, Wildenthal K. Altered distribution of lysosomal cathepsin D in ischemic myocardium. *J Clin Invest* 1977;59:911–921.
18. Mathew S, Menon PV, Kurup PA. Changes in glycoproteins in isoproterenol-induced myocardial infarction in rats. *Indian J Biochem Biophys* 1982;19:41–43.
19. Ravichandran LV, Puvanakrishnan R, Joseph KT. Influence of isoproterenol-induced myocardial infarction on certain glycohydrolases and cathepsins in rats. *Biochem Med Metab Biol* 1991;45:6–15.
20. Takahashi S, Barry AC, Factor SM. Collagen degradation in ischaemic rat hearts. *Biochem J* 1990;265:233–241.
21. Nirmala C, Puvanakrishnan R. Protective role of curcumin against isoproterenol induced myocardial infarction in rats. *Mol Cell Biochem* 1996;159:85–93.
22. Jain U. Myocardial infarction during coronary artery bypass surgery. *J Cardiothorac Vasc Anesth* 1992;6:612–623.

ELSEVIER

Archives of Medical Research ■ (2012) ■

Archives of Medical Research

ORIGINAL ARTICLE

Calcium-induced Cardiac Mitochondrial Dysfunction Is Predominantly Mediated by Cyclosporine A-dependent Mitochondrial Permeability Transition Pore But Not Mitochondrial Calcium Uniporter

Q1 Chontida Yarana,[a] Jirapas Sripetchwandee,[a] Jantira Sanit,[a] Siriporn Chattipakorn,[a,b] and Nipon Chattipakorn[a,c]

[a]*Cardiac Electrophysiology Research and Training Center, Faculty of Medicine,* [b]*Department of Oral Biology and Diagnostic Science, Faculty of Dentistry,* [c]*Biomedical Engineering Center, Chiang Mai University, Chiang Mai, Thailand*

Received for publication January 16, 2012; accepted June 6, 2012 (ARCMED-D-12-00035).

Background and Aims. Cardiac mitochondrial Ca^{2+} overload plays a critical role in mechanical and electrical dysfunction leading to cardiac cell death and fatal arrhythmia. Because Ca^{2+} overload is related to mitochondrial permeability transition, reactive oxygen species (ROS) production and membrane potential ($\Delta\Psi m$) dissipation, we probed the mechanistic association between Ca^{2+} overload, oxidative stress, mitochondrial permeability transition pore (mPTP) and mitochondrial calcium uniporter (MCU) in isolated cardiac mitochondria.

Methods. Various concentrations of Ca^{2+} (5−200 μM) were used to induce mitochondrial dysfunction. Cyclosporin A (CsA, an mPTP blocker) and Ru360 (an MCU blocker) were used to test its protective effects on Ca^{2+}-induced mitochondrial dysfunction.

Results. High concentrations of Ca^{2+} (≥100 μM) caused overt mitochondrial swelling and $\Delta\Psi m$ collapse. However, only slight increases in ROS production were detected. Blocking the MCU by Ru360 is less effective in protecting mitochondrial dysfunction.

Conclusions. A dominant cause of Ca^{2+}-induced cardiac mitochondrial dysfunction was mediated through the mPTP rather than MCU. Therefore, CsA could be more effective than Ru360 in preventing Ca^{2+}-induced cardiac mitochondrial dysfunction. © 2012 IMSS. Published by Elsevier Inc.

Key Words: Cardiac mitochondria, Calcium, Permeability transition, Reactive oxygen species, Membrane potential.

Introduction

Intracellular Ca^{2+} overload of cardiomyocytes can lead to both electrical and mechanical dysfunction (1). Mitochondria play a crucial role in buffering cytosolic Ca^{2+} for maintaining physiological Ca^{2+} signals (2). When mitochondrial Ca^{2+} uptake exceeds a certain threshold level, the mitochondria can no longer regulate the intramitochondrial Ca^{2+}, resulting in the opening of mitochondrial permeability transition pore (mPTP) (3,4). Opening of mPTP allows the influx of water and solutes (<1500 Da) into the matrix causing mitochondrial swelling, mitochondrial membrane potential ($\Delta\Psi m$) collapse, and eventually cell death (2). However, the mechanism by which Ca^{2+} mediates the mPTP opening in cardiac cells is still controversial and varies in different models (5). Ca^{2+} overload also leads to the increase in reactive oxygen species (ROS) production (6−8). However, the relationship between Ca^{2+} overload, mPTP opening, $\Delta\Psi m$ change and oxidative stress is still elusive.

Cyclosporin A (CsA) is regarded as a potent inhibitor of mPTP by preventing the interaction of cyclophilin D and adenine nucleotide translocator (ANT). It has long been used to identify mPTP activity in various tissues (9,10) and has been proven to be a cardioprotective agent (11). Therefore, in this study we investigated the mechanistic association between Ca^{2+} overload, mitochondrial

Address reprint requests to: Nipon Chattipakorn, MD, PhD, Cardiac Electrophysiology Research and Training Center, Faculty of Medicine, Chiang Mai University, Chiang Mai 50200, Thailand; Phone: +66-53-945329; FAX: +66-53-945368; E-mail: nchattip@gmail.com

0188-4409/$ - see front matter.
http://dx.doi.org/10.1016/j.arcmed.2012.06.010

dysfunction, oxidative stress and the mPTP opening in cardiac mitochondria. Moreover, because the mitochondrial calcium uniporter (MCU) has been proposed as a principal portal for Ca^{2+} influx (12−14), we also investigated the effect of Ru360, a selective MCU blocker, against mitochondrial dysfunction. In the present study we tested the hypotheses that the mechanism of Ca^{2+}- induced cardiac mitochondrial dysfunction is mainly via the mPTP and the MCU.

Materials and Methods

Ethics Approval

This study was approved by the Institutional Animal Care and Use Committee at the Faculty of Medicine, Chiang Mai University.

Animals

Male Wistar rats (n = 18, 350−400 g) were obtained from the National Laboratory Animal Center, Mahidol University, Bangkok, Thailand. All animals were housed in a room with controlled temperature maintaining between 22 and 25°C with a constant 12 h light/dark cycle. Rats were fed with standard rat pellet diet and water ad libitum.

Experimental Protocols

Isolated cardiac mitochondria were used in all experiments. Various doses of $CaCl_2$ (5, 10, 100, 200 μM) were applied to isolated cardiac mitochondria for 10 min before the measurement of mitochondrial swelling, ROS production and ΔΨm dissipation. In addition, the effect of the mPTP blocker (CsA) and the MCU blocker (Ru360) on attenuating Ca^{2+}-induced mitochondrial dysfunction was also investigated. Isolated cardiac mitochondria were pretreated with CsA at the concentration of 5 μM for 30 min before the application of $CaCl_2$ (15) or with Ru360 10 μM for 5 min (16).

Isolation of Cardiac Mitochondria

Cardiac mitochondria were isolated according to the method described previously (17,18). Male Wistar rats weighing 350−400 g were anesthetized by isoflurane and thiopental (80 mg/kg), and the hearts were perfused with ice-cold normal saline. The heart was then removed, minced with razors, and homogenized in ice-cold isolation buffer containing sucrose 300 mM, TES 5 mM and EGTA 0.2 mM, pH 7.2 (4°C). The homogenate was centrifuged at 800 g for 5 min. The supernatant was collected and centrifuged at 8800 g for 5 min. The mitochondrial pellet was resuspended in ice-cold isolation buffer and finally centrifuged at 8800 g for 5 min. The mitochondrial pellet was suspended in 2 ml of respiration buffer containing 100 mM KCl, 50 mM sucrose, 10 mM HEPES, and 5 mM KH_2PO_4, pH 7.4, at 37°C. Mitochondrial protein concentration was measured using bicinchoninic acid (BCA) assay (19).

Identification of Cardiac Mitochondria with Electron Microscopy

Electron microscopy was used to identify the morphology of cardiac mitochondria (20). Isolated mitochondria were fixed overnight by mixing 2.5% glutaraldehyde in 0.1 M cacodylate buffer, pH 7.4, at 4°C. The pellet was then rinsed in cacodylate buffer and postfixed in 1% cacodylate-buffered osmium tetroxide for 2 h at room temperature. Next, the mitochondrial pellet was dehydrated in a graded series of ethanol and embeded in Epon-Araldite. The pellet was then cut into ultrathin sections (60−80 nm thick) using a diamond knife, placed on copper grids and stained with uranyl acetate and lead citrate. Finally, mitochondria were observed with a transmission electron microscope.

Measurement of Cardiac Mitochondrial Swelling

Mitochondria suspension was added with respiration buffer to a final concentration of 0.4 mg/ml. Cardiac mitochondrial swelling was determined by the decrease of light absorbance at 540 nm using a microplate reader (18−21).

Measurement of ROS Production

Cardiac mitochondria (0.4 mg/mL) were incubated with 2 μM dichlorohydro-fluorescein diacetate (DCFDA) at 25°C for 20 min. In the presence of ROS, DCFDA was oxidized to DCF and the fluorescence increased. Fluorescence was determined at 485 nm for excitation and 530 for emission. The ROS level was expressed in arbitrary units of fluorescence intensity of DCF (18).

Measurement of Mitochondrial Membrane Potential Change (ΔΨm)

The mitochondrial membrane potential change of isolated cardiac mitochondria were evaluated by using the dye 5,5′,6,6′- tetrachloro-1,1′,3,3′-tetraethylbenzimidazolcarbocyanine iodide (JC-1) (22,23). JC-1 is a lipophilic, cationic dye which can pass into mitochondria. When mitochondria have high ΔΨm, JC-1 is in the aggregate form, which shows red fluorescence. With low ΔΨm (i.e., depolarized state), it remains in monomeric form showing green fluorescence. The isolated mitochondria (0.4 mg/mL) were incubated with 310 nM JC-1 at 37°C for 30 min (18). Fluorescence intensity was measured using a fluorescent microplate reader. The green fluorescence of JC-1 monomer was excited at 485 nm and the emission was noticed at 530 nm. The red fluorescence of J-aggregates was excited at 485 nm and the emission was detected at 590

nm. The mitochondrial depolarization was indicated by a decrease in red/green fluorescence intensity ratio.

Statistical Analysis

Data were presented as mean ± SEM. Evaluation of the differences was made by two-way ANOVA followed by the Fisher post-hoc test. Statistical significance was considered at $p < 0.05$.

Chemicals

All reagents used in this study were purchased from Sigma (St. Louis, MO).

Results

Effects of Ca^{2+} on Cardiac Mitochondrial Swelling

When exposed with Ca^{2+} at 5 and 10 μM, cardiac mitochondrial swelling was not observed, whereas when exposed with Ca^{2+} at 100 μM and 200 μM, cardiac mitochondrial swelling was obviously seen as indicated by markedly decreased absorbance (Figure 1A). At 30 min after Ca^{2+} incubation, only the absorbance in the cardiac mitochondria exposed to 100 and 200 μM Ca^{2+} was significantly decreased, indicating cardiac mitochondrial swelling, compared to the control (Figure 1A). Data from the decrease in absorbance were confirmed by the morphology of mitochondria taken from the electron microscope. Ca^{2+} at 200 μM caused severe morphological change of cardiac mitochondria, evidenced by matrix expansion and unfolding of the cristae (Figure 1B).

Effect of Ca^{2+} on Cardiac Mitochondrial ROS Production and ΔΨm Change

At low doses of Ca^{2+} (5 and 10 μM), the ROS level was not different from the control (Figure 2A). When the cardiac mitochondria were exposed to high doses of Ca^{2+} (100 and 200 μM), a small but significant increase of ROS level was observed. However, data from ΔΨm showed that 10 μM Ca^{2+} could trigger mitochondrial membrane depolarization without the change in ROS production (Figure 2B). Further, a high concentration of Ca^{2+} (100 and 200 μM) induced more ΔΨm dissipation than the low concentration (Figure 2B).

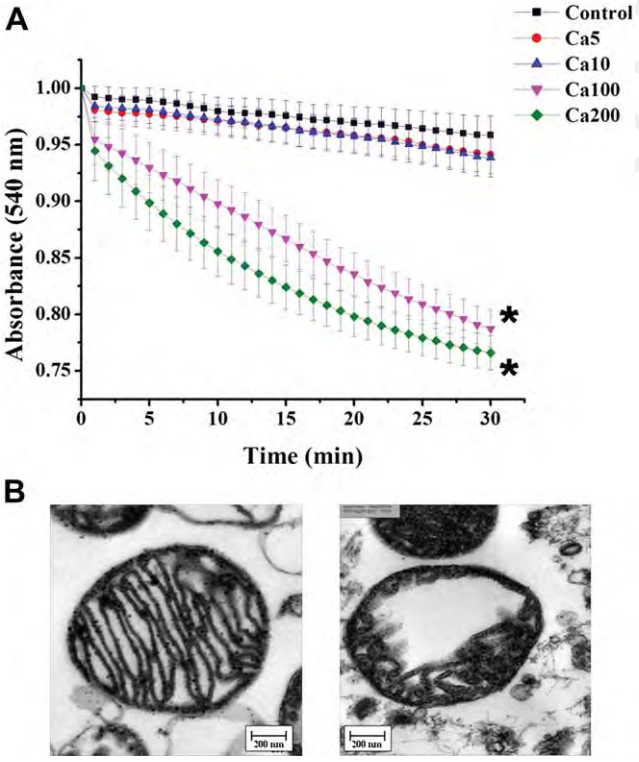

Figure 1. Cardiac mitochondrial swelling in response to increasing concentration of Ca^{2+}. (A) Kinetic study of cardiac mitochondrial swelling. (B) Effect of Ca^{2+}on morphological change of cardiac mitochondria. Isolated cardiac mitochondria without Ca^{2+} (left) and with 200 μM Ca^{2+} (right), Magnifications: 1:15,000. Control: isolated cardiac mitochondria without Ca^{2+} exposure. Ca5, Ca10, Ca100, Ca200: Ca^{2+}-treated mitochondria at 5, 10, 100, and 200 μM, respectively. *$p < 0.05$ vs. control.

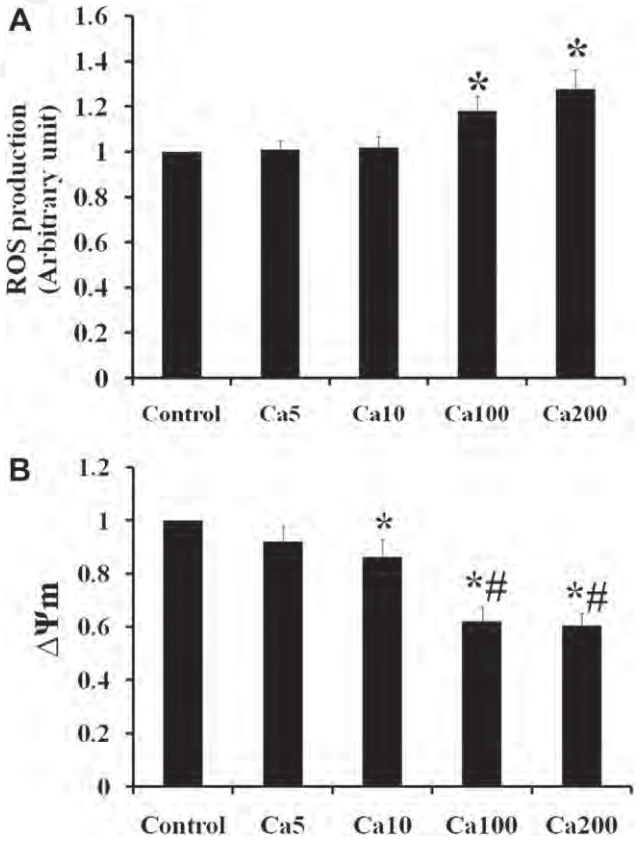

Figure 2. Effects of Ca^{2+} on cardiac mitochondrial ROS production (A) and ΔΨm change (B). Control: isolated cardiac mitochondria without Ca^{2+} exposure, Ca5, Ca10, Ca100, Ca200: Ca^{2+}-treated mitochondria at 5, 10, 100, and 200 μM, respectively. *$p < 0.05$ vs. control, #$p < 0.05$ vs. Ca10.

Effects of CsA and Ru360 on Mitochondrial Dysfunction

From the kinetic curve of the absorbance, it was found that CsA could apparently protect cardiac mitochondrial swelling especially in early Ca^{2+}-overloaded time points, i.e., the first 15 min (Figure 3A). However, Ru360 could modestly protect cardiac mitochondria from Ca^{2+}-induced swelling (Figure 3A). At 15 min after 200 μM Ca^{2+} loading, CsA could completely protect cardiac mitochondrial swelling, whereas Ru360 provided only partial protection (Figure 3B). Nevertheless, at 30 min after Ca^{2+} exposure, CsA could only partially protect mitochondrial swelling and Ru360 could no longer mitigate the swelling (Figure 3C). CsA and Ru360 alone did not alter mitochondrial ROS and membrane potential (Figure 4). CsA, as well as Ru360, could completely prevent Ca^{2+}-induced ROS production of cardiac mitochondria. However, the level of ROS attenuation by CsA is larger than Ru360 (Figure 4A). For the mitochondrial membrane potential, both CsA and Ru360 could only partially attenuate ΔΨm collapse in cardiac mitochondria (Figure 4B). When the concentration of CsA and Ru360 was decreased in half, it was still effective in attenuating mitochondrial dysfunction (Figure 4). However, CsA at a lower dose had lower effectiveness in preventing mitochondrial depolarization.

Discussion

In the present study the major findings are that in cardiac mitochondria overloaded with Ca^{2+}: 1) mitochondrial swelling, elevated ROS production and mitochondrial membrane depolarization were observed; 2) CsA pretreatment could completely prevent cardiac mitochondrial swelling in the first 15 min after Ca^{2+} exposure, protect ROS production, and partially alleviate ΔΨm dissipation; and 3) Ru360 pretreatment could not completely avert mitochondrial swelling, although it could attenuate ROS production and partially block ΔΨm collapse.

In the heart under physiological condition, Ca^{2+} plays an important part in mitochondrial oxidative-phosphorylation which enhances ATP production to support contractile activity and ion transport systems of myocardium (24). However, excessive Ca^{2+} loading occurring during cardiac ischemia/reperfusion can trigger mPTP opening and lead to apoptotic cell death (25,26). In the present study we found that Ca^{2+} at 5 μM did not cause cardiac mitochondrial swelling, ROS production, and ΔΨm collapse. However, 10 μM Ca^{2+} could induce slight mitochondrial depolarization. This finding may represent the role of low-dose Ca^{2+} in physiological process. Depolarization of cardiac mitochondria following 10 μM Ca^{2+} may be due to Ca^{2+} influx down a potential gradient (27) and be related to Ca^{2+} uptake through the MCU, which occurs only when the concentration of Ca^{2+} reaches 10 μM (28). With exposure of high concentrations of Ca^{2+} (100 and 200 μM), cardiac

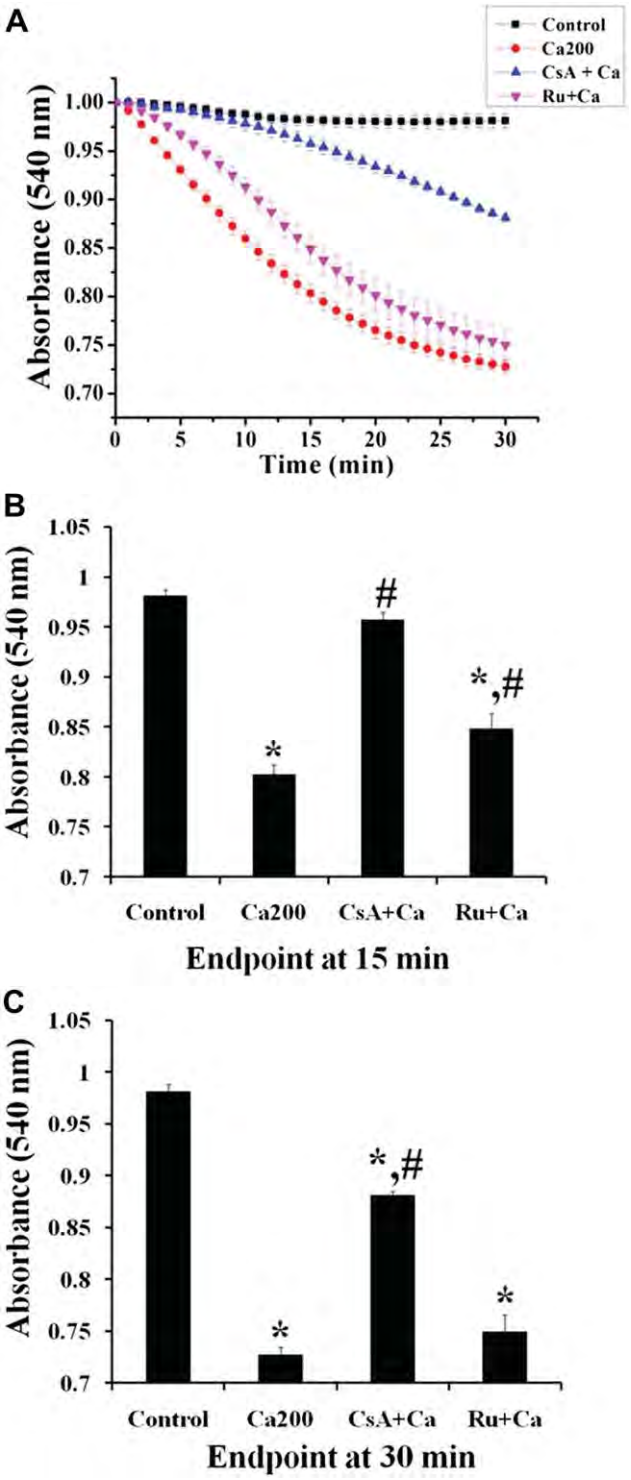

Figure 3. Effects of CsA and Ru360 on cardiac mitochondrial swelling. (A) Kinetic study of cardiac mitochondrial swelling. (B) Mitochondrial swelling at 15 min after 200 μM Ca^{2+} exposure. (C) Mitochondrial swelling at 30 min after 200 μM Ca^{2+} exposure. Control: isolated cardiac mitochondria without Ca^{2+} exposure, Ca200: Ca^{2+}-treated mitochondria at 200 μM, CsA + Ca: mitochondria pretreated with CsA followed by 200 μM Ca^{2+} application, Ru + Ca: mitochondria pretreated with Ru360 followed by 200 μM Ca^{2+} application. *p <0.05 vs. control, #p <0.05 vs. Ca200.

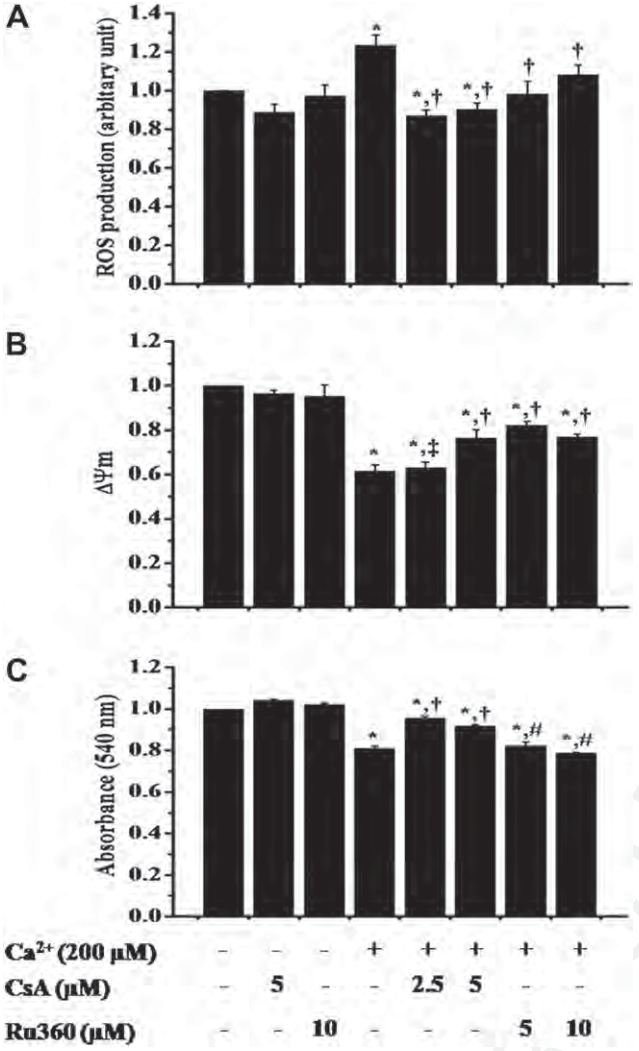

Figure 4. Effects of CsA and Ru360 on cardiac mitochondrial ROS production. (A) ΔΨm dissipation (B) and mitochondrial swelling. (C) Neither CsA nor Ru360 alone altered any determined parameters. CsA at 2.5 and 5 μM, and Ru360 at 5 and 10 μM provided similar results on ROS production and mitochondrial swelling. *p <0.05 vs. control, †p <0.05 vs. Ca^{2+} treatment, ‡p <0.05 vs. 5 μM CsA+Ca^{2+}, #p <0.05 vs. CsA+Ca^{2+}.

mitochondria became more depolarized and obviously swelling, observed by the decreasing of absorbance and severe morphological changes in electron microscopy. These high concentrations of Ca^{2+} could also induce oxidative stress by increasing ROS production. However, in cardiac mitochondria, Ca^{2+}-induced ROS production was observed in the condition in which complex III in the electron transport chain was inhibited (29). The increase in ROS production, which enhanced by Ca^{2+} alone, has been shown to be due to the loss of cytochrome c or glutathione-antioxidant enzymes through the mPTP (30,31). Our findings supported the hypothesis of Ca^{2+} threshold for the mPTP opening (32).

For the protective effects of CsA, our results demonstrated that within 15 min after Ca^{2+} exposure, CsA could completely prevent cardiac mitochondria from swelling, consistent with the effect on protecting ROS production. Therefore, it could be implied that the opening of mPTP plays a critical role in cardiac mitochondrial dysfunction in conditions of early Ca^{2+} overload. However, CsA could only partially prevent ΔΨm collapse because inhibition of mPTP did not block Ca^{2+} influx and, therefore, did not prevent alteration of the electron gradient across the inner membrane. The protective effect of CsA was attenuated in the next 15 min after Ca^{2+} exposure when the extent of mitochondrial swelling was so large that CsA no longer prevented mitochondrial swelling. Because the CsA could not inhibit Ca^{2+} influx into the mitochondria, high Ca^{2+} accumulation occurred in late Ca^{2+} exposure and could competitively interfere with the effect of CsA at mPTP, resulting in partial mPTP opening and later mitochondrial swelling (33,34).

As mitochondrial Ca^{2+} overload is a key factor of mPTP opening and the MCU has been proposed as a dominant portal of Ca^{2+} influx (12−14), we also further investigated the effect of Ru360, a selective MCU blocker against cardiac mitochondrial dysfunction. We found that Ru360 could decrease ROS production, although to a lesser extent than CsA. Moreover, Ru360 could not prevent mitochondrial swelling from Ca^{2+} overload in both early and late Ca^{2+} exposure. Considering the partial effect of Ru360 on inhibition of ΔΨm collapse, this finding suggested that Ca^{2+} may possibly enter the matrix through alternative pathways other than the MCU. Recently, growing bodies of evidence of other mechanisms related to mitochondrial Ca^{2+} influx have been reported. These mechanisms include mitochondrial ryanodine receptor (35,36), a rapid mode of Ca^{2+} uptake (36), mitochondrial uncoupling proteins (37), and leucine zipper EF hand-containing transmembrane protein 1 (LETM1) Ca^{2+}/H^{+} antiporter (38). Ca^{2+} influx through these alternative Ca^{2+} uptake channels could also trigger mPTP opening. Therefore, Ru360 may not be a promising agent for protecting cardiac mitochondrial dysfunction from calcium overload. Nevertheless, because this was an *in vitro* study performed in isolated cardiac mitochondria, there may be some limitations in that isolated mitochondria lack the effects of the cellular environment, which can interfere with the biological response. Also, direct intracellular calcium measurement, as well as calcium retention capacity, was not investigated in the present study. Future *in vivo* studies are needed to confirm the efficacy of both agents as well as to seek for the roles of those possible alternative portals for calcium entry to warrant their possible therapeutic use.

In conclusion, our finding suggested that Ca^{2+}-induced cardiac mitochondrial swelling, ROS production and ΔΨm dissipation is due to mPTP opening. Moreover, MCU may not be the principal pathway for cardiac mitochondrial Ca^{2+} uptake. CsA but not Ru360, was shown to be an effective agent against calcium-induced cardiac mitochondrial dysfunction.

Acknowledgments

This study is supported by research grants from the Thailand Research Fund RTA5280006 (NC), BRG5480003 (SC) and Chiang Mai University Young Researcher Fund (CY).

References

1. Vassalle M, Lin CI. Calcium overload and cardiac function. J Biomed Sci 2004;11:542−565.
2. Smaili SS, Hsu YT, Youle RJ, et al. Mitochondria in Ca2+ signaling and apoptosis. J Bioenerg Biomembr 2000;32:35−46.
3. Gustafsson AB, Gottlieb RA. Heart mitochondria: gates of life and death. Cardiovasc Res 2008;77:334−343.
4. Odagiri K, Katoh H, Kawashima H, et al. Local control of mitochondrial membrane potential, permeability transition pore and reactive oxygen species by calcium and calmodulin in rat ventricular myocytes. J Mol Cell Cardiol 2009;46:989−997.
5. Lemasters JJ, Theruvath TP, Zhong Z, et al. Mitochondrial calcium and the permeability transition in cell death. Biochim Biophys Acta 2009;1787:1395−1401.
6. Paradies G, Petrosillo G, Pistolese M, et al. Decrease in mitochondrial complex I activity in ischemic/reperfused rat heart: involvement of reactive oxygen species and cardiolipin. Circ Res 2004;94:53−59.
7. Petrosillo G, Ruggiero FM, Paradies G. Role of reactive oxygen species and cardiolipin in the release of cytochrome c from mitochondria. FASEB J 2003;17:2202−2208.
8. Pasdois P, Parker JE, Griffiths EJ, et al. The role of oxidized cytochrome c in regulating mitochondrial reactive oxygen species production and its perturbation in ischaemia. Biochem J 2011;436:493−505.
9. Halestrap AP, Connern CP, Griffiths EJ, et al. Cyclosporin A binding to mitochondrial cyclophilin inhibits the permeability transition pore and protects hearts from ischaemia/reperfusion injury. Mol Cell Biochem 1997;174:167−172.
10. Kilbaugh TJ, Bhandare S, Lorom DH, et al. Cyclosporin A preserves mitochondrial function after traumatic brain injury in the immature rat and piglet. J Neurotrauma 2011;28:763−774.
11. Arbustini E, Narula J. Cyclosporin a in reperfusion injury: not opening to cell death knocking at the door? Ann Thorac Surg 2010;89:1349−1351.
12. Kirichok Y, Krapivinsky G, Clapham DE. The mitochondrial calcium uniporter is a highly selective ion channel. Nature 2004;427:360−364.
13. Matlib MA, Zhou Z, Knight S, et al. Oxygen-bridged dinuclear ruthenium amine complex specifically inhibits Ca2+ uptake into mitochondria in vitro and in situ in single cardiac myocytes. J Biol Chem 1998; 273:10223−10231.
14. Garcia-Rivas Gde J, Carvajal K, Correa F, et al. Ru360, a specific mitochondrial calcium uptake inhibitor, improves cardiac post-ischaemic functional recovery in rats in vivo. Br J Pharmacol 2006; 149:829−837.
15. Kobayashi T, Kuroda S, Tada M, et al. Calcium-induced mitochondrial swelling and cytochrome c release in the brain: its biochemical characteristics and implication in ischemic neuronal injury. Brain Res 2003;960:62−70.
16. Zhang SZ, Gao Q, Cao CM, et al. Involvement of the mitochondrial calcium uniporter in cardioprotection by ischemic preconditioning. Life Sci 2006;78:738−745.
17. Larche J, Lancel S, Hassoun SM, et al. Inhibition of mitochondrial permeability transition prevents sepsis-induced myocardial dysfunction and mortality. J Am Coll Cardiol 2006;48:377−385.
18. Thummasorn S, Kumfu S, Chattipakorn S, et al. Granulocyte-colony stimulating factor attenuates mitochondrial dysfunction induced by oxidative stress in cardiac mitochondria. Mitochondrion 2011;11: 457−466.
19. Walker JM. The bicinchoninic acid (BCA) assay for protein quantitation. Methods Mol Biol 1994;32:5−8.
20. Chelli B, Falleni A, Salvetti F, et al. Peripheral-type benzodiazepine receptor ligands: mitochondrial permeability transition induction in rat cardiac tissue. Biochem Pharmacol 2001;61:695−705.
21. Ruiz-Meana M, Garcia-Dorado D, Miro-Casas E, et al. Mitochondrial Ca2+ uptake during simulated ischemia does not affect permeability transition pore opening upon simulated reperfusion. Cardiovasc Res 2006;71:715−724.
22. Tong V, Teng XW, Chang TK, et al. Valproic acid II: effects on oxidative stress, mitochondrial membrane potential, and cytotoxicity in glutathione-depleted rat hepatocytes. Toxicol Sci 2005;86: 436−443.
23. Di Lisa F, Blank PS, Colonna R, et al. Mitochondrial membrane potential in single living adult rat cardiac myocytes exposed to anoxia or metabolic inhibition. J Physiol 1995;486(Pt 1):1−13.
24. Balaban RS. The role of Ca^{2+} signaling in the coordination of mitochondrial ATP production with cardiac work. Biochim Biophys Acta 2009;1787:1334−1341.
25. Halestrap AP, Pasdois P. The role of the mitochondrial permeability transition pore in heart disease. Biochim Biophys Acta 2009;1787: 1402−1415.
26. Di Lisa F, Bernardi P. Mitochondria and ischemia-reperfusion injury of the heart: fixing a hole. Cardiovasc Res 2006;70:191−199.
27. Gunter TE, Pfeiffer DR. Mechanisms by which mitochondria transport calcium. Am J Physiol 1990;258(5 Pt 1):C755−C786.
28. Santo-Domingo J, Demaurex N. Calcium uptake mechanisms of mitochondria. Biochim Biophys Acta 2010;1797:907−912.
29. Cadenas E, Boveris A. Enhancement of hydrogen peroxide formation by protophores and ionophores in antimycin-supplemented mitochondria. Biochem J 1980;188:31−37.
30. Peng TI, Jou MJ. Oxidative stress caused by mitochondrial calcium overload. Ann NY Acad Sci 2010;1201:183−188.
31. Luetjens CM, Bui NT, Sengpiel B, et al. Delayed mitochondrial dysfunction in excitotoxic neuron death: cytochrome c release and a secondary increase in superoxide production. J Neurosci 2000;20: 5715−5723.
32. Schild L, Keilhoff G, Augustin W, et al. Distinct Ca2+ thresholds determine cytochrome c release or permeability transition pore opening in brain mitochondria. FASEB J 2001;15:565−567.
33. Halestrap AP, Clarke SJ, Javadov SA. Mitochondrial permeability transition pore opening during myocardial reperfusion−a target for cardioprotection. Cardiovasc Res 2004;61:372−385.
34. Halestrap AP, Brenner C. The adenine nucleotide translocase: a central component of the mitochondrial permeability transition pore and key player in cell death. Curr Med Chem 2003;10:1507−1525.
35. Altschafl BA, Beutner G, Sharma VK, et al. The mitochondrial ryanodine receptor in rat heart: a pharmaco-kinetic profile. Biochim Biophys Acta 2007;1768:1784−1795.
36. Beutner G, Sharma VK, Lin L, et al. Type 1 ryanodine receptor in cardiac mitochondria: transducer of excitation-metabolism coupling. Biochim Biophys Acta 2005;1717:1−10.
37. Waldeck-Weiermair M, Duan X, Naghdi S, et al. Uncoupling protein 3 adjusts mitochondrial Ca^{2+} uptake to high and low Ca^{2+} signals. Cell Calcium 2010;48:288−301.
38. Waldeck-Weiermair M, Jean-Quartier C, Rost R, et al. Leucine zipper EF hand-containing transmembrane protein 1 (Letm1) and uncoupling proteins 2 and 3 (UCP2/3) contribute to two distinct mitochondrial Ca2+ uptake pathways. J Biol Chem 2011;286:28444−28455.

Life Sciences 90 (2012) 808–814

Contents lists available at SciVerse ScienceDirect

Life Sciences

journal homepage: www.elsevier.com/locate/lifescie

Synaptic and nonsynaptic mitochondria demonstrate a different degree of calcium-induced mitochondrial dysfunction

Chontida Yarana [a], Jantira Sanit [a], Nipon Chattipakorn [a,b], Siriporn Chattipakorn [a,c,*]

[a] Neuroelectrophysiology Unit, Cardiac Electrophysiology Research and Training Center, Faculty of Medicine, Chiang Mai University, Chiang Mai, Thailand
[b] Biomedical Engineering Center, Chiang Mai University, Chiang Mai, Thailand
[c] Department of Oral Biology and Diagnostic Science, Faculty of Dentistry, Chiang Mai University, Chiang Mai, Thailand

ARTICLE INFO

Article history:
Received 30 September 2011
Accepted 5 April 2012

Keywords:
Synaptic
Nonsynaptic
Mitochondria
Ca^{2+}
ROS production
Membrane potential

ABSTRACT

Aims: Since variety in response to Ca^{2+}-induced mitochondrial dysfunction in different neuronal mitochondrial populations is associated with the pathogenesis of several neurological diseases, we investigated the effects of Ca^{2+} overload on synaptic (SM) and nonsynaptic mitochondrial (NM) dysfunction and probed the effects of cyclosporin A (CsA), 4′-chlorodiazepam (CDP) and Ru360 on relieving mitochondrial damage.
Main methods: SM and NM mitochondria were isolated from rats' brains (n = 5/group) and treated with various concentrations (5, 10, 100, and 200 μM) of Ca^{2+}, with and without CsA (mPTP blocker), CDP (PBR/TSPO blocker) and Ru360 (MCU blocker) pretreatments. Mitochondrial function was determined by mitochondrial swelling, ROS production and mitochondrial membrane potential changes (ΔΨm).
Key findings: At 200-μM Ca^{2+}, SM presented mitochondrial swelling to a greater extent than NM. At 100 and 200-μM Ca^{2+}, the ROS production of SM was higher than that of NM and ΔΨm dissipation of SM was also larger. CsA, CDP and Ru360 could reduce ROS production of SM and NM with exposure to 200-μM Ca^{2+}. However, only Ru360 could completely inhibit ROS generation in both SM and NM, whereas CsA and CDP could only partially reduce the ROS level in SM. Moreover, CsA and CDP pretreatments were not able to restore ΔΨm. However, Ru360 pretreatment could protect ΔΨm dissipation in both SM and NM, with complete protection observed only in NM.
Significance: Our findings suggested that mitochondrial calcium uniporter is a possible major pathway for calcium uptake in both mitochondrial populations. However, SM might have additional pathways involved in the calcium uptake.

Introduction

Mitochondria are critical regulators of neuronal cell survival and cell death (Boitier et al., 1999; Hyder et al., 2006; Murchison and Griffith, 2007; Yuan and Yankner, 2000). The pathophysiology of numerous neurological disorders, such as ischemic-reperfusion injury (Blomgren et al., 2003; Pandya et al., 2011), traumatic brain injury (Friberg and Wieloch, 2002; Norenberg and Rao, 2007) and neurodegenerative diseases (Reddy and Reddy, 2011; Reeve et al., 2008), is related to mitochondrial dysfunction, which leads to neuronal apoptosis. The most important factor inducing mitochondrial dysfunction is Ca^{2+} overload, which primarily occurs during neuroexcitotoxicity (Duchen, 2004; Nicholls, 2009; Starkov et al., 2004). Ca^{2+} overload is involved with mitochondrial membrane potential depolarization (ΔΨm dissipation), which has been proposed as an initiator as well as a consequence of mitochondrial transition pore (mPTP) opening (Ly et al., 2003; Wadia et al., 1998). Reactive oxygen species (ROS) are also crucial players in neuronal mitochondrial dysfunction (Wang et al., 2011). However, the relationship between Ca^{2+} overload and ROS in brain mitochondria is diverse depending on experimental conditions (Gyulkhandanyan and Pennefather, 2004; Komary et al., 2008; Panov et al., 2007; Petrosillo et al., 2004; Schonfeld and Reiser, 2007; Votyakova and Reynolds, 2005). Moreover, the correlation between Ca^{2+}-induced mitochondrial damage, ΔΨm dissipation, and ROS production is still controversial (Adam-Vizi and Starkov, 2010).

Brain mitochondria are classified into two groups, the synaptic mitochondria (SM) and the nonsynaptic mitochondria (NM). The properties of these two types of mitochondria especially in Ca^{2+} handling are different (Guo et al., 2005; Li et al., 2004). SM, which are located around the synapse, are exposed to extensive Ca^{2+} fluctuations and are at high risk for oxidative stress and Ca^{2+} accumulative damages (Banaclocha et al., 1997; Martinez et al., 1996). A previous study reported that the difference in the Ca^{2+}-induced mPTP opening could be due to the higher level of cyclophilin D (CypD) in SM (Naga et al., 2007). However, direct inhibition of CypD by cyclosporine A (CsA) cannot increase the Ca^{2+} accumulation capacity in SM (Brown et al., 2006), suggesting that additional mechanisms are likely

* Corresponding author at: Department of Oral Biology and Diagnostic Science, Faculty of Dentistry, Chiang Mai University, Chiang Mai, 50200, Thailand. Tel.: +66 53 945329; fax: +66 53 945368.
E-mail address: s.chat@chiangmai.ac.th (S. Chattipakorn).

0024-3205/$ – see front matter © 2012 Elsevier Inc. All rights reserved.
doi:10.1016/j.lfs.2012.04.004

responsible for the differences in Ca^{2+} handling in SM and NM. The main portal pathway for Ca^{2+} uptake of neuronal mitochondria proposed by previous studies is the mitochondrial calcium uniporter (MCU). However, subsequent studies of other tissues have discovered additional Ca^{2+} uptake mechanisms such as the rapid mode of Ca^{2+} uptake (RAM) (Buntinas et al., 2001; Sparagna et al., 1995), and the mitochondrial ryanodine receptor (mRYR) (Altschafl et al., 2007; Beutner et al., 2001; Beutner et al., 2005). Moreover, the Ca^{2+} uptake mechanism of SM and NM in the Ca^{2+} overload condition has not been investigated and whether Ca^{2+} entry via MCU in the SM and NM is different is not known. Therefore, in this study, we tested the hypothesis that 1) SM respond to Ca^{2+} overload conditions in a different way from NM, and 2) the mechanisms for Ca^{2+} entry via MCU in the SM and NM are different.

Materials and methods

Reagents

All of the reagents used in this study were purchased from Sigma (St. Louis, MO., USA), except Ru360, which was purchased from Calbiochem (San Diego, CA., USA).

Bovine serum albumin (BSA) and pyruvic acid were purchased from Amresco (Solon, OH., USA). CsA and CDP were prepared in DMSO and further diluted to final concentrations by 2% DMSO. Ru360 was prepared in deionized water.

Animal preparation

This study was approved by the Institutional Animal Care and Use Committee at the Faculty of Medicine, Chiang Mai University. Wistar rats (300–400 g) were obtained from the National Laboratory Animal Center, Mahidol University, Bangkok, Thailand. All animals were housed in a controlled room temperature maintained between 22 and 25 °C in a constant 12-h light/dark cycle. They were fed with standard pellet rat diet and water ad libitum.

Experimental protocols

Isolated mitochondria from synaptosomes and nonsynaptosomes of rat cortical brains were used as in a previous study (Chelli et al., 2001; Novalija et al., 2003; Thummasorn et al., 2011; Tong et al., 2005). The first protocol was to investigate the effect of Ca^{2+}-induced mitochondrial dysfunction on synaptic versus nonsynaptic mitochondria in the morphological aspects of mitochondrial swelling, ROS production and $\Delta\Psi m$ dissipation. In this study, $CaCl_2$ at concentrations of 5, 10, 100 and 200 μM were used (n = 6/group for ROS and $\Delta\Psi m$ measurements). Various doses of $CaCl_2$ were applied for 10 min to isolated mitochondria before the assessment of all parameters. In the second protocol, the mechanism underlying the differences in Ca^{2+} responses of SM and NM was investigated by several pharmacological interventions: cyclosporine A (CsA), 4′-chlorodiazepam (CDP) and Ru360 (as shown in Fig. 1). CsA is known as a mitochondrial permeability transition pore blocker, CDP is the specific peripheral benzodiazepine receptor (or presently known as translocator protein; TPSO) antagonist, and Ru360 is the mitochondrial calcium uniporter blocker. In the second protocol, both SM and NM were randomly assigned into eight groups: control (vehicle), CsA (5 μM), CDP (100 μM), Ru360 (10 μM), $CaCl_2$ (200 μM), $CaCl_2$ pretreated with CsA, $CaCl_2$ pretreated with CDP and $CaCl_2$ pretreated with Ru360 (n = 5/group). CsA and CDP were applied to the mitochondria for 30 min prior to exposure to Ca^{2+} or vehicle for 30 min, while Ru360 was added at 3 min before Ca^{2+} exposure. Doses of all blockers were used according to those reported previously (Thummasorn et al., 2011; Zhang et al., 2006).

Isolation of nonsynaptic brain mitochondria

Nonsynaptic brain mitochondria were isolated from 300–350 g male Wistar rats using a method modified from that described in a previous study (Lai and Clark, 1979; Clark and Nicklas, 1970; Krasnikov et al., 2005). Following decapitation, brains were rapidly removed and placed in ice-cold isolation buffer containing 320 mM sucrose, 10 mM HEPES, and 0.5 mM EGTA at pH 7.4. All homogenization and centrifugation steps were carried out at 4 °C. The cortices were chopped into small pieces with razors. Then, the brains were homogenized by the homogenizer containing 10 ml of isolation buffer. The homogenate was centrifuged at 1300 *g* for 3 min. The supernatant was centrifuged at 1300 *g* for 3 min. The supernatant was collected and centrifuged at 17,000 *g* for 8 min. The pellets obtained from this step were suspended in 3 ml of isolation buffer and applied to the top of 3 ml of 10% (w/v) Ficoll overlaid by 3 ml of 7.5% (w/v) Ficoll. After centrifugation at 99,000 *g* for 20 min, aliquots were removed. The nonsynaptic mitochondria-containing pellets at the bottom of the tube were resuspended in isolation buffer and recentrifuged at 12,000 *g* for 8 min. The pellet was resuspended in an isolation buffer supplemented with 0.5 mg/ml BSA and centrifuged at 12,000 *g* for 8 min. Protein concentration was determined using a Bicinchoninic Acid (BCA) assay with bovine serum albumin used as a concentration standard (Walker, 1994).

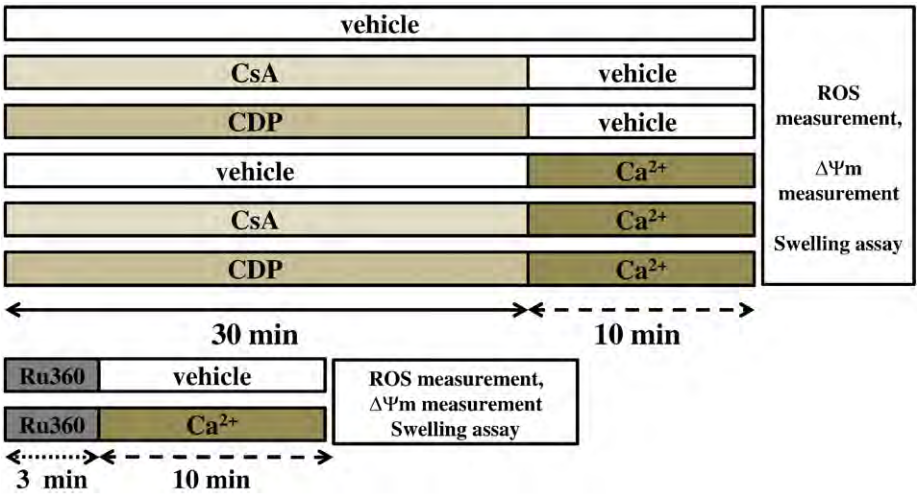

Fig. 1. Study protocol to determine the effects of cyclosporine A (CsA), 4′-chlorodiazepam (CDP) and Ru360 on Ca^{2+}-induced mitochondrial dysfunction.

Isolation of synaptic brain mitochondria

Brain synaptic mitochondria from male Wistar rats (300–350 g) were isolated according to the method described in a previous study (Kudin et al., 2004; Pallotti and Lenaz, 2007; Berman et al., 2000; Gangolf et al., 2010; Rosenthal et al., 1987) using 0.02% digitonin to free mitochondria from the synaptosomal fraction. After decapitation, the brain was transferred to ice-cold MSE solution (225 mM mannitol, 75 mM sucrose, 1 mM EGTA, 5 mM HEPES, 1 mg/ml BSA, pH 7.4), minced and transferred to 10 ml of MSE solution containing 0.05% nagarse for homogenizations. Then, the homogenate was centrifuged at 2 000 *g* for 4 min. The supernatant was centrifuged at 12,000 *g* for 9 min. The synaptosome-enriched pellets were resuspended in MSE containing 0.02% digitonin and centrifuged at 12,000 *g* for 11 min.

Identification of mitochondria with electron microscopy

Isolated mitochondria were fixed overnight in 2.5% glutaraldehyde in 0.1 M cacodylate buffer, pH 7.4 at 4 °C, postfixed with 1% cacodylate-buffered osmium tetroxide for 2 h at room temperature. Then, the pellets were dehydrated in a graded series of ethanol and embedded in Epon–Araldite as described in a previous study (Chelli et al., 2001).

After being cut with a diamond knife, ultrathin sections were placed on copper grids, stained with uranyl acetate and lead citrate, and observed with a transmission electron microscope.

Mitochondria were classified into two categories; intact mitochondria and damaged mitochondria. Intact mitochondria were characterized by condensed cristae and an uninterrupted outer membrane. Conversely, damaged mitochondria or mitochondrial swelling is described as fragmented cristae or an interrupted outer membrane and expanding matrix (Lifshitz et al., 2003).

Measurement of mitochondrial ROS production

ROS production in mitochondria was determined spectrofluorometrically, using dichlorohydro-fluorescein diacetate (DCFDA) (Novalija et al., 2003). Synaptic or nonsynaptic mitochondria (0.4 mg/ml) were incubated with 2 μM DCFDA at 25 °C for 20 min. Fluorescence was determined at 485 nm for excitation and 530 nm for emission. The ROS level was manifested as arbitrary units of fluorescence intensity of DCF as described in a previous study (Thummasorn et al., 2011).

Measurement of mitochondrial membrane potential (ΔΨm)

The dye 5,5′,6,6′-tetrachloro-1,1′,3,3′-tetraethylbenzimidazolcarbocyanine iodide (JC-1) was used to assess the change in ΔΨm as described in a previous study (Tong et al., 2005). Decreased red/green fluorescent intensity ratio indicates mitochondrial depolarization (Perry et al., 2011). The isolated mitochondria (0.4 mg/ml) were incubated with 310 nM JC-1 at 37 °C for 30 min.

Fluorescence intensity was measured by a fluorescence microplate reader using 485- and 530-nm (green) wavelengths for the excitation and 485- and 590 nm (red) for the emission.

Measurement of mitochondrial swelling

Mitochondrial swelling was assessed by measuring changes in the absorbance of the suspension at the 540-nm wavelength using a microplate reader. SM or NM (0.4 mg/ml) were incubated in a 2-ml respiration buffer (containing 150 mM KCl, 5 mM HEPES, 5 mM $K_2HPO_4.3H_2O$, 2 mM L-glutamate, 5 mM pyruvate sodium salt). Decreased absorbance indicated mitochondrial swelling (Thummasorn et al., 2011).

Data analysis

All data were expressed as means ± SEM. Comparisons were made by one-way ANOVA followed by the Fisher post-hoc test. Results were statistically significant with $P<0.05$.

Results

Ca^{2+}-induced oxidative stress and mitochondrial membrane depolarization in SM and NM

At baseline, there was no significant difference between the ROS level in the SM (137.19 ± 21.53 au) and NM (155.48 ± 23.60 au), and the ΔΨm between SM (1.12 ± 0.20) and NM (0.67 ± 0.22). Ca^{2+} at 5 μM did not cause any changes in ROS production in either SM or NM (Fig. 2). However, Ca^{2+} at 10 μM increased the mitochondrial ROS production in NM, but not SM (Fig. 2). Ca^{2+} at 100 and 200 μM increased ROS production in a dose-dependent manner in both SM and NM (Fig. 2). We also found that SM generated significantly higher levels of ROS in response to 200-μM Ca^{2+} than did NM (Fig. 2). Low concentrations of Ca^{2+} (5, 10 μM) did not change the ΔΨm in either SM or NM (Fig. 3). When Ca^{2+} concentration was increased to 100 and 200 μM, the SM encountered mitochondrial depolarization in a dose dependent manner, as shown by an obvious decrease in ΔΨm dissipation. In NM, however, mitochondrial depolarization occurred only when treated with 200-μM Ca^{2+} (Fig. 3). Moreover, when applied with 100 and 200-μM Ca^{2+}, the level of SM ΔΨm dissipation was greater than that of NM (Fig. 3). In the swelling assay, we found that 5, 10 and 100-μM Ca^{2+} did not cause NM swelling, while the 100-μM Ca^{2+} started to cause SM swelling (Fig. 4). However, the 200-μM Ca^{2+} could cause both SM and NM swelling (Fig. 4). Consistent with the morphology changes (as shown in Fig. 5), the exposure of 200-μM Ca^{2+} in both SM and NM caused severe mitochondrial swelling. However, SM exhibited greater swelling and morphological changes than those from NM (Figs. 4 and 5).

Effects of CsA, CDP, and Ru360 on SM and NM ROS production

The levels of ROS production were not altered in either SM or NM applied with CsA, CDP or Ru360, alone (Fig. 6). The ROS levels were dramatically increased in both SM and NM treated with 200-μM Ca^{2+}

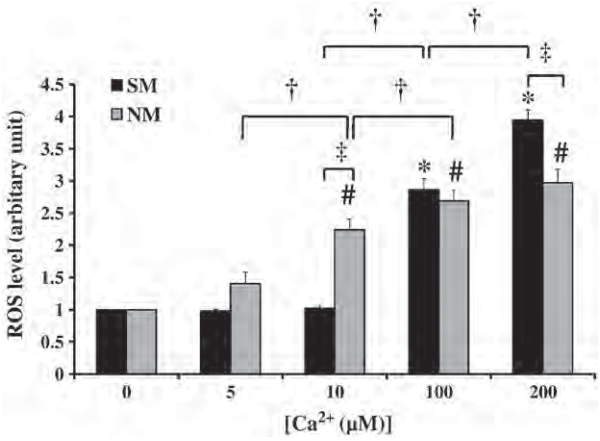

Fig. 2. ROS production in response to increasing concentration of Ca^{2+} in mitochondria isolated from synaptosomes and nonsynaptosomes (n = 8/group). 0, 5, 10, 100, and 200 = control group and $CaCl_2$-treated mitochondria at 5, 10, 100, and 200 μM, respectively. SM: synaptic mitochondria, NM: nonsynaptic mitochondria, *$P<0.05$ compared to the control group for SM, #$P<0.05$ compared to the control group for NM, †$P<0.05$ differences between different calcium concentrations at the same group, ‡$P<0.05$ differences between different groups at the same calcium concentration.

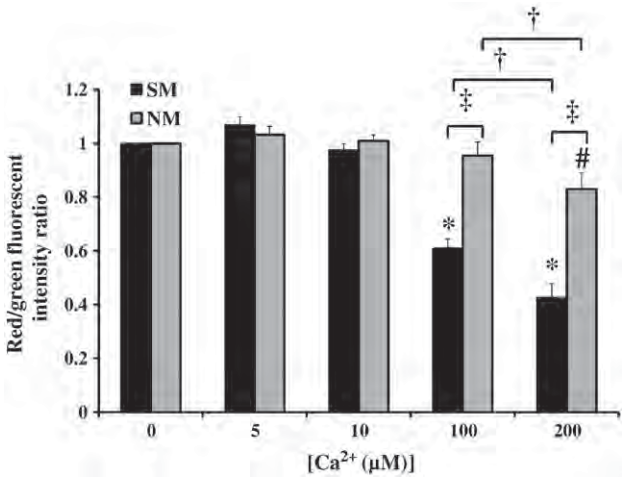

Fig. 3. Ca^{2+}-induced ΔΨm dissipation rates of mitochondria isolated from synaptosomes and nonsynaptosomes (n = 8/group). SM: synaptic mitochondria, NM: nonsynaptic mitochondria, *$P<0.05$ compared to the control group for SM, #$P<0.05$ compared to the control group for NM, †$P<0.05$ differences between different calcium concentrations in the same group, ‡$P<0.05$ differences between different groups at the same calcium concentration.

(Fig. 6). The ROS level, however, was increased to a much higher level in SM, than in NM. When CsA, CDP and Ru360 were applied to SM and NM prior to 200-μM Ca^{2+} application, the ROS levels were significantly reduced, compared to the Ca^{2+}-treated group. However, the ROS level in CsA and CDP pretreatment groups of SM was still greater than that in the control group, whereas the ROS level in NM was reduced to the same levels as the control group. In addition, the ROS levels in Ru360 pretreatment of both SM and NM were at the same levels as in the control group (Fig. 6).

Effects of CsA, CDP, and Ru360 on SM and NM membrane potential dissipation (ΔΨm)

At the baseline, CsA and CDP caused a significant decrease of ΔΨm, but Ru360 did not (Fig. 7). With exposure to 200-μM Ca^{2+}, both SM and NM underwent mitochondrial depolarization. As shown in Fig. 7, CsA and CDP pretreatment did not help in attenuating

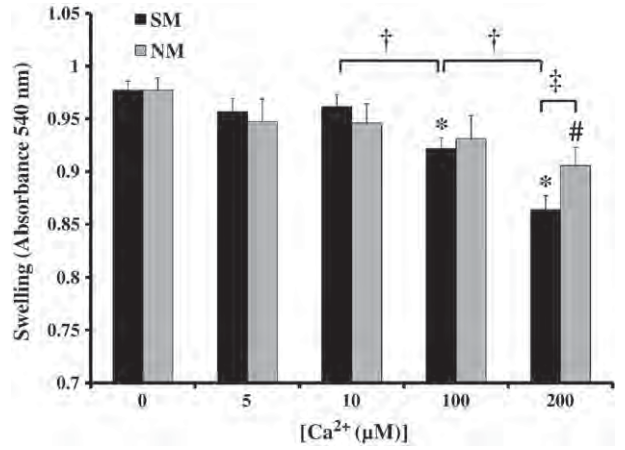

Fig. 4. Ca^{2+}-induced mitochondrial swelling of SM and NM (N = 8/group) after 10-min of Ca^{2+} application. SM: synaptic mitochondria, NM: nonsynaptic mitochondria, *$P<0.05$ compared to the control group for SM, #$P<0.05$ compared to the control group for NM, †$P<0.05$ differences between different calcium concentrations in the same group, ‡$P<0.05$ differences between different groups at the same calcium concentration.

the ΔΨm collapse in either SM or NM. However, Ru360 pretreatment completely restored the membrane potential of NM to the normal level, whereas it only partially prevented ΔΨm collapse in SM (Fig. 7).

Effect of CsA, CDP, and Ru360 on SM and NM swelling

CsA, CDP and Ru360 alone did not alter the absorbance in both SM and NM, compared to the control group. Among all pharmacological interventions, only Ru360 could completely prevent both SM and NM swelling following a 200-μM Ca^{2+} application (Fig. 8). For CsA and CDP, they could completely prevent mitochondrial swelling only in NM. In SM, both CsA and CDP could only partially prevent mitochondrial swelling (Fig. 8).

Discussion

Mitochondrial Ca^{2+} overload is a crucial pathogenesis of numerous neurological disorders including neurodegenerative diseases, ischemic brain injury, inflammatory processes and epilepsy (Zundorf and Reiser, 2010). Previous studies in isolated mitochondria have shown that excessive Ca^{2+} triggered mitochondrial permeability transition (mPT) evidenced by mitochondrial membrane potential (ΔΨm) collapse, ROS production, mitochondrial swelling, and outer membrane rupture leading to apoptotic cascade activation (Pivovarova and Andrews, 2010). In the CNS, differences in Ca^{2+} handling have been observed in different brain regions and neuronal mitochondrial populations. Synaptic mitochondria are at high risk for accumulative mitochondrial perturbation and consequently become more challenging to therapeutic interventions (Du et al., 2010). Mitochondrial swelling is one of the most important markers of the mPTP opening (Bernardi, 1996; Friberg and Wieloch, 2002). In the present study, we demonstrated that morphological changes in SM exposed to 200-μM Ca^{2+} were greater than those in the NM which reflected that SM underwent more mPTP opening as compared to the NM during Ca^{2+} exposure. This finding is consistent with that of a previous study which reported that SM had less capacity for Ca^{2+} accumulation than did NM prior to mitochondrial permeability transition (mPT), suggesting that Ca^{2+}-induced mPT in SM is more intense than in NM (Brown et al., 2006).

Ca^{2+} overload can also give rise to oxidative stress. Several mechanisms have been proposed to be involved in Ca^{2+}-induced ROS production. Under physiologic conditions, Ca^{2+} may be both a stimulator for oxidative-phosphorylation and a partial inhibitor of the electron transport chain, each of which actions leads to ROS production (Brookes et al., 2004). Another mechanism is the Ca^{2+}-triggered mPTP-opening when intramitochondrial Ca^{2+} reaches a threshold level (Ow et al., 2008). Opening of the mPTP leads to cytochrome c release causing an increase in ROS production (Starkov et al., 2004). According to the critical ROS threshold hypothesis, ROS at a certain level could trigger mitochondrial membrane depolarization (Zorov et al., 2006). Hence, it is possible that Ca^{2+}, which surges to the threshold level, might induce an increase of the ROS level high enough to cause ΔΨm dissipation.

In this study, we demonstrated that 100-μM Ca^{2+} or higher caused ROS production, ΔΨm dissipation, and mitochondrial swelling in SM. This finding implies that ROS level caused by 100-μM Ca^{2+} could reach the threshold level of SM to cause SM dysfunction. However, in NM, 10-μM and 100-μM Ca^{2+} triggered ROS production without causing ΔΨm dissipation or mitochondrial swelling, while 200-μM Ca^{2+} triggered both ROS generation, ΔΨm collapse, and mitochondrial swelling in NM. This finding suggests that the ROS levels caused by 10-μM and 100-μM Ca^{2+} were not high enough to induce ΔΨm collapse and mitochondrial swelling. Nevertheless, the ROS level caused by 200-μM Ca^{2+} reached the critical threshold of NM to undergo NM dysfunction. Therefore, from the data of ROS, ΔΨm and mitochondrial swelling, it may be concluded that the critical

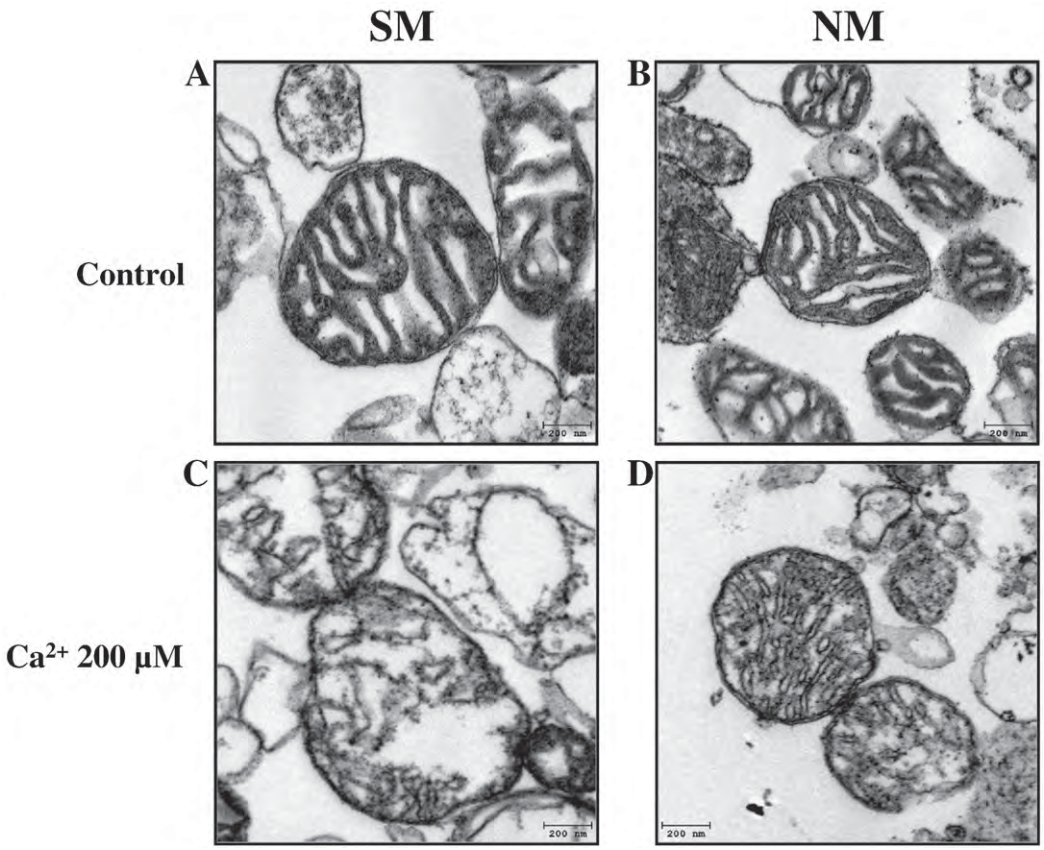

Fig. 5. Effect of Ca^{2+} overload on mitochondrial morphology of SM and NM. SM or NM (0.4 mg/ml) was incubated with respiration buffer (A, B) or with respiration buffer plus 200 μM Ca^{2+} (C, D) for 10 min before fixation. SM: synaptic mitochondria, NM: nonsynaptic mitochondria, magnification: 1:15,000 (A–D).

threshold levels of Ca^{2+} induced mitochondrial dysfunction in NM were higher than that in SM.

Since the heterogeneity of mitochondrial membrane channel properties of different mitochondrial populations might determine diverse sensitivities to Ca^{2+} insult and underlie pathogenesis of neuronal dysfunction, we examined the pharmacological effects on ROS production, ΔΨm dissipation, and mitochondrial swelling. In the present study, we found that pretreatment with CsA or CDP greatly reduced ROS levels of NM to the normal levels but only partially decreased ROS levels of SM. Since CsA and CDP directly interact with the mPTP components, the differences in response to these agents suggest the possibility that the quantity of both CypD and TSPO or their susceptibility to Ca^{2+} on the

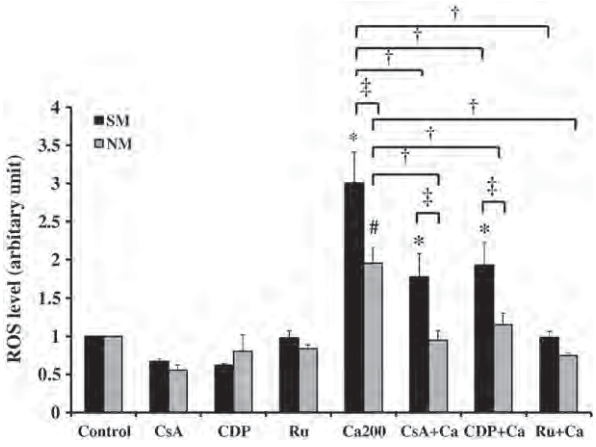

Fig. 6. Effects of CsA (5 μM), CDP (100 μM) and Ru360 (10 μM) on synaptic and nonsynaptic mitochondrial ROS production (n = 5/group). CsA, CDP, and Ru: mitochondria treated with 5-μM CsA, 100-μM CDP, and 10-μM Ru360, respectively. Ca200: mitochondria treated with $CaCl_2$ 200 μM. CsA + Ca, CDP + Ca, Ru + Ca: mitochondria pretreated with 5 μM CsA, 100 μM CDP, and 10 μM Ru360 followed by $CaCl_2$ application, respectively. SM: synaptic mitochondria, NM: nonsynaptic mitochondria, $^{*}P<0.05$ compared to the control group for SM, #$P<0.05$ compared to the control group for NM, †$P<0.05$ compared to 200 μM Ca^{2+} in the same group, ‡$P<0.05$ compared to SM at the same pretreatment group.

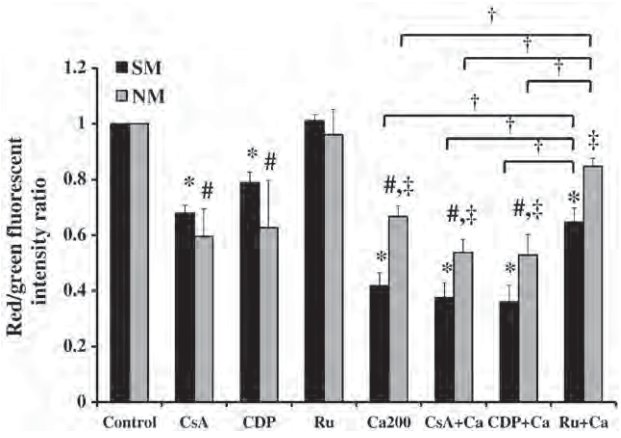

Fig. 7. Effects of CsA, CDP, and Ru360 on synaptic and nonsynaptic mitochondrial ΔΨm dissipation (n = 5/group). CsA, CDP, and Ru: mitochondria treated with 5-μM CsA, 100-μM CDP, and 10-μM Ru360, respectively. Ca200: mitochondria treated with $CaCl_2$ 200 μM. CsA + Ca, CDP + Ca, Ru + Ca: mitochondria pretreated with 5-μM CsA, 100-μM CDP, and 10-μM Ru360 followed by $CaCl_2$ application, respectively. SM: synaptic mitochondria, NM: nonsynaptic mitochondria, $^{*}P<0.05$ compared to the control group for SM, #$P<0.05$ compared to the control group for NM, †$P<0.05$ compared to 200 μM Ca^{2+} in the same group, ‡$P<0.05$ compared to SM at the same pretreatment group.

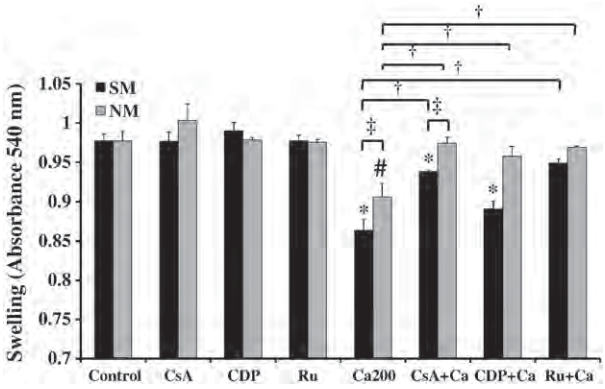

Fig. 8. Effects of CsA, CDP, and Ru360 on synaptic and nonsynaptic mitochondrial swelling (n = 5/group). CsA, CDP, and Ru: mitochondria treated with 5-μM CsA, 100-μM CDP, and 10-μM Ru360, respectively. Ca200: mitochondria treated with 200-μM $CaCl_2$. CsA + Ca, CDP + Ca, Ru + Ca: mitochondria pretreated with 5-μM CsA, 100-μM CDP, and 10-μM Ru360 followed by $CaCl_2$ application, respectively. SM: synaptic mitochondria, NM: nonsynaptic mitochondria, *$P<0.05$ compared to the control group for SM, #$P<0.05$ compared to the control group for NM, †$P<0.05$ compared to 200 μM Ca^{2+} in the same group, ‡$P<0.05$ compared to SM of the same treatment group.

mitochondrial membranes of SM might be greater than on NM. This finding was consistent with that of a recent study which reported the larger amount of CypD in SM compared with NM (Naga et al., 2007). That finding and our findings may be a major factor underlying the differences in Ca^{2+}-induced mitochondrial dysfunction between SM and NM. However, pretreatment with higher concentrations of CsA and CDP did not decrease the ROS levels in SM to the normal level (data not shown), suggesting that other mechanisms besides mPTP might be responsible for ROS production in SM. The findings that CsA and CDP could completely prevent mitochondrial swelling in NM, but not SM, support this hypothesis.

In the present study, a specific MCU inhibitor Ru360 could decrease ROS production and mitochondrial swelling caused by excess Ca^{2+} in both SM and NM to normal levels, suggesting that Ca^{2+} influx could occur directly via MCU. By inhibiting MCU, extramitochondrial Ca^{2+} could not influx into the matrix, leading to the blockage of Ca^{2+}-induced ROS production processes. These finding suggested that MCU could play a key role in increased ROS production induced by Ca^{2+} in both SM and NM. Furthermore, our results on the pharmacological interventions on mitochondrial membrane potential changes demonstrated that only Ru360 can attenuate the Ca^{2+}-induced mitochondrial depolarization in both SM and NM, whereas CsA and CDP could not. Although both CsA and CDP could reduce ROS production, they did not prevent mitochondrial depolarization. Mitochondrial depolarization due to excess Ca^{2+} could also involve the mechanism unrelated to the mPTP opening. Excess Ca^{2+} influx via the MCU could cause mitochondrial depolarization directly since Ca^{2+} uptake through MCU occurs down a potential gradient, thus allowing a large amount of positive charges into the mitochondria (Gunter and Pfeiffer, 1990). Although CsA and CDP directly inhibited mPTP opening and prevented loss of cytochrome c and ROS production, they could not prevent Ca^{2+} entry via MCU. Instead, Ru360 (MCU blocker), which directly inhibited Ca^{2+} influx, could protect mitochondrial depolarization. The findings that Ru360 could reduce ROS production greater than that by CsA and CDP could be another reason for the effect of Ru360 on relieving $\Delta\Psi m$ dissipation. Since Ca^{2+} entry into the mitochondria is the main cause of increased ROS production in this case, inhibiting Ca^{2+} influx could directly prevent excess ROS production as observed in the present study. However, the effect of Ru360 on $\Delta\Psi m$ in SM and NM was not similar. Ru360 could completely prevent $\Delta\Psi m$ dissipation in NM but partially prevent $\Delta\Psi m$ dissipation in SM, suggesting that MCU can be defined as a key pathway of Ca^{2+} sequestration in NM, but the additional alternative channels such as mitochondrial RyR or RAM may also take part in the Ca^{2+} uptake mechanism of SM.

Limitation of the study

Although the methods for NM and SM isolation we used in the present study have been used previously, they were different buffer systems, and may in part affect the mitochondrial physiological function. Therefore, the responses of SM and NM to the pharmacological interventions could be similar or different if the NM and SM were isolated with the same buffer system. Future studies are needed to investigate the effects of the buffer systems on mitochondrial responses to the drugs.

Conclusion

The findings in this study established that isolated mitochondria derived from synaptosomes presented more severe mitochondrial dysfunction in response to Ca^{2+} overload than did mitochondria derived from nonsynaptosomes. This divergence is not only the result of differences in mPTP components but also the differences in the Ca^{2+} uptake mechanism. Finally, the MCU may be the major portal for Ca^{2+} entry in NM. However, both MCU and other pathways such as RyR or RAM could be portals of Ca^{2+} entry in SM.

Although alternative mechanisms are still undiscovered, our results provided additional insights and explanation for the susceptibility of synaptic mitochondria, which could be useful for further therapeutic approach in numerous neuronal disorders, particularly disorders due to the calcium overload condition.

Conflict of interest statement

The authors state that there are no conflicts of interest.

Acknowledgments

This study is supported by research grants from the Thailand Research Fund RTA 5280006 (NC) and BRG 5480003 (SC) and the Chiang Mai University Young Researcher Fund (CY). The authors wish to thank Dr. M. Kevin O Carroll, Professor Emeritus of the University of Mississippi School of Dentistry, USA and Faculty Consultant at Faculty of Dentistry, Chiang Mai University, Thailand, for his assistance in the preparation of the manuscript.

References

Adam-Vizi V, Starkov AA. Calcium and mitochondrial reactive oxygen species generation: how to read the facts. J Alzheimers Dis 2010;20(Suppl. 2):S413–26.
Altschafl BA, Beutner G, Sharma VK, Sheu SS, Valdivia HH. The mitochondrial ryanodine receptor in rat heart: a pharmaco-kinetic profile. Biochim Biophys Acta 2007;1768:1784–95.
Banaclocha MM, Hernandez AI, Martinez N, Ferrandiz ML. N-acetylcysteine protects against age-related increase in oxidized proteins in mouse synaptic mitochondria. Brain Res 1997;762:256–8.
Berman SB, Watkins SC, Hastings TG. Quantitative biochemical and ultrastructural comparison of mitochondrial permeability transition in isolated brain and liver mitochondria: evidence for reduced sensitivity of brain mitochondria. Exp Neurol 2000;164:415–25.
Bernardi P. The permeability transition pore. Control points of a cyclosporin A sensitive mitochondrial channel involved in cell death. Biochim Biophys Acta 1996;1275:5–9.
Beutner G, Sharma VK, Giovannucci DR, Yule DI, Sheu SS. Identification of a ryanodine receptor in rat heart mitochondria. J Biol Chem 2001;276:21482–8.
Beutner G, Sharma VK, Lin L, Ryu SY, Dirksen RT, Sheu SS. Type 1 ryanodine receptor in cardiac mitochondria: transducer of excitation-metabolism coupling. Biochim Biophys Acta 2005;1717:1-10.
Buntinas L, Gunter KK, Sparagna GC, Gunter TE. The rapid mode of calcium uptake into heart mitochondria (RaM): comparison to RaM in liver mitochondria. Biochim Biophys Acta 2001;1504:248–61.
Blomgren K, Zhu C, Hallin U, Hagberg H. Mitochondria and ischemic reperfusion damage in the adult and in the developing brain. Biochem Biophys Res Commun 2003;304:551–9.
Boitier E, Rea R, Duchen MR. Mitochondria exert a negative feedback on the propagation of intracellular Ca^{2+} waves in rat cortical astrocytes. J Cell Biol 1999;145:795–808.
Brookes PS, Yoon Y, Robotham JL, Anders MW, Sheu SS. Calcium, ATP, and ROS: a mitochondrial love–hate triangle. Am J Physiol Cell Physiol 2004;287:C817–33.

Brown MR, Sullivan PG, Geddes JW. Synaptic mitochondria are more susceptible to Ca^{2+} overload than nonsynaptic mitochondria. J Biol Chem 2006;281:11658–68.
Chelli B, Falleni A, Salvetti F, Gremigni V, Lucacchini A, Martini C. Peripheral-type benzodiazepine receptor ligands: mitochondrial permeability transition induction in rat cardiac tissue. Biochem Pharmacol 2001;61:695–705.
Clark JB, Nicklas WJ. The metabolism of rat brain mitochondria. Preparation and characterization. J Biol Chem 1970;245:4724–31.
Du H, Guo L, Yan S, Sosunov AA, McKhann GM, Yan SS. Early deficits in synaptic mitochondria in an Alzheimer's disease mouse model. Proc Natl Acad Sci U S A 2010;107:18670–5.
Duchen MR. Mitochondria in health and disease: perspectives on a new mitochondrial biology. Mol Aspects Med 2004;25:365–451.
Friberg H, Wieloch T. Mitochondrial permeability transition in acute neurodegeneration. Biochimie 2002;84:241–50.
Gangolf M, Wins P, Thiry M, El Moualij B, Bettendorff L. Thiamine triphosphate synthesis in rat brain occurs in mitochondria and is coupled to the respiratory chain. J Biol Chem 2010;285:583–94.
Gunter TE, Pfeiffer DR. Mechanisms by which mitochondria transport calcium. Am J Physiol 1990;258:C755–86.
Guo X, Macleod GT, Wellington A, Hu F, Panchumarthi S, et al. The GTPase dMiro is required for axonal transport of mitochondria to Drosophila synapses. Neuron 2005;47:379–93.
Gyulkhandanyan AV, Pennefather PS. Shift in the localization of sites of hydrogen peroxide production in brain mitochondria by mitochondrial stress. J Neurochem 2004;90:405–21.
Hyder F, Patel AB, Gjedde A, Rothman DL, Behar KL, Shulman RG. Neuronal-glial glucose oxidation and glutamatergic–GABAergic function. J Cereb Blood Flow Metab 2006;26:865–77.
Komary Z, Tretter L, Adam-Vizi V. H2O2 generation is decreased by calcium in isolated brain mitochondria. Biochim Biophys Acta 2008;1777:800–7.
Krasnikov BF, Kim SY, McConoughey SJ, Ryu H, Xu H, et al. Transglutaminase activity is present in highly purified nonsynaptosomal mouse brain and liver mitochondria. Biochemistry 2005;44:7830–43.
Kudin AP, Bimpong-Buta NY, Vielhaber S, Elger CE, Kunz WS. Characterization of superoxide-producing sites in isolated brain mitochondria. J Biol Chem 2004;279:4127–35.
Lai JC, Clark JB. Preparation of synaptic and nonsynaptic mitochondria from mammalian brain. Methods Enzymol 1979;55:51–60.
Li Z, Okamoto K, Hayashi Y, Sheng M. The importance of dendritic mitochondria in the morphogenesis and plasticity of spines and synapses. Cell 2004;119:873–87.
Lifshitz J, Friberg H, Neumar RW, Raghupathi R, Welsh FA, et al. Structural and functional damage sustained by mitochondria after traumatic brain injury in the rat: evidence for differentially sensitive populations in the cortex and hippocampus. J Cereb Blood Flow Metab 2003;23:219–31.
Ly JD, Grubb DR, Lawen A. The mitochondrial membrane potential (deltapsi(m)) in apoptosis; an update. Apoptosis 2003;8:115–28.
Martinez M, Hernandez AI, Martinez N, Ferrandiz ML. Age-related increase in oxidized proteins in mouse synaptic mitochondria. Brain Res 1996;731:246–8.
Murchison D, Griffith WH. Calcium buffering systems and calcium signaling in aged rat basal forebrain neurons. Aging Cell 2007;6:297–305.
Naga KK, Sullivan PG, Geddes JW. High cyclophilin D content of synaptic mitochondria results in increased vulnerability to permeability transition. J Neurosci 2007;27:7469–75.
Nicholls DG. Mitochondrial calcium function and dysfunction in the central nervous system. Biochim Biophys Acta 2009;1787:1416–24.
Norenberg MD, Rao KV. The mitochondrial permeability transition in neurologic disease. Neurochem Int 2007;50:983–97.
Novalija E, Kevin LG, Eells JT, Henry MM, Stowe DF. Anesthetic preconditioning improves adenosine triphosphate synthesis and reduces reactive oxygen species formation in mitochondria after ischemia by a redox dependent mechanism. Anesthesiology 2003;98:1155–63.
Ow YP, Green DR, Hao Z, Mak TW. Cytochrome c: functions beyond respiration. Nat Rev Mol Cell Biol 2008;9:532–42.
Pallotti F, Lenaz G. Isolation and subfractionation of mitochondria from animal cells and tissue culture lines. Methods Cell Biol 2007;80:3-44.
Pandya JD, Sullivan PG, Pettigrew LC. Focal cerebral ischemia and mitochondrial dysfunction in the TNFalpha-transgenic rat. Brain Res 2011;1384:151–60.
Panov A, Dikalov S, Shalbuyeva N, Hemendinger R, Greenamyre JT, Rosenfeld J. Species- and tissue-specific relationships between mitochondrial permeability transition and generation of ROS in brain and liver mitochondria of rats and mice. Am J Physiol Cell Physiol 2007;292:C708–18.
Perry SW, Norman JP, Barbieri J, Brown EB, Gelbard HA. Mitochondrial membrane potential probes and the proton gradient: a practical usage guide. Biotechniques 2011;50:98-115.
Petrosillo G, Ruggiero FM, Pistolese M, Paradies G. Ca2+-induced reactive oxygen species production promotes cytochrome c release from rat liver mitochondria via mitochondrial permeability transition (MPT)-dependent and MPT-independent mechanisms: role of cardiolipin. J Biol Chem 2004;279:53103–8.
Pivovarova NB, Andrews SB. Calcium-dependent mitochondrial function and dysfunction in neurons. FEBS J 2010;277:3622–36.
Reddy PH, Reddy TP. Mitochondria as a therapeutic target for aging and neurodegenerative diseases. Curr Alzheimer Res 2011;8:393–409.
Reeve AK, Krishnan KJ, Turnbull DM. Age related mitochondrial degenerative disorders in humans. Biotechnol J 2008;3:750–6.
Rosenthal RE, Hamud F, Fiskum G, Varghese PJ, Sharpe S. Cerebral ischemia and reperfusion: prevention of brain mitochondrial injury by lidoflazine. J Cereb Blood Flow Metab 1987;7:752–8.
Schonfeld P, Reiser G. Ca^{2+} storage capacity of rat brain mitochondria declines during the postnatal development without change in ROS production capacity. Antioxid Redox Signal 2007;9:191–9.
Sparagna GC, Gunter KK, Sheu SS, Gunter TE. Mitochondrial calcium uptake from physiological-type pulses of calcium. A description of the rapid uptake mode. J Biol Chem 1995;270:27510–5.
Starkov AA, Chinopoulos C, Fiskum G. Mitochondrial calcium and oxidative stress as mediators of ischemic brain injury. Cell Calcium 2004;36:257–64.
Thummasorn S, Kumfu S, Chattipakorn S, Chattipakorn N. Granulocyte-colony stimulating factor attenuates mitochondrial dysfunction induced by oxidative stress in cardiac mitochondria. Mitochondrion 2011;11:457–66.
Tong V, Teng XW, Chang TK, Abbott FS. Valproic acid II: effects on oxidative stress, mitochondrial membrane potential, and cytotoxicity in glutathione-depleted rat hepatocytes. Toxicol Sci 2005;86:436–43.
Votyakova TV, Reynolds IJ. Ca2+-induced permeabilization promotes free radical release from rat brain mitochondria with partially inhibited complex I. J Neurochem 2005;93:526–37.
Wadia JS, Chalmers-Redman RM, Ju WJ, Carlile GW, Phillips JL, et al. Mitochondrial membrane potential and nuclear changes in apoptosis caused by serum and nerve growth factor withdrawal: time course and modification by (−)-deprenyl. J Neurosci 1998;18:932–47.
Walker JM. The bicinchoninic acid (BCA) assay for protein quantitation. Methods Mol Biol 1994;32:5–8.
Wang YC, Lee CM, Lee LC, Tung LC, Hsieh-Li HM, Lee-Chen GJ, et al. Mitochondrial dysfunction and oxidative stress contribute to the pathogenesis of spinocerebellar ataxia type 12 (SCA12). J Biol Chem 2011;286:21742–54.
Yuan J, Yankner BA. Apoptosis in the nervous system. Nature 2000;407:802–9.
Zhang SZ, Gao Q, Cao CM, Bruce IC, Xia Q. Involvement of the mitochondrial calcium uniporter in cardioprotection by ischemic preconditioning. Life Sci 2006;78:738–45.
Zorov DB, Juhaszova M, Sollott SJ. Mitochondrial ROS-induced ROS release: an update and review. Biochim Biophys Acta 2006;1757:509–17.
Zundorf G, Reiser G. Calcium dysregulation and homeostasis of neural calcium in the molecular mechanisms of neurodegenerative diseases provide multiple targets for neuroprotection. Antioxid Redox Signal 2010;14:1275–88.

EUROPEAN JOURNAL OF Haematology

European Journal of Haematology 88 (535–548)

ORIGINAL ARTICLE

T-type calcium channel blockade improves survival and cardiovascular function in thalassemic mice

Sirinart Kumfu[1], Siriporn Chattipakorn[1,2], Kroekkiat Chinda[1], Suthat Fucharoen[3], Nipon Chattipakorn[1,4]

[1]Cardiac Electrophysiology Research and Training Center, Department of Physiology, Faculty of Medicine, Chiang Mai University, Chiang Mai; [2]Department of Oral Biology and Diagnostic Science, Faculty of Dentistry, Chiang Mai University, Chiang Mai; [3]Thalassemia Research Center, Mahidol University, Bangkok; [4]Biomedical Engineering Center, Chiang Mai University, Chiang Mai, Thailand

Abstract

Objectives: Iron-overload cardiomyopathy is a major cause of morbidity and mortality in patients with thalassemia. However, the precise mechanisms of iron entry and sequestration in the heart are still unclear. Our previous study showed that Fe^{2+} uptake in thalassemic cardiomyocytes are mainly mediated by T-type calcium channels (TTCC). Nevertheless, the role of TTCC as well as other transporters such as divalent metal transporter1 (DMT1) and L-type calcium channels (LTCC) as possible portals for iron entry into the heart in *in vivo* thalassemic mice under an iron-overload condition has not been investigated. *Methods:* An iron-overload condition was induced in genetically altered β-thalassemic mice and adult wild-type mice by feeding them with an iron diet (0.2% ferrocene w/w) for 3 months. Then, blockers for LTCC (verapamil and nifedipine), TTCC (efonidipine), and DMT1 (ebselen) as well as iron chelator desferoxamine (DFO) were given for 1 month with continuous iron feeding. *Results:* Treatment with LTCC, TTCC, DMT1 blockers, and DFO reduced cardiac iron deposit, cardiac malondialdehyde (MDA), plasma non-transferrin-bound iron, and improved heart rate variability and left ventricular (LV) function in thalassemic mice with iron overload. Only TTCC and DMT1 blockers and DFO reduced liver iron accumulation, liver MDA, plasma MDA, and decreased mortality rate in iron-overloaded thalassemic mice. *Conclusions:* DMT1, LTCC, and TTCC played important roles for iron entry in the thalassemic heart under an iron-overloaded condition. Unlike LTCC blocker, TTCC blocker provided all benefits including attenuating iron deposit in both the heart and liver, reduced oxidative stress, and decreased mortality in iron-overloaded mice.

Key words cardiac iron; left ventricular function; heart rate variability; calcium channel; iron overload

Correspondence Nipon Chattipakorn, MD, PhD, Cardiac Electrophysiology Research and Training Center, Faculty of Medicine, Chiang Mai University, Chiang Mai 50200, Thailand. Tel: +66 53 945329; Fax: +66 53 945368; e-mail: nchattip@gmail.com

Accepted for publication 4 March 2012 doi:10.1111/j.1600-0609.2012.01779.x

Beta-thalassemia is an inherited hemoglobin disorder, resulting in chronic hemolytic anemia, which is typically required for regular blood transfusion (1, 2). It is prevalent in people of Mediterranean origin, Middle East, North India, and Southeast Asia (3, 4). The iron-overload condition in thalassemia can lead to iron accumulation in various organs, especially in the heart (5, 6), leading to iron-overload cardiomyopathy, which is the major cause of mortality in patients with thalassemia (7, 8). However, the mechanisms of iron uptake into the heart leading to abnormal left ventricular (LV) function are still unclear. A previous study showed that the L-type calcium channels (LTCC) played a role for iron uptake into the heart of the isolated perfused rat heart (9) and in an *in vivo* rat model of iron overload (10). However, inconsistent findings were reported in cultured cardiomyocyte studies (11, 12). Recently, using the thalassemic mouse model, our study demonstrated for the first time that T-type calcium channels (TTCC) were reexpressed in thalassemic mouse hearts (11). We also demonstrated that the TTCC blocker (efonidipine), but not the LTCC blocker (verapamil), prevented Fe^{2+} uptake into thalassemic cardiomyocytes (11).

Normally, iron can enter the cell such as enterocyte, hepatocyte, and cardiomyocyte via the divalent metal transporter1 (DMT1) and transferrin receptor1 (TfR1)

(13–15). However, under iron-overload conditions, previous studies demonstrated that TfR1 and DMT1 mRNA and protein expressions in the heart were suppressed (16, 17), suggesting that they may not be major transporters for iron uptake into the hearts under this condition. Moreover, it has been shown that TfR1 and DMT1 did not play important roles in Fe^{2+} uptake in cultured thalassemic cardiomyocytes (11). Nevertheless, the role of TTCC, LTCC, and DMT1 as iron transporters in '*in vivo*' thalassemic mice under iron-overload conditions has never been investigated.

Heart rate variability (HRV) is a measure of variation in the heart rate. Variation in the beat-to-beat interval is a physiological phenomenon, involving the sympathetic and parasympathetic nervous system (18, 19). HRV has been proposed as a new risk stratifier in postmyocardial infarction and heart failure patients (20). In patients with thalassemia, several studies demonstrated that the HRV was depressed indicating cardiac autonomic imbalance in these patients (18, 19). Similar findings, that is, depressed HRV, were also demonstrated in a mouse model of β-thalassemia (21). However, the effects of TTCC, LTCC, and DMT1 blockers on HRV as well as on LV function in iron-overloaded thalassemic mice have never been investigated.

In this study, we tested the hypothesis that pharmacological interventions with TTCC, LTCC, and DMT1 blockers and iron chelator desferoxamine (DFO) attenuate cardiac iron accumulation, improve HRV and LV function, and reduce cardiac oxidative stress in iron-overloaded thalassemic mice.

Materials and methods

Animal models

Two types of adult C57/BL6 mice (3–6 months old): wild type (mu$\beta^{+/+}$, WT) and heterozygous β^{KO} type (mu$\beta^{th-3/+}$, HT), were used in this study (11, 21). All animal studies were approved by the Institutional Animal Care and Use Committee (IACUC) of the Faculty of Medicine, Chiang Mai University, and conformed to the *Guide for the Care and Use of Laboratory Animals* published by the US National Institutes of Health (NIH Publication No. 85-23, revised 1996). All animals were housed in controlled temperature and humidity rooms with 12-h light–dark cycles.

Iron treatment and pharmacological interventions

Iron overload was induced by feeding WT and HT mice (FE group) with FE diet (0.2% ferrocene w/w), whereas WT and HT mice in the control group were fed with a normal diet for 90 d. Then, the mice in the FE group were randomly divided into six subgroups (n = 8 each) and were treated with drugs while being fed an FE diet for another 30 d. Group I (FE) mice were given intraperitoneal (IP) injections with 0.5% DMSO daily. Group II (FE/DFO) mice were injected with deferoxamine (DFO, 42 mg/kg) in 0.5% DMSO IP daily (22). Group III (FE/verapamil) mice were injected with verapamil (10 mg/kg) in 0.5% DMSO twice daily (alternating subcutaneous and IP) (23). Group IV (FE/nifedipine) mice were injected with nifedipine (5 mg/kg) in 0.5% DMSO IP daily (24). Group V (FE/efonidipine) mice were injected with efonidipine (4 mg/kg) in 0.5% DMSO IP daily (25). Group VI (FE/ebselen) mice were injected with ebselen (5 mg/kg) in 0.5% DMSO IP daily (26). Mice in the control group were injected with 0.5% DMSO IP daily and fed with the normal diet. Each group of mice were injected with drug at 6 pm each day except Fe/verapamil group, which were injected twice daily at 6 am and 6 pm each day. At the end of treatments (i.e., 4 months after iron-loading and treatment), the LV function, HRV, and cardiac iron deposition were assessed in all mice. The mortality rate was also determined in all groups.

Quantification of plasma non-transferrin-bound iron

The non-transferrin-bound iron (NTBI) concentration was measured using the NTA chelation/HPLC method established by Singh *et al*. (27) with the aluminum blocking step. Plasma was incubated with NTA solution (a final concentration of 80 mM) pH 7.0 for 30 min at room temperature to produce an Fe^{3+}-$(NTA)_2$ complex. Afterward, the Fe^{3+}-$(NTA)_2$ was separated from the plasma proteins by spinning the plasma mixture through a membrane filter (NanoSep®, 30-kDa cut off, polysulfone type; Pall Life Sciences, Ann Arbor, MI, USA). The concentration of the Fe^{3+}-$(NTA)_2$ representing NTBI in the ultrafiltrate was determined using a non-metallic HPLC system. The analytes were fractionated onto a glass analytical column (ChromSep-ODS1, 100 × 3.0 mm, 5 μm) and eluted with mobile-phase solvent (3 mM CP22 in 19% acetronitrile/MOPS buffer pH 7.0) at a flow rate of 1.0 mL/min. The effluents were monitored at 450 nm using a flow cell detector (SpecMonitor2300; LDC Milton-Roy Inc., Riviera Beach, FL, USA) and conducted with BDS software (BarSpec Ltd., Rehovot, Israel). The NTBI concentration was calculated from a calibration curve made with different iron concentrations Fe^{3+}-$(NTA)_2$ in 80 mM NTA, pH 7.0 ranging 0–16 μM.

Measurement of heart rate variability

Cardiac autonomic nervous activity was evaluated by spectral analysis of the RR interval variability. All mice

underwent measurement of HRV at month 0 (M0), three (M3), and four (M4). The lead II electrocardiogram (ECG) was recorded using needle electrodes (21) and recorded continuously using Power Lab with chart 5.0 (21). During the recording of the ECG, mice were placed in a familiar environment with unnecessary noise, put to calm, and prohibited from movement. The ECG data were analyzed using MATLAB program (21). The RR interval was determined using the peaks of QRS complex and stored as an interval tachogram. From the section of tachogram of at least 300 consecutive interval values, the standard deviation of all RR intervals (SDNN) and root mean square of successive difference (rMSSD) were calculated. The power spectra of RR interval variability were obtained using fast Fourier transform algorithm, and the high-frequency (HF: 0.6–3 Hz) and the low-frequency (LF: 0.2–0.6 Hz) components were determined (21). The power below 0.2 Hz is considered as a very low frequency (VLF). Each spectral component was calculated by determining the area under the respective part of the power spectral density function and was presented in absolute unit (ms^2). To minimize the effect of changes in total power on the LF and HF components, LF and HF were expressed as normalized units (LFnu and HFnu) by dividing the LF and HF by the total power minus VLF (19, 21). The LF/HF ratio is considered an index of autonomic balance (19, 21).

Left ventricular pressure-volume loops (P-V loops) analysis

The WT and HT mice were anesthetized and maintained under physiological conditions. Anesthesia was induced with zoletil (20 mg/kg body weight), injected intraperitoneally (28). The endotracheal tube was inserted, and respiration was maintained by the Harvard rodent ventilator model 683 (Harvard Apparatus, Holliston, MA, USA), which started immediately with room air using a volume of 200–250 μL and ventilator rate at 110–130 breaths/min to maintain PCO_2, PO_2, and pH parameters (29). The abdomen was opened subcostally. The diaphragm was incised by a transverse substernal approach leaving the pericardium intact. The left ventricle was entered through an apical stab with a 23 1/2 G needle, followed immediately by the pressure-volume conductance catheter (SciSense, ON, Canada) for measuring the LV pressure and volume (29). The end-systolic pressure (ESP) and end-diastolic pressure (EDP), maximum pressure (P_{max}) and minimum pressure (P_{min}), maximum and minimum dP/dt (dP/dt_{max}, dP/dt_{min}), stroke volume (SV), cardiac output (CO), and stroke work (SW) were measured using the P-V conductance catheter system (29, 30).

Percent of organ weight index

The heart, liver, spleen, and kidney were removed and weighed. The weight index was determined by using the equation: weight index (%) = (organ weight/body weight) × 100 (31). All organs were remained frozen at −80°C for further analysis.

Prussian blue staining for iron tissue

Iron deposition in HT heart and liver tissues was determined by fixing the dissected tissues in 10% neutral buffer formalin, embedding in paraffin boxes, cutting with a sliding microtome (5-μm-thick section), and staining with Prussian blue dye solution. Prussian blue–stained tissue slides were examined under a light microscope (Olympus Corporation, Philadelphia, PA, USA) (40× magnification objective lens) and recorded with a digital camera (Sony Corp., Minato-ku, Japan).

Cardiac iron determination

At the end of the PV loop determination, the hearts were removed and homogenated in deionized water 1 : 10 (w/v). Then, 100 μL of heart tissue homogenates were precipitated in precipitation solution (1 N HCl and 10% trichloroacetic acid) and heated at 95°C for 1 h. Then, the tubes were cooled down at room temperature for 2 min, vortex mixed, and then centrifuged at 8200 ***g*** for 10 min. The supernatants (50 μL) were mixed with 50 μL of chromogen solution [0.508 mM ferrozine, 1.5 M sodium acetate and 0.1% or 1.5% (v/v) thioglycolic acid] and incubated at room temperature for 30 min. After incubation, the absorbance was measured at 562 nm, and the cardiac iron concentration was compared with the iron standard curve (32).

Hepatic iron content determination

The hepatic iron content (HIC) was determined using a colorimetric technique (33) and expressed in milligrams of non-heme iron per gram of dry weight. The liver tissue was dried at 120°C for 24 h and weighed. The tissue was digested with the acid mixture (concentrated sulfuric acid : concentrated nitric acid = 1 : 1, *v/v*) at room temperature and adjusted to the final volume of 10 mL with deionized water. The tissue hydrolysate (50 μL) was incubated with hydroxylamine hydrochloride solution (50 μL) to reduce the ferric ion to ferrous ion at room temperature for 10 min. The pH of the mixture was adjusted to 5.0 with 0.1 M acetate buffer pH 5.0 solution, and the Fe^{2+} present in the solution was allowed to react with a 2,4,6-tripyridyl-*s*-triazine (TPTZ) solution to form a violet-colored product. The OD of the product was measured at 593 nm against the reagent blank. The hepatic

iron concentration was calculated from a calibration curve made from different concentrations of ferrous ammonium sulfate ranging from 12.5 to 200 μM. Data of HIC were expressed as mg/g dry weight.

Determination of malondialdehyde concentration

The heart, liver, and plasma malondialdehyde (MDA) concentrations were measured by using the HPLC method (34). The dry liver tissues (100 mg) or heart tissues (30 mg) were homogenized in the solution containing 50 mM phosphate buffer pH 2.8 (0.8 mL), methanol (0.1 mL) and butyrated hydroxytoluene (BHT) (50 ppm) in an ice bath. A 0.5-mL aliquot of the homogenate or plasma was mixed with 1.1 mL of 10% (*w/v*) trichloroacetic acid (TCA) containing BHT (50 ppm), heated at 90°C for 30 min and cooled down to room temperature. The mixture was centrifuged at 3300 ***g*** for 10 min to achieve a clear supernatant. The supernatant (0.5 mL) was mixed with 0.44 M H_3PO_4 (1.5 mL) and 0.6% (*w/v*) thiobarbituric acid (TBA) solution (1.0 mL) and incubated at 90°C for 30 min to produce pink-colored products called thiobarbituric acid-reactive substances (TBARS). The solution was passed through a syringe filter (polysulfone type membrane, pore size 0.45 μm; Whatman International, Maidstone, UK) and analyzed with the HPLC system. The TBARS were fractionated on the adsorption column (Water Spherosorb ODS2 type, 250 × 4.3 mm, 5 μm), eluted with mobile-phase solvent of 50 mM KH_2PO_4 : methanol (65 : 35 *v/v*) at flow rate of 1.0 mL/min and on-line detected at 532 nm. Data were collected and analyzed with the BDS software (BarSpec Ltd.).

A standard curve was constructed from the peak height of standard 1,1,3,3-tetramethoxypropane (standard reagent for MDA) at different concentrations (0–100 μM). Tissues and plasma TBARS concentration were determined directly from the standard curve and reported as a MDA equivalent concentration (34). The MDA concentrations were expressed in μM/mg protein for heart and liver tissues and in μM for plasma samples.

RNA isolation for microarray analysis

The heart samples of WT (n = 3) and HT (Fe group) (n = 3) mice were used for RNA isolation and microarray analysis. The method was similar to that described previously (11).

Real-time reverse-transcriptase polymerase chain reaction (real-time RT-PCR)

Real-time RT-PCR was used to assess mRNA transcript levels (35–37). Total RNA was extracted from the ventricles of all HT groups (n = 3–4), using purelink RNA mini purification kit (Invitrogen Corp., Grang Island, NY, USA) according to the manufacturer's instructions. RNA samples were treated with DNaseI (Invitrogen Corp.,) to eliminate genomic DNA contamination, and cDNA was synthesized using iScript cDNA synthesis kit (Bio-Rad Lab Ltd, Hercules, CA, USA) according to the manufacturer's instructions. The cDNA samples were prepared with SsoFast EvaGreen Supermix (Bio-Rad Lab Ltd.), and real-time PCR was performed in 96-well plates in triplicate and were cycled for 45 cycles with Chromo4 Real-time PCR detector (Bio-Rad). The cycling conditions included in a hot start at 95°C for 30 s, followed by 45 cycles at 95°C for 5 s, and 60°C for 10 s. To detect LTCC, TTCC and glyceraldehyde-3-phosphate dehydrogenase (GAPDH) mRNA expression, the gene-specific primers for these genes were used. Sense and antisense primers (10 nM) were forward (F) 5′-TCTGCCTCTCTAGGTCGAA-3′ and reverse (R) 5′-GGGAATGTGGTAGGAGAATG-3′ for LTCC(α1C) (38), forward (F) 5′-TGTGGAAATGGTGGTGAAGA-3′ and reverse (R) 5′-ACTGCGGAGAAGCTGACATT-3′ for TTCC(α1G) (38), forward (F) 5′-TGTGTCCGTCGTGGATCTGA-3′ and reverse (R) 5′-TTGCTGTTGAAGTCGCAGGAG-3′ for GAPDH (39). The fluorescent amplification curve of the product was determined, and the cycle at which the fluorescence reached a threshold was recorded (C_t) in triplicate and averaged. To control for variability in RNA quantity, the measured abundances of marker genes were normalized to that of GAPDH using the formula $\Delta C_t = C_t$ (Detected Genes) $- C_t$ (GAPDH). GAPDH mRNA was used as an internal control.

Statistical analysis

Data were reported as the mean ± standard error of mean (SEM) and were processed using the SPSS (Statistical Package for Social Sciences, Chicago, IL, USA) release 13.0 for Windows. One-way ANOVA analyses and Student's t-test were performed for group comparisons. Chi-square test was used for mortality rate comparisons between groups. P-value < 0.05 was considered statistically significant.

Results

Effect of iron administration on plasma non-transferrin-bound iron level

At the baseline (M0), the levels of plasma NTBI were not detected both in wild-type and in thalassemic mice (Fig. 1A). After exposing both types of mice (WT, HT) to a diet enriched with iron for 1 (M1), 2 (M2), 3 (M3), or 4 (M4) months, NTBI levels were significantly higher and followed a cumulative dose-dependent relationship (Fig. 1A).

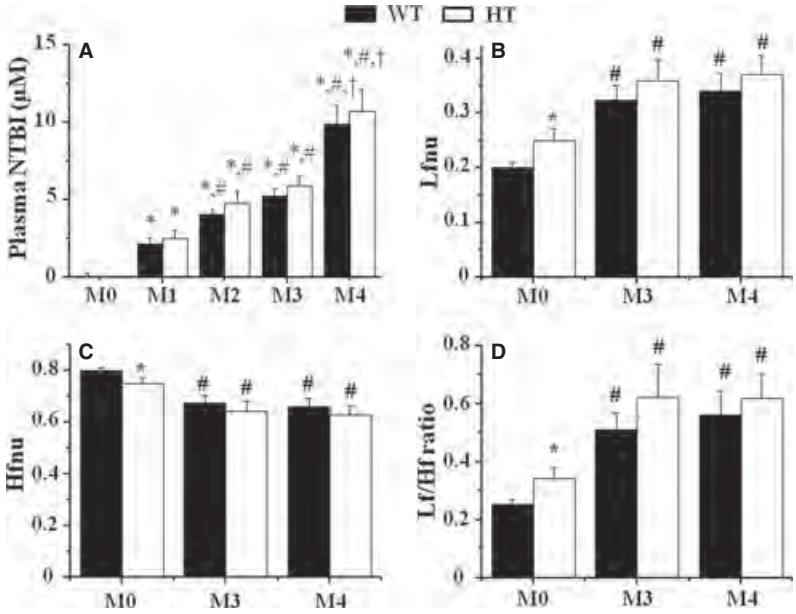

Figure 1 Effect of iron overload on plasma non-transferrin-bound iron (NTBI) level (A) and heart rate variability (HRV) (B–D) in wild-type (WT) and thalassemic mice (HT) without any pharmacological interventions at baseline (M0), 1 month (M1), 2 months (M2), 3 months (M3), and 4 months (M4) after iron feeding (n = 8–10/group). $^{*}P < 0.05$ vs. M0, $^{\#}P < 0.05$ vs. M1, †$P < 0.05$ vs. M3. Normalized low-frequency power (Lfnu) (B), normalized high-frequency power (Hfnu) (C) and Lf/Hf ratio (D). $^{*}P < 0.05$ vs. WT, $^{\#}P < 0.05$ vs. M0.

Effect of iron administration on heart rate variability

At the baseline (M0), thalassemic mice had a higher Lfnu (Fig. 1B), lower Hfnu (Fig. 1C), and higher Lf/Hf ratio (Fig. 1D) than those in the WT mice. After iron was administered for 3 and 4 months, both types of mice (WT, HT) showed a significantly increased Lfnu and Lf/Hf ratio and decreased Hfnu, compared with those at month 0 (Fig. 1). The heart rate, mean RR, SDNN, and rMSSD in both the WT (Table 1) and HT (Table 2) were not significantly different throughout the experiment (M0, M3, M4).

Effects of pharmacological interventions on organ weight index

In the control group, the liver weight indexes were not different between the WT and HT (Fig. 2A). After 4 months of iron feeding, both types of mice (WT, HT) showed a significantly increased liver weight index. Pharmacological interventions did not prevent elevation of liver weight index (Fig. 2A). The spleen weight index of the HT mice was significantly larger than the WT in the control group (Fig. 2B). After 4 months of iron feeding, both types of mice (WT, HT) showed a

Table 1 Effect of iron administration on heart rate variability in wild-type mice

Parameters	Month 0	Month 3	Month 4
RR_{max}	103 ± 2	105 ± 3	102 ± 2
RR_{min}	84 ± 1	85 ± 1	85 ± 1
Mean RR	92 ± 1	95 ± 1	93 ± 1
SDNN (ms)	2.92 ± 0.19	2.97 ± 0.31	3.00 ± 0.50
rMSSD (ms)	2.70 ± 0.19	2.61 ± 0.34	2.54 ± 0.57
HR_{max} (beats/min)	708 ± 4	710 ± 5	709 ± 9
HR_{min} (beats/min)	589 ± 9	586 ± 15	591 ± 14
Mean HR (beats/min)	647 ± 7	637 ± 7	644 ± 7

SDNN, standard deviation of all RR intervals; rMSSD, root mean square of successive difference of RR; HR, heart rate; Hfnu, normalized high-frequency power; Lfnu, normalized low-frequency power.

Table 2 Effect of iron administration on heart rate variability in thalassemic mice

Parameters	Month 0	Month 3	Month 4
RR_{max}	108 ± 3	103 ± 4	102 ± 2
RR_{min}	85 ± 1	87 ± 1	85 ± 1
Mean RR	92 ± 1	95 ± 1	93 ± 1
SDNN (ms)	3.69 ± 0.30	3.04 ± 0.54	3.00 ± 0.50
rMSSD (ms)	3.39 ± 0.32	3.38 ± 0.70	2.54 ± 0.57
HR_{max} (beats/min)	701 ± 4	703 ± 9	709 ± 9
HR_{min} (beats/min)	584 ± 15	587 ± 18	591 ± 14
Mean HR (beats/min)	654 ± 6	635 ± 8	644 ± 7

SDNN, standard deviation of all RR intervals; rMSSD, root mean square of successive difference of RR; HR, heart rate; Hfnu, normalized high-frequency power; Lfnu, normalized low-frequency power.

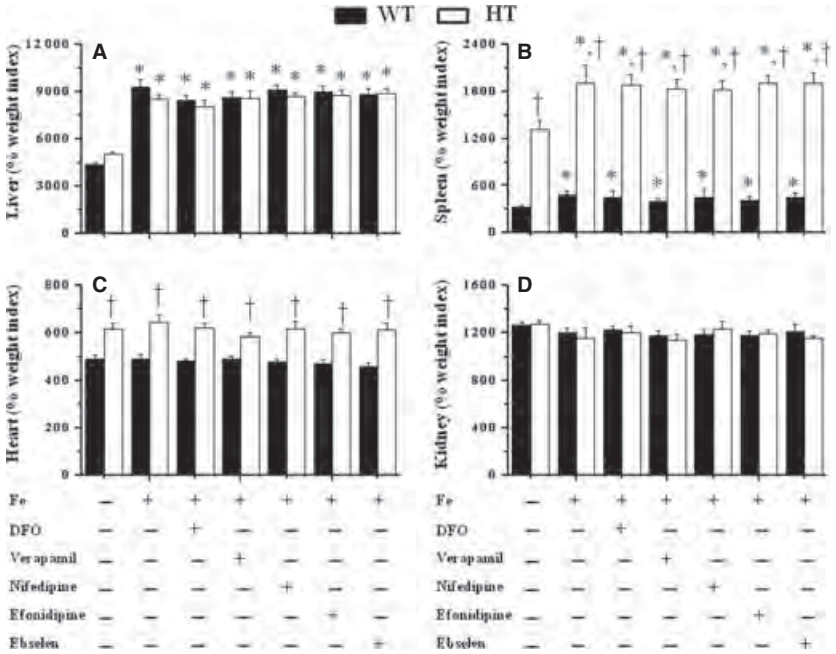

Figure 2 Effects of pharmacological interventions on percentage of organ weight index [i.e., liver (A), spleen (B), heart (C), kidney (D)] in wild-type (WT) and thalassemic mice (HT) (n = 8–10/group). *P < 0.05 vs. control, †P < 0.05 vs. WT.

significantly increased spleen weight index, and none of the pharmacological interventions prevented or attenuated it (Fig. 2B). The heart weight index of the HT mice was significantly larger than the WT in the control group (Fig. 2C). After 4 months of iron feeding and pharmacological interventions, the heart weight index in both types of mice (WT, HT) was not significantly different from the control group (Fig. 2C). Kidney weight indexes were not different in both types of mice (WT, HT) and in all groups throughout the experiment (Fig. 2D).

Effect of pharmacological interventions on heart rate variability

Wild-type mice in the FE group had increased Lf/Hf ratio, Lfnu and decreased Hfnu, suggesting that iron-overloaded conditions impaired cardiac autonomic regulation of heart rate compared with the control group (Table 3). In the treatment groups, verapamil, nifedipine, efonidipine, DMT1 blocker and iron chelator significantly decreased the Lf/Hf ratio, Lfnu and increased the Hfnu (Table 3). The results of the heart rate, RR, SDNN and rMSSD in WT mice after pharmacological

Table 3 Effects of pharmacological interventions on heart rate variability in wild-type mice

Parameters	Control	FE	FE/DFO	FE/Verapamil	FE/Nifedipine	FE/Efonidipine	FE/Ebselen
RR_{max}	100 ± 3	102 ± 2	104 ± 4	101 ± 7	106 ± 3	101 ± 3	101 ± 2
RR_{min}	83 ± 1	85 ± 1	86 ± 1	83 ± 1	85 ± 1	85 ± 1	85 ± 1
Mean RR	90 ± 1	93 ± 1	93 ± 1	92 ± 2	93 ± 2	94 ± 1	92 ± 1
SDNN (ms)	2.92 ± 0.46	3.00 ± 0.50	2.74 ± 0.63	2.83 ± 0.69	2.65 ± 0.44	2.73 ± 0.61	2.13 ± 0.43
rMSSD (ms)	2.85 ± 0.56	2.54 ± 0.57	2.55 ± 0.81	2.58 ± 0.73	2.45 ± 0.56	2.53 ± 0.56	2.34 ± 0.62
HR_{max} (beats/min)	714 ± 8	709 ± 9	702 ± 9	709 ± 8	704 ± 7	709 ± 8	710 ± 10
HR_{min} (beats/min)	602 ± 15	591 ± 14	605 ± 19	601 ± 25	608 ± 12	606 ± 24	603 ± 16
Mean HR (beats/min)	662 ± 8	644 ± 7	646 ± 9	652 ± 17	648 ± 15	645 ± 7	653 ± 8
Lf/Hf ratio	0.232 ± 0.021	0.707 ± 0.049*	0.224 ± 0.030#	0.294 ± 0.019#	0.317 ± 0.018#	0.263 ± 0.033#	0.283 ± 0.036#
Hfnu	0.812 ± 0.014	0.585 ± 0.017*	0.821 ± 0.021#	0.774 ± 0.012#	0.760 ± 0.012#	0.798 ± 0.020#	0.783 ± 0.023#
Lfnu	0.188 ± 0.014	0.415 ± 0.017*	0.179 ± 0.021#	0.226 ± 0.012#	0.240 ± 0.012#	0.202 ± 0.020#	0.218 ± 0.023#

SDNN, standard deviation of all RR intervals; rMSSD, root mean square of successive difference of RR; HR, heart rate; Hfnu, normalized high-frequency power; Lfnu, normalized low-frequency power.
*P < 0.05 vs. control, #P < 0.05 vs. FE.

interventions were not different from the control group throughout the experiment (Table 3).

Similar results were found in FE group of thalassemic mice. Increased Lf/Hf ratio and Lfnu, and decreased Hfnu were observed, suggesting that iron-overload conditions are associated with progressive deterioration of the already impaired cardiac autonomic function, compared with the control group (Table 4). Treatment with verapamil, nifedipine, efonidipine, DMT1 blocker and iron chelator decreased Lf/Hf ratio, Lfnu and increase Hfnu, which were back to the level observed in the control group (Table 4). The heart rate, RR, SDNN and rMSSD in thalassemic mice after pharmacological interventions were not significantly different from the control group throughout the experiment (Table 4).

Effect of pharmacological interventions on LV function

Wild-type mice in the FE group showed significantly decreased ESP, P_{max}, maximum dP/dt, SV, CO and SW, compared with the control group (Table 5). Treatment with verapamil, nifedipine, efonidipine, DMT1 blocker and iron chelator showed significantly increased ESP, P_{max}, SV, CO and SW, which were back to the level in the control group (Table 5). The heart rate, EDP, P_{min} and minimum dP/dt in WT mice after pharmacological interventions were not significantly different from the control group throughout the experiment (Table 5).

Similar results were found in the FE group of thalassemic mice, in which significantly decreased ESP, P_{max}, maximum dP/dt, SV, CO and SW were found, compared with the control group (Table 6). Treatment with verapamil, nifedipine, efonidipine, DMT1 blocker and iron chelator showed significantly increased ESP, P_{max}, SV, CO and SW, which were back to the level in the control group (Table 6). Moreover, in thalassemic mice with iron overload, treatment with efonidipine significantly increased the maximum dP/dt compared with the FE group (Table 6). The heart rate, EDP, P_{min} and minimum dP/dt in thalassemic mice after pharmacological interventions were not significantly different from the control group throughout the experiment (Table 6). The

Table 4 Effects of pharmacological interventions on heart rate variability in thalassemic mice

Parameters	Control	FE	FE/DFO	FE/Verapamil	FE/Nifedipine	FE/Efonidipine	FE/Ebselen
RR_{max}	103 ± 3	110 ± 3	105 ± 5	110 ± 7	103 ± 6	106 ± 6	108 ± 7
RR_{min}	84 ± 1	87 ± 1	86 ± 2	87 ± 1	85 ± 1	86 ± 1	87 ± 1
Mean RR	91 ± 1	94 ± 2	94 ± 2	94 ± 1	95 ± 2	93 ± 1	93 ± 1
SDNN (ms)	3.48 ± 0.51	3.53 ± 0.51	3.44 ± 0.77	3.55 ± 0.56	3.03 ± 0.70	3.13 ± 0.77	3.11 ± 0.51
rMSSD (ms)	3.37 ± 0.72	3.03 ± 0.85	3.89 ± 1.27	3.64 ± 0.84	3.68 ± 0.97	3.59 ± 1.09	3.36 ± 0.79
HR_{max} (beats/min)	693 ± 7	677 ± 13	689 ± 8	688 ± 7	693 ± 6	696 ± 8	686 ± 9
HR_{min} (beats/min)	580 ± 18	570 ± 7	576 ± 27	562 ± 19	571 ± 37	580 ± 15	593 ± 15
Mean HR (beats/min)	645 ± 11	615 ± 5	626 ± 12	646 ± 8	638 ± 7	641 ± 7	647 ± 7
Lf/Hf ratio	0.366 ± 0.027	0.673 ± 0.078*	0.324 ± 0.068#	0.316 ± 0.037#	0.355 ± 0.059#	0.346 ± 0.044#	0.334 ± 0.055#
Hfnu	0.734 ± 0.015	0.605 ± 0.027*	0.766 ± 0.035#	0.763 ± 0.021#	0.749 ± 0.028#	0.751 ± 0.024#	0.759 ± 0.031#
Lfnu	0.266 ± 0.015	0.395 ± 0.027*	0.234 ± 0.035#	0.237 ± 0.021#	0.251 ± 0.028#	0.249 ± 0.024#	0.241 ± 0.031#

SDNN, standard deviation of all RR intervals; rMSSD, root mean square of successive difference of RR; HR, heart rate; Hfnu, normalized high-frequency power; Lfnu, normalized low-frequency power.
*$P < 0.05$ vs. control, #$P < 0.05$ vs. FE.

Table 5 Effects of pharmacological interventions on left ventricular function in wild-type mice

Hemodynamic parameters	Control	FE	FE/DFO	FE/Verapamil	FE/Nifedipine	FE/Efonidipine	FE/Ebselen
HR (beats/min)	328 ± 21	327 ± 26	321 ± 15	334 ± 16	335 ± 12	329 ± 16	332 ± 24
ESP (mmHg)	112 ± 5	82 ± 3*	118 ± 9#	111 ± 8#	121 ± 10#	114 ± 6#	116 ± 6#
EDP (mmHg)	47 ± 4	41 ± 3	48 ± 3	45 ± 3	38 ± 3	42 ± 4	41 ± 4
P_{max} (mmHg)	118 ± 5	90 ± 4*	123 ± 8#	117 ± 8#	130 ± 6#	117 ± 6#	121 ± 5#
P_{min} (mmHg)	45 ± 4	38 ± 3	44 ± 4	41 ± 3	35 ± 3	40 ± 4	38 ± 4
dP/dt_{max} (mmHg/s)	7957 ± 2160	5282 ± 1893*	8112 ± 2156#	7154 ± 1433	6217 ± 2197	6996 ± 2196	6701 ± 2386
dP/dt_{min} (mmHg/s)	−4740 ± 176	−4972 ± 448	−5484 ± 736	−5908 ± 824	−6312 ± 688	−5944 ± 362	−5142 ± 906
Stroke volume (μL)	16 ± 1	10 ± 1*	19 ± 3#	18 ± 1#	17 ± 1#	19 ± 2#	21 ± 3#
Cardiac output (μL/min)	5.07 ± 0.38	3.15 ± 0.20*	5.42 ± 0.96#	6.22 ± 0.39#	5.43 ± 0.27#	5.64 ± 0.56#	5.97 ± 0.69#
Stroke work (mmHg/μL)	1721 ± 211	683 ± 82*	1480 ± 145#	1287 ± 93#	1671 ± 334#	1314 ± 153#	1699 ± 287#

HR, heart rate; ESP, EDP, end-systolic and end-diastolic pressure; P_{max}, P_{min}, maximum and minimum pressure; dP/dt_{max}, dP/dt_{min}, maximum and minimum dP/dt.
*$P < 0.05$ vs. control, #$P < 0.05$ vs. FE.

Table 6 Effects of pharmacological interventions on left ventricular function in thalassemic mice

Hemodynamic parameters	Control	FE	FE/DFO	FE/Verapamil	FE/Nifedipine	FE/Efonidipine	FE/Ebselen
HR (beats/min)	334 ± 13	322 ± 21	336 ± 13	320 ± 20	318 ± 18	323 ± 11	335 ± 26
ESP (mmHg)	122 ± 6	82 ± 6*	118 ± 6#	111 ± 2#	116 ± 6#	115 ± 3#	112 ± 6#
EDP (mmHg)	42 ± 1	39 ± 1	36 ± 1	38 ± 1	40 ± 2	41 ± 1	39 ± 2
P_{max} (mmHg)	125 ± 6	88 ± 6*	122 ± 6#	115 ± 1#	119 ± 6#	120 ± 3#	122 ± 6#
P_{min} (mmHg)	38 ± 1	36 ± 1	33 ± 1	34 ± 1	36 ± 2	37 ± 1	35 ± 1
dP/dt_{max} (mmHg/s)	8335 ± 2229	5957 ± 1156*	6158 ± 2267*	5105 ± 1840*	6516 ± 1080*	7753 ± 1999#	5456 ± 1523*
dP/dt_{min} (mmHg/s)	−6552 ± 822	−6878 ± 1362	−7536 ± 394	−6938 ± 464	−6176 ± 414	−5976 ± 506	−7594 ± 638
Stroke volume (μL)	36 ± 9	14 ± 2*	33 ± 5#	31 ± 4#	32 ± 5#	31 ± 3#	31 ± 6#
Cardiac output (μL/min)	9.85 ± 0.68	3.93 ± 0.35*	9.66 ± 1.58#	7.77 ± 0.62#	9.42 ± 0.93#	8.52 ± 0.64#	9.88 ± 2.01#
Stroke work (mmHg/μL)	2432 ± 363	1061 ± 142*	2010 ± 284#	2069 ± 283#	2315 ± 366#	2098 ± 247#	2792 ± 406#

HR, heart rate; ESP, EDP, end-systolic and end-diastolic pressure; P_{max}, P_{min}, maximum and minimum pressure; dP/dt_{max}, dP/dt_{min}, maximum and minimum dP/dt.
*$P < 0.05$ vs. control, #$P < 0.05$ vs. FE.

CO in HT mice was higher than that in WT mice, indicating the high-output state in HT mice, which is similar to that found in patients with thalassemia (3).

Prussian blue iron staining in the heart and liver of thalassemic mice

Prussian blue iron staining showed increased iron accumulation in heart and liver tissues in HT/Fe group, compared with the control HT group (Fig. 3B). DFO, verapamil, nifedipine, efonidipine and ebselen decreased the cardiac iron accumulation in HT heart under iron-overload condition (Fig. 3). Only DFO, efonidipine and ebselen decreased the liver iron accumulation in HT under iron-overload condition (Fig. 3).

Effects of pharmacological interventions on cardiac iron concentration and cardiac MDA content

At 4 months of iron administration, increased cardiac iron was significantly higher in the FE group (WT, HT), compared with the control group (Fig. 4A,B). DFO, verapamil, nifedipine, efonidipine and ebselen decreased the cardiac iron concentration in both types of mice, compared with the FE group, and were not different among groups of treatment (Fig. 4A,B). Similar results were found in cardiac MDA content, in which both types of mice in the FE group (WT, HT) had a significantly increased cardiac MDA content, compared with the control group (Fig. 4C,D). All of pharmacological interventions decreased the cardiac MDA concentration in both types of mice, compared with the FE group, and were not different among groups of treatment (Fig. 4C,D).

Effects of pharmacological interventions on liver iron concentration and liver MDA content

In the control group, the liver iron (0.74 ± 0.05 vs. 0.28 ± 0.04 mg/g dry weight) and liver MDA (8.87 ± 1.04 vs. 5.46 ± 0.47 μM/mg protein) of HT mice were significantly higher than WT mice ($P < 0.01$) (Fig. 5A,B). At 4 months of iron administration, increased liver iron in the FE group (WT, HT) was demonstrated, compared with the control group (Fig. 5A,B). Only DFO, efonidipine and ebselen decreased the liver iron concentration in both types of mice, compared with the FE group (Fig. 5A,B). Similar results were found in the liver MDA content, in which mice in the FE group (WT, HT) had significantly increased liver MDA content, compared with the control group (Fig. 5C,D). Only DFO, efonidipine and ebselen decreased the liver MDA concentration in both types of mice, compared with the FE group (Fig. 5C,D).

Effects of pharmacological interventions on plasma non-transferrin-bound iron and plasma MDA level

In the control group, the levels of plasma NTBI were not detected both in wild-type and in thalassemic mice (Fig. 6A,B). At 4 months of iron administration, both types of mice in the FE group (WT, HT) had significantly increased plasma NTBI, compared with the control group (Fig. 6A,B). DFO, verapamil, nifedipine, efonidipine and ebselen decreased plasma NTBI in both types of mice, compared with the FE group, and was not different among groups of treatment (Fig. 6A,B). At 4 months of iron administration, increased plasma MDA in the FE group (WT, HT) was demonstrated compared with the control group (Fig. 6C,D). In both types of mice (WT, HT), only DFO, efonidipine and ebselen decreased the plasma MDA, compared with the FE group (Fig. 6C,D).

Effect of pharmacological intervention on mortality rate

Iron-overloaded wild-type mice had an increased mortality rate, compared with the control group (Fig. 6E).

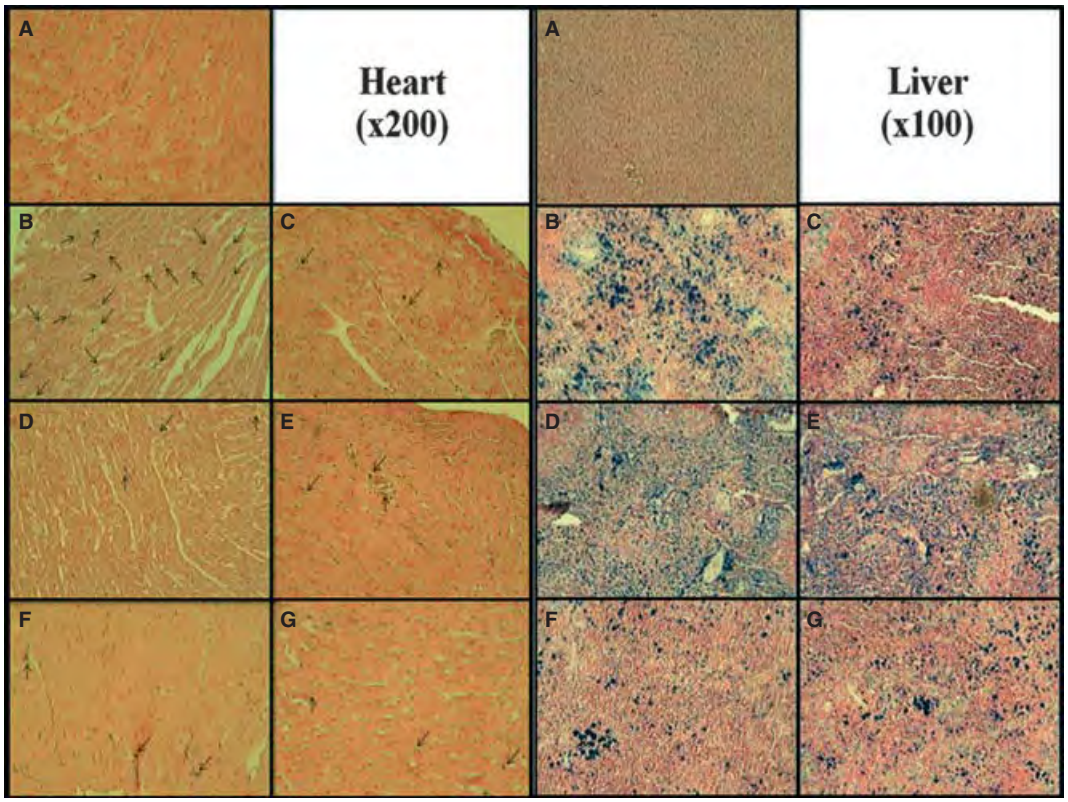

Figure 3 Prussian blue iron staining in the heart (×200) and liver (×100) of thalassemic mice. Control (A), Fe group (B), Fe/DFO (C), Fe/Verapamil (D), Fe/Nifedipine (E), Fe/Efonidipine (F), Fe/Ebselen (G). Arrow indicated iron staining in blue color.

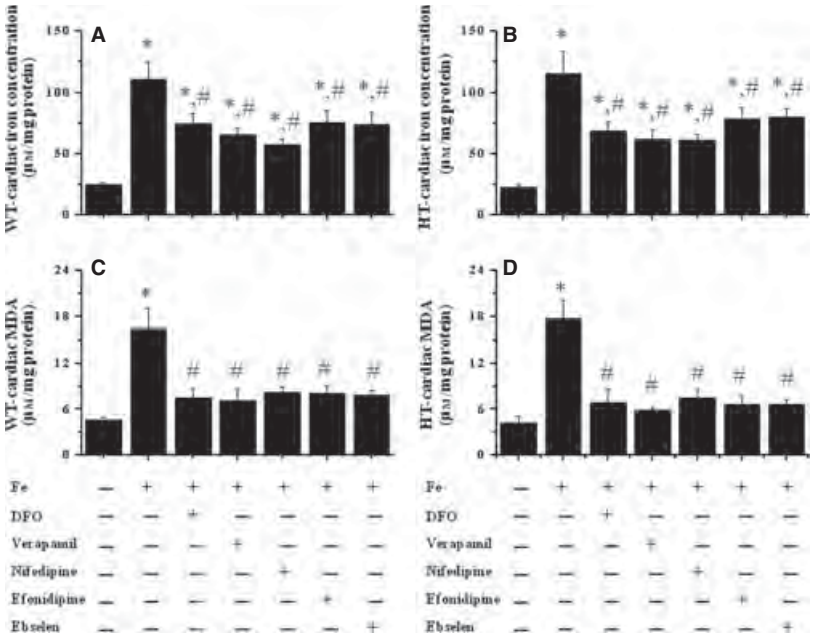

Figure 4 Effects of pharmacological interventions on cardiac iron concentration and cardiac malondialdehyde (MDA) content in wild-type (WT) and thalassemic mice (HT) (n = 8–10/group). $^{*}P < 0.05$ vs. control, $^{\#}P < 0.05$ vs. FE.

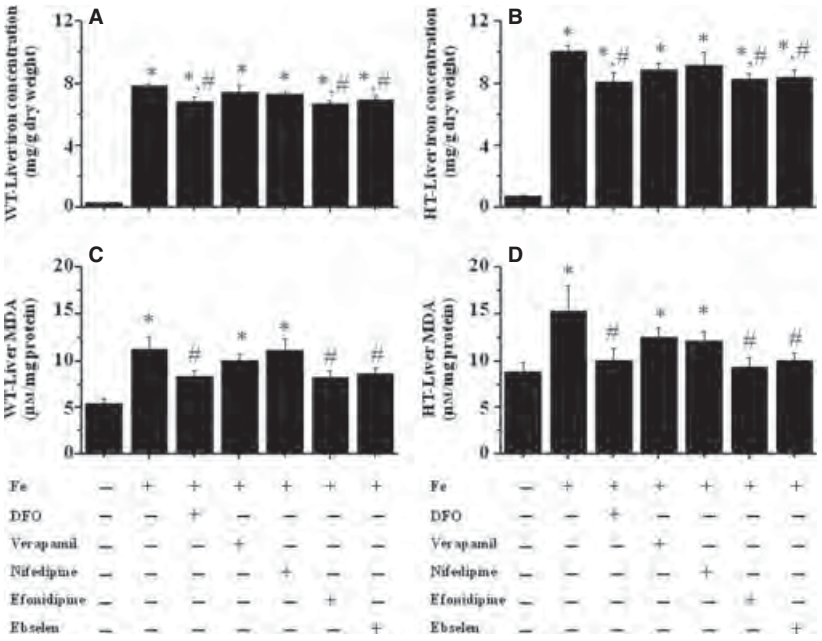

Figure 5 Effects of pharmacological interventions on liver iron concentration and liver malondialdehyde (MDA) content in wild-type (WT) and thalassemic mice (HT) (n = 8–10/group). $^{*}P < 0.05$ vs. control, $^{\#}P < 0.05$ vs. FE.

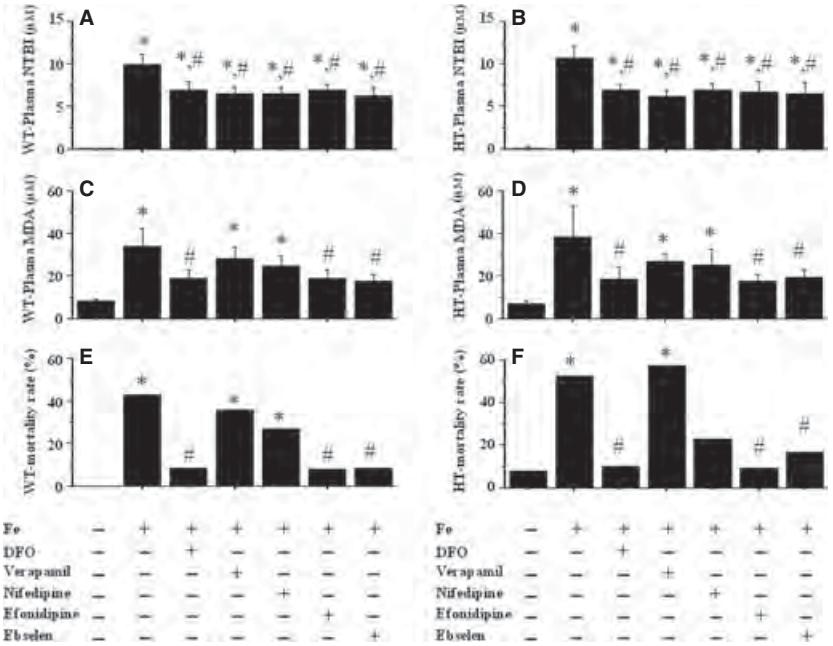

Figure 6 Effects of pharmacological interventions on plasma non-transferrin-bound iron (NTBI) level (A, B), plasma malondialdehyde (MDA) content (C, D) and mortality rate (E, F) in wild-type (WT) and thalassemic mice (HT) (n = 8–10/group). $^{*}P < 0.05$ vs. control, $^{\#}P < 0.05$ vs. FE.

Treatment with iron chelator (DFO), TTCC blocker (efonidipine) and DMT1 blocker (ebselen) decreased the mortality rate. However, the LTCC blockers verapamil and nifedipine did not decrease the mortality rate (Fig. 6E).

In iron-overloaded thalassemic mice, an increased mortality rate was found in the iron-loaded group, compared with the control group (Fig. 6F). Treatment with iron chelator (DFO), TTCC blocker (efonidipine) and DMT1 blocker (ebselen) decreased the mortality rate.

However, the LTCC blocker verapamil and nifedipine did not decrease the mortality rate (Fig. 6F). TTCC blocker (efonidipine) could reduce the mortality rate from 43% to 8% in WT and 53% to 9% in HT, whereas LTCC blocker did not provide this benefit (Fig. 6E,F).

Microarray study on LTCC and TTCC gene expressions in thalassemic heart

Microarray analysis showed that in the heart of iron-overload HT mice (HT/Fe group), calcium channel, voltage-dependent, T-type, alpha 1G subunit (Cacna1g) (NM_009783.1) was up-regulated (1.560263 fold), whereas calcium channel, voltage-dependent, L-type, alpha 1C subunit (Cacna1c) (NM_009781.1) was not altered, compared with the heart of HT mice without iron overload.

Real-time RT-PCR study on TTCC and LTCC mRNA expression

In iron-overloaded HT mice, an increased TTCC mRNA expression was found in the iron-loaded group, compared with the control group (Fig. 7A). Treatment with DFO, verapamil, nifedipine, efonidipine and ebselen did not alter TTCC mRNA expression. In contrast, LTCC mRNA expression was not changed in all groups of HT mice (Fig. 7B).

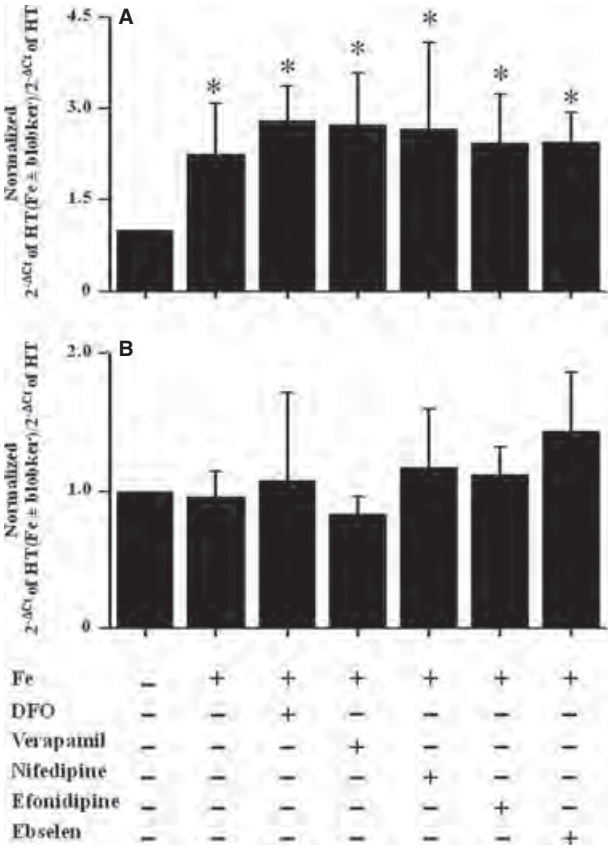

Figure 7 Real-time RT-PCR quantitation of TTCC and LTCC mRNA expression in the heart of thalassemic mice (HT). $*P < 0.05$ vs. control. LTCC, L-type calcium channels.

Discussion

The major findings in this study are that (i) iron-overload conditions are associated with increased Lf/Hf ratio, cardiac and liver iron, cardiac and liver MDA, plasma NTBI and plasma MDA, mortality rate and impaired LV function; (ii) treatment with LTCC, TTCC, DMT1 blocker and iron chelator (DFO) decreased the Lf/Hf ratio, cardiac iron and MDA, plasma NTBI and improved cardiac dysfunction in both types of mice (WT, HT), compared with the FE group; (iii) only TTCC and DMT1 blockers and iron chelator (DFO) decreased liver iron, liver MDA, plasma MDA and mortality rate in both types of mice (WT, HT), compared with the FE group, whereas LTCC blocker could not; (iv) in HT mice, only the TTCC blocker efonidipine increased EDP, P_{min} and maximum dP/dt; (v) in HT/Fe group, TTCC was up-regulated compared with HT, and all of treatment did not changed TTCC expression.

In this study, the development of LV systolic dysfunction was observed in iron-overloaded mice as indicated by decreased ESP, P_{max}, SV, CO and SW. LTCC blockers, verapamil and nifedipine, prevented this harmful effect of cardiac iron overload in both types of mice (WT, HT), which is consistent with a previous study in which the LTCC blockers, verapamil and amlodipine, improved cardiac dysfunction in iron-overloaded mice (10). Moreover, our results demonstrated that TTCC and DMT1 blockers as well as the iron chelator (DFO) could also attenuate cardiac dysfunction caused by iron overload in both WT and HT mice. In cultured thalassemic cardiomyocytes, a previous study demonstrated that treatment with the TTCC blocker, efonidipine, significantly reduced the cardiac iron uptake (11). In this study, our '*in vivo*' iron-overload model demonstrated similar benefits of the TTCC blocker, emphasizing that TTCC could play an important role on cardiac iron uptake under iron-overload conditions. As the improvement of LV function was also observed in conjunction with the improved HRV following these pharmacological interventions, these findings suggested that LTCC, TTCC and DMT1 could play an important role in cardiac iron uptake.

It has been shown that chronic iron overload can lead to increased plasma NTBI, which can catalyze the production of highly toxic free hydroxyl radicals via Haber–Weiss and Fenton reactions (40, 41). The excess of free

radicals can damage cellular lipids, proteins, and DNA (40, 41), causing increased lipid peroxidation and leading to the increased cytotoxic aldehyde products such as 4-hydroxynonenal (HNE) and MDA (40, 41). The aldehyde products can form covalent links to proteins leading to the loss of cellular protein function (42). In this study, the increased cardiac iron concentrations in both types of mice under iron-overload conditions were associated with the increased cardiac MDA content, indicating the cardiac cellular damage caused by iron overload. This similar benefit of all pharmacological interventions in this study could be responsible for improved LV function and HRV found in these iron-overloaded mice.

Although all pharmacological interventions in this study could similarly reduce the cardiac iron concentration in both types of mice, the effects on MDA reduction in the plasma and liver were not the same. The TTCC blocker and DMT1 blocker as well as the DFO could reduce the liver iron concentration, liver MDA and plasma MDA to a greater extent than the LTCC blockers could in both WT and HT mice. In this study, LTCC blockers did not decrease liver iron, liver MDA and plasma MDA, suggesting that LTCC did not play an important role in iron uptake in the liver. These findings are consistent with previous studies which showed that efonidipine and ebselen could have an antioxidant effect (43, 44), whereas the LTCC blockers verapamil and amlodipine did not decrease liver iron in iron-overloaded mice as hepatocytes did not express LTCC (10). Our findings indicated that in addition to a beneficial cardiac effect, a TTCC blocker could also provide systemic protective effects, at least for plasma MDA and liver iron and MDA reduction, whereas an LTCC blocker did not. Considering all of these protective benefits, this could be the reason for the higher mortality rate observed in the LTCC blocker groups.

T-type Ca^{2+} channels are abundantly expressed in the embryonic cardiomyocytes, but their expression is suppressed in the adult cells (45). In addition, T-type Ca^{2+} channel current has been shown to reappear in ventricular myocytes under some pathological conditions such as ventricular hypertrophy (46, 47) and postmyocardial infarction (48). Our findings indicated that iron-overload conditions increased TTCC mRNA expression in HT mice. Although all of pharmacological treatment did not effect on gene expression, it might inhibit TTCC function, thus leading to improved LV function. These findings suggested that under pathologic conditions such as iron overload, TTCC expression was reexpressed in adult hearts and could play an important role in iron-overload cardiomyopathy.

In conclusion, as the TTCC blocker, efonidipine, could provide broader beneficial effects including the heart, liver, and plasma, and antioxidant in iron-overload condition in both WT and HT mice, it is possible that efonidipine could be another drug of choice, in addition to an iron chelator and DMT1 blocker, for the treatment of the iron-overload condition. It is important to note here that although efonidipine is not a specific TTCC blocker as it could also block LTCC, its efficacy in blocking TTCC is much greater than that of LTCC (11, 49). Our findings conclude that efonidipine provided better protective effects than the LTCC blocker, indicating that the TTCC blocker effect of efonidipine could play an important role in the present study. Future clinical studies are also needed to validate the clinical significance for its use in iron-overload patients.

Study limitation

Although our findings indicated that TTCC expression was up-regulated, while LTCC was not altered in iron-overload hearts, the function of TTCC was not directly explored. Future studies are needed to investigate the TTCC current and the role of pharmacological interventions in iron-overload cardiomyocytes. Moreover, genetic manipulation of TTCC is needed to directly study its impact on iron uptake under iron-overload condition.

Acknowledgements

We would like to thank Assist. Prof. Jongkolnee Settakorn for her assistance on microarray data. This work is supported by grants from the Thailand Research Fund RTA 5280006 (N.C.), BRG 5480003 (S.C.), and the Thailand Research Fund Royal Golden Jubilee PhD project (S.K. and N.C.)

Conflict of interests

The authors declare that there are no conflicts of interest.

References

1. Weatherall DJ, Clegg JB. Inherited haemoglobin disorders: an increasing global health problem. *Bull World Health Organ* 2001;**79**:704–12.
2. Olivieri NF. The beta-thalassemias. *N Engl J Med* 1999;**341**:99–109.
3. Kremastinos DT, Farmakis D, Aessopos A, Hahalis G, Hamodraka E, Tsiapras D, Keren A. Beta-thalassemia cardiomyopathy: history, present considerations, and future perspectives. *Circ Heart Fail* 2010;**3**:451–8.
4. Cohen AR, Galanello R, Pennell DJ, Cunningham MJ, Vichinsky E. Thalassemia. *Hematology Am Soc Hematol Educ Program* 2004;14–34.
5. Breuer W, Hershko C, Cabantchik ZI. The importance of non-transferrin bound iron in disorders of iron metabolism. *Transfus Sci* 2000;**23**:185–92.

6. Templeton DM, Liu Y. Genetic regulation of cell function in response to iron overload or chelation. *Biochim Biophys Acta* 2003;**1619**:113–24.
7. Zurlo MG, De Stefano P, Borgna-Pignatti C, Di Palma A, Piga A, Melevendi C, Di Gregorio F, Burattini MG, Terzoli S. Survival and causes of death in thalassaemia major. *Lancet* 1989;**2**:27–30.
8. Wood JC, Enriquez C, Ghugre N, Otto-Duessel M, Aguilar M, Nelson MD, Moats R, Coates TD. Physiology and pathophysiology of iron cardiomyopathy in thalassemia. *Ann N Y Acad Sci* 2005;**1054**:386–95.
9. Tsushima RG, Wickenden AD, Bouchard RA, Oudit GY, Liu PP, Backx PH. Modulation of iron uptake in heart by L-type Ca^{2+} channel modifiers: possible implications in iron overload. *Circ Res* 1999;**84**:1302–9.
10. Oudit GY, Sun H, Trivieri MG, *et al*. L-type Ca^{2+} channels provide a major pathway for iron entry into cardiomyocytes in iron-overload cardiomyopathy. *Nat Med* 2003;**9**:1187–94.
11. Kumfu S, Chattipakorn S, Srichairatanakool S, Settakorn J, Fucharoen S, Chattipakorn N. T-type calcium channel as a portal of iron uptake into cardiomyocytes of beta-thalassemic mice. *Eur J Haematol* 2011;**86**:156–66.
12. Parkes JG, Olivieri NF, Templeton DM. Characterization of Fe^{2+} and Fe^{3+} transport by iron-loaded cardiac myocytes. *Toxicology* 1997;**117**:141–51.
13. Oudit GY, Trivieri MG, Khaper N, Liu PP, Backx PH. Role of L-type Ca^{2+} channels in iron transport and iron-overload cardiomyopathy. *J Mol Med* 2006;**84**:349–64.
14. Chua AC, Graham RM, Trinder D, Olynyk JK. The regulation of cellular iron metabolism. *Crit Rev Clin Lab Sci* 2007;**44**:413–59.
15. Wallander ML, Leibold EA, Eisenstein RS. Molecular control of vertebrate iron homeostasis by iron regulatory proteins. *Biochim Biophys Acta* 2006;**1763**:668–89.
16. Ke Y, Chen YY, Chang YZ, Duan XL, Ho KP, Jiang DH, Wang K, Qian ZM. Post-transcriptional expression of DMT1 in the heart of rat. *J Cell Physiol* 2003;**196**: 124–30.
17. Parkes JG, Liu Y, Sirna JB, Templeton DM. Changes in gene expression with iron loading and chelation in cardiac myocytes and non-myocytic fibroblasts. *J Mol Cell Cardiol* 2000;**32**:233–46.
18. Kardelen F, Tezcan G, Akcurin G, Ertug H, Yesilipek A. Heart rate variability in patients with thalassemia major. *Pediatr Cardiol* 2008;**29**:935–9.
19. Rutjanaprom W, Kanlop N, Charoenkwan P, Sittiwangkul R, Srichairatanakool S, Tantiworawit A, Phrommintikul A, Chattipakorn S, Fucharoen S, Chattipakorn N. Heart rate variability in beta-thalassemia patients. *Eur J Haematol* 2009;**83**:483–9.
20. Chattipakorn N, Incharoen T, Kanlop N, Chattipakorn S. Heart rate variability in myocardial infarction and heart failure. *Int J Cardiol* 2007;**120**:289–96.
21. Incharoen T, Thephinlap C, Srichairatanakool S, Chattipakorn S, Winichagoon P, Fucharoen S, Vadolas J, Chattipakorn N. Heart rate variability in beta-thalassemic mice. *Int J Cardiol* 2007;**121**:203–4.
22. Walker EM Jr, Morrison RG, Dornon L, Laurino JP, Walker SM, Studeny M, Wehner PS, Rice KM, Wu M, Blough ER. Acetaminophen combinations protect against iron-induced cardiac damage in gerbils. *Ann Clin Lab Sci* 2009;**39**:378–85.
23. Paquette F, Jasmin G, Dumont L. Cardioprotective efficacy of verapamil and mibefradil in young UM-X7.1 cardiomyopathic hamsters. *Cardiovasc Drugs Ther* 1999;**13**:525–30.
24. Ludwiczek S, Theurl I, Muckenthaler MU, *et al*. Ca^{2+} channel blockers reverse iron overload by a new mechanism via divalent metal transporter-1. *Nat Med* 2007;**13**:448–54.
25. Matsumura T, Furuichi H, Izumi J, Suda H, Ito S, Takei M, Nishi N, Mori T, Tanaka Y, Kurimoto T. [Effect of efonidipine hydrochloride, a calcium channel blocker, on the experimental cerebral ischemia/anoxia]. *Nippon Yakurigaku Zasshi* 1995;**105**:437–46.
26. Dhanarajan R, Abraham P, Isaac B. Protective effect of ebselen, a selenoorganic drug, against gentamicin-induced renal damage in rats. *Basic Clin Pharmacol Toxicol* 2006;**99**:267–72.
27. Singh S, Hider RC, Porter JB. A direct method for quantification of non-transferrin-bound iron. *Anal Biochem* 1990;**186**:320–3.
28. Lee DW, Lee TK, Cho IS, Park HE, Jin S, Cho HJ, Kim SH, Oh S, Kim HS. Creation of myocardial fibrosis by transplantation of fibroblasts primed with survival factors. *Am J Physiol Heart Circ Physiol* 2011;**301**:H1004–14.
29. Pacher P, Nagayama T, Mukhopadhyay P, Batkai S, Kass DA. Measurement of cardiac function using pressure-volume conductance catheter technique in mice and rats. *Nat Protoc* 2008;**3**:1422–34.
30. Lips DJ, van der Nagel T, Steendijk P, Palmen M, Janssen BJ, van Dantzig JM, de Windt LJ, Doevendans PA. Left ventricular pressure-volume measurements in mice: comparison of closed-chest versus open-chest approach. *Basic Res Cardiol* 2004;**99**:351–9.
31. van Acker FA, Boven E, Kramer K, Haenen GR, Bast A, van der Vijgh WJ. Frederine, a new and promising protector against doxorubicin-induced cardiotoxicity. *Clin Cancer Res* 2001;**7**:1378–84.
32. Rebouche CJ, Wilcox CL, Widness JA. Microanalysis of non-heme iron in animal tissues. *J Biochem Biophys Methods* 2004;**58**:239–51.
33. Cheng CS, Sullivan TD, Li PK. Iron toxicity screening. *JACEP* 1979;**8**:238–40.
34. Grotto D, Santa Maria LD, Boeira S, Valentini J, Charao MF, Moro AM, Nascimento PC, Pomblum VJ, Garcia SC. Rapid quantification of malondialdehyde in plasma by high performance liquid chromatography-visible detection. *J Pharm Biomed Anal* 2007;**43**:619–24.
35. Niwa N, Yasui K, Opthof T, Takemura H, Shimizu A, Horiba M, Lee JK, Honjo H, Kamiya K, Kodama I.

Cav3.2 subunit underlies the functional T-type Ca^{2+} channel in murine hearts during the embryonic period. *Am J Physiol Heart Circ Physiol* 2004;**286**:H2257–63.
36. Mizuta E, Miake J, Yano S, *et al*. Subtype switching of T-type Ca^{2+} channels from Cav3.2 to Cav3.1 during differentiation of embryonic stem cells to cardiac cell lineage. *Circ J* 2005;**69**:1284–9.
37. Chiang CS, Huang CH, Chieng H, *et al*. The Ca(v)3.2 T-type Ca(2+) channel is required for pressure overload-induced cardiac hypertrophy in mice. *Circ Res* 2009;**104**:522–30.
38. Mizuta E, Shirai M, Arakawa K, *et al*. Different distribution of Cav3.2 and Cav3.1 transcripts encoding T-type Ca(2+) channels in the embryonic heart of mice. *Biomed Res* 2010;**31**:301–5.
39. Han LQ, Yang GY, Zhu HS, Wang YY, Wang LF, Guo YJ, Lu WF, Li HJ, Wang YL. Selection and use of reference genes in mouse mammary glands. *Genet Mol Res* 2010;**9**:449–56.
40. Bartfay WJ, Bartfay E. Iron-overload cardiomyopathy: evidence for a free radical – mediated mechanism of injury and dysfunction in a murine model. *Biol Res Nurs* 2000;**2**:49–59.
41. Lekawanvijit S, Chattipakorn N. Iron overload thalassemic cardiomyopathy: iron status assessment and mechanisms of mechanical and electrical disturbance due to iron toxicity. *Can J Cardiol* 2009;**25**:213–8.
42. Houglum K, Filip M, Witztum JL, Chojkier M. Malondialdehyde and 4-hydroxynonenal protein adducts in plasma and liver of rats with iron overload. *J Clin Invest* 1990;**86**:1991–8.
43. Davis MT, Bartfay WJ. Ebselen decreases oxygen free radical production and iron concentrations in the hearts of chronically iron-overloaded mice. *Biol Res Nurs* 2004;**6**:37–45.
44. Oshima T, Ozono R, Yano Y, Higashi Y, Teragawa H, Miho N, Ishida T, Ishida M, Yoshizumi M, Kambe M. Beneficial effect of T-type calcium channel blockers on endothelial function in patients with essential hypertension. *Hypertens Res* 2005;**28**:889–94.
45. Yasui K, Niwa N, Takemura H, *et al*. Pathophysiological significance of T-type Ca^{2+} channels: expression of T-type Ca^{2+} channels in fetal and diseased heart. *J Pharmacol Sci* 2005;**99**:205–10.
46. Nuss HB, Houser SR. T-type Ca^{2+} current is expressed in hypertrophied adult feline left ventricular myocytes. *Circ Res* 1993;**73**:777–82.
47. Martinez ML, Heredia MP, Delgado C. Expression of T-type Ca(2+) channels in ventricular cells from hypertrophied rat hearts. *J Mol Cell Cardiol* 1999;**31**:1617–25.
48. Huang B, Qin D, Deng L, Boutjdir M, El-Sherif N. Reexpression of T-type Ca^{2+} channel gene and current in post-infarction remodeled rat left ventricle. *Cardiovasc Res* 2000;**46**:442–9.
49. Vassort G, Talavera K, Alvarez JL. Role of T-type Ca^{2+} channels in the heart. *Cell Calcium* 2006;**40**:205–20.

International Journal of Cardiology xxx (2012) xxx–xxx

Contents lists available at SciVerse ScienceDirect

International Journal of Cardiology

journal homepage: www.elsevier.com/locate/ijcard

Cardioprotective effect of dipeptidyl peptidase-4 inhibitor during ischemia–reperfusion injury

Kroekkiat Chinda [a,b], Siripong Palee [a,b], Sirirat Surinkaew [a,b], Mattabhorn Phornphutkul [a], Siriporn Chattipakorn [a,c], Nipon Chattipakorn [a,b,*]

[a] Cardiac Electrophysiology Research and Training Center, Faculty of Medicine, Chiang Mai University, Chiang Mai, Thailand
[b] Cardiac Electrophysiology Unit, Department of Physiology, Faculty of Medicine, Chiang Mai University, Chiang Mai, Thailand
[c] Faculty of Dentistry, Chiang Mai University, Chiang Mai, Thailand

ARTICLE INFO

Article history:
Received 13 September 2011
Received in revised form 30 December 2011
Accepted 6 January 2012
Available online xxxx

Keywords:
DPP-4 inhibitor
Ischemia–reperfusion injury
Mitochondria
Electrophysiology
Infarct size

ABSTRACT

Background: Dipeptidyl peptidase-4 (DPP-4) inhibitor is a new anti-diabetic drug for type-2 diabetes mellitus patients. Despite its benefits on glycemic control, the effects of DPP-4 inhibitor on the heart during ischemia–reperfusion (I/R) periods are not known. We investigated the effect of DPP-4 inhibitor on cardiac electrophysiology and infarct size in a clinically relevant I/R model in swine and its underlying cardioprotective mechanism.

Methods: Fourteen pigs were randomized to receive either DPP-4 inhibitor (vildagliptin) 50 mg or normal saline intravenously prior to a 90-min left anterior descending artery occlusion, followed by a 120-min reperfusion period. The hemodynamic, cardiac electrophysiological and arrhythmic parameters, and the infarct size were determined before and during I/R. Rat cardiac mitochondria were used to study the protective effects of DPP-4 inhibitor on cardiac mitochondrial dysfunction caused by severe oxidative stress induced by H_2O_2 to mimic the I/R condition.

Results: Compared to the saline group, DPP-4 inhibitor attenuated the shortening of the effective refractory period (ERP), decreased the number of PVCs, increased the ventricular fibrillation threshold (VFT) during the ischemic period, and also decreased the infarct size. In cardiac mitochondria, DPP-4 inhibitor decreased the reactive oxygen species (ROS) production and prevented cardiac mitochondrial depolarization caused by severe oxidative stress.

Conclusions: During I/R, DPP-4 inhibitor stabilized the cardiac electrophysiology by preventing the ERP shortening, decreasing the number of PVCs, increasing the VFT, and decreasing the infarct size. This cardioprotective effect could be due to its prevention of cardiac mitochondrial dysfunction caused by severe oxidative stress during I/R.

1. Introduction

Diabetes mellitus has been an important health problem in most nations with the number of patients dramatically soaring and expected to reach 366 million by the year 2030 [1]. Patients with type-2 diabetes mellitus (T2DM) have been shown to have a 2- to 4-fold higher risk in coronary heart disease and stroke mortality [2–6], and have a worse prognosis after cardiovascular events [7–9]. Although several new anti-diabetic drugs have been discovered in the past decades, the therapies have been limited by their adverse effects such as weight gain, hypoglycemia, fluid retention [10], and an unexpected cardiovascular risk [11–13]. Therefore, new anti-diabetic drugs that could control hyperglycemia and reduce the risk of cardiovascular events are of potential benefits to T2DM patients.

In the past few years, a potent dipeptidyl peptidase-4 (DPP-4) inhibitor, which is a novel anti-diabetic drug, has been shown to be effective in treating T2DM patients. Its action is to inhibit the proteolytic enzyme DPP-4 activity, resulting in postponing the degradation of glucagon-like peptide-1 (GLP-1), thus improving glycemic control [14,15]. Although previous studies demonstrated the cardioprotective actions of GLP-1 in an ischemic heart model of ex vivo isolated rodent Langendorff heart [16,17], in vivo rats, rabbits, canine, and swine [18–21], as well as in acute myocardial infarction patients [22], reports on the cardioprotective effect of DPP-4 inhibitor are scant and controversial [23–26]. Furthermore, the effect of DPP-4 inhibitor on cardiac electrophysiology during ischemia–reperfusion (I/R) has never been investigated.

* Corresponding author at: Cardiac Electrophysiology Research and Training Center, Faculty of Medicine, Chiang Mai University, Chiang Mai 50200, Thailand. Tel.: +66 53 945329; fax: +66 53 945368.
E-mail address: nchattip@gmail.com (N. Chattipakorn).

0167-5273/$ – see front matter © 2012 Elsevier Ireland Ltd. All rights reserved.
doi:10.1016/j.ijcard.2012.01.011

The purpose of this study was to investigate the effect of vildagliptin, a DPP-4 inhibitor, on cardiac electrophysiology and infarct size in a clinically relevant I/R model in swine. We hypothesized that vildagliptin can attenuate the occurrence of cardiac arrhythmias, increase the ventricular fibrillation threshold (VFT), improve defibrillation efficacy by lowering the defibrillation threshold (DFT), and reduce the infarct size during I/R in the swine heart. To study the cardioprotective mechanism, we determined the effect of vildagliptin in isolated rat's cardiac mitochondria. We tested the hypothesis that the cardioprotective mechanism of vildagliptin is via its prevention of cardiac mitochondrial dysfunction caused by severe oxidative stress during I/R.

2. Materials and methods

2.1. Animal preparation

All experiments were approved by the Institutional Animal Care and Use Committees of the Faculty of Medicine, Chiang Mai University, Chiang Mai, Thailand. Pigs were anesthetized by intramuscular injection of a combination of atropine (0.04 mg/kg), zoletil® (4.4 mg/kg) and xylazine (2.2 mg/kg). After endotracheal intubation, anesthesia was maintained by 1.5–3.0% isoflurane delivered in 100% oxygen. Surface electrocardiogram (lead II), femoral arterial blood pressure (BP), heart rates (HR), core body temperature as well as blood gases and electrolytes were continuously monitored to maintain a normal physiological condition. Platinum coated titanium coil electrodes (34- and 68-mm) were advanced into the right ventricular apex (RV) and junction between right atrium and superior vena cava, respectively, to deliver electrical stimulus during VFT and DFT determinations [27]. After a median sternotomy, two pacing electrodes were attached to the epicardium at the right ventricular outflow tract (RVOT) and left ventricular apex (LV) to evaluate the effective refractory period (ERP) and diastolic pacing threshold (DPT) at each site. The electrode at the tip of the endocardial RV apex catheter was also used to determine the ERP and DPT at this site.

2.2. Experimental protocols

Fourteen domestic pigs (25 to 30 kg) were randomly divided into 2 groups (n = 7/group). The first group was assigned to receive 30 ml of normal saline solution and the second group received vildagliptin (prepared by dissolving 50-mg vildagliptin in 30-ml saline solution). Both normal saline solution and vildagliptin (2 mg/Kg) were administered intravenously at a rate of 1.0 ml/min prior to the left anterior descending artery (LAD) occlusion. Hemodynamic and cardiac electrophysiological parameters including HR, systolic (SBP) and diastolic blood pressure (DBP), DPT, ERP, corrected QT interval (QT_C), VFT and DFT were determined at the beginning of the study as a baseline. Myocardial ischemia was induced by LAD occlusion at 5 cm above the distal end [28]. During the first 60 min of occlusion, if spontaneous ventricular fibrillation (VF) occurred, the defibrillation shock was delivered to determine the DFT. On the other hand, if VF did not occur, it was electrically induced with 50-Hz alternating current. Both VFT and DFT were determined using a three-reversal up/down protocol [28]. After 90 min of occlusion, LAD ligation was released to promote reperfusion for 120 min. All parameters were determined again at the end of the reperfusion. Ventricular arrhythmia, e.g. ventricular premature contractions (PVCs), ventricular tachycardia (VT) and spontaneous VF, was recorded throughout the experiment.

2.3. Diastolic pacing threshold (DPT) determination

A train of 10 S1 stimuli was delivered via the electrode at the tip of RV catheter. Current strength was begun with 0.1 mA and was increased in 0.1-mA steps until all stimuli in a train elicited a ventricular response (capture) [28]. The minimum current strength which captures ventricular response was defined as the DPT.

2.4. Effective refractory period (ERP) determination

An S2 stimulus (2× DPT strength) was introduced in late diastole of the last S1 beat of a train of 10 S1 to elicit a capture. S1–S2 coupling interval was decreased in 10-ms steps until S2 failed to elicit a capture. ERP was defined as the longest S1–S2 interval which S2 stimulus failed to capture [28].

2.5. Ventricular fibrillation threshold (VFT) determination

The interval between the last S1 and the mid T-wave was determined for 3 times. An average was used as a coupling interval between the last S1 and S2 shock. VFT was performed by delivering S2 shocks starting at 100 V. If this shock induced VF, the decrement of 10-V step was used for each successive shock until VF was no longer induced. If the 100-V S2 shock did not induce VF, the increment of 10-V step was used for each successive shock until VF was induced. VFT was defined as the lowest shock strength that successfully induced VF [28].

2.6. Defibrillation threshold (DFT) determination

Defibrillation shock was delivered after 10 s of VF to determine the DFT using a three-reversal up/down protocol [28]. However, if the tested shock failed to defibrillate, a rescue shock (600–700 V) was delivered to successfully defibrillate the heart. The DFT was defined as the lowest shock strength required for successful defibrillation. A 4-minute interval was allowed between each VF induction episode to set the heart back to physiologic condition [28].

2.7. Infarct size determination

The infarct size was assessed with 0.5% Evans Blue and 1.0% Triphenyltetrazolium Chloride (TTC) staining as previously described [28]. In brief, at the end of the study, the LAD was re-occluded at the exact same location as during ischemia. Evans Blue was infused into the left and right coronary arteries to evaluate the area at risk (AAR). After being frozen overnight, the heart was cut into 5-mm thick slices perpendicular to the LAD from apex to the occlusion site. Each slice was incubated in TTC for 15 min to discriminate the infarct tissues from the viable myocardium. After overnight fixation with 4% paraformaldehyde, each slice was photographed with a digital camera. An area measurement was performed using Image Tool software version 3.0.

2.8. Histological analysis

Both infarct and normal myocardium were fixed with 4% neural buffered formaldehyde for 24 h at room temperature, followed by embedding in paraffin wax, and slicing into 5-μm slices for subsequent Hematoxylin–Eosin staining [29,30]. The infarct tissues were evaluated for microscopic changes using the Lodge–Patch classification [31–33].

2.9. Isolated cardiac mitochondria study protocol

Male Wistar rats (300–350 g) were used for cardiac mitochondrial isolation as described previously [34]. H_2O_2 (2 mM, incubated for 5 min) was used to induce oxidative stress in cardiac mitochondria to mimic I/R condition [34]. Isolated cardiac mitochondria were divided into 6 groups (n = 5/group): 1) Control, 2) Mitochondria treated with H_2O_2, 3) Mitochondria treated with vildagliptin for 30 min, 4) Mitochondria pretreated with vildagliptin for 5 min followed by H_2O_2 treatment, 5) Mitochondria pretreated with vildagliptin for 15 min followed by H_2O_2 treatment, 6) Mitochondria pretreated with vildagliptin for 30 min followed by H_2O_2 treatment. Vildagliptin at doses of 0.33 mM, and 3.30 mM were used in this study.

The measurement of cardiac mitochondrial reactive oxygen species (ROS) production and mitochondrial membrane potential changes ($\Delta\Psi_M$) was determined in all groups as previously described [34]. In short, dichlorohydro-fluorescein diacetate dye was used to determine the level of ROS production in cardiac mitochondria. The ROS level was expressed as arbitrary units of fluorescence intensity determined at $\lambda_{excitation}$ 485 nm and $\lambda_{emission}$ 530 nm [34]. JC-1 was used to determine the change of cardiac mitochondrial membrane potential at $\lambda_{excitation}$ 485 nm and $\lambda_{emission}$ 530 nm for green and $\lambda_{emission}$ 590 nm for red [34]. Cardiac mitochondrial depolarization was indicated by a decrease in the red/green fluorescence intensity ratio.

2.10. Statistical analysis

Data were expressed as mean ± SEM. Statistical comparison of cardiac electrophysiological, hemodynamic, and arrhythmic parameters as well as cardiac mitochondria results was performed with the Student's *t* test. Chi-square test was performed to compare VT/VF incidence, and comparison of the infarct size was analyzed using Mann–Whitney's *U* test. All statistical analysis was performed with SPSS version 10.0. A p-value less than 0.05 was considered significant.

3. Results

The hemodynamic parameters including HR, SBP, DBP and cardiac electrophysiological parameters including QT_C, QRS complex, and DPT were not significantly different between the saline-treated group and the vildagliptin-treated group during baseline, ischemia, and reperfusion periods (Table 1). Pretreatment with vildagliptin significantly increased both VFT energy and VFT voltage at ischemic period compared with the saline-treated group (Fig. 1). However, there was no difference between the DFT of the vildagliptin-treated group and the saline-treated group at any time period (Fig. 2). For the ERP, no differences were found among ERPs recorded at three sites at baseline and reperfusion periods in both saline and vildagliptin treated groups (Fig. 3A and 3C). However, during ischemia the ERP at the LV epicardium (i.e. ischemic site) was significantly shortened, compared to the other two sites in the saline-treated group (Fig. 3B), thus creating the dispersion of the ERP in the heart during this period. In the

Please cite this article as: Chinda K, et al, Cardioprotective effect of dipeptidyl peptidase-4 inhibitor during ischemia–reperfusion injury, Int J Cardiol (2012), doi:10.1016/j.ijcard.2012.01.011

Table 1
Basic electrophysiological and hemodynamic parameters.

Parameters	Baseline		Ischemia 60 min		Reperfusion	
	NSS	Vil	NSS	Vil	NSS	Vil
HR (beat/min)	88.4 ± 5.2	98.0 ± 5.7	91.3 ± 3.6	95.3 ± 4.6	102.7 ± 8.5	107.6 ± 4.2
SBP (mm Hg)	101.1 ± 7.4	102.9 ± 5.1	87.1 ± 6.1	84.6 ± 6.1	86.1 ± 3.4	85.6 ± 4.7
DBP (mm Hg)	63.3 ± 5.4	64.0 ± 3.9	55.6 ± 4.1	52.0 ± 4.6	54.4 ± 2.3	53.9 ± 2.9
QT_C (ms)	466.7 ± 7.1	466.1 ± 14.0	451.2 ± 17.2	459.2 ± 18.5	441.7 ± 15.8	435.2 ± 20.3
QRS (ms)	64.4 ± 2.0	58.0 ± 5.0	59.6 ± 2.0	57.6 ± 4.5	60.8 ± 3.2	58.0 ± 2.2
DPT RV (mA)	0.20 ± 0.02	0.21 ± 0.01	0.29 ± 0.03	0.31 ± 0.05	0.33 ± 0.05	0.36 ± 0.04
DPT RVOT (mA)	0.19 ± 0.04	0.17 ± 0.02	0.14 ± 0.02	0.16 ± 0.03	0.40 ± 0.13	0.23 ± 0.07
DPT LV (mA)	0.11 ± 0.01	0.14 ± 0.02	0.22 ± 0.08	0.18 ± 0.04	0.42 ± 0.20	0.21 ± 0.04

NSS = Normal saline solution; Vil = Vildagliptin; HR = Heart rate; SBP = Systolic blood pressure; DBP = Diastolic blood pressure; QT_C = Corrected QT interval; QRS = QRS complex; DPT = Diastolic pacing threshold; RV = Right ventricle; RVOT = Right ventricular outflow tract; LV = Left ventricle.

vildagliptin-treated group, the ERP from all 3 sites were not different during the ischemic period, indicating less dispersion of the ERP during ischemia in this group.

Regarding the occurrence of arrhythmias, the number of PVCs was markedly decreased in pigs treated with vildagliptin during 90 min of ischemia, compared to the saline-treated group (Fig. 4A). The number of PVCs during reperfusion was also smaller in the vildagliptin group, but it did not reach statistical significance (Fig. 4A). The VT/VF incidence (Fig. 4B) and the number of VT/VF episodes (Fig. 4C) were also smaller in the vildagliptin-treated group, but were not statistically significant. The time to the first VT/VF onset was not different between the vildagliptin and the saline treated groups (Fig. 4D). The area at risk (AAR) was not different between the saline (36.8 ± 2.7%) and the vildagliptin treated groups (33.4 ± 3.2%). However, the infarct size in the vildagliptin-treated group was significantly smaller than that in the saline-treated group (Fig. 5A), accounting for a 17% reduction in the infarct size. To determine stages of myocardial damage caused by I/R injury, myocardial tissues were obtained and evaluated based on microscopic changes. In the infarct area, thinning and waviness of myocardial fibers with distinct nuclei were observed (Fig. 5B).

In cardiac mitochondria, vildagliptin alone at doses 0.1 mg/ml (0.33 mM) and 1.0 mg/ml (3.30 mM) did not affect the mitochondrial ROS production and the mitochondrial membrane potential change (Fig. 6). H_2O_2 caused a markedly increased ROS level and decreased the red/green fluorescent intensity ratio (i.e. an indication of mitochondrial depolarization). Vildagliptin at 0.1 mg/ml neither attenuated cardiac mitochondrial ROS production nor prevented mitochondrial depolarization caused by H_2O_2 (Fig. 6A and 6B). However, treatment with 1.0 mg/ml of vildagliptin for 5, 15, and 30 min ameliorated cardiac mitochondrial dysfunction caused by H_2O_2, as indicated by lower ROS production (Fig. 6C) and less mitochondrial membrane potential changes (Fig. 6D), compared to those in H_2O_2-treated cardiac mitochondria.

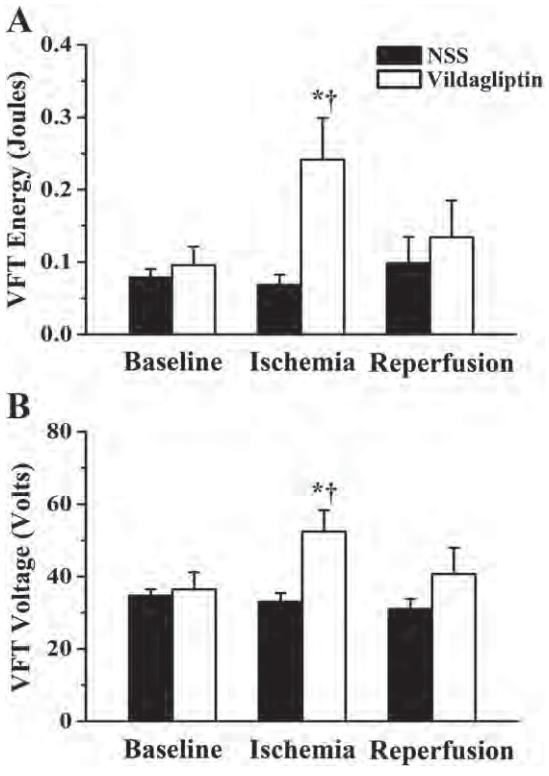

Fig. 1. Effect of vildagliptin on the VFT. During the ischemic period, vildagliptin significantly increased both VFT energy (panel A) and voltage (panel B) compared to normal saline group. * $p<0.05$ vs. NSS at ischemic period; † $p<0.05$ vs. vildagliptin at baseline.

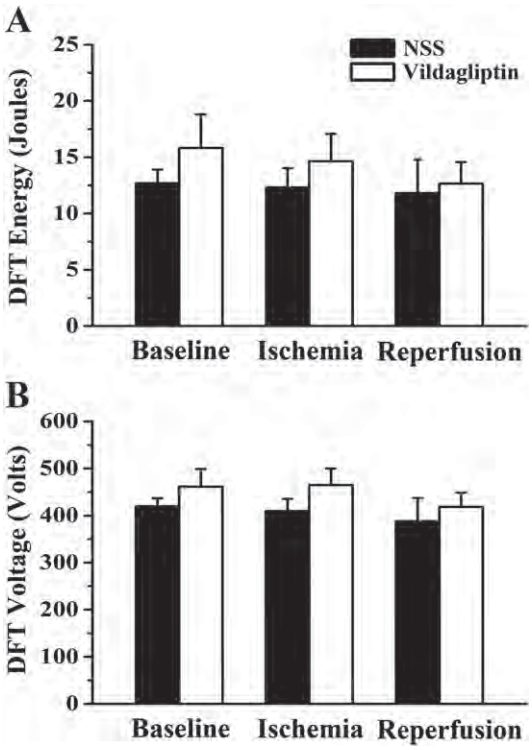

Fig. 2. Effect of vildagliptin on the DFT. Both vildagliptin and normal saline did not change the DFT energy (panel A) and DFT voltage (panel B).

Please cite this article as: Chinda K, et al, Cardioprotective effect of dipeptidyl peptidase-4 inhibitor during ischemia–reperfusion injury, Int J Cardiol (2012), doi:10.1016/j.ijcard.2012.01.011

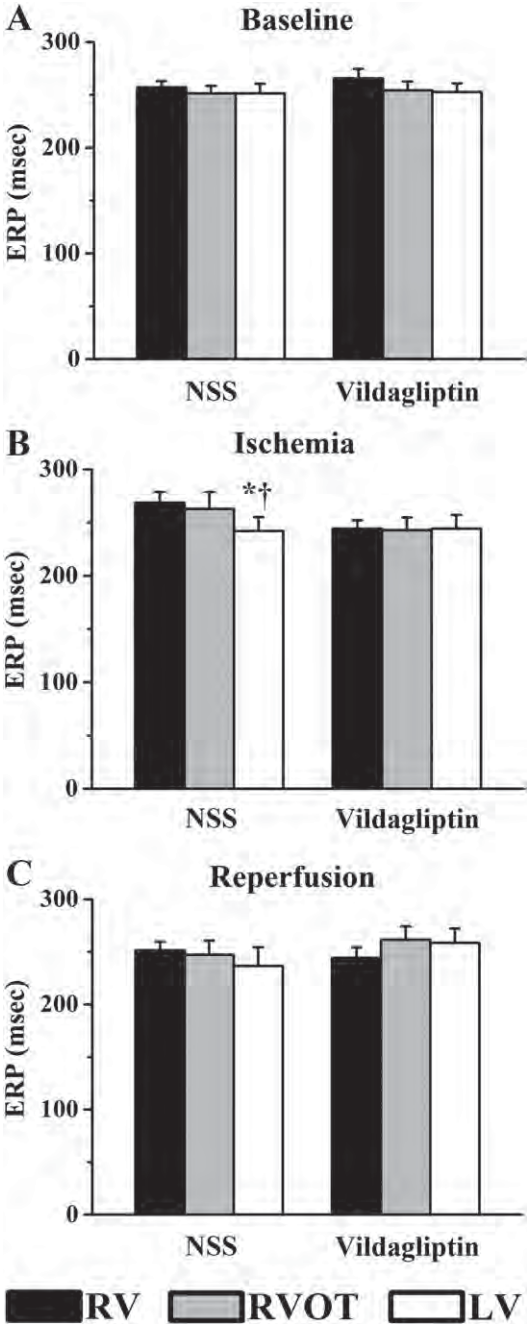

Fig. 3. Effect of vildagliptin on the ERP. ERP at baseline was not different among all 3 recording sites in both normal saline and vildagliptin groups (panel A). During ischemia, LV ERP was decreased compared to the other two recorded sites in the normal saline group (panel B), whereas the LV ERP was not different from the other two recorded sites in the vildagliptin treated group (panel B), indicating that vildagliptin prevented the ERP dispersion among all recording sites at ischemic period. At reperfusion, the ERPs were not different among all three recorded sites in both normal saline and vildagliptin treated groups (panel C). * $p<0.05$ vs. RV; † $p<0.05$ vs. RVOT. RV = Right ventricle; RVOT = Right ventricular outflow tract; LV = Left ventricle.

4. Discussion

In this study, we assessed the cardioprotective effects of vildagliptin in a clinically relevant swine I/R model. The major findings of this study were as follows. Vildagliptin demonstrated its cardioprotective effects by 1) attenuating ERP shortening caused by myocardial ischemia, thus decreasing the ERP dispersion in the heart during ischemia, 2) increasing the VFT, 3) reducing the number of PVCs, 4) decreasing the infarct size, and 5) attenuating cardiac mitochondrial dysfunction due to oxidative stress caused by H_2O_2.

In the present study, we demonstrated for the first time the cardiac electrophysiological effects of DPP-4 inhibitor, vildagliptin, in the I/R heart. Our study demonstrated that vildagliptin could attenuate the ERP shortening in the ischemic myocardium, thus decreasing the degree of the dispersion of refractoriness caused by cardiac ischemia. Since dispersion of refractoriness plays an important role in facilitating arrhythmias [35], prevention of the ERP dispersion in the heart during ischemia could attenuate the occurrence of arrhythmia in this study. Our study also demonstrated the decreased number of PVCs and the reduced VFT in the vildagliptin treated pigs, suggesting that vildagliptin could stabilize cardiac electrophysiology during ischemia, thus attenuating myocardial vulnerability to arrhythmia during ischemia.

In the present study, the AAR in both saline and vildagliptin treated groups was not different, indicating the similar extent of ischemic myocardium caused by an LAD occlusion in both groups. However, vildagliptin significantly decreased the infarct size, compared with that in the saline-treated group. The histological appearance of the infarct tissues represented an early myocardial infarction (stage 1) according to Lodge–Patch classification [31,33], which was consistent with the duration of I/R in this study. The beneficial effect on the infarct size reduction of vildagliptin in the swine I/R model as shown in our study was consistent with previous reports in I/R model in mice using DPP-4 inhibitor sitagliptin [24], and in pre-diabetic insulin resistance rat using vildagliptin [23]. Since a reduced infarct size has been shown to be associated with a decreased myocardial vulnerability to arrhythmias during I/R, the reduction of infarct size and decreased ERP dispersion caused by vildagliptin could help attenuate arrhythmia and reduce the VFT as found in this study. However, not all reports on the effects of DPP-4 inhibitors on the infarct size are consistent. In ischemic study of DPP-4 gene deleted mice and DPP-4 inhibitor treated mice, no infarct size reduction was observed in that study [26]. Furthermore, treatment with vildagliptin or valine pyrrolidide did not reduce the infarct size in rat I/R model [18,23]. This discrepancy in results could be due to the difference in animal models. Nevertheless, our study is the first study to demonstrate the infarct limiting effect of DPP-4 inhibitor in the swine I/R model. This finding suggests that the effect of DPP-4 inhibitor on the infarct size reduction could differ in different animal species. In the clinically relevant swine I/R model, the augmentation of GLP-1 level by GLP-1 analog could also reduce infarct size [21]. However, Kavianipour et al. [36] and Kristensen et al. [37] failed to show infarct size limiting profit. This inconsistent finding could be due to different type of drug, routes, and the timing of drug administration. In a swine study that showed infarct limiting benefit, exendin-4 (GLP-1 analog) was given at 10 μg subcutaneously and intravenously prior to reperfusion and 10 μg subcutaneously twice daily until day 3 of reperfusion [21]. However, in two swine studies that failed to show infarct limiting benefit, liraglutide (GLP-1 analog) was given at 10 μg/kg/day subcutaneously for 3 days prior to the I/R conduction [37], and recombinant GLP-1 was given at 3 pmol/kg/min intravenously starting at 15 min before ischemia to the end of reperfusion [36]. All of these findings indicate the importance of species, type of drug, routes, and timing of drug administration in I/R models.

The present study further demonstrated the protective effect of vildagliptin on cardiac mitochondria. We demonstrated for the first time that DPP-4 inhibitor could effectively attenuate cardiac mitochondrial dysfunction caused by severe oxidative stress as found in the heart during I/R, suggesting that this mitochondrial protection could play a crucial role in the cardioprotective effect of vildagliptin. During I/R, it has been shown that the level of ROS could be markedly increased [38], resulting in the deterioration of the electron transport chain [39] and activation of the apoptotic pathway [40], and eventually myocardial death. In addition, the elevation of ROS level

Please cite this article as: Chinda K, et al, Cardioprotective effect of dipeptidyl peptidase-4 inhibitor during ischemia–reperfusion injury, Int J Cardiol (2012), doi:10.1016/j.ijcard.2012.01.011

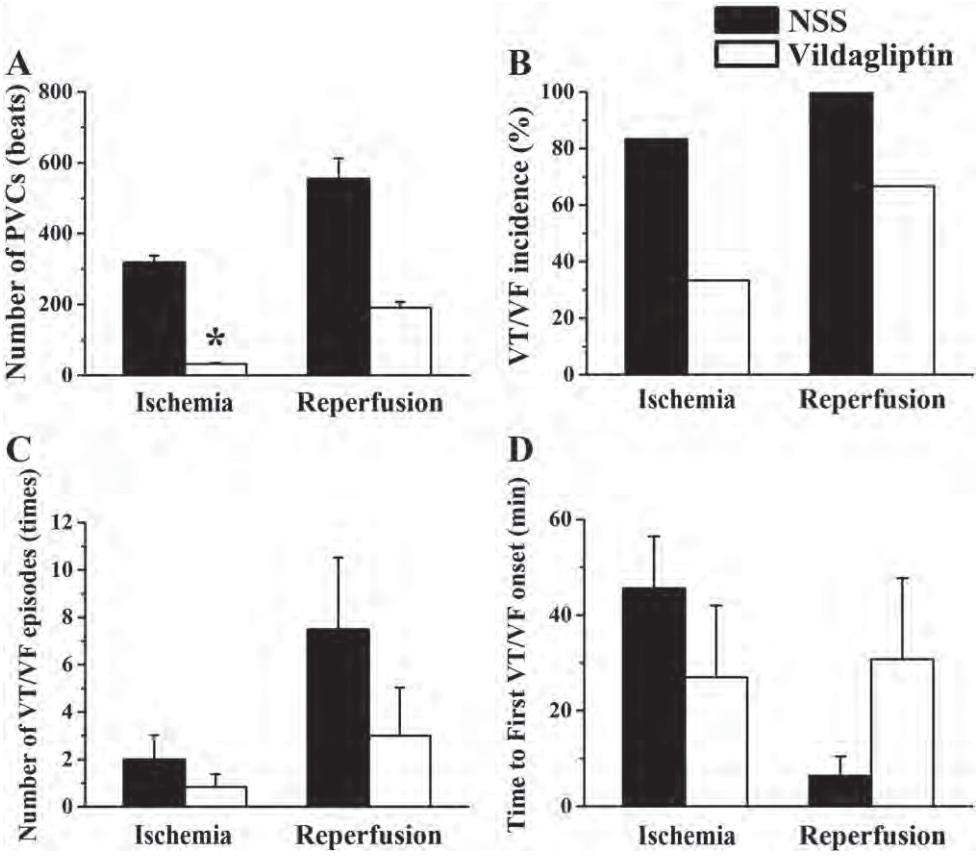

Fig. 4. Vildagliptin and the occurrence of cardiac arrhythmia. PVCs were markedly decreased in the vildagliptin treated group at the ischemic period and tended to decrease at reperfusion period, compared with normal saline group (panel A). Ventricular tachycardia (VT) and ventricular fibrillation (VF) incidence (panel B), VT/VF episode (panel C) and time to the first VT/VF onset (panel D) were not significantly different between vildagliptin and normal saline groups. * $p<0.05$ vs. baseline.

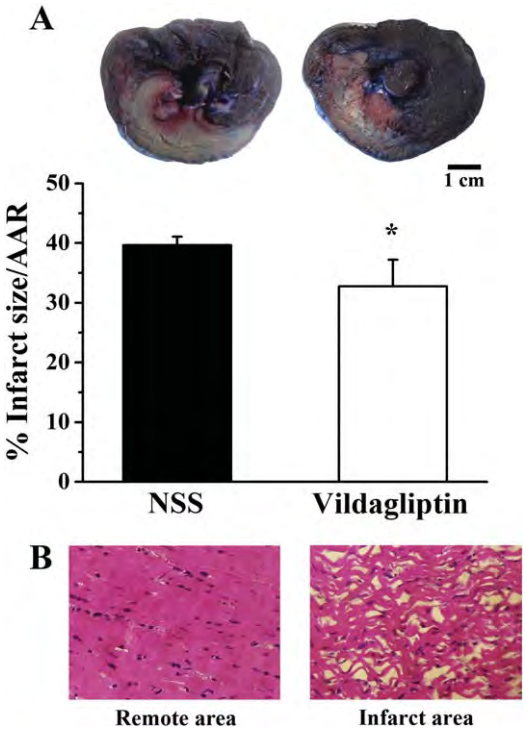

Fig. 5. Effect of vildagliptin on the infarct size. Panel A: The AAR was not different between the vildagliptin and normal saline treated groups. Vildagliptin could attenuate the infarct size by 17%, compared with normal saline treated group. Panel B: a microscopic appearance of the myocardium from the remote area (left) and infarct area (right). Thinning and waviness of myocardial fibers with distinct nuclei were found in the infarct area. * $p<0.05$ vs. NSS. AAR = Area at risk.

could cause cardiac mitochondrial membrane depolarization, a condition that has been shown to be responsible for cardiac arrhythmias [41]. In our study, administration of vildagliptin at 3.30 mM to cardiac mitochondria could attenuate cardiac mitochondrial dysfunction caused by H_2O_2, as indicated by the reduction of ROS production and attenuation of mitochondrial membrane potential changes. These effects could be a mechanism responsible for reduced myocardial vulnerability to arrhythmia and decreased infarct size found in the present study [42].

5. Conclusions

A DPP-4 inhibitor vildagliptin stabilized cardiac electrophysiology by attenuating ERP shortening and reducing the infarct size, resulting in decreasing myocardial vulnerability to cardiac arrhythmia during I/R. The cardioprotective effect of vildagliptin could be due to its ability to prevent cardiac mitochondrial dysfunction caused by severe oxidative stress during I/R.

Conflict of interest

None declared.

Acknowledgments

This study is supported by grants from the Thailand Research Fund RTA5280006 (NC), BRG5480003 (SC), and the Thailand Research Fund's Royal Golden Jubilee PhD program (NC and KC).

The authors of this manuscript have certified that they comply with the Principles of Ethical Publishing in the International Journal of Cardiology [43].

Please cite this article as: Chinda K, et al, Cardioprotective effect of dipeptidyl peptidase-4 inhibitor during ischemia–reperfusion injury, Int J Cardiol (2012), doi:10.1016/j.ijcard.2012.01.011

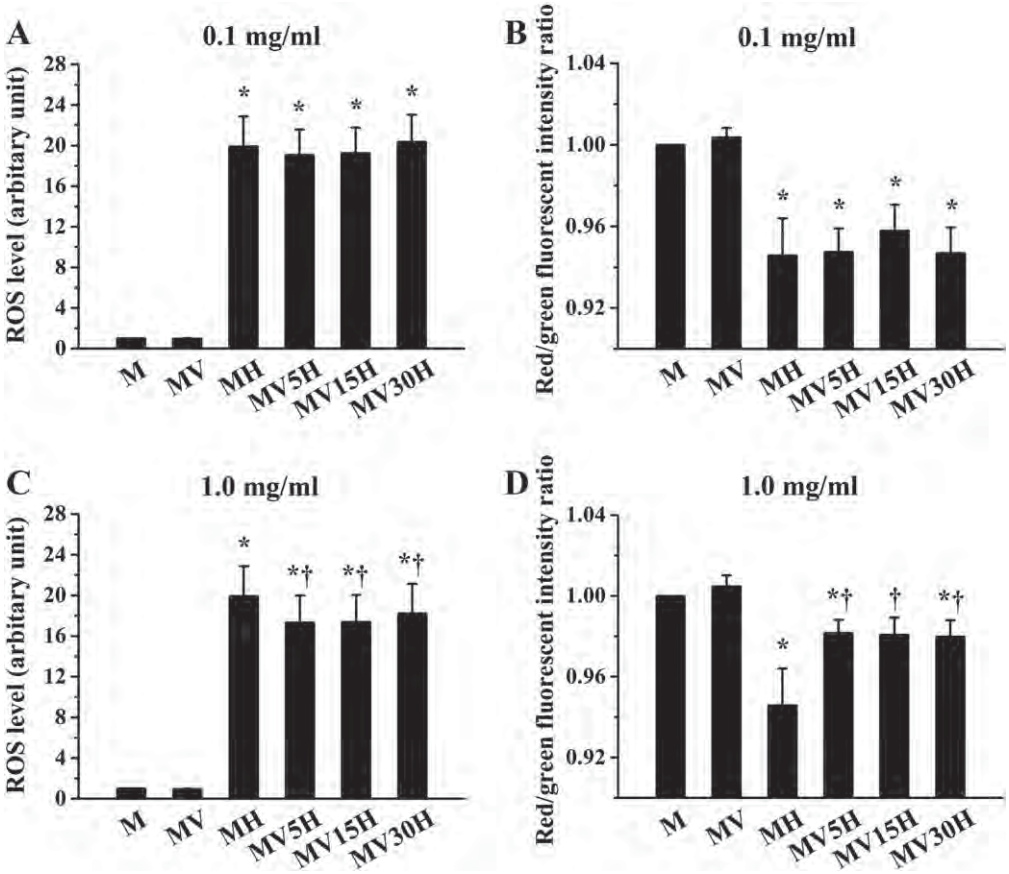

Fig. 6. Effect of vildagliptin on cardiac mitochondria. H_2O_2 caused markedly increased ROS level and decreased red/green florescent ratio. Vildagliptin at 0.1 mg/ml could not reduce ROS level (panel A) or prevent the red/green florescent ratio reduction (panel B) caused by H_2O_2. However, 1.0-mg/ml vildagliptin treated for 5, 15, and 30 min could significantly decrease ROS level (panel C) and attenuate mitochondrial depolarization (panel D) caused by H_2O_2. * $p<0.05$ vs. M; † $p<0.05$ vs. MH. M = Mitochondria; MV = Mitochondria + Vildagliptin; MH = Mitochondria + H_2O_2; MV5H = Mitochondria + $Vildagliptin_{5\ min}$ + H_2O_2; MV15H = Mitochondria + $Vildagliptin_{15\ min}$ + H_2O_2; MV30H = Mitochondria + $Vildagliptin_{30\ min}$ + H_2O_2.

References

[1] Smyth S, Heron A. Diabetes and obesity: the twin epidemics. Nat Med 2006;12:75–80.
[2] Huang PL. Unraveling the links between diabetes, obesity, and cardiovascular disease. Circ Res 2005;96:1129–31.
[3] Grundy SM, Benjamin IJ, Burke GL, et al. Diabetes and cardiovascular disease: a statement for healthcare professionals from the American Heart Association. Circulation 1999;100:1134–46.
[4] Becker A, Bos G, de Vegt F, et al. Cardiovascular events in type 2 diabetes: comparison with nondiabetic individuals without and with prior cardiovascular disease. 10-year follow-up of the Hoorn Study. Eur Heart J 2003;24:1406–13.
[5] Fox CS, Coady S, Sorlie PD, et al. Increasing cardiovascular disease burden due to diabetes mellitus: the Framingham Heart Study. Circulation 2007;115:1544–50.
[6] Lee CD, Folsom AR, Pankow JS, Brancati FL. Cardiovascular events in diabetic and nondiabetic adults with or without history of myocardial infarction. Circulation 2004;109:855–60.
[7] Timmer JR, Ottervanger JP, Thomas K, et al. Long-term, cause-specific mortality after myocardial infarction in diabetes. Eur Heart J 2004;25:926–31.
[8] Rosamond W, Flegal K, Furie K, et al. Heart disease and stroke statistics—2008 update: a report from the American Heart Association Statistics Committee and Stroke Statistics Subcommittee. Circulation 2008;117:e25–146.
[9] Deedwania P, Kosiborod M, Barrett E, et al. Hyperglycemia and acute coronary syndrome: a scientific statement from the American Heart Association Diabetes Committee of the Council on Nutrition, Physical Activity, and Metabolism. Circulation 2008;117:1610–9.
[10] Mudaliar S, Henry RR. Effects of incretin hormones on beta-cell mass and function, body weight, and hepatic and myocardial function. Am J Med 2010;123:S19–27.
[11] Lu L, Reiter MJ, Xu Y, Chicco A, Greyson CR, Schwartz GG. Thiazolidinedione drugs block cardiac KATP channels and may increase propensity for ischaemic ventricular fibrillation in pigs. Diabetologia 2008;51:675–85.
[12] Nissen SE, Wolski K. Effect of rosiglitazone on the risk of myocardial infarction and death from cardiovascular causes. N Engl J Med 2007;356:2457–71.
[13] Graham DJ, Ouellet-Hellstrom R, MaCurdy TE, et al. Risk of acute myocardial infarction, stroke, heart failure, and death in elderly Medicare patients treated with rosiglitazone or pioglitazone. JAMA 2010;304:411–8.
[14] Barnett A. DPP-4 inhibitors and their potential role in the management of type 2 diabetes. Int J Clin Pract 2006;60:1454–70.
[15] He YL, Sadler BM, Sabo R, et al. The absolute oral bioavailability and population-based pharmacokinetic modelling of a novel dipeptidylpeptidase-IV inhibitor, vildagliptin, in healthy volunteers. Clin Pharmacokinet 2007;46:787–802.
[16] Zhao T, Parikh P, Bhashyam S, et al. Direct effects of glucagon-like peptide-1 on myocardial contractility and glucose uptake in normal and postischemic isolated rat hearts. J Pharmacol Exp Ther 2006;317:1106–13.
[17] Sonne DP, Engstrom T, Treiman M. Protective effects of GLP-1 analogues exendin-4 and GLP-1(9–36) amide against ischemia–reperfusion injury in rat heart. Regul Pept 2008;146:243–9.
[18] Bose AK, Mocanu MM, Carr RD, Brand CL, Yellon DM. Glucagon-like peptide 1 can directly protect the heart against ischemia/reperfusion injury. Diabetes 2005;54:146–51.
[19] Matsubara M, Kanemoto S, Leshnower BG, et al. Single dose GLP-1-Tf ameliorates myocardial ischemia/reperfusion injury. J Surg Res 2011;165:38–45.
[20] Nikolaidis LA, Doverspike A, Hentosz T, et al. Glucagon-like peptide-1 limits myocardial stunning following brief coronary occlusion and reperfusion in conscious canines. J Pharmacol Exp Ther 2005;312:303–8.
[21] Timmers L, Henriques JP, de Kleijn DP, et al. Exenatide reduces infarct size and improves cardiac function in a porcine model of ischemia and reperfusion injury. J Am Coll Cardiol 2009;53:501–10.
[22] Nikolaidis LA, Mankad S, Sokos GG, et al. Effects of glucagon-like peptide-1 in patients with acute myocardial infarction and left ventricular dysfunction after successful reperfusion. Circulation 2004;109:962–5.
[23] Huisamen B, Genis A, Marais E, Lochner A. Pre-treatment with a DPP-4 inhibitor is infarct sparing in hearts from obese, pre-diabetic rats. Cardiovasc Drugs Ther 2011;25:13–20.
[24] Ye Y, Keyes KT, Zhang C, Perez-Polo JR, Lin Y, Birnbaum Y. The myocardial infarct size-limiting effect of sitagliptin is PKA-dependent, whereas the protective effect of pioglitazone is partially dependent on PKA. Am J Physiol Heart Circ Physiol 2010;298:H1454–65.

Please cite this article as: Chinda K, et al, Cardioprotective effect of dipeptidyl peptidase-4 inhibitor during ischemia–reperfusion injury, Int J Cardiol (2012), doi:10.1016/j.ijcard.2012.01.011

[25] Read PA, Khan FZ, Heck PM, Hoole SP, Dutka DP. DPP-4 inhibition by sitagliptin improves the myocardial response to dobutamine stress and mitigates stunning in a pilot study of patients with coronary artery disease. Circ Cardiovasc Imaging 2010;3:195–201.
[26] Sauve M, Ban K, Momen MA, et al. Genetic deletion or pharmacological inhibition of dipeptidyl peptidase-4 improves cardiovascular outcomes after myocardial infarction in mice. Diabetes 2010;59:1063–73.
[27] Kanlop N, Shinlapawittayatorn K, Sungnoon R, Chattipakorn S, Lailerd N, Chattipakorn N. Sildenafil citrate on the inducibility of ventricular fibrillation and upper limit of vulnerability in swine. Med Sci Monit 2008;14:BR205–9.
[28] Kanlop N, Thommasorn S, Palee S, et al. Granulocyte colony-stimulating factor stabilizes cardiac electrophysiology and decreases infarct size during cardiac ischaemic/reperfusion in swine. Acta Physiol (Oxf) 2011;202:11–20.
[29] Gu R, Zheng D, Bai J, Xie J, Dai Q, Xu B. Altered melusin pathways involved in cardiac remodeling following acute myocardial infarction. Cardiovasc Pathol 2011.
[30] Driesen RB, Zalewski J, Driessche NV, et al. Histological correlate of a cardiac magnetic resonance imaged microvascular obstruction in a porcine model of ischemia–reperfusion. Cardiovasc Pathol 2011.
[31] Lodge-Patch I. The ageing of cardiac infarcts, and its influence on cardiac rupture. Br Heart J 1951;13:37–42.
[32] Ishikawa Y, Akasaka Y, Ishii T, et al. Changes in the distribution pattern of gelatin-binding protein of 28 kDa (adiponectin) in myocardial remodelling after ischaemic injury. Histopathology 2003;42:43–52.
[33] Akasaka Y, Morimoto N, Ishikawa Y, et al. Myocardial apoptosis associated with the expression of proinflammatory cytokines during the course of myocardial infarction. Mod Pathol 2006;19:588–98.
[34] Thummasorn S, Kumfu S, Chattipakorn S, Chattipakorn N. Granulocyte-colony stimulating factor attenuates mitochondrial dysfunction induced by oxidative stress in cardiac mitochondria. Mitochondrion 2011;11:457–66.
[35] Frazier DW, Wolf PD, Wharton JM, Tang AS, Smith WM, Ideker RE. Stimulus-induced critical point. Mechanism for electrical initiation of reentry in normal canine myocardium. J Clin Invest 1989;83:1039–52.
[36] Kavianipour M, Ehlers MR, Malmberg K, et al. Glucagon-like peptide-1 (7–36) amide prevents the accumulation of pyruvate and lactate in the ischemic and non-ischemic porcine myocardium. Peptides 2003;24:569–78.
[37] Kristensen J, Mortensen UM, Schmidt M, Nielsen PH, Nielsen TT, Maeng M. Lack of cardioprotection from subcutaneously and preischemic administered liraglutide in a closed chest porcine ischemia reperfusion model. BMC Cardiovasc Disord 2009;9:31.
[38] Zorov DB, Juhaszova M, Sollott SJ. Mitochondrial ROS-induced ROS release: an update and review. Biochim Biophys Acta 2006;1757:509–17.
[39] Tompkins AJ, Burwell LS, Digerness SB, Zaragoza C, Holman WL, Brookes PS. Mitochondrial dysfunction in cardiac ischemia–reperfusion injury: ROS from complex I, without inhibition. Biochim Biophys Acta 2006;1762:223–31.
[40] Loor G, Kondapalli J, Iwase H, et al. Mitochondrial oxidant stress triggers cell death in simulated ischemia–reperfusion. Biochim Biophys Acta 2011;1813:1382–94.
[41] Aon MA, Cortassa S, Akar FG, Brown DA, Zhou L, O'Rourke B. From mitochondrial dynamics to arrhythmias. Int J Biochem Cell Biol 2009;41:1940–8.
[42] Moncada S. Mitochondria as pharmacological targets. Br J Pharmacol 2010;160:217–9.
[43] Shewan LG, Coats AJ. Ethics in the authorship and publishing of scientific articles. Int J Cardiol 2010;144:1–2.

Please cite this article as: Chinda K, et al, Cardioprotective effect of dipeptidyl peptidase-4 inhibitor during ischemia–reperfusion injury, Int J Cardiol (2012), doi:10.1016/j.ijcard.2012.01.011

Eur J Clin Pharmacol
DOI 10.1007/s00228-011-1193-2

REVIEW ARTICLE

Role of p38 inhibition in cardiac ischemia/reperfusion injury

Sarawut Kumphune · Siriporn Chattipakorn · Nipon Chattipakorn

Received: 3 November 2011 / Accepted: 29 November 2011

Abstract The p38 mitogen-activated protein kinases (p38s) are Ser/Thr kinases that are activated as a result of cellular stresses and various pathological conditions, including myocardial ischemia/reperfusion. p38 activation has been shown to accentuate myocardial injury and impair cardiac function. Inhibition of p38 activation and its activity has been proposed to be cardioprotective by slowing the rate of myocardial damage and improving cardiac function. The growing body of evidence on the use of p38 inhibitors as therapeutic means for responding to heart problems is controversial, since both beneficial as well as a lack of protective effects on the heart have been reported. In this review, the outcomes from studies investigating the effect of p38 inhibitors on the heart in a wide range of study models, including *in vitro*, *ex vivo*, and *in vivo* models, are discussed. The correlations of experimental models with practical clinical usefulness, as well as the need for future studies regarding the use of p38 inhibitors, are also addressed.

Keywords p38 Mitogen-activated protein kinase · Myocardial ischemia/reperfusion · p38 Inhibitors · Therapy

S. Kumphune
Department of Medical Technology,
Faculty of Allied Health Sciences, Naresuan University,
Phitsanulok 65000, Thailand

S. Kumphune · S. Chattipakorn · N. Chattipakorn (✉)
Cardiac Electrophysiology Research and Training Center,
Faculty of Medicine, Chiang Mai University,
Chiang Mai 50200, Thailand
e-mail: nchattip@gmail.com

S. Chattipakorn
Department of Oral Biology and Diagnostic Science,
Faculty of Dentistry,
Chiang Mai University,
Chiang Mai 50200, Thailand

N. Chattipakorn
Cardiac Electrophysiology Unit, Department of Physiology,
Faculty of Medicine, Chiang Mai University,
Chiang Mai 50200, Thailand

Introduction

Ischemic heart disease is considered to be the leading cause of death worldwide and is predicted to be the major cause of deaths in the future [1]. Myocardial ischemia exists when the reduction of the coronary flow is so severe that the supply of oxygen to the myocardium is inadequate for the oxygen demands of the tissue [2], resulting in the accumulation of metabolites in the ischemic region [2]. Severe and prolonged ischemia ultimately results in cellular necrosis. Currently, the most efficient method of reducing mortality in such patients experiencing ischemia is to achieve rapid reperfusion by thrombolysis or mechanical disruption of the occlusion. The mortality from acute myocardial infarction under these circumstances is inversely related to the amount of myocardial salvage achieved by reperfusion [3]. However, reperfusion itself can also be harmful, since it can damage the myocardium, a process known as "reperfusion injury" [4]. Different intracellular signaling pathways are considered to play a crucial role in the myocardial response to ischemia/reperfusion injury and consequent pathological remodeling. Many highly conserved serine/threonine mitogen-activated protein kinases (MAPK) are activated in response to myocardial ischemia/reperfusion [5]. In particular, the p38 MAPK has been widely studied.

A growing body of evidence from preclinical investigations indicates that the inhibition of p38 activation could reduce myocardial injury [6], suggesting the therapeutic

Published online: 29 December 2011

potential of p38 inhibitors in ischemic heart disease. However, the findings of not all studies consistent, and these inconsistencies raise the question of whether p38 inhibition is truly cardioprotective. Only a few published reports on clinical trials with p38 inhibitor in cardiovascular disorders are currently available [7–10]. The aim of this article is, therefore, to comprehensively review the findings of relevant studies regarding the use of p38 inhibitors in the cardiac ischemia/reperfusion model, including *in vitro*, *ex vivo*, and *in vivo* models in both animal and clinical studies. Findings both consistent and inconsistent with the therapeutic potential of p38 inhibition are discussed, and the future direction of p38 inhibitor therapy in the cardiac ischemia/reperfusion model is addressed in the hope of elucidating the possible usefulness of p38 inhibitors in patients in the future.

Biological and biochemical properties of p38

The p38 MAPK is a family of serine/threonine protein kinases that plays an important role in cellular responses to external stress signaling and also functions in many cellular processes, including inflammation, cell differentiation, cell growth and death [11]. The human p38 was originally isolated as a 38-kDa protein that is rapidly tyrosine phosphorylated in response to lipopolysaccharide stimulation in human monocytes [11]. It was also identified as a target of a pyridinyl imidazole drug that blocked the production of tumor necrosis factor-alpha (TNFα), and was consequently called cytokine-suppressive anti-inflammatory drug-binding protein [11], and as a reactivating kinase for MAP kinase-activated protein (MAPKAP) kinase-2 [12], Human p38 cDNA cloning revealed that the amino acid sequence of human p38 is 94% identical to mouse p38 [13, 14].

The activity of p38 is controlled by the dual phosphorylation of the Thr^{180}-Gly^{181}-Tyr^{182} motif within the activation loop/lip [15]. The traditional view is that this dual phosphorylation event is achieved by upstream, dual specificity MAPK kinases (MAPKKs) or MKKs. The major activators of p38 *in vivo* are MKK3, MKK6 [16, 17], and MKK4 [18]. This serial phosphorylation relay from MKKK to MKK3/6 to p38, and finally to substrates is termed the "transphosphorylation" mechanism due to the transfer of the phosphate group from ATP to downstream signaling molecules. The pharmacological inhibitor, SB203580, inhibits p38 activity and attenuates the phosphorylation processes downstream of p38 [19, 20]. Although it is unlikely that SB203580 will inhibit dual phosphorylation of p38 itself, growing evidence demonstrates that the inhibitory effect of SB203580 and of structurally related compounds acts on p38 phosphorylation [21]. These findings could possibly be explained by the finding that p38 can phosphorylate itself, a mechanism called "autophosphorylation" [22–24].

There are four isoforms of p38 that have been identified, including p38 α, β, γ, and δ. Sequence comparisons have revealed that each p38 isoform has more than 69% identity within this group, but only 40–45% to the other MAP kinase family members [25]. Among all isoforms, p38α and β are highly homologous [26] and sensitive to pyridinyl imidazole molecules, such as SB203580 [27], but they have only 60% homology with p38γ and δ, which are resistant to SB203580 [27]. p38α is ubiquitously expressed in several tissues and is the best characterized and perhaps the most physiologically relevant kinase involved in inflammatory responses [26, 28]; it is also the isoform predominantly involved in myocardial ischemic injury [24].

p38 MAPK activation in myocardial ischemia/reperfusion

Myocardial ischemia is a potent stimulant of p38 activation, which is an important pro-apoptotic kinase in cardiomyocytes [29]. Evidence has been accumulating from preclinical investigations that the inhibition of p38 during prolonged ischemia slows the rate of infarction/death and inhibits the production of inflammatory cytokines, such as TNFα, interleukin-1 (IL-1), and IL-8, which are known to aggravate ischemic injury [6, 30]. In the clinical context, prompt reperfusion following coronary artery occlusion remains the most effective intervention to re-establish arterial patency and reduce ischemic myocardial injury [29]. However, reperfusion can re-activate p38, perhaps in response to stimuli such as reactive oxygen species (ROS) and osmotic stress [29]. Although this field of research is still evolving, compelling evidence supports a causative role of p38 in myocardial injury and dysfunction following ischemia/reperfusion [29, 31–33]. Many studies have elucidated the mechanisms, such as apoptosis and inflammation, through which p38 activation might contribute to ischemia/reperfusion injury [29]. Bogoyevitch et al. were the first to demonstrate that p38α and β isoforms are activated in response to ischemia/reperfusion in the heart [34]. Later studies using ectopic gene expression found that the α isoform is implicated in cardiomyocyte apoptosis and that this isoform alone is sufficient to cause cell death following ischemia [24, 34–36].

Study models of p38 inhibitors on myocardial ischemia/reperfusion

The pro-apoptotic role of p38 in cardiomyocytes during ischemic injury has been highlighted in many studies using

a selective p38 inhibitor [34, 37]. These studies demonstrated that the inhibition of p38, using pharmacological inhibitors, could reduce the infarct size [38–43] and improve cardiac function [40, 42, 44–48] after myocardial infarction. However, there are some inconsistent findings indicating that treatment with p38 inhibitor neither reduced the infarct size nor improved cardiac function and that it abolished the beneficial effect of ischemic preconditioning [49–53]. These studies were performed in various model systems, including multiple *in vitro*, *ex vivo* (isolated whole heart), and *in vivo* animal models.

Reports of p38 inhibitor in an *in vitro* model of ischemia/reperfusion

Reports from *in vitro* experiments on the p38 inhibitor in the model of ischemia/reperfusion injury, either a cardiac cell line or isolated cardiomyocytes from many species, are summarized in Table 1. *In vitro* treatment with a p38 inhibitor, mainly SB203580, prior to ischemia at concentrations ranging from 1 to 15 μM was found to protect the cardiac cells from ischemia/reperfusion injury, suggesting an undesired effect of p38 activation in myocardial ischemia/reperfusion [36, 50, 54–63]. However, there have been some reports of beneficial effects following p38 activation, in which its activation could lead to the protection against injury rather than a harmful effect. Nagarkatti et al. [50] and Weinbrenner et al. [53] showed that the inhibition of p38 activation before ischemic preconditioning abolished the protective effect of preconditioning. Interestingly, in the same published work, applications with the same inhibitor and at a similar concentration before and during ischemia showed protection of the cardiac cell from ischemic injury [50]. These inconsistent findings could be due to the conditions of the heart at the time of p38 inhibition. The signal transduction cascade of ischemia can be divided into triggers and mediators. Triggers are important during the episode of preconditioning ischemia and reperfusion, while mediators are important during the prolonged index ischemia [64]. More importantly, the different signal transduction pathways and the consequences can possibly be due to differences in p38 downstream signalings or even end-effectors, which are specifically and differently activated according to prolonged ischemia or ischemic preconditioning (IPC). Identification of these specific targets of p38 is a challenge, as this information could prove helpful in understanding the complexity of p38 signaling, such as cross-talk between kinase pathways, desensitization to stimulation, and signal amplification, and ultimately lead to the discovery of powerful therapeutic agents with less harmful side effects.

Despite the fact that the *in vitro* model provides some valuable mechanistic information, which is also crucial to a better understanding of the mechanism of p38 activation during ischemia/reperfusion, and in the hope that this will allow circumstance-specific inhibition and/or the identification of the harmful downstream pathways, it is important to note that the major limitation of *in vitro* studies is that they determine cell viability based on the release of metabolic enzymes as outcome measures and do not provide sufficient information on cardiac function. Therefore, studying the role of p38 in the whole heart would provide much insight into the function of the heart as an organ in the body.

Reports of p38 inhibitors in an *ex vivo* model of ischemia/reperfusion

A summary of *ex vivo* studies with cardiac ischemia/reperfusion is shown in Table 2. Studies of the inhibitory effect of p38 inhibitors in an *ex vivo* model were performed with concentrations of the inhibitor ranging from 1 to 10 μM, similar to most *in vitro* experiments. The pre-treatment of SB203580 and other p38 inhibitors prior to the ischemic period had a protective effect by reducing infarct size [38–43] and improving left ventricular (LV) function [40, 42, 44–48]. However, inconsistent findings were also reported in which inhibitor treatment in low-flow ischemia failed to reduce the infarct size [65] or abolished the protective effect of preconditioning [49, 66], which can also be seen in some *in vitro* data [50, 53]. There are many factors that possibly explain these inconsistent findings, such as dose of the inhibitor, timing of the treatment, study protocol of ischemia, and the specific animal model. For example, Gorog et al. [65] demonstrated that treatment with 1 μM of p38 inhibitor for 5 min before low-flow ischemia in a mouse model could not reduce the size of the infarct, whereas treatment with the same type and concentration of inhibitor in the same animal model for 10–15 min prior to the onset of ischemia did limit infarct size [43, 67]. However, treatment with 1 μM of p38 inhibitor for 5 min before ischemia was able to reduce infarct size in the rabbit model [38], suggesting different effects of the inhibitor in different species. The timing of the administration of p38 inhibitor in these experiments could be one of the major factors that should be considered. The concentration of p38 inhibitor used in most of these studies ranged from 1 to 10 μM, but the outcomes were apparently inconsistent. Some studies using either 1 or 10 μM p38 inhibitor showed that the therapy was protective [24, 38–41, 43, 45–48, 65, 67], whereas others reported no effect [42, 46, 49, 51]. These results suggest that timing of p38 inhibition is crucial for its cardioprotective effects during cardiac ischemia/reperfusion injury.

Similar to the findings in *in vitro* studies, inhibition of p38 activation prior to ischemic preconditioning also abolished the protective effect of preconditioning in an *ex vivo* model. In one study using the isolated rat heart model, 10 μM of p38 inhibitor given 5 min before the first precondition cycle

Table 1 Summary of reports on p38 inhibitor in an *in vitro* model

Species	Study model	Dosage of inhibitor	Treatment conditions	Readout	Outcomes	References
Rat	H9c2 rat cardiac myoblast cell line	15 μM	1 hour before and during simulated ischemia	Cell viability by MTT assay	SB203580 increased cell viability	[50]
		1 μM	30 min before and maintain during 7 hr sI	Cell viability by MTT assay	SB203580 increased cell viability	[36]
	HL-1 cardiac muscle cell line	10 μM	SB before 45-min hypoxia SB before reoxygenation	Mitochondrial ROS, Apoptosis by propidium iodide (PI) staining	SB203580 decreased mitochondrial ROS and apoptosis	[63]
		10 μM	2-h sI/5-h reperfusion SB203580 at and during 5-h reperfusion	Irreversible cellular injury by GFP-Bax or mCherry-Bax distribution	SB203580 decreased mitochondrial ROS	[54]
	Isolate neonatal rat cardiac myocytes	1 or 10 μM	During 2-h sI	LDH release, and cell viability by MTT assay	SB203580 increased cell viability, reduced LDH release	[61]
		1 μM	During 18-h hypoxia/1-h reoxygenation	Cell viability by trypan blue Annexin V-FITC, TUNEL, propidium iodide staining	SB203580 prevented hypoxia/ reoxygenation induced cell death	[57]
	Isolate neonatal rat cardiac myocytes	1 or 10 μM	1 μM SB30 min before 2 h of hypoxia 1-or 10 μM 30 min before IPC	Cell viability by trypan blue exclusion assay	SB203580 increased cell viability did not block protective effect of IPC	[59]
		2–10 μM	During 90-min ischemia	Cell viability by calcein acetoxymethyl ester and propidium iodide (PI) staining, LDH release	SB203580 reduced LDH release in a dose-dependent manner and significantly decreased cell death	[58]
		10 μM	During 6-h sI/2-h reoxygenation	CK release, LDH release, and cell viability by MTT	SB203580 increased cell viability, reduced CK, LDH release	[35]
		10 μM SB242719/ SB203580	15 min before and during ischemia/reperfusion	Apoptosis (TUNEL)	Both of SB242719 and SB203580 reduced apoptosis	[83]
	Isolate neonatal rat cardiac myocytes (NRCMs)	10 mM	During 7-h ischemia	LDH release	Reduced LDH release	[84]
		10 μM	15 min before and during sI and reoxygenation	Cytochrome C release, caspase 3 activation, DNA fragmentation	SB203580 prevented LDH release, cytochrome C release, caspase 3 activation, and DNA fragmentation	[60]
	Isolate neonatal rat cardiac myocytes (NRCMs)	500 nM–1 μM RWJ	30 min before exposed to H_2O_2 for 24 h	TUNEL	RWJ reduced apoptosis	[33]
	Isolate adult rat ventricular myocytes (ARVMs)	1 and 10 μM	30 min before and during 4-h sI	LDH release	SB203580 reduced LDH release	[36]
	Isolate adult rat cardiac ribroblasts (ARCFs)	10 μM	20 min before exposured to H_2O_2	apoptosis by Annexin V-FITC	SB203580 reduced apoptosis	[55]
		10 μM	Throughout experiment of sI	Cell viability by MTS assay	SB203580 reduced apoptosis	[56]
Dog	Isolate cardiac cells	10 μM	During 3-h hypoxia	TUNEL	SB203580 reduced apoptosis	[62]
Rat	H9c2 Rat cardiac myoblast cell line	15 μM	1 hour before and during preconditioning and wash away after preconditioning	Cell viability by MTT	SB203580 blocked protective effect of IPC	[50]
Rabbit	Isolate ventricular myocytes	10 μM	5 min before IPC	Cell viability by trypan blue exclusion assay	SB203580 blocked protective effect of IPC	[53]

sI, simulated ischemia; IPC, ischemia preconditioning

The p38 inhibitor used in all of the *in vitro* models is SB203580, except where stated otherwise

Table 2 Summary of reports on p38 inhibitor in an *ex vivo* (isolated heart) model

Species	Study model	Dosage of inhibitor	Treatment conditions	Readout	Outcomes	References
Mouse	30 min global ischemia/ 120 min reperfusion	1 μM SB203580	10 min before global ischemia	Infarct size	SB203580 reduced infarct size	[43]
	120 min of low-flow or moderate flow ischemia	1 μM SB203580	5 min or 60 min after the onset of low-flow or moderate flow ischemia until the end of protocol	Infarct size and left ventricular function	Early SB203580 treatment in both low/ moderate flow reduced infarct size, but failed to attenuate contractile dysfunction	[65]
	30 min low-flow ischemia/ 30 min of reperfusion or 60 min of low-flow ischemia/120 min of reperfusion	2 μM SB203580	15 min before and 15 min after onset of ischemia/15 min before and after onset of reperfusion	Infarct size	SB203580 reduced infarct size	[39]
	30-min global ischemia/ 120-min reperfusion in p38α drug-resistant mice	- 1 or 10 μM SB203580 - 1 μM BIRB-796	10 min before global ischemia	Infarct size, hemodynamic parameters	- SB203580 reduced infarct size and improved hemodynamic parameters in wildtype mice, but not in p38α drug resistant (DR) mice - BIRB 796 reduced infarct size in both wildtype and p38αDR mice	[24]
Rat	Heart was perfused with 300 mM H_2O_2 for 80 min	1 mM SB203580	Perfused 5 min before exposure to H_2O_2	Developed pressure coronary flow, end-diastolic pressure, and creatine kinase in effluent	SB203580 reduced cell death and myocardial dysfunction	[47]
	30-min global ischemia/ 120 min reperfusion	10 μM SB203580	10 min before ischemia, throughout the period of reperfusion	DNA fragmentation, TUNEL assay, contractile function, CK activity	SB203580 before ischemia and during reperfusion reduced apoptosis and contractile function recovery	[46]
	20 min ischemia/ 25 min reperfusion -5 min I/5min R IPC before 20 min ischemia	10 μM SB202190	- 5 min before index ischemia - 2 min before first cycle of IPC	Left ventricular developed pressure (LVDP), infarct size	- SB202190 reduced infarct size and enhanced function recovery - SB202190 had no effect on IPC	[41]
	30-min ischemia/ 180 min reperfusion	0.5-2 mg/kg FR 167653	1 hour via i.p. before ischemia and 1 mg/L in perfusion buffer	Apoptosis by TUNEL, CK activity in effluent, Left ventricular function	FR 167653 reduced apoptosis, CK leakage, and improved cardiac contractile function during reperfusion	[44]
	25 min global ischemia/ 40 min reperfusion	20 μM SB203580	5 min before ischemia/reperfusion	Left ventricular function and caspase activity	SB203580 reduced caspase-1,3,11 activation, and improved left ventricular function	[48]
	Rat heart subjected to hypothermic storage (8 h, 3°C) and rewarming (10 min, 37°C) before normothermic reperfusion (30 min)	10 μM SB202190	during reperfusion	Left ventricular function	SB202190 improved Left ventricular function recovery	[45]
	30-min global ischemia/ 45-min reperfusion	10 μM SB203580	10 min before ischemia	Infarct size, left ventricular function and CK and LDH activity in effluent, Apoptosis by TUNEL, caspase-3 assay	SB203580 reduced infarct size, improved Left ventricular function recovery, reduced cellular apoptosis and injury	[40]
	35-min regional ischemia/ 120-min reperfusion	1 μM SB203580	10 min before ischemia/reperfusion	Infarct size, caspase-3 activation, and PARP cleavage	SB203580 before ischemia reduced apoptosis. SB203580 did not abolish protective effect of IPC	[67]
Rabbit	30-min focal ischemia/ 120-min reperfusion	1 μM SB203580	SB203580 5 min before I/R and 5 min after ischemia before reperfusion	Infarct size	SB203580 reduced infarct size	[38]
Mouse	30-min ischemia/120-min reperfusion in C57BL/6 or $mkk3^{-/-}$	1 μM SB203580	15 min before ischemia or at perfuse Antimycin A	Infarct size and left ventricular function	SB203580 co-administered with Antimycin A abolished protective effect of Antimycin A preconditioning	[66]
	20-min ischemia/120 min reperfusion	10 μM SB203580	After the onset of reperfusion for 30 min	Infarct size, left ventricular function and CK activity	SB203580 during reperfusion improved contractility but increased CK release and infarct size	[42]
	4×4-min ischemia/6-min reperfusion followed by 30-min Ischemia/120-reperfusion in p38α or p38β DR mice	10 μM SB203580	During IPC	Infarct size	SB203580 abolished protective effect of IPC in wildtype and p38βDR but not p38αDR	[85]
Rat	30-min global ischemia/ 120-min reperfusion	10 μM SB203580	10 min after the onset of reperfusion	DNA fragmentation, TUNEL assay, contractile function, CK activity and NBT staining	Perfusion of SB203580 at 10 min after reperfusion failed to protect the heart from ischemic injury	[46]
	35-min regional ischemia/ 120-min reperfusion	10 μM SB203580	5 min before first preconditioning cycle and wash out/5 min after preconditioning and continued until 15 min into sustained ischemia SB 20 min before ischemia and during first 15 min of ischemia	Infarct size, left ventricular function	SB203580 blocked the protective effect of preconditioning SB203580 had no effect on infarct size	[49]
Rabbit	30-min focal ischemia/120-min reperfusion -5 min of global ischemia and 10 min reperfusion before the 30-min period of ischemia	2 μM SB203580	20 min before ischemia	Infarct size	SB203580 alone had no effect on infarct size, treatment of SB203580 before ischemic precondition blocked the protective effect of preconditioning	[51]

prevented the cardioprotective effect of preconditioning [49]. However, treatment with a tenfold lower concentration of the same inhibitor for 10 min before ischemia, which is known to reduce infarct size in a similar animal model, could not abolish the subsequent protective effect of ischemic preconditioning [67]. These findings suggest that, in the ischemic preconditioning model, the dosage of the inhibitor has more influence on the cardioprotection effect than the timing of administration of the inhibitor. Similar to the finding in the heart of small rodents, infusion of p38 inhibitor in the isolated rabbit heart model also exerted a significant cardioprotective effect during sustained ischemia [38, 46], although this same inhibitor again blocked the cardioprotective effect of ischemic preconditioning [51]. Therefore, it may be concluded that p38 activation only during sustained ischemia appears to be proapoptotic, whereas its activation in ischemia preconditioning seemed to be more anti-apoptosis. Again, this inconsistency could possibly be explained by p38 activation playing different roles, namely, as a trigger or mediator, when subjected to different stimuli.

Reports of p38 inhibitors in an *in vivo* model of ischemia/reperfusion

The cardioprotective effect of p38 inhibitor that was demonstrated in *in vivo* studies was similar to the findings from both *in vitro* and *ex vivo* models. The *in vivo* study model provides valuable functional information which is closely related to the pathophysiology of myocardial ischemia/reperfusion. To date, *in vivo* studies on the use of p38 inhibitors have been reported with different doses, modes of treatment, duration of treatment, and animal species (Table 3).

Many studies have demonstrated the benefit of p38 inhibitors in the *in vivo* model of sustained ischemia, either in the small animal or large animal model, where p38 inhibitors were found to reduce the infarct size [21, 32, 68, 69] and improve LV function [33, 69–74]. Nevertheless, inconsistent reports do exist, mostly from studies performed in the large animal model. It is noticeable that, in large animal models such as pigs or dogs, p38 activation does not appear to be as clearly proapoptotic as found in rodents [32]. Kaiser et al. reported that SB239063 reduced the infarct size in the mouse model, but failed to protect the pig heart from ischemic injury [32]. The failure of the p38 inhibitor to protect the pig heart from ischemic injury was also reported in another study using different p38 inhibitors, such as BIX-645 and SB203580 [75]. The potential explanation for these inconsistent findings could be species, which can be explained by the concept that signal transduction varies among species. The findings in the large animal model also showed some inconsistencies.

The mode of drug administration and degree of coronary occlusion have been shown to play important roles in the cardioprotective effects of p38 inhibitor in a large animal model [75, 76]. Intracoronary infusion of SB203580 in low-flow ischemia failed to reduce the infarct size and limited the beneficial effect of IPC [75], whereas an intramyocardial injection of SB203580 in the ischemic area in complete coronary occlusion was able to reduce infarct size and did not abolish the IPC effect [76]. These findings emphasize the importance of the intensity of the ischemic stimuli that may cause variable degrees of signal transduction activation and responses. Nevertheless, in a dog model, the intracoronary infusion of SB203580 prior to ischemia/reperfusion or during IPC failed to reduce the infarct size and abrogated the protective effect of IPC, whereas the continuous treatment of SB203580 during sustained ischemia had a cardioprotective effect [52]. This report again emphasizes the importance of the timing and duration of p38 inhibitor administration in terms of its cardioprotective effect during ischemia/reperfusion.

It is widely accepted that an *in vivo* model is the best study model to determine the long-term effect of both drugs and physiological responses. Chronic studies investigating the long-term (1–14 weeks) effect of p38 inhibitor in ischemia/reperfusion have been reported. Most of these studies demonstrated that long-term treatment with p38 inhibitors following the induction of myocardial infarction had beneficial effects, such as improved cardiac function [33, 70–74, 77], inhibited infarct expansion [33], reduced scar size [77], and suppressed myocardial fibrosis [74].

p38 inhibitor: where do we go from here?

The important questions that still need to be clarified are whether p38 inhibitors really do have therapeutic potential in real clinical settings and if so, is the background information sufficient to ensure that the p38 inhibitor can be used effectively in real clinical treatment? It is noticeable that the majority of the experimental findings that initially indicated the efficiency of p38 inhibitors in reducing myocardial injury and impaired cardiac function were associated with pre-ischemic treatment. Prevention of p38 activation by the inhibitor prior to ischemia seems to be impractical in the actual clinical setting, as myocardial ischemia is an unpredictable episodic condition. Therefore, the timing of treatment and its therapeutic potential are critical issues that need to be addressed. It will be clinically more useful if the inhibition of p38 activation at the postischemic state, which includes the reperfusion period, can provide a cardioprotective effect. Nevertheless, the roles of p38 activation and the consequences of its inhibition in postischemic and reperfusion periods, especially in an *in vivo* model, have not been

Table 3 Summary of reports on p38 inhibitor in an *in vivo* model

Species	Study model	Dosage of inhibitor	Treatment conditions	Readout	Outcomes	References
Mouse	30-min regional ischemia/ 120-min reperfusion (LAD ligation)	2 mg/ kg FR167653	Intraperitoneal injection 24 hours before ischemia	Infarct size	FR167653 reduced infarct size	[21]
	60-min regional ischemia/ 24-hr reperfusion (LAD ligation)	7 μg SB239063	Injected into tail vein 5 min before ischemia	Infarct size	SB239063 5 min before ischemia had 25% reduction infarct size compared to control	[32]
Rat	Regional ischemia/ reperfusion (LAD ligation)	2 mg/kg SB203580-HCl	Intraperitoneal injection immediately after LAD ligation	Cardiomyocytes mitosis, Cardiac functions: % left ventricular fractional shortening (FS), end diastolic dimension, and end systolic dimension.	24 h after MI SB203580 treatment induced cardiomyocytes mitosis and significantly increased %FS.	[77]
	20-min regional ischemia/ 24-hr reperfusion (LAD ligation)	30 mg/kg SB239063 orally	Administered per oral 20 min before ischemia	Infarct size, myocardial myeloperoxidase	SB239063 reduced infarct size and polymorphonuclear cell accumulation	[68]
	Regional ischemia/ reperfusion (LAD ligation)	1 mg/kg SB203580	Jugular vein injection 5 min before reperfusion	Rate-pressure product value, ±delta pressure/delta time max, apoptotic index, CK-MB activity, Area at risk (AAR)	SB203580 injection before reperfusion (postconditioning) improved cardiac function and reduce AAR.	[69]
Rabbit	1-hr regional Ischemia/ 3-hr reperfusion (LAD ligation)	1 mg/kg PD169316	Intravenous bolus injection 55 min after LAD ligation	Area at risk (AAR), plasma CK activity, myocardial myeloperoxidase	PD169316 reduced AAR, plasma CK activity and PMN accumulation	[86]
Pig	Regional ischemia/ reperfusion (LAD ligation)	40 nM SB203580 or 5 mg/kg	Local intramyocardial infusion 1hr before index ischemia or 5 mg/animal 10 min before the onset of 1hr coronary occlusion	Infarct size	SB203580 reduced infarct size. Both local or systemic perfusion of SB203580 before and during IPC had no effect on IPC	[76]
Dog	Transplant dog heart	FR167653 (dose not mentioned)	Hearts from donor were left in situ for 30 min after cardiac arrest and subjected to coronary flushing and immersed in Celsior solution for 4 h with and without FR167653	Cardiac output, LV pressure, End-systolic maximal elastance (EMax)	FR167653 improved heart-graft viability and cardiac function	[87]
	90-min occlusion/ 6-hr reperfusion	1.18 μg/kg/ min SB203580	during sustained ischemia	Infarct size	Continuous treatment of SB203580 during sustained ischemia reduced the infarct size	[52]
Mouse	Long-term treatment: regional ischemia/ reperfusion (LAD ligation) of MKK6bE transgenic mice	1200 ppm SB239068 in chow or food	SB239068 in drinking water for a total of 2–14 weeks (for hemodynamic and biochemical studies) or 12 weeks (for survival observations).	Hemodynamic measurement by Pressure-volume loop analysis	SB239068 treatment reduced end-diastolic and end-systolic chamber stiffening; net chamber filling and output were restored toward baseline despite persistently depressed systolic function. SB prolonged life span.	[71]
	Long-term treatment: regional ischemia/reperfusion (LAD ligation)	30 mg/kg/day SC-409 in chow	Long-term treatment with SC-409 for 2- to 14-weeks post-MI.	Cardiac geometry and function by echocardiography	SC-409 reduced systolic blood pressure, increased LV ejection fraction and cardiac output, and decreased LV area at diastole	[72]

Table 3 (continued)

Species	Study model	Dosage of inhibitor	Treatment conditions	Readout	Outcomes	References
Rat	Long-term treatment: regional ischemia/reperfusion (LAD ligation)	50 mg/kg/day R WJ-67657	Daily treatment by gavage 21 days post-MI	Anterior and posterior wall thickness and LV fractional shortening, infarct size	Improved LV function and but had no effect on infarct size	[33]
	Long-term treatment: regional ischemia/reperfusion (LAD ligation)	2 mg/kg SB203580-HCl	Long-term treatment of SB203580 by intraperitoneal injection once every 3 days for 4 weeks	Cardiomyocytes mitosis, cardiac functions were assessed by percentage left ventricular fractional shortening (%FS), end diastolic dimension (EDD), and end systolic dimension (ESD).	-2 weeks after MI SB203580 treatment significantly increased %FS, prevented cardiac dilation as measured by EDD and ESD -at 3 months after injury, 4 weeks of SB203580 increased %FS by 30% and reduced scar size	[77]
	Long-term treatment: regional ischemia/reperfusion	2 mg/kg SB203580-HCl	Intraperitoneal injection once every 3 days for 1 and 4 weeks	Cardiac function by echocardiography, myocardial fibrosis	SB203580 suppressed myocardial fibrosis and LV remodeling	[74]
	Long-term treatment: regional ischemia/reperfusion (LAD ligation)	50 mg/kg/day RWJ-67657	Treatment by gavage for 7 days after MI compared with 12 weeks treatment	Cardiac function by echocardiography and hemodynamic measurement	Long-term RWJ treatment improved fractional shortening and attenuated the rise in LVEDP, and prevented the reduction in dP/dtmax	[70]
	Long-term treatment: regional ischemia/reperfusion (LAD ligation)	2 μM SB239063	Intramyocardial injection with SB239063 encapsulated in microsphere formulated from the polymer (PCADK) and inject (0.5 mg/ml corresponding to 2 μM SB239063) after LAD ligation	Cardiac function using MRI and Echocardiography 7 and 21 day post-MI	No significant improvement of cardiac function at 7 day post-MI but significantly improved cardiac function at 21 days post-MI	[73]
Pig	Regional 60-min ischemia/ 4-hr reperfusion (LAD ligation)	7 mg SB239063	SB directly injected into LV lumen and perfused for 5 min before LAD occlusion	Infarct size	SB239063 had no effect on infarct size	[32]

LAD, left anterior descending coronary artery; MI, myocardial infarction; LV, left ventricle; LVEDP, left ventricular end-diastolic pressure

intensively investigated. Studies in an *in vivo* model, either acute or long-term treatment, are essential and will provide significant and clinically useful information, which may be used to develop therapeutic strategies during the actual pathophysiological events that occur in humans.

In addition to the timing of drug administration, another important issue is the effect of p38 inhibition on potentially fatal cardiac arrhythmia during myocardial ischemia/reperfusion. Although a number of ischemia/reperfusion studies reported the incidence of fatal arrhythmias during ischemia/reperfusion [78, 79], no *in vivo* study has yet investigated the effect of p38 inhibitors on a lethal arrhythmia during ischemia/reperfusion. Similar to the postischemic mortality rate, no work has presented mortality data in animals treated with p38 inhibitors, which would support the long-term effect of using a p38 inhibitor. This crucial information needs to be obtained if the effect of p38 inhibitors in myocardial ischemia/reperfusion is to be of significant relevance.

The small molecule inhibitors of p38 have been studied for almost 20 years, predominantly in terms of the anti-inflammatory effect of the inhibitors [80]. However, most of the outcomes of using the p38 inhibitors in clinical trials have been disappointing as a result of adverse events stemming from drug toxicity [81]. Although many studies of the p38 inhibitor in myocardial ischemia seem to support the benefit of the p38 inhibitor in reducing myocardial injury and improving cardiac function, the majority of clinical trials with p38 inhibitors have been mainly aimed at studying its anti-inflammatory effect, not for myocardial infarctions. Therefore, at this point do we still have faith in the p38 inhibitor for attenuating cardiac damage in ischemic heart disease? Although there have been some clinical trials on a p38 inhibitor in cardiovascular disease [7–10], only one study has focused on the acute coronary syndrome [82], namely, the first clinical study of the p38 inhibitor GW856553 or Losmapimod (NCT00910962; GlaxoSmithKline, London, UK). In this trial, changes in high-sensitivity C-reactive protein and cardiac biomarkers are being measured as primary outcomes, as well as the infarct size and cardiac functions based on magnetic resonance imaging data in the sub-study [82]. This study is still ongoing, and the primary outcome data are expected to be available in April 2012 [82]. At the same time, it is necessary to look back to the pre-clinical data set derived from p38 inhibitors during myocardial ischemia/reperfusion in order to determine whether there are still some crucial gap(s) of information as these should be filled in an attempt to obtain useful information. This is an essential prerequisite to the exploitation of the wealth of pre-clinical data which suggests that the inhibition of p38 activation will benefit patients with ischemic heart disease.

Acknowledgments This study was supported by the Thailand Research Fund grants MRG5480017 (SK), BRG5480003 (SC), and RTA5280006 (NC).

References

1. World Health Organization (2008) World Heath Statistics 2008. World Health Organization, Geneva
2. Jennings RB, Reimer KA (1991) The cell biology of acute myocardial ischemia. Annu Rev Med 42:225–246. doi:10.1146/annurev.me.42.020191.001301
3. Braunwald E (1998) Evolution of the management of acute myocardial infarction: a 20th century saga. Lancet 352(9142):1771–1774. doi:10.1016/s0140-6736(98)03212-7
4. Gottlieb RA, Burleson KO, Kloner RA, Babior BM, Engler RL (1994) Reperfusion injury induces apoptosis in rabbit cardiomyocytes. J Clin Invest 94(4):1621–1628. doi:10.1172/JCI117504
5. Schulz R (2005) A new paradigm: cross talk of protein kinases during reperfusion saves life! Am J Physiol Heart Circ Physiol 288 (1):H1–H2. doi:10.1152/ajpheart.00886.2004
6. Clark JE, Sarafraz N, Marber MS (2007) Potential of p38-MAPK inhibitors in the treatment of ischaemic heart disease. Pharmacol Therapeutics 116(2):192–206
7. U.S. National Institutes of Health (2011) A study to evaluate the effects of 3 months dosing with GW856553, as assessed FDG-PET/CT imaging. Available at: http://clinicaltrials.gov/ct2/show/study/NCT00633022. Accessed 26 Sept 2011
8. U.S. National Institutes of Health (2011) Efficacy study of p38 kinase inhibitor to treat patients with atherosclerosis. Available at: http://clinicaltrials.gov/ct2/show/NCT00570752?term=NCT00570752&rank=1. Accessed 26 Sept 2011
9. U.S. National Institutes of Health (2011) A pharmacokinetic study of SB-681323 in subjects with coronary heart disease undergoing percutaneous intervention. Available at: http://clinicaltrials.gov/ct2/show/NCT00291902?term=SB-681323&rank=9. Accessed 26 Sept 2011
10. Sarov-Blat L, Morgan JM, Fernandez P, James R, Fang Z, Hurle MR, Baidoo C, Willette RN, Lepore JJ, Jensen SE, Sprecher DL (2010) Inhibition of p38 mitogen-activated protein kinase reduces inflammation after coronary vascular injury in humans. Arterioscler Thromb Vac Biol 30(11):2256–2263. doi:10.1161/atvbaha.110.209205
11. Lee JC, Laydon JT, McDonnell PC, Gallagher TF, Kumar S, Green D, McNulty D, Blumenthal MJ, Keys JR, Land Vatter SW, Strickler JE, McLaughlin MM, Siemens IR, Fisher SM, Livi GP, White JR, Adams JL, Young PR (1994) A protein kinase involved in the regulation of inflammatory cytokine biosynthesis. Nature 372(6508):739–746
12. Rouse J, Cohen P, Trigon S, Morange M, Alonso-Llamazares A, Zamanillo D, Hunt T, Nebreda AR (1994) A novel kinase cascade triggered by stress and heat shock that stimulates MAPKAP kinase-2 and phosphorylation of the small heat shock proteins. Cell 78(6):1027–1037. doi:10.1016/0092-8674(94)90277-1
13. Han J, Lee JD, Bibbs L, Ulevitch RJ (1994) A MAP kinase targeted by endotoxin and hyperosmolarity in mammalian cells. Science 265(5173):808–811
14. Han J, Richter B, Li Z, Kravchenko VV, Ulevitch RJ (1995) Molecular cloning of human p38 MAP kinase. Biochim Biophys Acta 1265(2–3):224–227. doi:10.1016/0167-4889(95)00002-a
15. Hanks SK, Hunter T (1995) Protein kinases 6. The eukaryotic protein kinase superfamily: kinase (catalytic) domain structure and classification. FASEB J 9(8):576–596
16. Derijard B, Raingeaud J, Barrett T, Wu IH, Han J, Ulevitch RJ, Davis RJ (1995) Independent human MAP-kinase signal

transduction pathways defined by MEK and MKK isoforms. Science 267(5198):682–685
17. Raingeaud J, Whitmarsh AJ, Barrett T, Derijard B, Davis RJ (1996) MKK3- and MKK6-regulated gene expression is mediated by the p38 mitogen-activated protein kinase signal transduction pathway. Mol Cell Biol 16(3):1247–1255
18. Brancho D, Tanaka N, Jaeschke A, Ventura JJ, Kelkar N, Tanaka Y, Kyuuma M, Takeshita T, Flavell RA, Davis RJ (2003) Mechanism of p38 MAP kinase activation *in vivo*. Genes Dev 17(16):1969–1978. doi:10.1101/gad.1107303
19. Kumar S, Jiang MS, Adams JL, Lee JC (1999) Pyridinylimidazole compound SB 203580 inhibits the activity but not the activation of p38 mitogen-activated protein kinase. Biochem Biophys Res Commun 263(3):825–831. doi:10.1006/bbrc.1999.1454
20. Lee JC, Kumar S, Griswold DE, Underwood DC, Votta BJ, Adams JL (2000) Inhibition of p38 MAP kinase as a therapeutic strategy. Immunopharmacology 47(2–3):185–201. doi:10.1016/s0162-3109(00)00206-x
21. Yada M, Shimamoto A, Hampton CR, Chong AJ, Takayama H, Rothnie CL, Spring DJ, Shimpo H, Yada I, Pohlman TH, Verrier ED (2004) FR167653 diminishes infarct size in a murine model of myocardial ischemia-reperfusion injury. J Thorac Cardiovasc Surg 128(4):588–594. doi:10.1016/j.jtcvs.2004.02.007
22. Cheung PC, Campbell DG, Nebreda AR, Cohen P (2003) Feedback control of the protein kinase TAK1 by SAPK2a/p38alpha. EMBO J 22(21):5793–5805. doi:10.1093/emboj/cdg552
23. Ge B, Gram H, Di Padova F, Huang B, New L, Ulevitch RJ, Luo Y, Han J (2002) MAPKK-independent activation of p38alpha mediated by TAB1-dependent autophosphorylation of p38alpha. Science 295(5558):1291–1294. doi:10.1126/science.1067289
24. Kumphune S, Bassi R, Jacquet S, Sicard P, Clark JE, Verma S, Avkiran M, O'Keefe SJ, Marber MS (2010) A chemical genetic approach reveals that p38alpha MAPK activation by diphosphorylation aggravates myocardial infarction and is prevented by the direct binding of SB203580. J Biol Chem 285(5):2968–2975. doi:10.1074/jbc.M109.079228
25. Ono K, Han J (2000) The p38 signal transduction pathway: activation and function. Cell Signal 12(1):1–13
26. Jiang Y, Chen C, Li Z, Guo W, Gegner JA, Lin S, Han J (1996) Characterization of the structure and function of a new mitogen-activated protein kinase (p38beta). J Biol Chem 271(30):17920–17926
27. Eyers PA, Craxton M, Morrice N, Cohen P, Goedert M (1998) Conversion of SB 203580-insensitive MAP kinase family members to drug-sensitive forms by a single amino-acid substitution. Chem Biol 5(6):321–328
28. Kumar S, McDonnell PC, Gum RJ, Hand AT, Lee JC, Young PR (1997) Novel homologues of CSBP/p38 MAP kinase: activation, substrate specificity and sensitivity to inhibition by pyridinyl imidazoles. Biochem Biophys Res Commun 235(3):533–538. doi:10.1006/bbrc.1997.6849
29. See F, Kompa A, Krum H (2004) p38 MAP kinase as a therapeutic target in cardiovascular disease. Drug Discovery Today 1(2):149–154. doi:10.1016/j.ddstr.2004.08.024
30. Young PR, McLaughlin MM, Kumar S, Kassis S, Doyle ML, McNulty D, Gallagher TF, Fisher S, McDonnell PC, Carr SA, Huddleston MJ, Seibel G, Porter TG, Livi GP, Adams JL, Lee JC (1997) Pyridinyl imidazole inhibitors of p38 mitogen-activated protein kinase bind in the ATP site. J Biol Chem 272(18):12116–12121
31. Kaiser RA, Bueno OF, Lips DJ, Doevendans PA, Jones F, Kimball TF, Molkentin JD (2004) Targeted inhibition of p38 mitogen-activated protein kinase antagonizes cardiac injury and cell death following ischemia-reperfusion *in vivo*. J Biol Chem 279(15):15524–15530. doi:10.1074/jbc.M313717200
32. Kaiser RA, Lyons JM, Duffy JY, Wagner CJ, McLean KM, O'Neill TP, Pearl JM, Molkentin JD (2005) Inhibition of p38 reduces myocardial infarction injury in the mouse but not pig after ischemia-reperfusion. Am J Physiol Heart Circ Physiol 289(6):H2747–H2751. doi:10.1152/ajpheart.01280.2004
33. See F, Thomas W, Way K, Tzanidis A, Kompa A, Lewis D, Itescu S, Krum H (2004) p38 mitogen-activated protein kinase inhibition improves cardiac function and attenuates left ventricular remodeling following myocardial infarction in the rat. J Am Coll Cardiol 44(8):1679–1689. doi:10.1016/j.jacc.2004.07.038
34. Bogoyevitch MA, Gillespie-Brown J, Ketterman AJ, Fuller SJ, Ben-Levy R, Ashworth A, Marshall CJ, Sugden PH (1996) Stimulation of the stress-activated mitogen-activated protein kinase subfamilies in perfused heart. p38/RK mitogen-activated protein kinases and c-Jun N-terminal kinases are activated by ischemia/reperfusion. Circ Res 79(2):162–173
35. Saurin AT, Martin JL, Heads RJ, Foley C, Mockridge JW, Wright MJ, Wang Y, Marber MS (2000) The role of differential activation of p38-mitogen-activated protein kinase in preconditioned ventricular myocytes. FASEB J 14(14):2237–2246. doi:10.1096/fj.99-0671com
36. Martin JL, Avkiran M, Quinlan RA, Cohen P, Marber MS (2001) Antiischemic effects of SB203580 are mediated through the inhibition of p38alpha mitogen-activated protein kinase: Evidence from ectopic expression of an inhibition-resistant kinase. Circ Res 89(9):750–752
37. Wang Y, Huang S, Sah VP, Ross J Jr, Brown JH, Han J, Chien KR (1998) Cardiac muscle cell hypertrophy and apoptosis induced by distinct members of the p38 mitogen-activated protein kinase family. J Biol Chem 273(4):2161–2168
38. Gysembergh A, Simkhovich BZ, Kloner RA, Przyklenk K (2001) p38 MAPK activity is not increased early during sustained coronary artery occlusion in preconditioned versus control rabbit heart. J Mol Cell Cardiol 33(4):681–690. doi:10.1006/jmcc.2000.1331
39. House SL, Branch K, Newman G, Doetschman T, Schultz Jel J (2005) Cardioprotection induced by cardiac-specific overexpression of fibroblast growth factor-2 is mediated by the MAPK cascade. Am J Physiol Heart Circ Physiol 289(5):H2167–H2175. doi:10.1152/ajpheart.00392.2005
40. Khan M, Varadharaj S, Ganesan LP, Shobha JC, Naidu MU, Parinandi NL, Tridandapani S, Kutala VK, Kuppusamy P (2006) C-phycocyanin protects against ischemia-reperfusion injury of heart through involvement of p38 MAPK and ERK signaling. Am J Physiol Heart Circ Physiol 290(5):H2136–H2145. doi:10.1152/ajpheart.01072.2005
41. Schneider S, Chen W, Hou J, Steenbergen C, Murphy E (2001) Inhibition of p38 MAPK alpha/beta reduces ischemic injury and does not block protective effects of preconditioning. Am J Physiol Heart Circ Physiol 280(2):H499–H508
42. Sumida T, Otani H, Kyoi S, Okada T, Fujiwara H, Nakao Y, Kido M, Imamura H (2005) Temporary blockade of contractility during reperfusion elicits a cardioprotective effect of the p38 MAP kinase inhibitor SB-203580. Am J Physiol Heart Circ Physiol 288(6):H2726–H2734. doi:10.1152/ajpheart.01183.2004
43. Tanno M, Bassi R, Gorog DA, Saurin AT, Jiang J, Heads RJ, Martin JL, Davis RJ, Flavell RA, Marber MS (2003) Diverse mechanisms of myocardial p38 mitogen-activated protein kinase activation: evidence for MKK-independent activation by a TAB1-associated mechanism contributing to injury during myocardial ischemia. Circ Res 93(3):254–261. doi:10.1161/01.res.0000083490.43943.85
44. Aleshin A, Sawa Y, Ono M, Funatsu T, Miyagawa S, Matsuda H (2004) Myocardial protective effect of FR167653; a novel cytokine inhibitor in ischemic-reperfused rat heart. Eur J Cardiothorac Surg 26(5):974–980. doi:10.1016/j.ejcts.2004.06.021
45. Clanachan AS, Jaswal JS, Gandhi M, Bottorff DA, Coughlin J, Finegan BA, Stone JC (2003) Effects of inhibition of myocardial extracellular-responsive kinase and P38 mitogen-activated protein

kinase on mechanical function of rat hearts after prolonged hypothermic ischemia. Transplantation 75(2):173–180. doi:10.1097/01.tp.0000040429.40245.3a
46. Ma XL, Kumar S, Gao F, Louden CS, Lopez BL, Christopher TA, Wang C, Lee JC, Feuerstein GZ, Yue TL (1999) Inhibition of p38 mitogen-activated protein kinase decreases cardiomyocyte apoptosis and improves cardiac function after myocardial ischemia and reperfusion. Circulation 99(13):1685–1691
47. Meldrum DR, Dinarello CA, Cleveland JC Jr, Cain BS, Shames BD, Meng X, Harken AH (1998) Hydrogen peroxide induces tumor necrosis factor alpha-mediated cardiac injury by a P38 mitogen-activated protein kinase-dependent mechanism. Surgery 124(2):291–296, discussion 297
48. Wang M, Tsai BM, Turrentine MW, Mahomed Y, Brown JW, Meldrum DR (2005) p38 mitogen activated protein kinase mediates both death signaling and functional depression in the heart. Ann Thorac Surg 80(6):2235–2241. doi:10.1016/j.athoracsur.2005.05.070
49. Mocanu MM, Baxter GF, Yue Y, Critz SD, Yellon DM (2000) The p38 MAPK inhibitor, SB203580, abrogates ischaemic preconditioning in rat heart but timing of administration is critical. Basic Res Cardiol 95(6):472–478
50. Nagarkatti DS, Sha'afi RI (1998) Role of p38 MAP kinase in myocardial stress. J Mol Cell Cardiol 30(8):1651–1664
51. Nakano A, Cohen MV, Critz S, Downey JM (2000) SB 203580, an inhibitor of p38 MAPK, abolishes infarct-limiting effect of ischemic preconditioning in isolated rabbit hearts. Basic Res Cardiol 95(6):466–471
52. Sanada S, Kitakaze M, Papst PJ, Hatanaka K, Asanuma H, Aki T, Shinozaki Y, Ogita H, Node K, Takashima S, Asakura M, Yamada J, Fukushima T, Ogai A, Kuzuya T, Mori H, Terada N, Yoshida K, Hori M (2001) Role of phasic dynamism of p38 mitogen-activated protein kinase activation in ischemic preconditioning of the canine heart. Circ Res 88(2):175–180
53. Weinbrenner C, Liu GS, Cohen MV, Downey JM (1997) Phosphorylation of tyrosine 182 of p38 mitogen-activated protein kinase correlates with the protection of preconditioning in the rabbit heart. J Mol Cell Cardiol 29(9):2383–2391. doi:10.1006/jmcc.1997.0473
54. Brady NR, Hamacher-Brady A, Gottlieb RA (2006) Proapoptotic BCL-2 family members and mitochondrial dysfunction during ischemia/reperfusion injury, a study employing cardiac HL-1 cells and GFP biosensors. Biochim Biophys Acta 1757(5–6):667–678. doi:10.1016/j.bbabio.2006.04.011
55. Colston JT, de la Rosa SD, Freeman GL (2004) Impact of brief oxidant stress on primary adult cardiac fibroblasts. Biochem Biophys Res Commun 316(1):256–262. doi:10.1016/j.bbrc.2004.02.042
56. Cooper M, Ytrehus K (2004) Cell survival signalling in heart derived myofibroblasts induced by preconditioning and bradykinin: the role of p38 MAP kinase. Mol Cell Biochem 259(1–2):83–90
57. Kim JK, Pedram A, Razandi M, Levin ER (2006) Estrogen prevents cardiomyocyte apoptosis through inhibition of reactive oxygen species and differential regulation of p38 kinase isoforms. J Biol Chem 281(10):6760–6767. doi:10.1074/jbc.M511024200
58. Mackay K, Mochly-Rosen D (1999) An inhibitor of p38 mitogen-activated protein kinase protects neonatal cardiac myocytes from ischemia. J Biol Chem 274(10):6272–6279
59. Marais E, Genade S, Huisamen B, Strijdom JG, Moolman JA, Lochner A (2001) Activation of p38 MAPK induced by a multi-cycle ischaemic preconditioning protocol is associated with attenuated p38 MAPK activity during sustained ischaemia and reperfusion. J Mol Cell Cardiol 33(4):769–778. doi:10.1006/jmcc.2001.1347
60. Okada T, Otani H, Wu Y, Kyoi S, Enoki C, Fujiwara H, Sumida T, Hattori R, Imamura H (2005) Role of F-actin organization in p38 MAP kinase-mediated apoptosis and necrosis in neonatal rat cardiomyocytes subjected to simulated ischemia and reoxygenation. Am J Physiol Heart Circ Physiol 289(6):H2310–H2318. doi:10.1152/ajpheart.00462.2005
61. Rakhit RD, Kabir AN, Mockridge JW, Saurin A, Marber MS (2001) Role of G proteins and modulation of p38 MAPK activation in the protection by nitric oxide against ischemia-reoxygenation injury. Biochem Biophys Res Commun 286(5):995–1002. doi:10.1006/bbrc.2001.5477
62. Sharov VG, Todor A, Suzuki G, Morita H, Tanhehco EJ, Sabbah HN (2003) Hypoxia, angiotensin-II, and norepinephrine mediated apoptosis is stimulus specific in canine failed cardiomyocytes: a role for p38 MAPK, Fas-L and cyclin D1. Eur J Heart Fail 5(2):121–129
63. Sucher R, Gehwolf P, Kaier T, Hermann M, Maglione M, Oberhuber R, Ratschiller T, Kuznetsov AV, Bosch F, Kozlov AV, Ashraf MI, Schneeberger S, Brandacher G, Ollinger R, Margreiter R, Troppmair J (2009) Intracellular signaling pathways control mitochondrial events associated with the development of ischemia/ reperfusion-associated damage. Transpl Int 22(9):922–930. doi:10.1111/j.1432-2277.2009.00883.x
64. Schulz R, Cohen MV, Behrends M, Downey JM, Heusch G (2001) Signal transduction of ischemic preconditioning. Cardiovasc Res 52(2):181–198
65. Gorog DA, Tanno M, Cao X, Bellahcene M, Bassi R, Kabir AM, Dighe K, Quinlan RA, Marber MS (2004) Inhibition of p38 MAPK activity fails to attenuate contractile dysfunction in a mouse model of low-flow ischemia. Cardiovasc Res 61(1):123–131
66. Kabir AM, Cao X, Gorog DA, Tanno M, Bassi R, Bellahcene M, Quinlan RA, Davis RJ, Flavell RA, Shattock MJ, Marber MS (2005) Antimycin A induced cardioprotection is dependent on pre-ischemic p38-MAPK activation but independent of MKK3. J Mol Cell Cardiol 39(4):709–717. doi:10.1016/j.yjmcc.2005.07.012
67. Moolman JA, Hartley S, Van Wyk J, Marais E, Lochner A (2006) Inhibition of myocardial apoptosis by ischaemic and beta-adrenergic preconditioning is dependent on p38 MAPK. Cardiovasc Drugs Ther 20(1):13–25. doi:10.1007/s10557-006-6257-7
68. Gao F, Yue TL, Shi DW, Christopher TA, Lopez BL, Ohlstein EH, Barone FC, Ma XL (2002) p38 MAPK inhibition reduces myocardial reperfusion injury via inhibition of endothelial adhesion molecule expression and blockade of PMN accumulation. Cardiovasc Res 53(2):414–422
69. Zhang GM, Su SP, Wang Y, Li TD, Li XY, Tan H, Zhang DW, Zhang H, Liu LF (2010) Effect of ischemic postconditioning on activation of p38 mitogen activated protein kinase and cardiocyte apoptosis in rats. Zhongguo Yi Xue Ke Xue Yuan Xue Bao 32(5):526–532. doi:10.3881/j.issn.1000-503X.2010.05.012
70. Kompa AR, See F, Lewis DA, Adrahtas A, Cantwell DM, Wang BH, Krum H (2008) Long-term but not short-term p38 mitogen-activated protein kinase inhibition improves cardiac function and reduces cardiac remodeling post-myocardial infarction. J Pharmacol Exp Ther 325(3):741–750. doi:10.1124/jpet.107.133546
71. Li M, Georgakopoulos D, Lu G, Hester L, Kass DA, Hasday J, Wang Y (2005) p38 MAP kinase mediates inflammatory cytokine induction in cardiomyocytes and extracellular matrix remodeling in heart. Circulation 111(19):2494–2502. doi:10.1161/01.cir.0000165117.71483.0c
72. Liu YH, Wang D, Rhaleb NE, Yang XP, Xu J, Sankey SS, Rudolph AE, Carretero OA (2005) Inhibition of p38 mitogen-activated protein kinase protects the heart against cardiac remodeling in mice with heart failure resulting from myocardial infarction. J Card Fail 11(1):74–81
73. Sy JC, Seshadri G, Yang SC, Brown M, Oh T, Dikalov S, Murthy N, Davis ME (2008) Sustained release of a p38 inhibitor from non-

inflammatory microspheres inhibits cardiac dysfunction. Nat Mater 7 (11):863–868. doi:10.1038/nmat2299
74. Yin H, Zhang J, Lin H, Wang R, Qiao Y, Wang B, Liu F (2008) p38 mitogen-activated protein kinase inhibition decreases TNFalpha secretion and protects against left ventricular remodeling in rats with myocardial ischemia. Inflammation 31(2):65–73. doi:10.1007/s10753-007-9050-2
75. Schulz R, Belosjorow S, Gres P, Jansen J, Michel MC, Heusch G (2002) p38 MAP kinase is a mediator of ischemic preconditioning in pigs. Cardiovasc Res 55(3):690–700
76. Barancik M, Htun P, Strohm C, Kilian S, Schaper W (2000) Inhibition of the cardiac p38-MAPK pathway by SB203580 delays ischemic cell death. J Cardiovasc Pharmacol 35(3):474–483
77. Engel FB, Hsieh PC, Lee RT, Keating MT (2006) FGF1/p38 MAP kinase inhibitor therapy induces cardiomyocyte mitosis, reduces scarring, and rescues function after myocardial infarction. Proc Natl Acad Sci USA 103(42):15546–15551. doi:10.1073/pnas.0607382103
78. Di Diego JM, Antzelevitch C (2011) Ischemic ventricular arrhythmias: Experimental models and their clinical relevance. Heart Rhythm 8:1963–1968. doi:10.1016/j.hrthm.2011.06.036
79. Chen Z, Luo H, Zhuang M, Cai L, Su C, Lei Y, Zou J (2011) Effects of ischemic preconditioning on ischemia/reperfusion-induced arrhythmias by upregulatation of connexin 43 expression. J Cardiothorac Surg 6:80. doi:10.1186/1749-8090-6-80
80. Marber MS, Molkentin JD, Force T (2010) Developing small molecules to inhibit kinases unkind to the heart: p38 MAPK as a case in point. Drug Discov Today Dis Mech 7(2):e123–e127. doi:10.1016/j.ddmec.2010.07.006
81. Sweeney SE (2009) The as-yet unfulfilled promise of p38 MAPK inhibitors. Nat Rev Rheumatol 5(9):475–477. doi:10.1038/nrrheum.2009.171
82. U.S. National Institutes of Health (2011) A study to evaluate the safety of 12 weeks of dosing with GW856553 and its effects on inflammatory markers, infarct size, and cardiac function in subjects with myocardial infarction without ST-segment elevation (Solstice). Available at: http://clinicaltrials.gov/ct2/show/study/NCT00910962?term=GW856553&rank=6. Accessed 26 Sept 2011
83. Yue TL, Wang C, Gu JL, Ma XL, Kumar S, Lee JC, Feuerstein GZ, Thomas H, Maleeff B, Ohlstein EH (2000) Inhibition of extracellular signal-regulated kinase enhances Ischemia/Reoxygenation-induced apoptosis in cultured cardiac myocytes and exaggerates reperfusion injury in isolated perfused heart. Circ Res 86(6):692–699
84. Mackay K, Mochly-Rosen D (2000) Involvement of a p38 mitogen-activated protein kinase phosphatase in protecting neonatal rat cardiac myocytes from ischemia. J Mol Cell Cardiol 32 (8):1585–1588. doi:10.1006/jmcc.2000.1194
85. Sicard P, Clark JE, Jacquet S, Mohammadi S, Arthur JS, O'Keefe SJ, Marber MS (2010) The activation of p38 alpha, and not p38 beta, mitogen-activated protein kinase is required for ischemic preconditioning. J Mol Cell Cardiol 48(6):1324–1328. doi:10.1016/j.yjmcc.2010.02.013
86. Schwertz H, Carter JM, Abdudureheman M, Russ M, Buerke U, Schlitt A, Muller-Werdan U, Prondzinsky R, Werdan K, Buerke M (2007) Myocardial ischemia/reperfusion causes VDAC phosphorylation which is reduced by cardioprotection with a p38 MAP kinase inhibitor. Proteomics 7(24):4579–4588. doi:10.1002/pmic.200700734
87. Koike N, Takeyoshi I, Ohki S, Tokumine M, Matsumoto K, Morishita Y (2004) Effects of adding P38 mitogen-activated protein-kinase inhibitor to celsior solution in canine heart transplantation from non-heart-beating donors. Transplantation 77 (2):286–292. doi:10.1097/01.TP.0000101039.12835.A4

International Endodontic Journal

doi:10.1111/j.1365-2591.2011.01986.x

$Na_V1.8$, but not $Na_V1.9$, is upregulated in the inflamed dental pulp tissue of human primary teeth

A. Suwanchai[1], U. Theerapiboon[1], N. Chattipakorn[2] & S. C. Chattipakorn[2,3]

[1]Division of Pediatric Dentistry, Department of Orthodontics and Pediatric Dentistry, Faculty of Dentistry, Chiang Mai University, Chiang Mai; [2]Cardiac Electrophysiology Research and Training Center, Department of Physiology, Faculty of Medicine, Chiang Mai; and [3]Department of Oral Biology and Diagnostic Science, Faculty of Dentistry, Chiang Mai University, Chiang Mai, Thailand

Abstract

Suwanchai A, Theerapiboon U, Chattipakorn N, Chattipakorn SC. $Na_V1.8$, but not $Na_V1.9$, is upregulated in the inflamed dental pulp tissue of human primary teeth. *International Endodontic Journal*, **45**, 372–378, 2012.

Aim To investigate alterations in $Na_V1.8$ and $Na_V1.9$ expression within inflamed dental pulp tissue of human primary teeth.

Methodology Dental pulp tissue obtained from both normal and inflamed pulps in primary teeth as well as pulps from normal and inflamed permanent teeth was used. The quantity of $Na_V1.8$ and $Na_V1.9$ expression in the dental pulp tissue was investigated using Western blot analysis. General neuron marker (PGP9.5) was used to quantify for neural density, and an increase in metalloproteinase-9 was used to indicate pulpal inflammation in inflamed teeth. Statistically significant differences for each determined parameter between normal and inflamed teeth of both primary and permanent teeth were tested using the Mann–Whitney rank sum test.

Results There was no significant difference in neural density of normal and inflamed dental pulp tissue, although degrees of inflammation were increased in the inflamed dental pulp of both permanent and primary teeth ($P < 0.05$). $Na_V1.8$ and $Na_V1.9$ expression in inflamed pulps of permanent teeth increased significantly compared with normal permanent teeth ($P < 0.05$). However, only $Na_V1.8$ expression was increased significantly in the inflamed dental pulp of primary teeth ($P < 0.05$).

Conclusions $Na_V1.8$ alone may be the therapeutic target for treatment of painful pulpitis in primary teeth.

Keywords: dental pulp, inflammation, $Na_V1.8$, $Na_V1.9$, primary teeth.

Received 8 August 2011; accepted 25 October 2011

Introduction

Voltage-gated sodium channels (VGSCs) are transmembrane ion channels involved in the initiation and propagation of action potentials, and the spontaneous activity of VGSCs can lead to spontaneous pain. VGSCs are found in excitable cells, including neurons and muscle cells (Goodman 2008). VGSCs can be categorized into two groups according to their resistance to the blocker, tetrodotoxin (TTX): TTX-sensitive (TTX-S) and TTX-resistant (TTX-R) channels (Cummins *et al.* 2007). $Na_V1.8$ and $Na_V1.9$ are a subfamily of TTX-R VGSCs, which are dominantly found in unmyelinated C fibres, the largest group of sensory nerve fibres innervating dental pulp tissue (Amir *et al.* 2006). $Na_V1.8$, with its slow inactivation kinetics and high activation threshold, is involved in the electrogenesis of action potentials in C-type peripheral neurons (Renganathan *et al.* 2001), whereas $Na_V1.9$ is responsible for the generation of persistent action potentials (Dib-Hajj *et al.* 2002). Both $Na_V1.8$ and $Na_V1.9$ are believed to be involved in prolonged action potentials during painful stimuli (Cummins *et al.* 2007). Several previous studies have shown that $Na_V1.8$ and $Na_V1.9$ are upregulated

Correspondence: Siriporn Chattipakorn, DDS, PhD, Department of Oral Biology and Diagnostic Science, Faculty of Dentistry, Chiang Mai University, Chiang Mai 50200, Thailand (Tel.: 011 66 53 944 451; fax: 011 66 53 222 844; e-mail: s.chat@chiangmai.ac.th).

in several chronic inflammatory pain models (Amaya *et al.* 2006, Joshi *et al.* 2006, Strickland *et al.* 2008).

Dental pulp innervation consists mostly of nociceptive nerve fibres that originate from the trigeminal ganglion, peripherally pass through the apical foramen, and terminate in the dental pulp as free nerve endings (Hildebrand *et al.* 1995). Dynamic changes in the density of pulpal innervation during pulpal inflammation have been found to be changed depending on the severity and timing of the inflammation (Byers *et al.* 1990). These changes can be either sprouting or degeneration of nerve fibres. Thus, the innervation density of dental pulp tissue may be either increased or decreased following inflammation. For example, a study by Rodd & Boissonade (2001) using immunohistochemistry revealed that neural density at the pulpal horn of inflamed dental pulp of human primary and permanent teeth increased with the depth of dental caries. In contrast, Western blot analysis indicated no significant difference in neural density of the dental pulp of inflamed human permanent teeth compared with normal teeth (Warren *et al.* 2008). In the dental pulp of permanent teeth with pulpitis, the upregulation of matrix metalloproteinase-9 (MMP-9), which is an enzyme responsible for extracellular matrix remodelling and degradation, was also found (Tsai *et al.* 2005). This finding indicates that MMP-9 is a marker for pulpal inflammation. The expression of $Na_V1.8$ and $Na_V1.9$ has been found at nerve endings in the dental pulp of permanent teeth (Renton *et al.* 2005, Wells *et al.* 2007), and the upregulation of those VGSC isoforms, $Na_V1.8$ and $Na_V1.9$, has been demonstrated during painful pulpitis of human permanent teeth (Renton *et al.* 2005, Wells *et al.* 2007, Warren *et al.* 2008). A recent study in rat dental pulp tissue found increased $Na_V1.8$ mRNA expression in association with an increased degree of pulpal inflammation (Esmaeili *et al.* 2011). In spite of the strong evidence for $Na_V1.8$ and $Na_V1.9$ expression in permanent human dental pulp tissue, no evidence of those sodium channel isoforms in the dental pulp of human primary teeth has been demonstrated. The innervation in primary teeth and in permanent teeth is different because the density of the dental nerve supply is lower in primary teeth (Rodd & Boissonade 2001, 2002). Therefore, the aim of this study was to investigate whether $Na_V1.8$ and $Na_V1.9$ expression is altered in human dental pulp of inflamed primary teeth compared with normal teeth. The hypothesis that the expression of $Na_V1.8$ and $Na_V1.9$ are altered following pulpal inflammation in primary teeth was tested.

Materials and methods

Subjects

The use of human subjects was approved by the Human Experimentation Committee, Faculty of Dentistry, Chiang Mai University. Informed consent was obtained from all the subjects or accompanying guardians, in the case of subjects under the age of 20.

Teeth from subjects were divided into four groups: intact premolars extracted for orthodontic purposes ($n = 18$), permanent teeth diagnosed with irreversible pulpitis that required extraction ($n = 7$), intact primary teeth diagnosed with prolonged retention that required extraction ($n = 7$) and primary teeth diagnosed with reversible or irreversible pulpitis that required extraction ($n = 16$). Teeth with deep caries or mechanical pulp exposures with a history of pain on stimulation that rapidly disappeared or no history of pain and no radiographic periapical changes were diagnosed with reversible pulpitis. Teeth with irreversible pulpitis had deep caries and/or restorations with spontaneous pain. Normal or enlarged periodontal space was detected on the radiograph of teeth with irreversible pulpitis. All primary teeth had physiologic root resorption of not more than 2/3 root length. All teeth had no history of trauma, and all teeth with inflamed pulps were from deep caries. The subjects were interviewed for their history of pain before extraction. The information related to history of dental pain included sites of dental pain, duration, stimulating factors and severity of maximum pain was obtained using visual analogue scales (VAS).

Pulpal tissue collection

Immediately after extraction, a vertical groove almost to the depth of the pulp chamber was cut along the buccal surface of each tooth from the incisal edge to the apex in anterior teeth, and to the furcation in molar teeth. Then, the teeth were split open along the groove using an elevator. Pulpal tissues were removed and stored in 1.5 mL Eppendorf tubes in liquid nitrogen, before being transferred to a freezer and stored at −80 °C for further investigation.

Western blot analysis

The method for Western blot analysis was modified from that of Warren *et al.* (2008). Frozen pulp tissue was weighed before being crushed with a plastic pestle

in a homogenization buffer at a ratio of 1 mg of pulpal tissue to 10 μL of buffer. The buffer consisted of RIPA (50 mmol L^{-1} of Tris-Cl pH7.5, 150 mmol L^{-1} of sodium chloride, 1 mmol L^{-1} of EDTA, 1% Triton X-100 and 0.1% SDS), two cocktails, of protease and phosphatase inhibitors (Roche Applied Science, Mannheim, Germany), and 1% of sodium deoxycholate. The protein concentration of each sample was determined using a Bio-Rad protein assay kit (Bio-Rad Laboratories, Hercules, CA, USA). The proteins were denatured by being boiled at 95 °C for 5 min and were detected via 10% sodium dodecyl sulphate polyacrylamide gel electrophoresis (SDS-PAGE), transferring of proteins from gels to nitrocellulose membranes, and incubation of the membranes in primary antibody overnight. The primary antibodies used in this study were rabbit polyclonal antibody to PGP9.5, a general neuronal marker (1 : 400 in 0.1% TBST with 10% nonfat dry milk, ab10404; Biomed Diagnostics, Cambridge, MA, USA), rabbit polyclonal antibody to MMP-9, used as a marker of inflammation (1 : 200 in 0.1% TBST with 5% nonfat dry milk, ab38904; Biomed Diagnostics), rabbit polyclonal antibody to $Na_V1.8$ (1 : 200 in 0.1% TBST with 5% bovine serum albumin, S2071; Sigma Aldrich Inc, St. Louis, MO, USA) and rabbit polyclonal antibody to $Na_V1.9$ (1 : 200 in 0.1% TBST with 5% bovine serum albumin; S2196, Sigma Aldrich Inc). The membranes were then incubated in a secondary goat anti-rabbit antibody, conjugated with horseradish peroxidase (1 : 5000 in 0.1% TBST; Bio-Rad Laboratories). The proteins were visualized via a chemiluminescent detection system (Amersham ECL Western blotting detection reagents; GE Healthcare, Piscataway, NJ, USA). Band intensity was quantified by the Scion Image program (Scion Corporation, Frederick, MD, USA). The data were normalized with β-actin to control for the amount of protein loading and transfer.

Data analysis

Data were shown as mean ± SE. Statistically significant differences for each determined parameter between normal and inflamed teeth of both primary and permanent teeth were tested using the Mann–Whitney rank sum test. Significance levels were set at $P < 0.05$.

Results

Mean ages of subjects with permanent teeth with normal pulps, permanent teeth with inflamed pulps, primary teeth with normal pulps and primary teeth with inflamed pulps were 17.3 ± 1.1, 35.4 ± 6.3, 9.4 ± 0.9 and 6.1 ± 0.7 (mean ± SE) years, respectively. The average duration of pain was 56 ± 51 days in the subjects with permanent teeth with inflamed pulps and 15 ± 6 days in subjects with primary teeth with inflamed pulps. No pain was reported in subjects with normal primary and normal permanent teeth. All permanent teeth with inflamed pulps were diagnosed with irreversible pulpitis. Of 16 inflamed primary teeth, eight were clinically diagnosed with irreversible pulpitis, whereas another eight were clinically diagnosed with reversible pulpitis.

To quantify the amount of nerve fibres in the dental pulp, the levels of PGP9.5 compared with β-actin in each dental pulp were measured. There was no significant difference in the relative amount of PGP9.5 between normal and inflamed dental pulp of either primary or permanent teeth (Fig. 1). The average levels of inflammation were represented by the ratio of MMP-9 to β-actin. The relative amounts of MMP-9 were significantly higher in inflamed primary teeth ($P < 0.05$) and inflamed permanent teeth ($P < 0.05$) than in normal teeth (Fig. 2). The expression

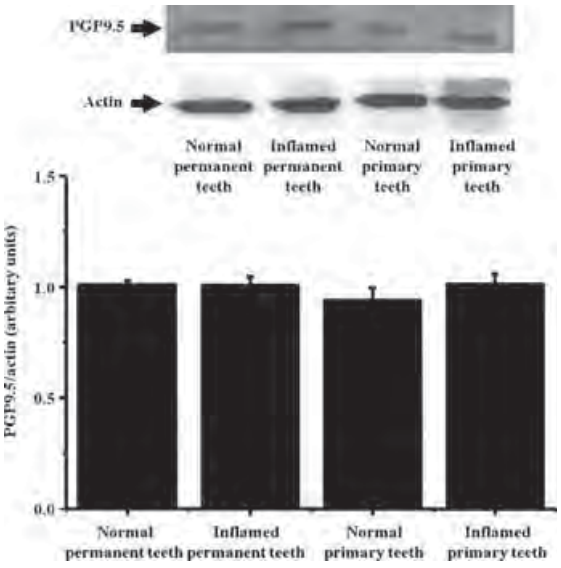

Figure 1 Relative amounts of PGP9.5 expression. PGP9.5, the neural marker, was detected in the dental pulp of permanent and primary teeth as indicated by the arrow. The band intensity of each sample was normalized with β-actin and shown as mean ± SE. The data show that the relative amount of PGP9.5 in dental pulp of inflamed permanent ($n = 7$) and primary teeth ($n = 16$) was not significantly different from that in normal permanent ($n = 18$) and primary ($n = 7$) teeth.

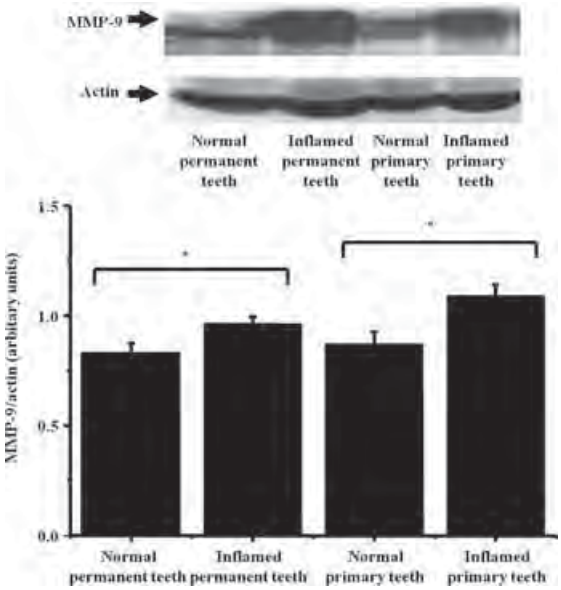

Figure 2 Relative amounts of metalloproteinase-9 (MMP-9) expression. The expected molecular weight of MMP-9 is indicated by the arrow. The band intensity of each sample was normalized with β-actin and shown as mean ± SE. There was a significant increase in MMP-9 in inflamed pulp compared with normal pulp of both permanent (n = 7 and 18, for inflamed and normal pulp, respectively) and primary teeth (n = 16 and 7, for inflamed and normal pulp, respectively) (*P < 0.05).

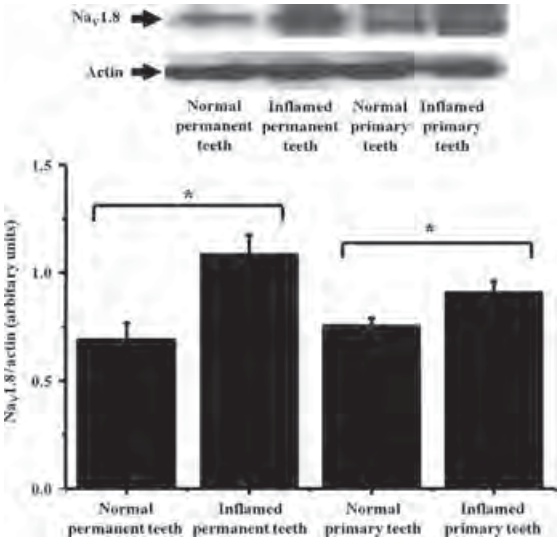

Figure 3 Relative amounts of $Na_V1.8$ expression. The expected molecular weight of $Na_V1.8$ is indicated by the arrow. The band intensity of each sample was normalized with β-actin and shown as mean ± SE. The data indicate a significant increase of $Na_V1.8$ in the inflamed dental pulp of permanent (n = 5) and primary teeth (n = 9) compared with normal dental pulp (n = 6 and 6, for normal permanent and primary teeth, respectively) (*P < 0.05).

of $Na_V1.8$ and $Na_V1.9$ in the dental pulp of permanent teeth with inflamed pulps was significantly greater than in normal permanent teeth (P < 0.05, as shown in Figs 3 and 4). In primary teeth, only $Na_V1.8$ expression was significantly higher in the inflamed dental pulp than in normal dental pulp (P < 0.05, Fig. 3). However, no significant difference between the amount of $Na_V1.9$ expression in inflamed and normal pulp tissues in primary teeth was observed (Fig. 4).

Only $Na_V1.8$ was correlated with maximum pain intensity in the group with permanent teeth (P < 0.05, r = 0.674), However, no correlation between all protein expression and pain intensity in groups with primary teeth was found (P > 0.05).

Discussion

The present study is the first to demonstrate the expression of $Na_V1.8$ and $Na_V1.9$ in dental pulp tissue of human primary teeth. $Na_V1.8$ was upregulated in the inflamed dental pulp of both permanent and primary teeth, whereas $Na_V1.9$ was upregulated only in the inflamed dental pulp of permanent teeth. The results also showed that there was no change in the overall amount of nerve fibres in inflamed pulps compared with normal pulps in both permanent and primary teeth.

Changes in pulpal innervation during inflammation by sprouting of nerve fibres have been reported (Byers *et al.* 1990). However, the depth of carious lesions and degrees of pulpal inflammation resulting in the degenerative changes of pulpal tissues may explain the findings with no change in the overall amount of innervation in teeth with and without pulpitis. The comparability of overall innervation between inflamed and normal dental pulp tissue may also suggest a similarity in the number of potential sites of sodium channel expression. Therefore, the increased expression of $Na_V1.8$ in primary and permanent teeth with pulpitis and of $Na_V1.9$ in permanent teeth with pulpitis results not only from an increase in the number of potential sites of their expression, but may also result directly from the upregulation of the $Na_V1.8$ and $Na_V1.9$ expression itself. The increased expression of $Na_V1.8$ and $Na_V1.9$ in human permanent dental pulp with painful pulpitis, as in the present study, has previously

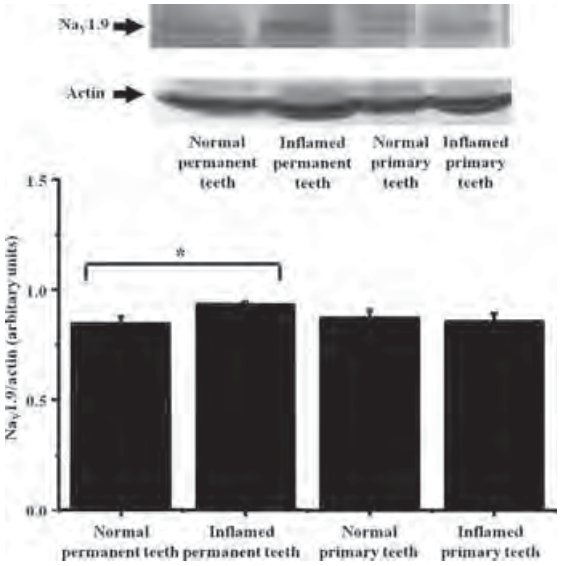

Figure 4 Relative amounts of $Na_V1.9$ expression. The expected molecular weight of $Na_V1.9$ is indicated by the arrow. The band intensity of each sample was normalized with β-actin and shown as mean ± SE. There was a significant increase of $Na_V1.9$ in the inflamed dental pulp of permanent teeth ($n = 5$) compared with normal permanent teeth ($n = 8$) ($^*P < 0.05$). However, there was no significant difference in $Na_V1.9$ expression between normal ($n = 5$) and inflamed ($n = 9$) dental pulp of primary teeth.

been reported (Renton *et al.* 2005, Wells *et al.* 2007, Warren *et al.* 2008), but the altered expression of $Na_V1.8$ and $Na_V1.9$ in primary teeth with pulpitis has never been investigated. Despite the dominant expression of $Na_V1.8$ and $Na_V1.9$ in nociceptive neurons, the localized expression of both sodium channel subtypes may not be similar. $Na_V1.8$ is remarkably localized in unmyelinated and small myelinated sensory neurons, whereas $Na_V1.9$ is located only in unmyelinated neurons (Amaya *et al.* 2000). The possible explanation for no upregulation of the $Na_V1.9$ expression in inflamed primary teeth could be due to the insufficient degree of pulpal inflammation in inflamed primary teeth to activate the upregulation of $Na_V1.9$ expression. Previous studies demonstrated that the expression of $Na_V1.8$ may be more sensitive to inflammatory pain stimuli, suggesting that the threshold for upregulation of $Na_V1.8$ may be lower than that of $Na_V1.9$ (Benn *et al.* 2001, Yu *et al.* 2011). As the inflammatory mediators secreted following injuries, such as prostaglandin E_2 (PGE2), serotonin and adenosine, are capable to modulate TTX-R currents, contributing to hyperalgesia (Gold 1999), and that inflammatory mediators have been found to be increased with age (Brüünsgaard & Pedersen 2003), it is possible that the levels of inflammatory mediators could be higher in the group with permanent teeth than the group with primary teeth.

Axonal demyelination is a common event in the inflamed dental pulp that causes a dynamic change in the proportion of myelinated and demyelinated fibres (Henry *et al.* 2009). The study of Henry *et al.* (2009) in human permanent inflammatory dental pulp showed that there was an increase in the atypical nodal sites, representing axonal demyelination. That study also found the accumulation of sodium channels at the atypical nodal sites but there was no overall upregulation of sodium channel expression (Henry *et al.* 2009). That finding suggested that pulpal inflammation can upregulate sodium channels at only some specific sites without changes in total sodium channel expression. The upregulation of $Na_V1.8$, but not $Na_V1.9$, expression in the inflamed primary teeth found in this study suggests that $Na_V1.8$, rather than $Na_V1.9$, should have a significant role in primary tooth pulpal inflammatory pain. However, the finding that $Na_V1.9$ did not increase in primary teeth with pulpitis does not mean that there was no change in $Na_V1.9$ expression, but there may be changes in specific sites of $Na_V1.9$ accumulation without overall quantitative changes. Further investigations to localize the sites of $Na_V1.8$ and $Na_V1.9$ expression and studies in the field of stimulating pathways of $Na_V1.8$ and $Na_V1.9$ are still required. It was also demonstrated that only $Na_V1.8$ expression in permanent teeth was correlated with pain score; therefore, the findings may emphasize that only $Na_V1.8$, but not $Na_V1.9$, plays a role in chronic pulpal inflammatory pain. However, the reasons for the absence of correlation between $Na_V1.8$ and pain scores in the group with primary teeth may be a result of the difference in their ability to recall previous pain between adults and children.

Conclusions

Evidence exists to support the concept that $Na_V1.8$ plays an important role in chronic inflammatory pain (Amaya *et al.* 2000, Joshi *et al.* 2006, Strickland *et al.* 2008). In contrast, the evidence for the involvement of $Na_V1.9$ in inflammatory pain is controversial (Porreca *et al.* 1999, Coggeshall *et al.* 2004, Amaya *et al.* 2006, Strickland *et al.* 2008). In the present study, there was an increase in both $Na_V1.8$ and $Na_V1.9$ expression in

permanent teeth with inflamed pulps compared with permanent teeth with normal pulps, and there was an increase of only $Na_V1.8$, but not $Na_V1.9$, expression in primary teeth with inflamed pulps compared with normal primary teeth. This suggests that, in permanent teeth, both $Na_V1.8$ and $Na_V1.9$ may be the targets for the development of novel analgesic drugs and novel anaesthetic agents for the treatment of pulpal inflammatory pain, whereas, in primary teeth, only $Na_V1.8$ may be the target for the treatment of pulpal inflammatory pain.

Acknowledgements

This research was supported by the Thailand Research Fund (RTA5280006, NC), Thailand Research Fund (BRG5480003, SC), Chiang Mai University Fund (UT), Faculty of Dentistry, Chiang Mai University (UT and SC). The authors wish to thank Dr. M. Kevin O Carroll, Professor Emeritus of the University of Mississippi School of Dentistry, USA, and Faculty Consultant at Faculty of Dentistry, Chiang Mai University, Thailand, for his assistance in the preparation of the manuscript. All authors have no conflict of interest to declare.

References

Amaya F, Decosterd I, Samad TA *et al.* (2000) Diversity of expression of the sensory neuron-specific TTX-resistant voltage-gated sodium ion channels SNS and SNS2. *Molecular and Cellular Neuroscience* **15**, 331–42.

Amaya F, Wang H, Costigan M *et al.* (2006) The voltage-gated sodium channel Na(v)1.9 is an effector of peripheral inflammatory pain hypersensitivity. *Journal of Neuroscience* **26**, 12852–60.

Amir R, Argoff CE, Bennett GJ *et al.* (2006) The role of sodium channels in chronic inflammatory and neuropathic pain. *Journal of Pain* **7**, S1–29.

Benn SC, Costigan M, Tate S, Fitzgerald M, Woolf CJ (2001) Developmental expression of the TTX-resistant voltage-gated sodium channels $Na_V1.8$ (SNS) and $Na_V1.9$ (SNS2) in primary sensory neurons. *Journal of Neuroscience* **21**, 6077–85.

Brüünsgaard H, Pedersen BK (2003) Age-related inflammatory cytokines and disease. *Immunology and Allergy Clinics of North America* **23**, 15–39.

Byers MR, Taylor PE, Khayat BG, Kimberly CL (1990) Effects of injury and inflammation on pulpal and periapical nerves. *Journal of Endodontics* **16**, 78–84.

Coggeshall RE, Tate S, Carlton SM (2004) Differential expression of tetrodotoxin-resistant sodium channels Nav1.8 and Nav1.9 in normal and inflamed rats. *Neuroscience Letters* **355**, 45–8.

Cummins TR, Sheets PL, Waxman SG (2007) The roles of sodium channels in nociception: implications for mechanisms of pain. *Pain* **131**, 243–57.

Dib-Hajj S, Black JA, Cummins TR, Waxman SG (2002) NaN/Nav1.9: a sodium channel with unique properties. *Trends in Neuroscience* **25**, 253–9.

Esmaeili A, Akhavan A, Bouzari M, Mousavi SB, Torabinia N, Adibi S (2011) Temporal expression pattern of sodium channel Nav 1.8 messenger RNA in pulpitis. *International Endodontic Journal* **44**, 499–504.

Gold MS (1999) Tetrodotoxin-resistant Na+ currents and inflammatory hyperalgesia. *Proceedings of the National Academy of Science of the United States of America* **96**, 7645–9.

Goodman BE (2008) Channels active in the excitability of nerves and skeletal muscles across the neuromuscular junction: basic function and pathophysiology. *Advances in Physiology Education* **32**, 127–35.

Henry MA, Luo S, Foley BD, Rzasa RS, Johnson LR, Levinson SR (2009) Sodium channel expression and localization at demyelinated sites in painful human dental pulp. *Journal of Pain* **10**, 750–8.

Hildebrand C, Fried K, Tuisku F, Johansson CS (1995) Teeth and tooth nerves. *Progress in Neurobiology* **45**, 165–222.

Joshi SK, Mikusa JP, Hernandez G *et al.* (2006) Involvement of the TTX-resistant sodium channel Nav 1.8 in inflammatory and neuropathic, but not post-operative, pain states. *Pain* **123**, 75–82.

Porreca F, Lai J, Bian D *et al.* (1999) A comparison of the potential role of the tetrodotoxin-insensitive sodium channels, PN3/SNS and NaN/SNS2, in rat models of chronic pain. *Proceedings of the National Academy of Science of the United States of America* **96**, 7640–4.

Renganathan M, Cummins TR, Waxman SG (2001) Contribution of Na(v)1.8 sodium channels to action potential electrogenesis in DRG neurons. *Journal of Neurophysiology* **86**, 629–40.

Renton T, Yiangou Y, Plumpton C, Tate S, Bountra C, Anand P (2005) Sodium channel Nav1.8 immunoreactivity in painful human dental pulp. *BMC Oral Health* **5**, 5.

Rodd HD, Boissonade FM (2001) Innervation of human tooth pulp in relation to caries and dentition type. *Journal of Dental Research* **80**, 389–93.

Rodd HD, Boissonade FM (2002) Comparative immunohistochemical analysis of the peptidergic innervation of human primary and permanent tooth pulp. *Archives of Oral Biology* **47**, 375–85.

Strickland IT, Martindale JC, Woodhams PL, Reeve AJ, Chessell IP, McQueen DS (2008) Changes in the expression of NaV1.7, NaV1.8 and NaV1.9 in a distinct population of dorsal root ganglia innervating the rat knee joint in a model of chronic inflammatory joint pain. *Eur Journal of Pain* **12**, 564–72.

Tsai CH, Chen YJ, Huang FM, Su YF, Chang YC (2005) The upregulation of matrix metalloproteinase-9 in inflamed human dental pulps. *Journal of Endodontics* **31**, 860–2.

Warren CA, Mok L, Gordon S, Fouad AF, Gold MS (2008) Quantification of neural protein in extirpated tooth pulp. *Journal of Endodontics* **34**, 7–10.

Wells JE, Bingham V, Rowland KC, Hatton J (2007) Expression of Nav1.9 channels in human dental pulp and trigeminal ganglion. *Journal of Endodontics* **33**, 1172–6.

Yu YQ, Zhao F, Guan SM, Chen J (2011) Antisense-mediated knockdown of $Na_V1.8$, but not $Na_V1.9$, generates inhibitory effects on complete Freund's adjuvant-induced inflammatory pain in rat. *PLoS One* **6**, e19865.

Cardioprotective effects of incretin during ischaemia-reperfusion

Kroekkiat Chinda, Siriporn Chattipakorn and Nipon Chattipakorn

Diabetes and Vascular Disease Research published online 11 April 2012
DOI: 10.1177/1479164112440816

Non-invited Review

Cardioprotective effects of incretin during ischaemia-reperfusion

Diabetes & Vascular Disease Research
0(0) 1–14

DOI: 10.1177/1479164112440816
dvr.sagepub.com
SAGE

Kroekkiat Chinda[1,2], Siriporn Chattipakorn[1,3] and Nipon Chattipakorn[1,2]

Abstract

Incretin is a gut derived peptide hormone secreted in the intestine after food ingestion, and is degraded rapidly after secretion by dipeptidyl peptidase (DPP)-4. Incretin-based therapy, such as glucagon-like peptide (GLP)-1 and the DPP-4 inhibitor, has been proposed as a new therapeutic approach for the treatment of type 2 diabetic patients. In the past few years, growing evidence also demonstrated the cardioprotective effects of incretin-based therapy, especially during ischaemia-reperfusion (I/R) injury in both the animal models and in clinical studies. However, inconsistent reports exist regarding the use of these pharmacological interventions. In this article, a comprehensive review regarding both basic and clinical studies reporting the effects of GLP-1 and DPP-4 inhibitors on I/R hearts is presented and discussed. The consistent findings as well as controversial results are summarised, focusing on the effects of incretin on the infarct size, left ventricular function and haemodynamic improvement during an I/R injury.

Keywords

Incretin, GLP-1, DPP-4 inhibitor, ischaemia-reperfusion injury, heart

Introduction

Diabetes mellitus (DM) has become a significant health problem in most nations with the number of patients dramatically soaring and expected to reach 366 million by the year 2030.[1] It has been shown that patients with type 2 diabetes mellitus (T2DM) have a two- to four-fold higher risk of coronary disease and stroke mortality.[2–6] Although several new anti-diabetic drugs have been discovered in the past decades, the therapies have been limited by their adverse effects such as weight gain, hypoglycaemia, fluid retention and an unexpected cardiovascular risk.[7–10] Therefore, new anti-diabetic drugs that could control hyperglycaemia and reduce the risk of cardiovascular events are of potential benefit to T2DM patients.

Incretin is a gut derived peptide hormone which enhances endogenous insulin secretion and reduces glucagon secretion, resulting in reduced blood glucose after food consumption.[11–14] Its secretion is greatly influenced by ingestion.[15] The incretin hormone has been classified into glucose-dependent insulinotropic peptide (GIP) and glucagon-like peptide (GLP)-1. GIP is secreted by the enteroendocrine K cell of the proximal intestine, while GLP-1 is released from the enteroendocrine L cell of the distal intestine. GLP-1 is responsible for the majority of the incretin effect on pancreatic β-cell function. The secretion of GLP-1 is lower in patients with T2DM than normal, suggesting that this hormone contributes to the pathogenesis of the disease.[16]

The circulating GLP-1 has two isotypes: GLP-1 (7-36) and GLP-1 (7-37), in which GLP-1 (7-36) is responsible for 80% of active GLP-1.[17] GLP-1 has insulinotropic, insulinomimetic and glucagonostatic effects.[18] GLP-1 binds to GLP-1 receptors (GLP-1Rs) leading to regulatory actions which are an enhancement of β-cell function and proliferation, enhancement of glucose-dependent insulin secretion from β-cell, activation of insulin biosynthesis, suppression of elevated glucagon secretion, suppression of food intake and slowing of gastric emptying.[11,19] However, the therapeutic drawback is that the circulating GLP-1 level decreases rapidly, i.e. less than two minutes, after secretion due to being degraded by dipeptidyl peptidase (DPP)-4 enzymes and renal clearance.[20–23] DPP-4 enzyme degrades GLP-1 (7-36) by removing an N-terminal

[1]Cardiac Electrophysiology Research and Training Centre, Faculty of Medicine, Chiang Mai University, Thailand
[2]Cardiac Electrophysiology Unit, Department of Physiology, Faculty of Medicine, Chiang Mai University, Thailand
[3]Faculty of Dentistry, Chiang Mai University, Thailand

Corresponding author:
Nipon Chattipakorn, Cardiac Electrophysiology Research and Training Centre, Faculty of Medicine, Chiang Mai University, Chiang Mai, 50200, Thailand.
Email: nchattip@gmail.com

dipeptide, resulting in its metabolite, GLP-1 (9-36), which has 1000-fold lower affinity to GLP-1Rs.[21] It has been shown that the inhibition of DPP-4 could enhance the level of intact GLP-1 and prolong its action time.[24] Thus, two classes of drugs have been recently used for incretin enhancement in T2DM, including GLP-1 analogues and DPP-4 inhibitors. While GLP-1 analogues (i.e. exenatide, liraglutide and albiglutide) increase the GLP-1 level to a supraphysiological level, DPP-4 inhibitors (i.e. vildagliptin, sitagliptin and saxagliptin) conserve and prolong intact GLP-1 availability within a physiological level.

Although the primary physiological function of GLP-1 is related to the control of plasma glucose, GLP-1Rs have been ubiquitously found in a variety of extra-pancreatic tissues including the central and peripheral nervous system, kidney, lung, gastrointestinal tract, blood vessel and heart both in rodents and humans.[13,25] Since GLP-1Rs in the heart are similar to in the pancreas,[25] it has been suggested that drugs targeting incretin enhancement may potentially affect the heart.

DM has been shown to increase cardiovascular risk including increased incidence of myocardial infarction.[2] With the undesirable effects of several anti-diabetic drugs such as those in the thiazolidinedione group, i.e. rosiglitazone, that increased the cardiovascular morbidity and mortality,[8,9] it is essential that any new anti-diabetic drug be investigated for both beneficial and harmful effects on the cardiovascular system. In this review, reports from basic and clinical studies regarding the effects of GLP-1 and DPP-4 inhibitor on cardiac function and infarct size in an ischaemic-reperfused heart are comprehensively summarised. Key results are critically discussed with emphasis placed on consistent findings. Inconsistent results are also highlighted to more fully explore what is known and what remains to be discovered.

Effects of GLP-1 on the infarct size

GLP-1 has been shown to have an infarct limiting effect in both in vitro and in vivo models of ischaemia-reperfusion (I/R) injury (Table 1). GLP-1 co-administered with DPP-4 inhibitor, valine pyrrolide (VP), could reduce the infarct size ranging from 39% to 58% in isolated Langendorff rat hearts whether given prior to ischaemia or during the reperfusion period.[26–29] However, the administration of GLP-1[28] or DPP-4 inhibitor[26–28] alone failed to reduce the infarct size. These studies suggested the synergistic effect of DPP-4 inhibition and exogenous GLP-1 on the infarct limiting effect in which DDP-4 inhibitor enhanced endogenous GLP-1 level and reduced exogenous GLP-1 degradation.

Another line of drug that has been used to enhance an incretin effect is a DPP-4 resistant GLP-1R agonist. Exendin-4, a hormone found in the saliva of the Gila monster, at 0.03 and 0.3 nM has been shown to reduce the infarct size, while 3.0 nM exendin-4 could not show this benefit, suggesting a biphasic infarct limiting effect.[30] Human transferrin (Tf) was also demonstrated to prolong the GLP-1 action. Administration of GLP-1-Tf could effectively reduce the infarct size in rabbits, given either before or after coronary occlusion.[31] Recently, albiglutide, another GLP-1 analogue, has been shown to increase cAMP in an ischaemic myocardium and improve cardiac metabolic efficiency by increasing glucose metabolism and reducing fat oxidation, which results in 26% reduction of infarct size.[32]

In a pig model, exenatide has been shown to reduce the infarct size,[33] whereas the other two studies with a shorter period of I/R using recombinant GLP-1 (rGLP-1)[34] or liraglutide[35] could not demonstrate any improvement in infarct size (Table 2). This discrepancy could be due to a different duration and site of occlusion, therapeutic drugs and drug concentrations. This hypothesis is supported by a report by Noyan-Ashraf and colleagues, demonstrating that the optimal time and dose of liraglutide, GLP-1 analogue, played an important role in infarct size reduction, improved survival rate and contractile function in both normoglycaemic and diabetic mice.[36]

Several mechanisms underlying the infarct limiting effect of GLP-1 have been proposed to be independent of weight loss.[36] First, GLP-1 has been shown to activate the cAMP-PKA pathway,[26,32,36] the pro-survival kinase associated with reperfusion injury signalling kinase (RISK) pathway,[37] including the following: PI3K, Akt, MAPK, PPARβ/δ, Nrf-2, HO-1 and Akt-p70s6K-BAD pathways.[18,26,27,33,36,38] Second, GLP-1 has been shown to reduce oxidative stress and increase antioxidants, leading to decreased apoptosis.[26,31,33,36] Third, since proinflammatory cells such as neutrophils (PMNs) play an important role during the time of blood return to the heart,[39,40] GLP-1 has been shown to attenuate the PMN activation and accumulation in the myocardium, thus reducing injuries caused by reperfusion.[41] Recent studies demonstrated that the infarct limiting effects were diminished with the administration of either GLP-1 metabolite, i.e. GLP-1 (9-36),[29,30] or when giving GLP-1 with the GLP-1R antagonist, namely GLP-1 (9-39).[26,29,30,36] Moreover, the administration of liraglutide failed to activate cardioprotective kinase in the GLP-1R depleted mice. Taken together, the effect of GLP-1 on the infarct size reduction is proposed to be a GLP-1R dependent mechanism.

Effects of GLP-1 on left ventricular function

Besides its infarct limiting effect, GLP-1 has been shown to improve left ventricular (LV) recovery from ischaemic myocardial stunning after reperfusion (Table 3). The administration of GLP-1 as a post-conditioning agent, which demonstrated a higher plasma GLP-1 level, could improve LV performance by decreasing the wall motion abnormality, and increasing the ejection fraction and LV

Table 1. Summary of the beneficial effects of GLP-1 on the infarct size.

Animal species	Study model	Drug/dose/route	Major findings	Interpretation	References
Rabbit	I/R LCX ligation 30-min ischaemia 180-min reperfusion	GLP-1-Tf 10 mg/kg Pretreatment 12 h, SC At reperfusion, IV	1. GLP-1-Tf decreased infarct size in both pretreatment and post-ischaemia by 23% and 25%, respectively. 2. GLP-1-Tf decreased apoptotic index.	GLP-1-Tf decreased infarct size by reducing myocardial apoptosis whether given pretreatment or post-ischaemia.	Matsubara et al.[31]
Normal mice High fat diet with streptozotocin-induced diabetic mice	MI LAD ligation 28-day ischaemia	Liraglutide Pretreatment 75 or 200 μg/kg, IP, twice daily for 7 days 75 μg/kg, IP, twice daily for 7 days	1. Liraglutide at dose 75 and 200 μg/kg increased survival rate in both normal and diabetic mice. 2. Liraglutide at dose 200 μg/kg reduced infarct size by 27% and reduced HW/BW ratio. 3. Liraglutide activated cardioprotective signalling pathway, e.g. pAkt, pGSK3β, PPARβ/δ, nNrf-2, and HO-1 before MI through GLP-1R. 4. Liraglutide increased pAkt, pGSK3β, and decreased caspase 3, ANP and MMP-9 after MI. 5. Liraglutide increased cAMP level and decreased caspase 3 in cardiomyocytes. 6. Concomitant administration of GLP-1R antagonist abolished effects of liraglutide on cardiomyocytes.	Liraglutide decreased infarct size. The mechanism could be due to activation of cardioprotective signalling pathway. e.g. pAkt, pGSK3β, and reduce caspase-3 activation through GLP-1R dependent pathway.	Noyan-Ashraf et al.[36]
Pig	I/R LCX ligation 75-min ischaemia 3-day reperfusion	Exenatide 10 μg, SC and IV 5 min before reperfusion 10 μg, SC, twice daily during reperfusion	1. Exenatide reduced infarct size by 39%. 2. Exenatide increased Akt and Bcl-2 phosphorylation. 3. Exenatide decreased caspase 3. 4. Exenatide decreased nuclear oxidative stress. 5. Exenatide increased antioxidant enzyme.	Exenatide decreased infarct size by activating pro-survival kinase, Akt and Bcl-2 phosphorylation as well as decreasing pro-apoptotic caspase 3. Exenatide also increased anti-oxidant, resulting in decreased nuclear oxidative stress.	Timmers et al.[33]
Rat	I/R LAD ligation 30-min ischaemia 120-min reperfusion	Pretreated with VP 20 mg/kg, SC, 30 min before experiment + infusion with GLP-1 4.8 pmol/kg per min throughout experiment	VP + GLP-1 reduced infarct size by 58%.	DPP-4 inhibitor combined with GLP-1 could reduce infarct size.	Bose et al.[26]
Rat	I/R LAD ligation 30-min ischaemia 120-min reperfusion	rGLP-1 30 pM/kg per min, infusion beginning at 28 min after occlusion until the end of reperfusion	1. rGLP-1 reduced infarct size by 79%. 2. rGLP-1 attenuated PMN activation. 3. rGLP-1 decreased PMN accumulation in ischaemic myocardium. 4. In vitro, rGLP-1 attenuated PMN activation; this effect was abolished by GLP-1R antagonist.	GLP-1 mitigated I/R injury by reduced infarct size and inhibited PMN-mediated reperfusion injury through GLP-1R dependent pathway.	Dokken et al.[41]
Rat	I/R LAD ligation 30-min ischaemia 24-h reperfusion	Albiglutide 1, 3, 10 mg/kg per day, SC, once daily, for 3 days	1. Albiglutide at doses 3 and 10 mg/kg reduced infarct size by 26%. 2. Albiglutide increased cAMP level in ischaemic myocardium. 3. Albiglutide increased myocardial glucose uptake. 4. Albiglutide increased carbohydrate oxidation and reduced fat oxidation.	Infarct limiting effect of albiglutide was associated with improvement of cardiac metabolic efficiency.	Bao et al.[32]

(Continued)

Table 1. (continued)

Animal species	Study model	Drug/dose/route	Major findings	Interpretation	References
Isolated rat heart	I/R Left main coronary artery ligation (regional ischaemia) 35-min ischaemia 120-min reperfusion	VP 20 mg/L + GLP-1 0.3 nM in perfusion buffer, throughout experiment	1. VP + GLP-1 reduced infarct size by 55%. 2. Using GLP-1 inhibitor, cAMP inhibitor, PI3K inhibitor and MAPK inhibitor abolished infarct limiting effect. 3. VP + GLP-1 treated group increased phosphorylated BAD.	Infarct limiting effect of GLP-1 could be due to activation of pro-survival kinase including cAMP, PI3K, MAPK and promote BAD phosphorylation.	Bose et al.[26]
Isolated rat heart	I/R Left main coronary artery ligation (regional ischaemia) 35-min ischaemia 120-min reperfusion	VP 20 mg/L + GLP-1 0.3 nM in perfusion buffer, throughout experiment	1. GLP-1 + VP reduced infarct size by 50%. 2. Rapamycin, p70s6K inhibitor, abolished infarct limiting effect. 3. GLP-1 + VP did not increase phosphorylated p70s6K.	GLP-1 with DPP-4 inhibitor could reduce infarct size by activation of Akt-p70s6K-BAD pathway.	Bose et al.[28]
Isolated rat heart	I/R Left main coronary artery ligation (regional ischaemia) 35-min ischaemia 120-min reperfusion	Pretreatment VP 20 mg/L + GLP-1 0.3 nM, 15 min before I/R VP 20 mg/L + GLP-1 0.3 nM, during 15 min of reperfusion	Given VP + GLP-1 before ischaemia or at reperfusion reduced infarct size by 49% and 48%, respectively.	GLP-1 with DPP-4 inhibitor could use as preconditioning or post-conditioning agent to reduce infarct size.	Bose et al.[27]
Isolated rat heart	I/R 35-min global no flow ischaemia 120-min reperfusion	VP 40 μM + GLP-1 0.3 nM, during 15 min of reperfusion	1. VP + GLP-1 reduced infarct size by 39%. 2. GLP-1 with GLP-1R antagonist could not reduce infarct size.	Infarct limiting effect of GLP-1 was mediated by GLP-1R.	Ossum et al.[29]
Isolated rat heart	I/R 45-min global no flow ischaemia 120-min reperfusion	Exendin-4 0.03, 0.3, 3.0 nM, during 15 min at reperfusion	1. Exendin-4 at 0.03 and 0.3 nM reduced infarct size by 53% and 56%, respectively. 2. Exendin-4 with GLP-1R antagonist cannot reduce infarct size.	Infarct limiting effect of exendin-4 was mediated by GLP-1R.	Sonne et al.[30]

I/R: ischaemic-reperfusion, LCX: left circumflex coronary artery; GLP-1-Tf: glucagon-like peptide-1-transferrin, SC: subcutaneous route, IV: intravenous route, MI: myocardial infarction, LAD: left anterior descending coronary artery, IP: intraperitoneal route, HW/BW: heart weight/body weight; GLP-1R: GLP-1 receptor; pAkt: phosphorylated Akt; pGSK: phosphorylated glycogen synthase kinase; PPAR: peroxisome proliferated-activated receptors; HO-1: heme-oxygenase-1; ANP: atrial natriuretic peptide; MMP: matrix metallopeptidase; VP: valine pyrrolide; rGLP-1: recombinant GLP-1; PMN: polymorphonuclear neutrophils; DPP-4: dipeptidyl peptidase-4; PI3K: phosphoinositide 3-kinase; MAPK: mitogen-activated peptide kinase; BAD: Bcl-2 associated death promoter.

Table 2. Summary of the neutral effects of GLP-1 on the infarct size.

Animal species	Study model	Drug/dose/route	Major findings	Interpretation	References
Pig	I/R LAD ligation 60-min ischaemia 120-min reperfusion	rGLP-1, 3 pmol/kg per min, 120 min before experiment + rGLP-1, 3 pmol/kg per min, IV perfusion during I/R rGLP-1, 3 pmol/kg per min, IV perfusion during I/R	1. rGLP-1 did not reduce infarct size. 2. rGLP-1 increased plasma insulin level. 3. rGLP-1 lowered blood glucose level. 4. rGLP-1 decreased interstitial levels of pyruvate and lactate.	rGLP-1 did not reduce infarct size, but altered myocardial glucose utilisation, which was associated with insulin level.	Kavianipour et al.[34]
Pig	I/R Balloon LAD occlusion 40-min ischaemia 150-min reperfusion	Liraglutide Pretreatment 10 μg/kg, SC, once daily for 3 days	1. Liraglutide did not reduce infarct size. 2. VF incidence and time to VF was not different between liraglutide and vehicle.	Liraglutide did not reduce infarct size.	Kristensen et al.[35]
Isolated rat heart	I/R Left main coronary artery ligation (regional ischaemia) 35-min ischaemia 120-min reperfusion	GLP-1 0.3 nM in perfusion buffer, throughout experiment	GLP-1 alone did not reduce infarct size.	GLP-1 alone could not reduce infarct size. DPP-4 inhibitor was important for exogenous GLP-1 function to reduce infarct size.	Bose et al.[28]
Isolated rat heart	I/R 35-min global no flow ischaemia 120-min reperfusion	VP 40 μM + GLP-1 (9-36) 0.3 nM, during 15 min of reperfusion	GLP-1 (9-36) + VP did not reduce infarct size.	GLP-1 metabolite with DPP-4 inhibitor did not reduce infarct size.	Ossum et al.[29]
Isolated rat heart	I/R 45-min global no flow ischaemia 120-min reperfusion	GLP-1 (9-36) 0.03, 0.3, 3.0 nM, during 15 min of reperfusion	GLP-1 (9-36) did not reduce infarct size.	GLP-1 metabolite did not reduce infarct size.	Sonne et al.[30]

I/R: ischaemia-reperfusion; LAD: left anterior descending coronary artery; rGLP-1: recombinant GLP-1; IV: intravenous route; SC: subcutaneous route; VP: valine pyrrolide; VF: ventricular fibrillation; DPP-4: dipeptidyl peptidase-4.

developed pressure,[29,31] compared with giving GLP-1 as a pre-conditioning agent, which has a lower plasma GLP-1 level.[31] Nevertheless, it is possible that the time for which GLP-1 was given as a preconditioning treatment in those studies was too short, thus allowing insufficient time for its action. This is supported by a report by Noyan-Ashraf and colleagues which demonstrated that the GLP-1 analogue required the optimal pre-treatment time and dose for the activation of the cardiac gene and protein to promote LV enhancement.[36] Other possible factors including routes and times of drug administration during I/R could also play an important role in this finding. Interestingly, like the infarct limiting effect, exendin-4 also improved the mechanical function in a biphasic manner.[30] In a clinically relevant swine model, exenatide improved regional and global systolic function.[33] In coronary artery disease patients with good LV function, a continuous infusion of rGLP-1 for 30 minutes before dobutamine stress echocardiography demonstrated an improved ejection fraction and LV regional wall function as well as mitigated post-ischaemic stunning, predominantly in the ischaemic wall segment.[42] The beneficial effect of a 72-hour GLP-1 infusion on the post-infarction recovery, including an increased ejection fraction and improvement of both global and regional wall motion was also observed in acute myocardial infarction patients with LV ejection fraction of less than 40% after successful primary percutaneous coronary intervention.[43] Long-term GLP-1 infusion also improved myocardial stunning, which was characterised by enhanced LV wall motion and relaxation in I/R dogs.[44]

Surprisingly, the benefit of exenatide and GLP-1 on LV function was also observed in the presence of GLP-1R antagonist and in GLP-1R deleted mice, suggesting that the improved LV function of GLP-1 may be mediated independent of GLP-1R.[30,38] However, a recent study demonstrated that GLP-1 co-administered with sitagliptin, DPP-4 inhibitor, could not improve contractile functional recovery in GLP-1R deleted mice, whereas this treatment provided the benefit in wild-type mice.[38] Taken together, unlike the infarct limiting effect, the LV function amelioration of

Table 3. Summary of the effects of GLP-1 on left ventricular function.

Animal species	Study model	Drug/dose/route	Major findings	Interpretation	References
Rabbit	I/R LCX ligation 30-min ischaemia 180-min reperfusion	GLP-1-Tf 10 mg/kg Pretreatment 12 h, SC At reperfusion, IV	1. GLP-1 level in post-ischaemic treatment significantly higher than pre-ischaemic treatment. 2. Given GLP-1-Tf at reperfusion decreased wall motion abnormality. 3. Given GLP-1-Tf at reperfusion improved ejection fraction. 4. Pretreatment with GLP-1-Tf failed to improve ejection fraction and wall motion abnormality.	GLP-1-Tf at higher concentration, post-ischaemic treatment, improved LV function by limiting myocardial stunning.	Matsubara et al.[31]
Dog	I/R Balloon LCX occlusion 10-min ischaemia 1-day reperfusion	GLP-1 1.5 pmol/kg per min, IV perfusion, during reperfusion	1. GLP-1 caused an earlier and completely recovered regional wall motion. 2. GLP-1 restored diastolic relaxation to normal. 3. GLP-1 did not improve fractional shortening. 4. GLP-1 did not improve LV contractility.	GLP-1 enhanced functional recovery from ischaemic myocardial stunning independently of changing systemic haemodynamic or global systolic function.	Nikolaidis et al.[44]
Pig	I/R LCX ligation 75-min ischaemia 3-day reperfusion	Exenatide 10 µg, SC and IV, 5 min before reperfusion + 10 µg, SC, twice daily during reperfusion	1. Exenatide increased systolic wall thickening. 2. Exenatide increased fractional area shortening. 3. Exenatide increased ejection fraction. 4. Exenatide reduced myocardial stiffness.	Exenatide improved systolic function	Timmers et al.[33]
Rat	I/R LAD ligation 30-min ischaemia 24-h reperfusion	Albiglutide 1, 3, 10 mg/kg per day, SC, once daily, for 3 days	1. Albiglutide increased dP/dt_{max}. 2. Albiglutide increased myocardial glucose uptake. 3. Albiglutide increased carbohydrate oxidation and reduced fat oxidation. 4. Albiglutide increased ejection fraction and end systolic volume.	Albiglutide increased cardiac function by improving cardiac metabolic efficiency.	Bao et al.[32]
Isolated mice heart	I/R 30-min global ischaemia 40-min reperfusion	Liraglutide 0.3, 3, 30 nM, in perfusion buffer, 20 min before ischaemia 30 nM, in perfusion buffer, at reperfusion for 20 min Pretreatment with liraglutide 200 µg/kg, IP, b.i.d., 1- or 7-day	1. Acute treatment with liraglutide before or after ischaemia failed to improve LVDP. 2. Pretreatment with liraglutide for 1- or 7-day improved LVDP.	LV improvement of liraglutide required optimal dose and pretreatment time.	Noyan-Ashraf et al.[36]
Isolated rat heart	I/R 35-min global no flow ischaemia 120-min reperfusion	VP 40 µM + GLP-1 0.3 nM, during 15 min of reperfusion	GLP-1 slightly increased LVDP, rate pressure product and maximal rate of LV systolic pressure development.	GLP- 1 + VP tended to improve LV function.	Ossum et al.[29]
Isolated rat heart	I/R 35 min global no flow ischaemia 120-min reperfusion	VP 40 µM + GLP-1 (9-36) 0.3 nM, during 15 min of reperfusion	GLP-1 (9-36) decreased LVDP, rate pressure product and maximal rate of LV systolic pressure development.	GLP-1 metabolite acted as a strong negative inotrope in post-ischaemic hearts.	Ossum et al.[29]

Table 3. (continued)

Animal species	Study model	Drug/dose/route	Major findings	Interpretation	References
Isolated rat heart	I/R 45-min global no flow ischaemia 120-min reperfusion	Exendin-4 0.03, 0.3, 3.0 nM, for 15 min at reperfusion GLP-1 (9-36) 0.03, 0.3, 3.0 nM, for 15 min at reperfusion	1. Exendin-4 at 0.03 and 0.3 nM improved LVDP and rate pressure product during the last 60 min of reperfusion. 2. GLP-1 (9-36) at 0.03 and 0.3 nM improved LVDP and rate pressure product during the last 60 min of reperfusion. 3. GLP-1 (9-39) partly affected on beneficial effect of LV performance of exendin-4 and GLP-1 (9-36).	GLP-1 and GLP-1 (9-36) increased ventricular performance. Action of GLP-1 and GLP-1 (9-36) was mediated independently with GLP-1R.	Sonne et al.[30]
Isolated rat heart	I/R 30-min global low flow ischaemia 30-min reperfusion	GLP-1 500 pmol/L in perfusion buffer, pretreatment 1 min before ischaemia and throughout reperfusion	1. GLP-1 enhanced LV end diastolic pressure. 2. GLP-1 increased LVDP. 3. GLP-1 increased myocardial glucose uptake. 4. GLP-1 increased GLUT-1 and GLUT-4 translocation.	GLP-1 improved post-ischaemic contractile dysfunction by enhancing myocardial glucose uptake.	Zhao et al.[18]
Isolated rat heart and isolated mitochondria	I/R 20-min global low flow ischaemia 30-min reperfusion	Exendin-4 1 nM/kg, SC, 6 day, once daily, after birth	**Juvenile age (4–6 weeks)** 1. HW, HW/BW, and HW/tibia length were similar between groups. 2. Exendin enhanced per cent recovery of LVDP. 3. Rates of state 3 and 4 respiration were comparable in control and exendin treated group. 4. Exendin did not reduce oxidative stress. 5. Exendin did not increase antioxidant, MnSOD. **Adult age (9 months)** 1. HW, HW/BW, and HW/tibia length were similar between groups. 2. Exendin improved recovery of LVDP. 3. Rates of state 3 respiration were lower in exendin-treated animal, while state 4 respiration was comparable. 4. Mitochondria from exendin-treated group took up less calcium.	Short course treatment with exendin-4 improved LV function in adult after I/R insult by alteration of mitochondrial phenotype which reduced rates of oxidative phosphorylation and mitochondrial calcium uptake.	Brown et al.[47]
Isolated mice heart of wild type and GLP-1R$^{-/-}$	I/R 30-min global no flow ischaemia 40-min reperfusion	GLP-1 Exendin-4 0.3, 3, 5 nM in perfusion buffer Pretreatment for 20 min before ischaemia Post-treatment for 20 min at reperfusion GLP-1 (9-36) 0.3, 3, 6 nM in perfusion buffer Pretreatment for 20 min before ischaemia Post-treatment for 20 min at reperfusion	1. Pretreatment with GLP-1 (0.3nM) and Exendin-4 (5 nM) increased LVDP in wild-type mice. 2. Pretreatment with GLP-1 (0.3 nM) increased LVDP in GLP-1R$^{-/-}$ mice. 3. Pretreatment with exendin-4 failed to increase LVDP in GLP-1R$^{-/-}$ mice. 4. Pretreatment with GLP-1 (9-36) worsened LV function in wild type mice. 5. Post treatment with GLP-1 (9-36) improved LVDP in both wild-type and GLP-1R$^{-/-}$ mice. 6. With sitagliptin, effect of GLP-1 on LVDP was diminished in GLP-1R$^{-/-}$ but improved in wild-type mice.	Effects of GLP-1 on LV performance were mediated via both GLP-1R dependent and independent pathways.	Ban et al.[38]

(Continued)

Table 3. (continued)

Animal species	Study model	Drug/dose/route	Major findings	Interpretation	References
Acute MI patients with EF<40%	After successful primary angioplasty	rGLP-1 1.5 pmol/kg per min 72 h after angioplasty	1. rGLP-1 improved LV ejection fraction. 2. rGLP-1 decreased global and regional wall motion score index.	Infusion of GLP-1 improved regional and global LV function in patient after successful primary angioplasty.	Nikolaidis et al.[43]
Patients	Coronary artery disease with normal resting LV function	GLP-1 1.2 pmol/kg per min, intravenous infusion starting at 30 min before dobutamine stress echocardiography	1. GLP-1 level was increased after GLP-1 administration. 2. GLP-1 lowered plasma glucose level. 3. Insulin level was increased in GLP-1 treated group during dobutamine stress. 4. Free fatty acid level was lowered in GLP-1 treated group. 5. GLP-1 improved ejection fraction and regional wall function during peak dobutamine stress and 30 min of recovery. 6. GLP-1 had a greater beneficial effect on ischaemic than on non-ischaemic segments.	GLP-1 improved both global and regional LV performance in response to stress and also reduced post-ischaemic stunning.	Read et al.[42]

I/R: ischaemia-reperfusion; LCX: left circumflex coronary artery; GLP-1-Tf: glucagon-like peptide-1-transferrin; SC: subcutaneous route; IV: intravenous route; LV: left ventricle; LAD: left anterior descending coronary artery; IP: intraperitoneal route; LVDP: left ventricular developed pressure; VP: valine pyrrolide; GLP-1R: GLP-1 receptor; GLUT: glucose transporter; MnSOD: manganese superoxide dismutase; HW: heart weight; BW: body weight; EF: ejection fraction; rGLP-1: recombinant GLP-1.

GLP-1 was mediated by both GLP-1R dependent and independent pathways. Although the administration of GLP-1 (9-36) could not reduce the infarct size,[29,30] it exerts a functional recovery benefit which might mediate through the GLP-1 (9-36)-cGMP-NO pathway, independent of GLP-1R activation.[30,38] However, the inotropic effect of GLP-1 (9-36) is still questionable.[29]

Enhanced myocardial glucose uptake by up-regulation of glucose transporter (GLUT)-1 and GLUT-4 may be one of the underlying mechanisms to explain the beneficial effect of GLP-1 on LV functional improvement.[18,32] In a normal physiological condition, the heart mainly uses fatty acid as a fuel in maintaining its function. Reduced availability of oxygen during low-flow ischaemia reduces the heart's ability to produce energy from fatty acid oxidation and carbohydrates. The enhancement of glycolysis through diverse mechanisms or pharmacologic interventions can delay and prevent ischaemic damage and improve the recovery of the contractile function.[45,46] GLP-1 has been shown to increase myocardial glucose uptake, which ameliorates the post-ischaemia myocardial dysfunction.[18,32] This action of GLP-1 might be used as a therapeutic target for high risk cardiovascular disease patients, especially in insulin resistant T2DM. The long-term effect of GLP-1 analogue has been demonstrated in neonatal rats receiving exenatide once daily for six days.[47] This persistent beneficial effect is mediated by an altered mitochondrial phenotype which decreased the cardiac mitochondria calcium uptake and reduced oxidative phosphorylation, resulting in improved functional recovery after ischaemia reperfusion injury. Surprisingly, the cardioprotective effect of GLP-1 and GLP-1 analogue was not associated with any improvement in haemodynamic parameters (Table 4).[26,31–35,44,47]

Unlike GLP-1, information regarding the effects of DPP-4 inhibitor on the I/R heart is scarce and controversial.[48–50] DPP-4 inhibitors inhibit the enzyme activity of DPP-4, resulting in decreasing degradation rate, thereby maintaining higher GLP-1 levels.[24,51,52] Although growing evidence demonstrated the infarct limiting effect of DPP-4 inhibitors (Table 5), many studies suggested that the physiological level of GLP-1 may not be sufficient to reduce the infarct size (Table 6). Besides the infarct limiting effect, the beneficial effect of DPP-4 inhibitors on LV function after I/R injury has also been documented (Table 7).

Effects of DPP-4 inhibitor on the infarct size

As DM increases cardiovascular risk including myocardial infarction, pretreatment with vildagliptin, DPP-4 inhibitor, has been shown to attenuate the infarct size in insulin resistant rats.[53] This cardioprotective effect was also observed in normoglycaemic rats with pretreatment of sitagliptin.[48] A longer period of pre-treatment with sitagliptin resulted in smaller infarct size, suggesting that the plasma drug level

Table 4. Summary of the effects of GLP-1 on haemodynamic parameters.

Animal species	Study model	Drug/dose/route	Major findings	Interpretation	References
Rabbit	I/R LCX ligation 30-min ischaemia 180-min reperfusion	GLP-1-Tf 10 mg/kg Pretreatment 12 h, SC At reperfusion, IV	Treatment with GLP-1-Tf did not affect heart rate and mean arterial blood pressure between groups.	GLP-1-Tf did not alter haemodynamic parameters.	Matsubara et al.[31]
Pig	I/R LAD ligation 60-min ischaemia 120-min reperfusion	rGLP-1, 3 pmol/kg per min, 120 min before experiment + rGLP-1, 3 pmol/kg per min, IV perfusion during I/R rGLP-1, 3 pmol/kg per min, IV perfusion during I/R	rGLP-1 did not affect heart rate, cardiac output, mean arterial blood pressure, pulmonary artery wedge pressure and central venous pressure.	rGLP-1 did not alter haemodynamic parameters.	Kavianipour et al.[34]
Pig	I/R Balloon LAD occlusion 40-min ischaemia 150-min reperfusion	Liraglutide Pretreatment 10 μg/kg, SC, once daily for 3 days	Liraglutide increased heart rate but had no effect on blood pressure and cardiac output.	Liraglutide slightly increased heart rate but had no effect on other haemodynamic parameters.	Kristensen et al.[35]
Pig	I/R LCX ligation 75-min ischaemia 3-day reperfusion	Exenatide 10 μg, SC and IV 5 min before reperfusion 10 μg, SC, twice daily during reperfusion	Exenatide did not affect heart rate, mean arterial blood pressure and cardiac output.	Exenatide did not alter haemodynamic parameters.	Timmers et al.[33]
Rat	I/R LAD ligation 30-min ischaemia 120-min reperfusion	Pretreated with VP 20 mg/kg, SC, 30 min before experiment + infusion with GLP-1 4.8 pmol/kg per min throughout experiment	VP + GLP-1 did not affect heart rate and mean arterial blood pressure.	GLP-1 with DPP-4 did not alter haemodynamic parameters.	Bose et al.[26]
Dog	I/R Balloon LCX occlusion 10-min ischaemia 1-day reperfusion	GLP-1 1.5 pmol/kg per min, IV perfusion, during reperfusion	GLP-1 did not affect heart rate, coronary blood flow, mean arterial blood pressure and LV end diastolic pressure.	Long term GLP-1 infusion did not alter haemodynamic parameters.	Nikolaidis et al.[44]
Isolated mice heart of wild type and GLP-1R$^{-/-}$	I/R 30-min global no flow ischaemia 40-min reperfusion	GLP-1 Exendin-4 0.3, 3, 5 nM in perfusion buffer Pretreatment for 20 min before ischaemia Post-treatment for 20 min at reperfusion GLP-1 (9-36) 0.3, 3, 6 nM in perfusion buffer Pretreatment for 20 min before ischaemia Post-treatment for 20 min at reperfusion	1. Pretreatment with GLP-1 improved pre- and post-ischaemic coronary flow. 2. Pretreatment with GLP-1 (9-36) improved pre-ischaemic coronary flow. 3. Post treatment with GLP-1 (9-36) improved post-ischaemic coronary flow. 4. GLP-1 and GLP-1 (9-36) increased cGMP level in wild-type and GLP-1R$^{-/-}$ mice. 5. Exendin-4 did not produce cGMP release. 6. Functional recovery after I/R was reduced in GLP-1 treated with L-NAME, NOS inhibitor.	Vascular effects of GLP-1 were mediated via GLP-1 (9-36) and GLP-1R independent pathway, through NOS-dependent cGMP formation.	Ban et al.[38]
Patients	Coronary artery disease with normal resting LV function	GLP-1 1.2 pmol/kg per min, IV infusion starting at 30 min before dobutamine stress echocardiography	GLP-1 did not affect heart rate, systolic and diastolic blood pressure, and rate-pressure product.	GLP-1 did not alter haemodynamic parameters.	Read et al.[42]

I/R: ischaemia-reperfusion; LCX: left circumflex coronary artery; GLP-1-Tf: glucagon-like peptide-1-transferrin; SC: subcutaneous route; LAD: left anterior descending coronary artery; IV: intravenous route; rGLP-1: recombinant GLP-1; VP: valine pyrrolide; DPP-4: dipeptidyl peptidase-4; LV: left ventricle; GLP-1R: GLP-1 receptor; L-NAME: NG-monomethyl-L-arginine; NOS: nitric oxide synthase.

Table 5. Summary of the beneficial effects of DPP-4 inhibitor on infarct size.

Animal species	Study model	Drug/dose/ route	Major findings	Interpretation	References
Diet-induced obesity, insulin resistant rat	I/R LAD ligation 35-min ischaemia 30-min reperfusion	Vildagliptin Pretreatment 10 mg/kg per day, PO, for 4 weeks	1. Vildagliptin reduced infarct size in diet induced obesity rat by 38%. 2. Vildagliptin increased plasma GLP-1 level to normal in diet-induced obesity rat. 3. Vildagliptin increased beta cell/alpha cell ratio to normal in diet-induced obesity rat. 4. Vildagliptin increased phosphorylation of Akt and ERK at serine 42.	Vildagliptin reduced infarct size in insulin resistance rat by increased phosphorylation of Akt and ERK at serine 42.	Huisamen et al.[53]
Rat	I/R LAD ligation 30-min ischaemia 4-hour reperfusion	Sitagliptin Pretreatment 300 mg/kg per day, PO, for 3 or 14 days	1. Pretreatment with sitagliptin for 3 and 14 days reduced infarct size by 47% and 64%, respectively. 2. Using PKA inhibitor completely abolished infarct limiting effect of sitagliptin. 3. Sitagliptin increased cAMP level.	Protective effect of sitagliptin was via cAMP-dependent PKA activation.	Ye et al.[48]

I/R: ischaemia-reperfusion; LAD: left anterior descending coronary artery; PO: per oral; GLP-1: glucagon-like peptide-1; ERK: extracellular regulated kinase; PKA: protein kinase A.

might influence its cardioprotective effect. The infarct limiting mechanism of DPP-4 inhibitor in these studies was proposed to be due to the activation of Akt and cAMP-PKA pro-survival kinase in RISK pathway as observed in GLP-1 administration.[48,53] However, some studies demonstrated that prolonged availability of intact GLP-1 caused by a DPP-4 inhibitor failed to demonstrate the infarct limiting effect.[26–28,54] Moreover, inhibition or reduction of DPP-4 activity using DPP-4 deleted mice or pretreatment with sitagliptin before ischaemia in high fat diet-induced diabetic mice could not reduce the infarct size, but improved the survival rate by activation of cardioprotection kinase such as GSK3β, ANP and Akt.[49] These discrepant results suggest that the different animal models, the duration of ischaemia in the heart models and the minimal dose for a specific time may play a pivotal role in the reduction of the infarct size. Tables 5 and 6 summarise significant effects of DPP-4 inhibitors on the infarct size.

Effects of DPP-4 inhibitor on left ventricular function

DPP-4 inhibitors also exert a cardioprotective effect by the improvement of post-ischaemia myocardial stunning. Table 7 summarises the effects of DPP-4 inhibitors on LV function. In DPP-4 deleted mice and mice pretreated with sitagliptin for 12 hours prior to aortic occlusion, improved LV developed pressure after I/R injury was observed.[49] However, acute treatment with sitagliptin for 20 minutes prior to I/R insult failed to improve ventricular performance.[49] The discrepancy in these findings could be due to the differences in the time of drug administration as well as study models (in vivo versus ex vivo), and might suggest that the benefit of DPP-4 inhibitor required an optimal time and an intact cardiovascular system process. However, a recent report in rats with ischaemic heart failure demonstrated that early or late treatment with vildagliptin had no beneficial effect on ventricular performance.[54] In a clinical study, single dose treatment with sitagliptin improved regional and global wall function, which improved post-ischaemic stunning in patients with coronary artery disease awaiting revascularisation.[50] These improvements are independent of insulin[50] or haemodynamic parameter alterations.[49,50,53] Table 8 summarises the effect of DPP-4 inhibitors on haemodynamic parameters.

Conclusion

Growing evidence suggests that incretin exerts a cardioprotective effect during I/R injury. The infarct limiting effect is mediated through GLP-1R, while LV function improvement is mediated through both GLP-1R dependent and independent (via GLP-1 (9-39)) pathways. The underlying mechanisms were due to the activation of pro-survival kinase, increased antioxidant and myocardium glucose utilisation, reduction of oxidative stress and pro-apoptotic kinase, and attenuation proinflammatory cell activation and accumulation in the myocardium. Although many mechanisms have been proposed, the exact mechanisms have never been fully elucidated. Therefore, further investigations are required to determine the cardioprotective mechanisms of incretin. Ultimately, large clinical trials are the essential step to validate those effects reported in animal studies and to warrant their clinical use in the I/R condition.

Table 6. Summary of the neutral effects of DPP-4 inhibitor on infarct size.

Animal species	Study model	Drug/dose/route	Major findings	Interpretation	References
Normoglycaemic rat	I/R LAD ligation 35-min ischaemia 30-min reperfusion	Vildagliptin Pretreatment 10 mg/kg per day, PO, for 4 weeks	Vildagliptin did not reduce infarct size in normal rat.	Vildagliptin did not reduce infarct size in normal rat.	Huisamen et al.[53]
DPP-4$^{-/-}$ mice	MI LAD ligation for 4 weeks	DPP-4$^{-/-}$ mice	1. DPP-4$^{-/-}$ mice had improved survival rate. 2. DPP-4$^{-/-}$ mice did not have reduced infarct size. 3. pGSK3β, pANP, pAkt were increased in DPP-4$^{-/-}$ mice.	DPP-4$^{-/-}$ did not reduce infarct size, but improved survival rate after MI in normoglycaemia. The mechanism could be due to activation of pGSK3β, pANP and pAkt.	Sauve et al.[49]
High fat diet with streptozotocin-induced diabetic mice	MI LAD ligation for 4 weeks	Sitagliptin Pretreatment 250 mg/kg per day, PO, 12 weeks	1. Sitagliptin improved survival rate. 2. Sitagliptin did not reduce infarct size. 3. Sitagliptin increased GLP-1 (7-36) amide level. 4. Sitagliptin lowered HbA1c level. 5. HO-1, ANP, pAkt increased in sitagliptin group. 6. pGSK3β tended to increase in sitagliptin-treated group.	Sitagliptin did not reduce infarct size, but improved survival rate after MI in diabetic mice. The mechanism could be due to activation of HO-1, ANP, pAkt and improved blood glucose.	Sauve et al.[49]
Rat	I/R LAD ligation 30-min ischaemia 120-min reperfusion	VP 20 mg/kg, SC, 30 min before ischaemia	VP did not reduce infarct size.	Intact GLP-1 alone did not reduce infarct size.	Bose et al.[26]
Rat	Ischaemic heart failure 12-week LAD occlusion	Vildagliptin 15 mg/kg per day, PO, 2 days prior to LAD occlusion 15 mg/kg per day, PO, beginning after LAD occlusion for 3 weeks	1. Vildagliptin increased active plasma GLP-1 level and decreased DPP-4 activity. 2. Vildagliptin did not mitigate the MI-induced decrease in capillary density. 3. Vildagliptin could not reduce cardiomyocyte size.	Early or late vildagliptin treatments had no infarct limiting effect on ischaemic cardiac remodelling.	Yin et al.[54]
Isolated rat heart	I/R Left main coronary artery ligation (regional ischaemia) 35-min ischaemia 120-min reperfusion	VP Pretreatment 20 mg/L VP 20 mg/L at reperfusion	VP did not reduce infarct size whether given as preconditioning or at reperfusion.	Intact GLP-1 alone did not reduce infarct size.	Bose et al.[27]
Isolated rat heart	I/R Left main coronary artery ligation (regional ischaemia) 35-min ischaemia 120-min reperfusion	VP 20 mg/L, in perfusion buffer, throughout experiment	VP alone did not reduce infarct size.	Intact GLP-1 alone did not reduce infarct size.	Bose et al.[28]

I/R: ischaemia-reperfusion; LAD: left anterior descending coronary artery; PO: per oral; MI: myocardial infarction; pGSK: phosphorylated glycogen synthase kinase; pANP: phosphorylated atrial natriuretic peptide; pAkt: phosphorylated Akt; GLP-1: glucagon-like peptide-1; HbA1c: haemoglobin A1c; HO-1: heme oxygenase-1; VP: valine pyrrolide; SC: subcutaneous route; DPP-4: dipeptidyl pepetidase-4.

Table 7. Summary of the effects of DPP-4 inhibitor on left ventricular function.

Animal species	Study model	Drug/dose/route	Major findings	Interpretation	References
Rat	Ischaemic heart failure 12-week LAD occlusion	Vildagliptin 15 mg/kg per day, PO for 2 days prior to LAD occlusion 15 mg/kg per day, PO for 3 weeks after LAD occlusion	1. Vildagliptin did not improve ejection fraction and fractional shortening. 2. Progressive LV dilatation and wall thinning after MI was attenuated in vildagliptin-treated groups. 3. Vildagliptin did not improve dP/dt_{max} and dP/dt_{min}.	Early and late treatment with vildagliptin had no beneficial effect on LV function.	Yin et al.[54]
Isolated mice heart	I/R 30-min global no flow ischaemia 40-min reperfusion	Sitagliptin 20 mg/kg, IP, 12 h and 1 h prior to heart excision DPP-$4^{-/-}$ mice Sitagliptin 5 μmol/L, in perfusion buffer, for 20 min before I/R insult	1. Sitagliptin improved LVDP in normoglycaemic mice. 2. LVDP was increased in DPP-$4^{-/-}$ mice compared with DPP-$4^{+/+}$ mice. 3. Administration of sitagliptin immediately before I/R injury failed to improve LVDP in normoglycaemic mice.	Genetic deletion and pharmacological inhibition of DPP-4 activity improved LV function. Acute reduction of cardiac DPP-4 activity was not sufficient to improve LV function.	Sauve et al.[49]
Patients	Coronary artery disease and preserved LV function	Sitagliptin 100 mg, single PO	1. Sitagliptin increased plasma GLP-1 level. 2. Sitagliptin lowered plasma glucose level. 3. Insulin level was comparable between groups. 4. Free fatty acid level was comparable between groups. 5. Sitagliptin improved ejection fraction and regional wall function during peak dobutamine stress and 30 min of recovery. 6. Sitagliptin had a greater beneficial effect on ischaemic than on non-ischaemic segments.	Sitagliptin improved both global and regional LV performance in response to stress and also reduced post-ischaemic stunning.	Read et al.[50]

LAD: left anterior descending coronary artery; PO: per oral; LV: left ventricle; MI: myocardial infarction; I/R: ischaemia-reperfusion; IP: intraperitoneal route; LVDP: left ventricle developed pressure; DPP-4: dipeptidyl pepetidase-4; GLP-1: glucagon-like peptide-1.

Table 8. Summary of the effects of DPP-4 inhibitor on haemodynamic parameters.

Animal species	Study model	Drug/dose/route	Major findings	Interpretation	References
Mice	MI LAD ligation for 4 weeks	DPP-$4^{-/-}$ mice	Aortic flow and mitral flow were comparable between DPP-$4^{-/-}$ mice and DPP-$4^{+/+}$ mice.	Genetic inhibition of DPP-4 activity did not alter haemodynamic parameters.	Sauve et al.[49]
Mice	MI LAD ligation for 4 days	Sitagliptin 250 mg/kg per day, PO, for 11 days	Aortic flow and mitral flow were comparable between sitagliptin and control group.	Pharmacological inhibition of DPP-4 activity did not alter haemodynamic parameters.	Sauve et al.[49]
Rat	Ischaemic heart failure 12-week LAD occlusion	Vildagliptin 15 mg/kg per day, PO for 2 days prior to LAD occlusion 15 mg/kg per day, PO for 3 weeks after LAD occlusion	Vildagliptin did not alter heart rate, systolic and diastolic blood pressure, LV systolic and end diastolic pressure.	Vildagliptin had no beneficial effect on haemodynamic parameters.	Yin et al.[54]
Isolated rat heart	I/R 45-min global low flow ischaemia 30-min reperfusion	Vildagliptin Pretreatment 10 mg/kg per day, PO, for 4 weeks	Vildagliptin did not improve basal aortic output and basal coronary flow in both normal and insulin resistant rat.	Vildagliptin did not alter haemodynamic parameters.	Huisamen et al.[53]
Patients	Coronary artery disease and preserved LV function	Sitagliptin 100 mg, single oral dose	Sitagliptin did not affect heart rate, systolic and diastolic blood pressure, and rate-pressure product.	Sitagliptin did not alter haemodynamic parameters.	Read et al.[50]

MI: myocardial infarction; LAD: left anterior descending coronary artery; DPP-4: dipeptidyl pepetidase-4; PO: per oral; LV: left ventricle; I/R: ischaemia-reperfusion.

Funding

This work was supported by the Thailand Research Fund Royal Golden Jubilee PhD Project (KC and NC) and the Thailand Research Fund (grants nos RTA5280007 (NC) and BRG5480003 (SC)).

Conflicts of interest

No conflicts of interest have been declared.

References

1. Smyth S and Heron A. Diabetes and obesity: The twin epidemics. *Nat Med* 2006; 12: 75–80.
2. Huang PL. Unraveling the links between diabetes, obesity, and cardiovascular disease. *Circ Res* 2005; 96: 1129–1131.
3. Grundy SM, Benjamin IJ, Burke GL, et al. Diabetes and cardiovascular disease: a statement for healthcare professionals from the American Heart Association. *Circulation* 1999; 100: 1134–1146.
4. Becker A, Bos G, de Vegt F, et al. Cardiovascular events in type 2 diabetes: comparison with nondiabetic individuals without and with prior cardiovascular disease. 10-year follow-up of the Hoorn Study. *Eur Heart J* 2003; 24: 1406–1413.
5. Fox CS, Coady S, Sorlie PD, et al. Increasing cardiovascular disease burden due to diabetes mellitus: The Framingham Heart Study. *Circulation* 2007; 115: 1544-1550.
6. Lee CD, Folsom AR, Pankow JS, et al. Cardiovascular events in diabetic and nondiabetic adults with or without history of myocardial infarction. *Circulation* 2004; 109: 855–860.
7. Mudaliar S and Henry RR. Effects of incretin hormones on beta-cell mass and function, body weight, and hepatic and myocardial function. *Am J Med* 2010; 123: S19–S27.
8. Lu L, Reiter MJ, Xu Y, et al. Thiazolidinedione drugs block cardiac KATP channels and may increase propensity for ischaemic ventricular fibrillation in pigs. *Diabetologia* 2008; 51: 675–685.
9. Nissen SE and Wolski K. Effect of rosiglitazone on the risk of myocardial infarction and death from cardiovascular causes. *N Engl J Med* 2007; 356: 2457–2471.
10. Graham DJ, Ouellet-Hellstrom R, MaCurdy TE, et al. Risk of acute myocardial infarction, stroke, heart failure, and death in elderly medicare patients treated with rosiglitazone or pioglitazone. *JAMA* 2010; 304: 411–418.
11. Verge D and Lopez X. Impact of GLP-1 and GLP-1 receptor agonists on cardiovascular risk factors in type 2 diabetes. *Curr Diabetes Rev* 2010; 6: 191–200.
12. Drucker DJ. The biology of incretin hormones. *Cell Metab* 2006; 3: 153–165.
13. Drucker DJ and Nauck MA. The incretin system: Glucagon-like peptide-1 receptor agonists and dipeptidyl peptidase-4 inhibitors in type 2 diabetes. *Lancet* 2006; 368: 1696–1705.
14. Drucker DJ. Enhancing incretin action for the treatment of type 2 diabetes. *Diabetes Care* 2003; 26: 2929–2940.
15. Elrick H, Stimmler L, Hlad Jr CJ, et al. Plasma insulin response to oral and intravenous glucose administration. *J Clin Endocrinol Metab* 1964; 24: 1076–1082.
16. Zander M, Madsbad S, Madsen JL, et al. Effect of 6-week course of glucagon-like peptide 1 on glycaemic control, insulin sensitivity, and beta-cell function in type 2 diabetes: A parallel-group study. *Lancet* 2002; 359: 824–830.
17. Orskov C, Rabenhoj L, Wettergren A, et al. Tissue and plasma concentrations of amidated and glycine-extended glucagon-like peptide I in humans. *Diabetes* 1994; 43: 535–539.
18. Zhao T, Parikh P, Bhashyam S, et al. Direct effects of glucagon-like peptide-1 on myocardial contractility and glucose uptake in normal and postischemic isolated rat hearts. *J Pharmacol Exp Ther* 2006; 317: 1106–1113.
19. Barnett A. DPP-4 inhibitors and their potential role in the management of type 2 diabetes. *Int J Clin Pract* 2006; 60: 1454–1470.
20. Green BD, Flatt PR and Bailey CJ. Dipeptidyl peptidase IV (DPP IV) inhibitors: A newly emerging drug class for the treatment of type 2 diabetes. *Diab Vasc Dis Res* 2006; 3: 159–165.
21. Deacon CF. Circulation and degradation of GIP and GLP-1. *Horm Metab Res* 2004; 36: 761–765.
22. Deacon CF, Pridal L, Klarskov L, et al. Glucagon-like peptide 1 undergoes differential tissue-specific metabolism in the anesthetized pig. *Am J Physiol* 1996; 271: E458–E464.
23. Orskov C, Andreasen J and Holst JJ. All products of proglucagon are elevated in plasma from uremic patients. *J Clin Endocrinol Metab* 1992; 74: 379–384.
24. Ahren B, Landin-Olsson M, Jansson PA, et al. Inhibition of dipeptidyl peptidase-4 reduces glycemia, sustains insulin levels, and reduces glucagon levels in type 2 diabetes. *J Clin Endocrinol Metab* 2004; 89: 2078–2084.
25. Wei Y and Mojsov S. Tissue-specific expression of the human receptor for glucagon-like peptide-I: Brain, heart and pancreatic forms have the same deduced amino acid sequences. *FEBS Lett* 1995; 358: 219–224.
26. Bose AK, Mocanu MM, Carr RD, et al. Glucagon-like peptide 1 can directly protect the heart against ischemia/reperfusion injury. *Diabetes* 2005; 54: 146–151.
27. Bose AK, Mocanu MM, Carr RD, et al. Glucagon like peptide-1 is protective against myocardial ischemia/reperfusion injury when given either as a preconditioning mimetic or at reperfusion in an isolated rat heart model. *Cardiovasc Drugs Ther* 2005; 19: 9–11.
28. Bose AK, Mocanu MM, Carr RD, et al. Myocardial ischaemia-reperfusion injury is attenuated by intact glucagon like peptide-1 (GLP-1) in the in vitro rat heart and may involve the p70s6K pathway. *Cardiovasc Drugs Ther* 2007; 21: 253–256.
29. Ossum A, van Deurs U, Engstrom T, et al. The cardioprotective and inotropic components of the postconditioning effects of GLP-1 and GLP-1(9-36)a in an isolated rat heart. *Pharmacol Res* 2009; 60: 411–417.
30. Sonne DP, Engstrom T and Treiman M. Protective effects of GLP-1 analogues exendin-4 and GLP-1(9-36) amide against ischemia-reperfusion injury in rat heart. *Regul Pept* 2008; 146: 243–249.

31. Matsubara M, Kanemoto S, Leshnower BG, et al. Single dose GLP-1-Tf ameliorates myocardial ischemia/reperfusion injury. *J Surg Res* 2011; 165: 38–45.
32. Bao W, Aravindhan K, Alsaid H, et al. Albiglutide, a long lasting glucagon-like peptide-1 analog, protects the rat heart against ischemia/reperfusion injury: Evidence for improving cardiac metabolic efficiency. *PLoS One* 2011; 6: e23570.
33. Timmers L, Henriques JP, de Kleijn DP, et al. Exenatide reduces infarct size and improves cardiac function in a porcine model of ischemia and reperfusion injury. *J Am Coll Cardiol* 2009; 53: 501–510.
34. Kavianipour M, Ehlers MR, Malmberg K, et al. Glucagon-like peptide-1 (7-36) amide prevents the accumulation of pyruvate and lactate in the ischemic and non-ischemic porcine myocardium. *Peptides* 2003; 24: 569–578.
35. Kristensen J, Mortensen UM, Schmidt M, et al. Lack of cardioprotection from subcutaneously and preischemic administered liraglutide in a closed chest porcine ischemia reperfusion model. *BMC Cardiovasc Disord* 2009; 9: 31.
36. Noyan-Ashraf MH, Momen MA, Ban K, et al. GLP-1R agonist liraglutide activates cytoprotective pathways and improves outcomes after experimental myocardial infarction in mice. *Diabetes* 2009; 58: 975–983.
37. Hausenloy DJ, Duchen MR and Yellon DM. Inhibiting mitochondrial permeability transition pore opening at reperfusion protects against ischaemia-reperfusion injury. *Cardiovasc Res* 2003; 60: 617–625.
38. Ban K, Noyan-Ashraf MH, Hoefer J, et al. Cardioprotective and vasodilatory actions of glucagon-like peptide 1 receptor are mediated through both glucagon-like peptide 1 receptor-dependent and -independent pathways. *Circulation* 2008; 117: 2340–2350.
39. Vinten-Johansen J. Involvement of neutrophils in the pathogenesis of lethal myocardial reperfusion injury. *Cardiovasc Res* 2004; 61: 481–497.
40. Duilio C, Ambrosio G, Kuppusamy P, et al. Neutrophils are primary source of O2 radicals during reperfusion after prolonged myocardial ischemia. *Am J Physiol Heart Circ Physiol* 2001; 280: H2649–H2657.
41. Dokken BB, La Bonte LR, Davis-Gorman G, et al. Glucagon-like peptide-1 (GLP-1), immediately prior to reperfusion, decreases neutrophil activation and reduces myocardial infarct size in rodents. *Horm Metab Res* 2011; 43: 300–305.
42. Read PA, Khan FZ and Dutka DP. Cardioprotection against ischaemia induced by dobutamine stress using glucagon-like peptide-1 in patients with coronary artery disease. *Heart* 2012; 98: 408–413.
43. Nikolaidis LA, Mankad S, Sokos GG, et al. Effects of glucagon-like peptide-1 in patients with acute myocardial infarction and left ventricular dysfunction after successful reperfusion. *Circulation* 2004; 109: 962–965.
44. Nikolaidis LA, Doverspike A, Hentosz T, et al. Glucagon-like peptide-1 limits myocardial stunning following brief coronary occlusion and reperfusion in conscious canines. *J Pharmacol Exp Ther* 2005; 312: 303–308.
45. Lee L, Horowitz J and Frenneaux M. Metabolic manipulation in ischaemic heart disease, a novel approach to treatment. *Eur Heart J* 2004; 25: 634–641.
46. Vanoverschelde JL, Janier MF, Bakke JE, et al. Rate of glycolysis during ischemia determines extent of ischemic injury and functional recovery after reperfusion. *Am J Physiol* 1994; 267: H1785–H1794.
47. Brown SB, Libonati JR, Selak MA, et al. Neonatal exendin-4 leads to protection from reperfusion injury and reduced rates of oxidative phosphorylation in the adult rat heart. *Cardiovasc Drugs Ther* 2010; 24: 197–205.
48. Ye Y, Keyes KT, Zhang C, et al. The myocardial infarct size-limiting effect of sitagliptin is PKA-dependent, whereas the protective effect of pioglitazone is partially dependent on PKA. *Am J Physiol Heart Circ Physiol* 2010; 298: H1454–H1465.
49. Sauve M, Ban K, Momen MA, et al. Genetic deletion or pharmacological inhibition of dipeptidyl peptidase-4 improves cardiovascular outcomes after myocardial infarction in mice. *Diabetes* 2010; 59: 1063–1073.
50. Read PA, Khan FZ, Heck PM, et al. DPP-4 inhibition by sitagliptin improves the myocardial response to dobutamine stress and mitigates stunning in a pilot study of patients with coronary artery disease. *Circ Cardiovasc Imaging* 2010; 3: 195–201.
51. Green BD, Flatt PR and Bailey CJ. Inhibition of dipeptidyl-peptidase IV activity as a therapy of type 2 diabetes. *Expert Opin Emerg Drugs* 2006; 11: 525–539.
52. Drucker DJ. Therapeutic potential of dipeptidyl peptidase IV inhibitors for the treatment of type 2 diabetes. *Expert Opin Investig Drugs* 2003; 12: 87–100.
53. Huisamen B, Genis A, Marais E, et al. Pre-treatment with a DPP-4 inhibitor is infarct sparing in hearts from obese, prediabetic rats. *Cardiovasc Drugs Ther* 2011; 25: 13–20.
54. Yin M, Sillje HH, Meissner M, et al. Early and late effects of the DPP-4 inhibitor vildagliptin in a rat model of post-myocardial infarction heart failure. *Cardiovasc Diabetol* 2011; 10: 85–94.

NUMBER 1 OF 1

AUTHOR QUERIES

DATE 6/16/2012
JOB NAME FJC

ARTICLE 201265
QUERIES FOR AUTHORS Weerateerangkul et al

THIS QUERY FORM MUST BE RETURNED WITH ALL PROOFS FOR CORRECTIONS

AU1) Please confirm all disclosures (funding and conflicts of interest) are indicated correctly.
AU2) Please spell out "cGMP" at all occurrences in the text.
AU3) Please update the reference 11 by providing the volume and page range.

Effects of *Kaempferia parviflora* Wall. Ex. Baker and Sildenafil Citrate on cGMP Level, Cardiac Function, and Intracellular Ca^{2+} Regulation in Rat Hearts

Punate Weerateerangkul, MSc, Siripong Palee, BSc,* Kroekkiat Chinda, DVM,* Siriporn C. Chattipakorn, DDS, PhD,*† and Nipon Chattipakorn, MD, PhD**

Abstract: Although *Kaempferia parviflora* extract (KPE) and its flavonoids have positive effects on the nitric oxide (NO) signaling pathway, its mechanisms on the heart are still unclear. Because our previous studies demonstrated that KPE decreased defibrillation efficacy in swine similar to that of sildenafil citrate, the phosphodiesterase-5 inhibitor, it is possible that KPE may affect the cardiac NO signaling pathway. In the present study, the effects of KPE and sildenafil citrate on cGMP level, modulation of cardiac function, and Ca^{2+} transients in ventricular myocytes were investigated. In a rat model, cardiac cGMP level, cardiac function, and Ca^{2+} transients were measured before and after treatment with KPE and sildenafil citrate. KPE significantly increased the cGMP level and decreased cardiac function and Ca^{2+} transient. These effects were similar to those found in the sildenafil citrate–treated group. Furthermore, the nonspecific NOS inhibitor could abolish the effects of KPE and sildenafil citrate on Ca^{2+} transient. KPE has positive effect on NO signaling in the heart, resulting in an increased cGMP level, similar to that of sildenafil citrate. This effect was found to influence the physiology of normal heart via the attenuation of cardiac function and the reduction of Ca^{2+} transient in ventricular myocytes.

Key Words: *Kaempferia parviflora*, sildenafil citrate, heart, cGMP, cardiac function, Ca^{2+} transient

(*J Cardiovasc Pharmacol*™ 2012;0:1–11)

INTRODUCTION

Kaempferia parviflora Wall. Ex. Baker or Krachai-dam belongs to the plant in Zingiberaceae family.[1] The rhizome has been used in Thai traditional medicine for several purposes such as the treatment of allergy, gastrointestinal disorders and rectifying male impotence.[1] Various studies demonstrated that the crude extract of *K. parviflora* rhizome and its flavonoids exert a positive effect on the nitric oxide (NO) signaling pathway both in the in vivo and in vitro studies.[2–6] *K. parviflora* extract (KPE) was shown to increase the expression of endothelial nitric oxide synthase (eNOS) mRNA and the protein level in primary cell culture of human umbilical vein endothelial cells.[2] Moreover, it has been shown recently that some flavonoids extracted from *K. parviflora* rhizome can inhibit the activity of phosphodiesterase type 5 (PDE-5),[3] the enzyme that specifically cleaves the NO mediator cGMP to 5′GMP.[7] These effects of *K. parviflora* results in an increased intracellular cGMP level.

Previous studies demonstrated that exposure to KPE produced vasodilation in both in vivo and ex vivo studies.[4–6,8,9] similar to the effects of NO on vasculature. It has been shown that L-N^G-nitroarginine methyl ester (L-NAME), a nonspecific nitric oxide synthase (NOS) inhibitor, can significantly decrease KPE-induced vasorelaxation of the aortic ring.[4] Moreover, the vasorelaxant effect of flavonoids extracted from *K. parviflora* rhizome was found to be related to NO signaling pathway.[5,6] In addition, KPE was shown to improve the endothelial dysfunction in streptozotocin-induced diabetic rats.[10] This effect was found to be due to the increase of NO bioavailability by the effect of *K. parviflora*.[10]

Our previous study in swine demonstrated that KPE decreased the defibrillation efficacy and increased the vulnerability to arrhythmia,[11] similar to that of the supratherapeutic concentration of sildenafil citrate, the PDE-5 inhibitor.[12,13] This finding suggested that KPE may affect the heart via NO/cGMP-dependent mechanism. However, the effect of KPE on NO signaling pathway in the heart is still unknown. In the present study, we hypothesized that KPE has the positive effect on NO signaling pathway in the heart via increased cGMP level. Because NO signaling pathway plays a crucial role in attenuating intracellular Ca^{2+} concentration [$(Ca2+)_i$] via the modulation of L-type Ca^{2+} channel and Ca^{2+} handling proteins of the heart,[14–17] the effects of KPE and sildenafil citrate on Ca^{2+} transient and cardiac function were also investigated in the present study. We hypothesized that KPE attenuates cardiac function via the reduction of Ca^{2+} transient amplitude similar to that of sildenafil citrate.

Received for publication January 18, 2012; accepted May 21, 2012.

From the *Department of Physiology and Cardiac Electrophysiology Research and Training Center, Cardiac Electrophysiology Unit, Faculty of Medicine, Chiang Mai University, Chiang Mai, Thailand; and †Department of Odontology and Oral Pathology, Faculty of Dentistry, Chiang Mai University, Chiang Mai, Thailand.

Supported by CHE-PhD-SW Scholarship, Office of the Higher Education Commission, Ministry of Education, Thailand (N.C. and P.W.); National Research Council of Thailand (N.C.); Faculty of Medicine Endowment Fund, Chiang Mai University (N.C. and P.W.); and the Thailand Research Fund grants BRG 5480003 (S.C.C.) and RTA 5280006 (N.C.).

The authors declare no conflicts of interest.

Reprints: Nipon Chattipakorn, MD, PhD, Cardiac Electrophysiology Research and Training Center, Faculty of Medicine, Chiang Mai University, Chiang Mai 50200, Thailand (e-mail: nchattip@gmail.com).

MATERIALS AND METHODS

Preparation of KPE

K. parviflora rhizomes were obtained in the form of coarsely ground powder from Thanyaporn Co, Ltd., Samutprakarn province, Thailand. The preparation of KPE was performed using the protocol as described previously.[11] Briefly, the coarse powder of *K. parviflora* rhizomes was weighed for 3000 mg, and extracted with 90°C saline 70 mL for 15 minutes. Then, the solution was filtered with Whatman filtered paper No.1 to collect the extract. The final volume of the extract was ~50 mL (the concentration of the extract stock solution was at 60 mg/mL).

In the present study, 2 different concentrations of KPE were used base on their effects on cardiac electrophysiological parameters as previously described.[11] The 100-mg/kg KPE, the highest concentration from our preclinical study was found to alter major cardiac electrophysiological parameters,[11] whereas the 12.5 mg/kg did not change any cardiac electrophysiological parameters.[11]

In an in vivo model, the extract was collected and diluted with saline for the final concentration of KPE at 12.5 or 100 mg/kg. In an in vitro model, the extract was added into the bath solution for the final concentrations at 75, 150, or 300 μg/mL.

The Experimental Protocol in an In Vivo Model

Animal Preparation and Cannulation for Intravenous Injection

The study was approved by the Institutional Animal Care and Use Committees of the Faculty of Medicine, Chiang Mai University. Rats were received standard pelted rat diet and water ad libitum before the study. Male Wistar rats (~300 g) were anesthetized with thiopental (100 mg/kg, intraperitoneally). Rats were operated to expose the left internal jugular vein and cannulated with polyethylene tubing (PE-60, Intramedic, Clay Adams, NJ) containing heparinized saline (40 U/mL) for subsequent infusion of KPE, drugs or saline vehicle.

The Measurement of cGMP Level in the Heart

The cardiac cGMP level was measured according to the modified method of Favory et al.[18] Briefly, frozen minced ventricular samples were weighed and homogenized with 6% trichloroacetic acid in deionized water at a ratio of 1 g wet weight: 3 mL trichloroacetic acid solution. The tissue suspension was vortexed briefly before centrifuging at 2000*g* at 4°C for 15 minutes. The supernatant was washed 3 times with water-saturated diethyl ether and the upper ether layer was discarded after each wash. The aqueous extract was heated with 70°C in water bath for 5 minutes to discard the remaining diethyl ether. The final solution was lyophilized and analyzed for cGMP by a commercial ELISA kit (Parameter, R&D Systems, Minneapolis, MN).

Western Blot Analysis for NOS Expression

Frozen minced samples were homogenized with ice-cold potassium phosphate buffer (pH 8.3) with protease inhibitor cocktail, and subsequently centrifuged at 800*g* for 10 minutes at 4°C. The supernatant was centrifuged at 15,000*g* for 20 minutes at 4°C, and the protein concentration in the resultant supernatant was measured. Equal amount of proteins were subjected to sodium dodecyl sulfate—polyacrylamide gel electrophoresis. Blots were probed with primary antibodies against eNOS, nNOS, and iNOS (Santa Cruz Biotechnology, Inc, Santa Cruz, CA), and secondary antibodies conjugated with horseradish peroxidase. Bound antibodies were detected with the ECL detection system (GE Healthcare Bio-sciences Corp, Piscataway, NJ). Subsequent detection of the specific proteins was normalized to β-actin using Scion Image for Windows.

Experimental Protocol for Studying the Effect of KPE on cGMP Level and NOS Expression in the Heart

The rats were divided into 4 groups (n = 8 in each group). Group 1: saline; group 2: sildenafil citrate (Pfizer; 4 mg/kg, comparable to the supratherapeutic concentration); groups 3 and 4: KPE (12.5 and 100 mg/kg, respectively).

After cannulation, the solutions including KPE, sildenafil citrate or saline (1 mL each) were administered (0.5 mL/min, intravenously (i.v.)). Thirty minutes after the end of the treatments, the ventricles were rapidly removed, cleaned in ice-cold saline, and then minced and divided into 2 halves for cGMP level measurement and Western blot analysis for NOS expression. The period of the study (30 min) was chosen because our previous study indicated that the effect of KPE on cardiac electrophysiology reached a peak 30 minutes after KPE infusion.[11]

Pharmacological Protocol for Studying the Effect of KPE on the Downstream Cascade From NOS in the Heart

The rats were divided into 5 groups (n = 8 in each group). Group 1: saline-treated in combination with NO-donor, nitroglycerin (NTG, Schwarz, Germany), and nonspecific NOS inhibitor, L-NAME (Sigma Chemical, St. Louis, MO); group 2: 12.5-mg/kg KPE with NTG and L-NAME; group 3: 12.5-mg/kg KPE combined with NTG only; group 4: 100-mg/kg KPE with NTG and L-NAME; and group 5: 100-mg/kg KPE combined with NTG only.

After internal jugular vein cannulation, rats in groups 1, 2, and 4 received a bolus of L-NAME (10 mg/kg,[19] 0.25 mL, intravenously). In other groups, saline was administered instead of L-NAME. After L-NAME or saline injection, the KPE or saline (1 mL each) were infused (0.5 mL/min). Subsequently, a bolus of NTG (150 μg/kg,[20] 0.25 mL, intravenously) was administered and maintained (50 μg/kg/min, intravenously) throughout the experiment in all groups. Thirty minutes after KPE or saline infusion, the ventricles were rapidly removed, cleaned in ice-cold saline. and processed to assess cGMP levels.

Experimental Protocol for Studying the Effect of KPE on Cardiac Function

The rats were divided into 6 groups (n = 8 in each group). Group 1: saline; groups 2 and 3: KPE (12.5 and

100 mg/kg, respectively); groups 4 and 5, sildenafil citrate (2 and 4 mg/kg, the latter concentration is comparable to the therapeutic concentration); groups 6: L-NAME (10 mg/kg).

After the surgery for the insertion of the cardiac pressure-conductance catheter (Scisense Inc, London, Ontario, Canada), left ventricular (LV) function was assessed. LV hemodynamic data was digitized and recorded using a data acquisition system. After each experiment, end-systolic pressure (ESP), end diastolic pressure, maximum +dP/dt and -dP/dt, end-systolic volume (ESV), end-diastolic volume (EDV), ejection fraction (EF), and heart rate (HR) were extracted during baseline and after administration of saline, KPE (12.5 and 100 mg/kg), sildenafil citrate (2 and 4 mg/kg), or L-NAME (1 mL each, 0.5 mL/min, intravenously) in groups 1–6, respectively. The LV hemodynamics were measured again after the end of saline, KPE, or sildenafil citrate infusion, and the data were compared against baseline.

The Experimental Protocol in an In Vitro Model

Preparation of Isolated Ventricular Myocytes

Rat ventricular myocytes were isolated using an enzymatic technique.[21] The rats were injected with 0.2 mL heparin intraperitoneally. After deep anesthesia, the hearts were excised, and the aortas were cannulated rapidly. The cannulated hearts were perfused on a Langendorff perfusion apparatus with oxygenated normal Tyrode solution containing (in mM): 130 NaCl, 5.4 KCl, 0.75 $CaCl_2$, 1.4 $MgCl_2$, 0.4 NaH_2PO_4, 10 glucose, 4.2 HEPES, 20 taurine, 10 creatine) at 37°C in the first column at constant flow (~2 mL/min) for 10 minutes. Then, the hearts were switched to the second column and perfused with oxygenated Ca^{2+}-free Tyrode solution. After 5 minutes, the hearts were switched to the third column (enzymatic buffer), where they were digested with the 30-mL normal Tyrode solution containing 1 mg/mL of collagenase type II (Gibco, Invitrogen Corporation, CA), for another 7 minutes. After that, the hearts were cut off the cannula, and the aortas and atria were removed from the hearts. The remaining ventricular tissues were cut into several pieces with scissors in the same enzymatic buffer from the third column. Then the cardiomyocytes in the solution were dispersed gently by a wide tipped pipette and filtered through nylon mesh into a plastic tube. After the cardiomyocytes were pelleted by gravity for ~6 minutes, the supernatant was aspirated and the cell pellet was resuspended and incubated in the warm normal Tyrode solution before the use.

The Measurement of Ca^{2+} Transient

The Ca^{2+} transient in rat ventricular myocytes was measured by a fluorimetric ratio technique.[22] The fluorescent Ca^{2+} indicator Fura-2 was loaded by incubating the cardiomyocytes at room temperature for 20–30 minutes with 25 μM of Fura-2/AM (Sigma Chemical, St. Louis, MO). The background and cell autofluorescence were cancelled out by zeroing the output using cells without Fura-2/AM loading. Ultraviolet light at the wavelengths of 340 and 387 nm were used for the excitation of the Fura-2 from a xenon arc lamp controlled by a microfluorometry system (Cell, Olympus, Tokyo, Japan), and the excitation light beam was directed into an inverted microscope (IX-81; Olympus). The ratio of emitted fluorescence signals from the Fura-2/AM loaded cardiomyocytes at 510 nm were recorded. The Ca^{2+} transient parameters including the Ca^{2+} transient amplitude, the Ca^{2+} transient rising and decay rate, and the diastolic Ca^{2+} level were measured during 1-Hz field-stimulation with 10-ms supramaximal threshold strength square-wave pulses. The fluorescence ratio data was processed and stored in a computer using Xcellence imaging software (Olympus).

Experimental Protocol for Studying the Effects of KPE and Sildenafil Citrate on Ca2+ Transient in Isolated Ventricular Myocytes

The ventricular myocytes were divided into 6 groups (n = 8–12 in each group). Before the saline, KPE, or sildenafil citrate superfusion, the Ca^{2+} transient in each group was measured as the baseline. After that, in group 1, saline was superfused to serve as a control group. In groups 2, 3, and 4, KPE at several concentrations (75, 150, and 300 μg/mL, respectively) was superfused. The 300 μg/mL KPE (approximately consistent with the 20-mg/kg KPE in our in vivo studies) was chosen because it decreased the Ca^{2+} transient in isolated ventricular myocytes within 5 minutes of superfusion. The concentration of KPE higher than 300 μg/mL was shown to have the cytotoxic effects; cells displayed obvious shrinkage within 5 minutes after superfusion of the extract.

In groups 5 and 6, sildenafil citrate (30 and 60 μg/mL, respectively, approximately comparable with the concentration of 2 and 4 mg/kg in our in vivo study), were superfused. The Ca^{2+} transient was measured again at 5 minutes after sildenafil citrate superfusion and at 5 and 10 minutes after KPE or saline superfusion.

Experimental Protocol for Studying the Effects of KPE and Sildenafil Citrate in Combination With L-Name On Ca^{2+} Transient in Isolated Ventricular Myocytes

The ventricular myocytes were treated with L-NAME (1 mM) for 5 minutes, after which the Ca^{2+} transient was measured as the baseline value. These L-NAME-treated cardiomyocytes were divided into 6 treatment groups (n = 8–12 in each group): saline, KPE (75, 150, and 300 μg/mL), or sildenafil citrate (30 and 60 μg/mL). In the sildenafil-treated groups, Ca^{2+} transients were measured at 5 minutes after sildenafil superfusion. In saline and KPE-treated groups, Ca^{2+} transients were measured at 10 minutes (the effective time obtained from the in vitro protocol) after saline or KPE superfusion.

Experimental Protocol for Studying the Effects of KPE and Silenafil Citrate in Combination With L-NAME and NTG on Ca^{2+} Transient in Isolated Ventricular Myocytes

The ventricular myocytes were treated with L-NAME (1 mM) in combination with NTG (10 μM) for 5 minutes, after which the Ca^{2+} transient was measured as the baseline. These cardiomyocytes were divided into 3 groups (n = 8–12

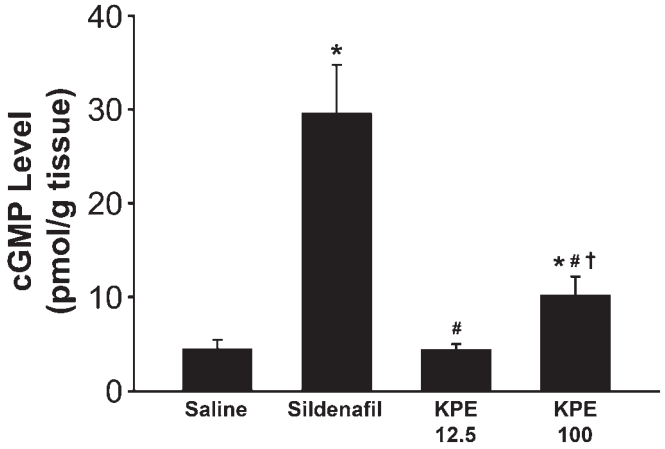

FIGURE 1. Effects of KPE (12.5 and 100 mg/kg), sildenafil citrate (4 mg/kg), and saline (n = 8 in each group) on the cGMP level in rat hearts. *$P < 0.05$ vs. saline; #$P < 0.05$ vs. sildenafil citrate; †$P < 0.05$ vs. KPE12.5.

in each group) as follows: saline, KPE (300 μg/mL), or sildenafil citrate (60 μg/mL). Five minutes after sildenafil citrate superfusion, Ca^{2+} transient was measured again to compare against baseline. In saline-treated and KPE-treated groups, Ca^{2+} transients were measured again at 10 minutes after superfusion of saline or the extract to compare against the baseline.

Statistical Analysis

Values are expressed as mean ± SD in all studies. Comparisons of variables at baseline and after saline, KPE, sildenafil citrate or L-NAME treatment in each group were performed using the Wilcoxon Signed Ranks test. Comparisons of variables between experimental groups were performed using the Mann–Whitney U test. $P < 0.05$ was considered statistically significant.

RESULTS

The In Vivo Studies

Effect of KPE on cGMP Level in the Hearts

At 30 minutes after treatment, the intravenous administration of both 100-mg/kg KPE and 4-mg/kg sildenafil citrate significantly increased cGMP level in the ventricles (Fig. 1). The level of cGMP in the sildenafil citrate–treated group (the positive control) was also higher than that of the 100-mg/kg KPE–treated group. However, the cGMP level in the 12.5-mg/kg KPE group was not changed compared with the saline-treated group (Fig. 1). F1

Effect of KPE and Sildenafil Citrate on NOS Expression in the Hearts

Figure 2 represents the expression of NOS in the ventricles after KPE, sildenafil citrate, or saline treatment. KPE at any concentration, sildenafil citrate (4 mg/kg), or saline did not alter the expression of eNOS and the other 2 types of NOS, nNOS and iNOS, in the ventricles at 30 minutes after intravenous administration of the treatment. F2

Effect of KPE on Downstream Cascade From NOS in the Hearts

Because we found that the 100-mg/kg KPE increased cGMP level but did not change the expression of any type of NOS in rat ventricles, we further hypothesized that KPE increases cGMP by inhibiting PDE-5, similar to that of sildenafil citrate. To test this hypothesis, L-NAME, the nonspecific NOS inhibitor, was used to inhibit all types of NOS, and NTG, the NO donor, was used as the source of NO to control the level of exogenous NO in all groups. This

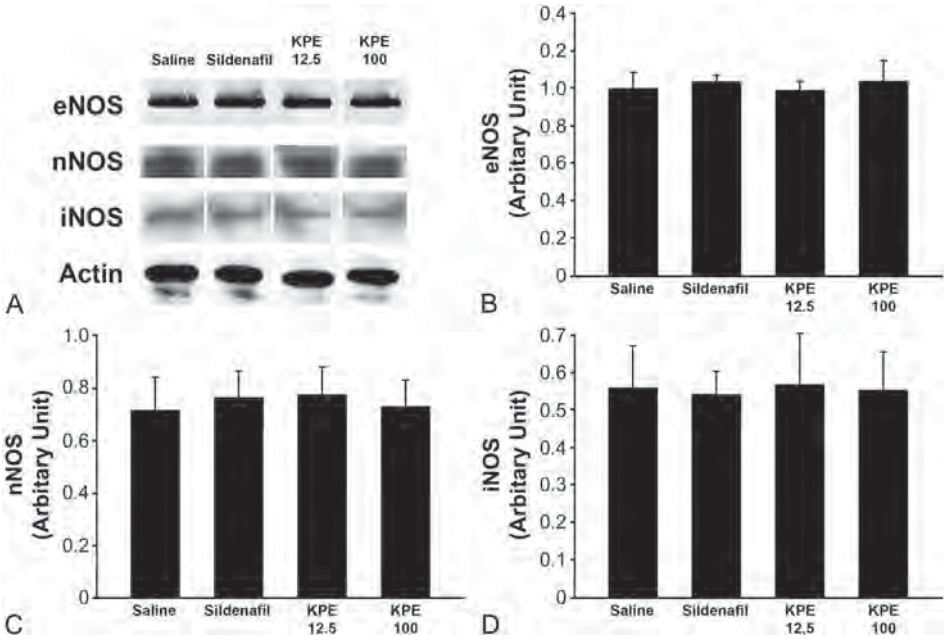

FIGURE 2. Effects of KPE (12.5 and 100 mg/kg), sildenafil citrate (4 mg/kg), and saline (n = 8 in each group) on NOS expression in rat hearts. A, Proteins by Western blot analysis in rat hearts; B, eNOS; C, nNOS; D, iNOS.

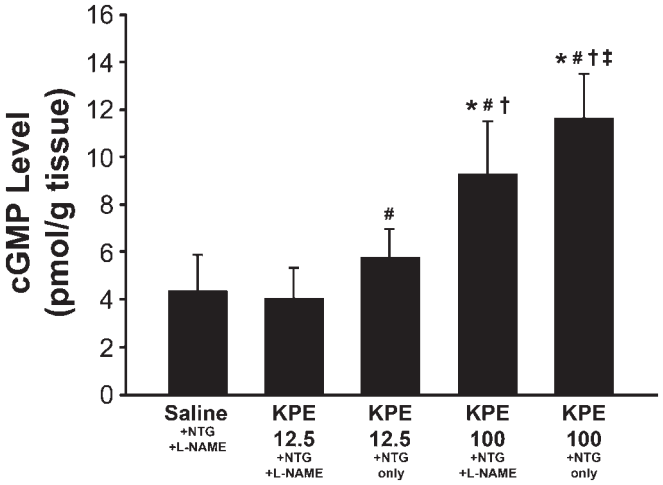

FIGURE 3. Effects of KPE (12.5 and 100 mg/kg) and saline combination with NO donor, NTG, and NOS inhibitor, L-NAME, or with NO donor only (n = 8 in each group) on the cGMP level in rat hearts. *$P < 0.05$ vs. saline; #$P < 0.05$ vs. KPE12.5 + NTG + L-NAME; †$P < 0.05$ vs. KPE12.5 + NTG only; ‡$P < 0.05$ vs. KPE100 + NTG + L-NAME.

would allow us to elucidate whether increased cGMP was caused by the effect of KPE on NOS or its downstream cascade. Our results demonstrated that in the group treated with 100-mg/kg KPE combined with L-NAME and NTG, the cGMP level in the ventricles was significantly higher than the control (ie, saline plus L-NAME and NTG) group (Fig. 3). Moreover, in the group treated with 100-mg/kg KPE combined with NTG only, the cGMP level was significantly higher than that in the KPE-treated group with L-NAME and NTG (Fig. 3). The cGMP level of both 12.5-mg/kg KPE–treated groups (in combination with NTG) with or without L-NAME was not different from that in the control group. However, the cGMP level in the group without L-NAME was significantly higher than that in the group with L-NAME (Fig. 3).

Effects of KPE and Sildenafil Citrate on Cardiac Function

Table 1 shows a tabulation of LV hemodynamic parameters including ESP, end-diastolic pressure, maximum +dP/dt and –dP/dt, ESV, EDV, EF, and HR after the treatments of KPE, sildenafil citrate, L-NAME, or saline compared with baseline. We found that after 30 minutes, KPE (100 mg/kg) degraded cardiac function as shown by the significantly decrease of ESP, maximum +dP/dt and –dP/dt, and ESV compared with baseline of the same group. Additionally, both concentrations of sildenafil citrate significantly degraded cardiac function by the same parameters as 100-mg/kg KPE–treated group within 5 minutes after the end of drug administration. In L-NAME–treated group, ESP, maximum +dP/dt and –dP/dt, ESV, and EDV were found to increase within 5 minutes after the end of L-NAME administration. However, EF and HR were not changed in these groups. KPE at 12.5 mg/kg or saline did not alter any LV hemodynamic parameters.

TABLE 1. Effects of KPE (12.5 and 100 mg/kg), Sildenafil Citrate (2 and 4 mg/kg), L-NAME (10 mg/kg), and Saline on the Cardiac Function (n = 8 in Each Group)

	Group 1		Group 2		Group 3	
Parameters	**Baseline**	**Saline**	**Baseline**	**KPE (12.5 mg/kg)**	**Baseline**	**KPE (100 mg/kg)**
ESP (mm Hg)	176 ± 16	178 ± 16	188 ± 21	191 ± 21	185 ± 12	171 ± 8*
EDP (mm Hg)	47 ± 4	48 ± 4	50 ± 3	51 ± 2	44 ± 3	43 ± 2
Maximum +dP/dt (mm Hg/s)	8821 ± 767	8839 ± 675	8954 ± 649	8827 ± 845	8424 ± 327	7840 ± 403*
Maximum -dP/dt (mmHg/s)	4554 ± 933	4407 ± 980	4698 ± 802	4794 ± 842	4145 ± 538	2963 ± 243*
ESV (% of baseline)	100	103 ± 14	100	104 ± 18	100	98 ± 16
EDV (% of baseline)	100	100 ± 4	100	99 ± 2	100	89 ± 6*
EF (% of baseline)	100	98 ± 7	100	98 ± 10	100	96 ± 10
HR (bpm)	442 ± 31	439 ± 35	425 ± 43	418 ± 50	420 ± 22	417 ± 14

	Group 4		Group 5		Group 6	
Parameters	**Baseline**	**Sildenafil Citrate (2 mg/kg)**	**Baseline**	**Sildenafil Citrate (4 mg/kg)**	**Baseline**	**L-NAME**
ESP (mm Hg)	187 ± 9	176 ± 14*	181 ± 6	165 ± 8*	186 ± 30	224 ± 43*
EDP (mm Hg)	52 ± 3	51 ± 2	43 ± 5	43 ± 4	45 ± 3	49 ± 6*
Maximum +dP/dt (mm Hg/s)	8791 ± 471	8173 ± 337*	8807 ± 499	7586 ± 603*	8433 ± 474	9476 ± 378*
Maximum -dP/dt (mmHg/s)	4459 ± 848	3058 ± 309*	4018 ± 430	2739 ± 697*	4298 ± 940	5053 ± 891*
ESV (% of baseline)	100	94 ± 17	100	97 ± 31	100	183 ± 54*
EDV (% of baseline)	100	92 ± 8*	100	89 ± 11*	100	138 ± 24*
EF (% of baseline)	100	99 ± 6	100	96 ± 21	100	86 ± 21
HR (bpm)	436 ± 16	444 ± 16	434 ± 37	439 ± 40	434 ± 22	416 ± 15

Values are expressed as mean ± SD.
*$P < 0.05$ versus baseline of the same group.
EDP, end diastolic pressure.

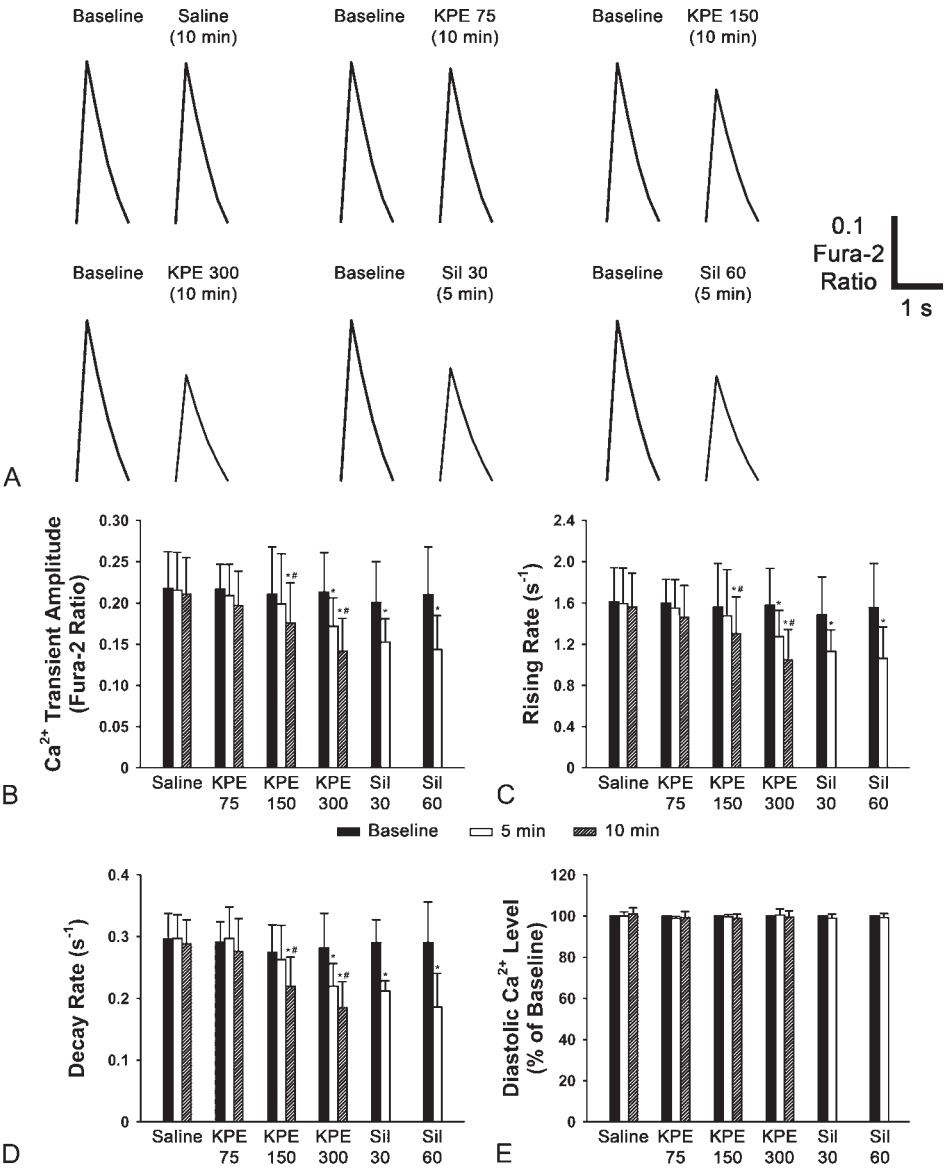

FIGURE 4. Effects of KPE at 75 (n = 9), 150 (n = 10), and 300 μg/mL (n = 8); sildenafil citrate (Sil) at 30 (n = 11) and 60 mg/mL (n = 12); and saline (n = 12) on the Ca^{2+} transient in ventricular myocytes. A, the representative Ca^{2+} transient tracings; B, Ca^{2+} transient amplitude; C, Ca^{2+} transient rising rate; D, Ca^{2+} transient decay rate; E, diastolic Ca^{2+} level. *$P < 0.05$ vs. baseline; #$P < 0.05$ vs. 5 minutes of the same group.

The In Vitro Studies

Effects of KPE and Sildenafil Citrate on Ca^{2+} Transient in Isolated Ventricular Myocytes

F4 Figure 4A represents the Ca^{2+} transient tracings of isolated ventricular myocytes treated with KPE, sildenafil citrate, and saline. KPE at the concentration of 300 μg/mL significantly decreased the Ca^{2+} transient amplitude (Fig. 4B), rising (Fig. 4C) and decay rate (Fig. 4D) within 5 minutes (19%, 19%, and 22% respectively) and showed the progressive decrease of these parameters at 10 minutes of KPE superfusion (33%, 33%, and 34%, respectively). The superfusion of KPE at 150 μg/mL decreased Ca^{2+} transient amplitude, rising and decay rate at 10 minutes of KPE superfusion (17%, 17%, and 20%, respectively). KPE at 75 μg/mL did not change the Ca^{2+} transient amplitude, rising and decay rate.

After the superfusion of sildenafil citrate at 60 and 30 μg/mL for 5 minutes, the Ca^{2+} transient amplitudes were decreased by 32% and 25%, respectively (Fig. 4B), the Ca^{2+} transient rising rates were decreased by 32% and 25%, respectively (Fig. 4C), and the Ca^{2+} transient decay rates were decreased by 36% and 27%, respectively (Fig. 4D). Saline did not alter Ca^{2+} transient amplitude, rising and decay rate. Additionally, the diastolic Ca^{2+} level was not altered from its baseline after being treated with any of the tested concentrations of KPE, sildenafil citrate, and saline (Fig. 4E).

Effects of KPE and Sildenafil Citrate on Ca^{2+} Transient in Combination With L-Name in Isolated Ventricular Myocytes

This study was performed to determine whether KPE and sildenafil citrate modulate Ca^{2+} transient through the

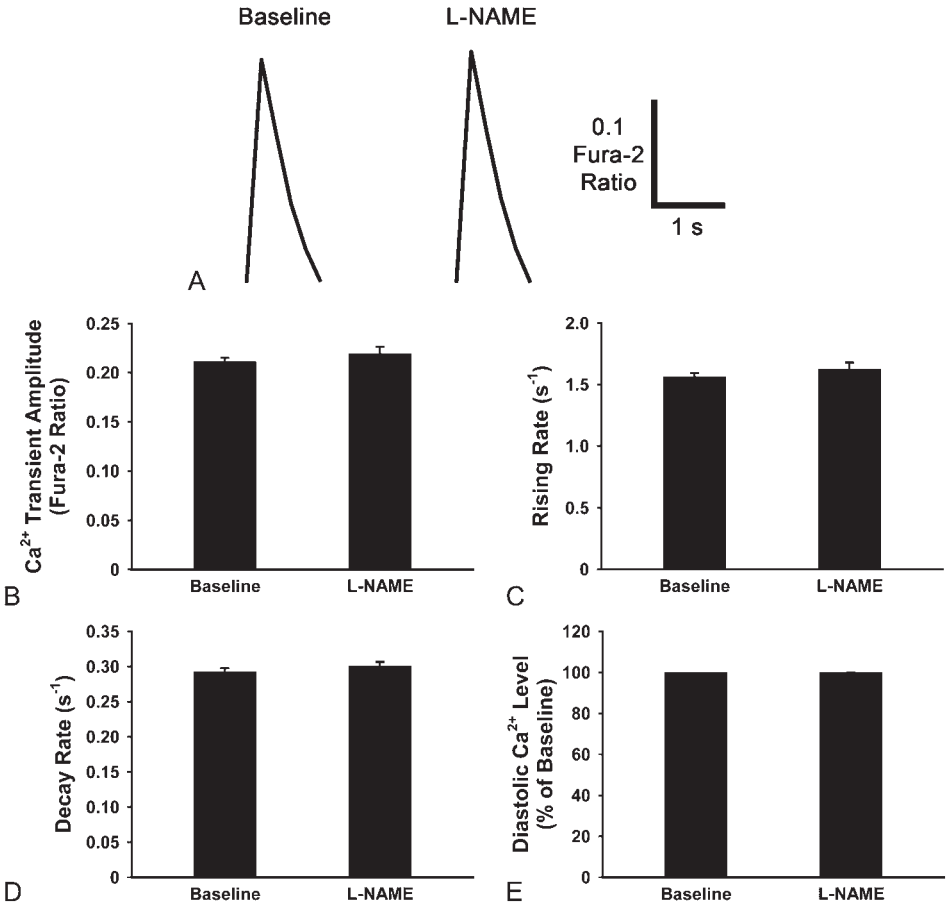

FIGURE 5. Effects of L-NAME (1 mM) on the Ca^{2+} transient in ventricular myocytes. A, the representative Ca^{2+} transient tracings; B, Ca^{2+} transient amplitude; C, Ca^{2+} transient rising rate; D, Ca^{2+} transient decay rate; E, diastolic Ca^{2+} level.

NO/cGMP signaling pathway. It is known that this pathway attenuates intracellular Ca^{2+} level via the regulation of L-type Ca^{2+} channel and Ca^{2+} handling proteins.[14–17] To prevent intracellular cGMP production via NO before KPE or sildenafil citrate was applied to the ventricular myocytes, all types of NOS were inhibited with nonspecific NOS inhibitor L-NAME in this series of experiment. We hypothesized that the disturbance of cGMP production by L-NAME could abolish the effects of KPE and sildenafil citrate on Ca^{2+} transient.

F5 Figure 5 represents the effect of L-NAME on the Ca^{2+} transient of isolated ventricular myocytes. It was found that after 5 minutes of L-NAME treatment, the Ca^{2+} transient amplitude, rising and decay rate or diastolic Ca^{2+} level did not change compared with the baseline. These effects of L-NAME–treated cardiomoycytes served as baseline for further studying the effects of KPE and sildenafil citrate treatments.

In L-NAME–treated cardiomyocytes, neither KPE of any concentrations nor sildenafil citrate altered the Ca^{2+} transient amplitude, rising or decay rate, compared with the ventricular myocytes treated with L-NAME alone (baseline) F6 (Fig. 6). Moreover, the diastolic Ca^{2+} level was not altered in any of these groups. Saline did not alter Ca^{2+} transient after L-NAME superfusion in isolated ventricular myocytes.

Experimental Protocol for Studying the Effects of KPE and Silenafil Citrate in Combination With L-NAME and NTG on Ca^{2+} Transient in Isolated Ventricular Myocytes

In L-NAME–treated cardiomyocytes in combination with NTG, KPE (300 μg/mL) and sildenafil citrate (6 μg/mL) decreased the Ca^{2+} transient amplitude, rising and decay rate, compared with the pretreatment of the extract or sildenafil citrate (Fig. 7). However, the diastolic Ca^{2+} level was not altered F7 in these groups. Saline did not alter Ca^{2+} transient after L-NAME combined with NTG superfusion in isolated ventricular myocytes.

DISCUSSION

The major findings of the present study are as follows: (1) The 100-mg/kg KPE increased cardiac cGMP level via downstream cascade from NOS; (2) The 100-mg/kg KPE and both supratherapeutic and therapeutic concentrations of sildenafil citrate decreased cardiac function in the normal rat heart; (3) The 100-mg/kg KPE and both supratherapeutic and therapeutic concentrations of sildenafil citrate decreased Ca^{2+} transient via the NO signaling pathway from its downstream cascade from NOS; (4) L-NAME increased cardiac function without the changing of Ca^{2+} transient.

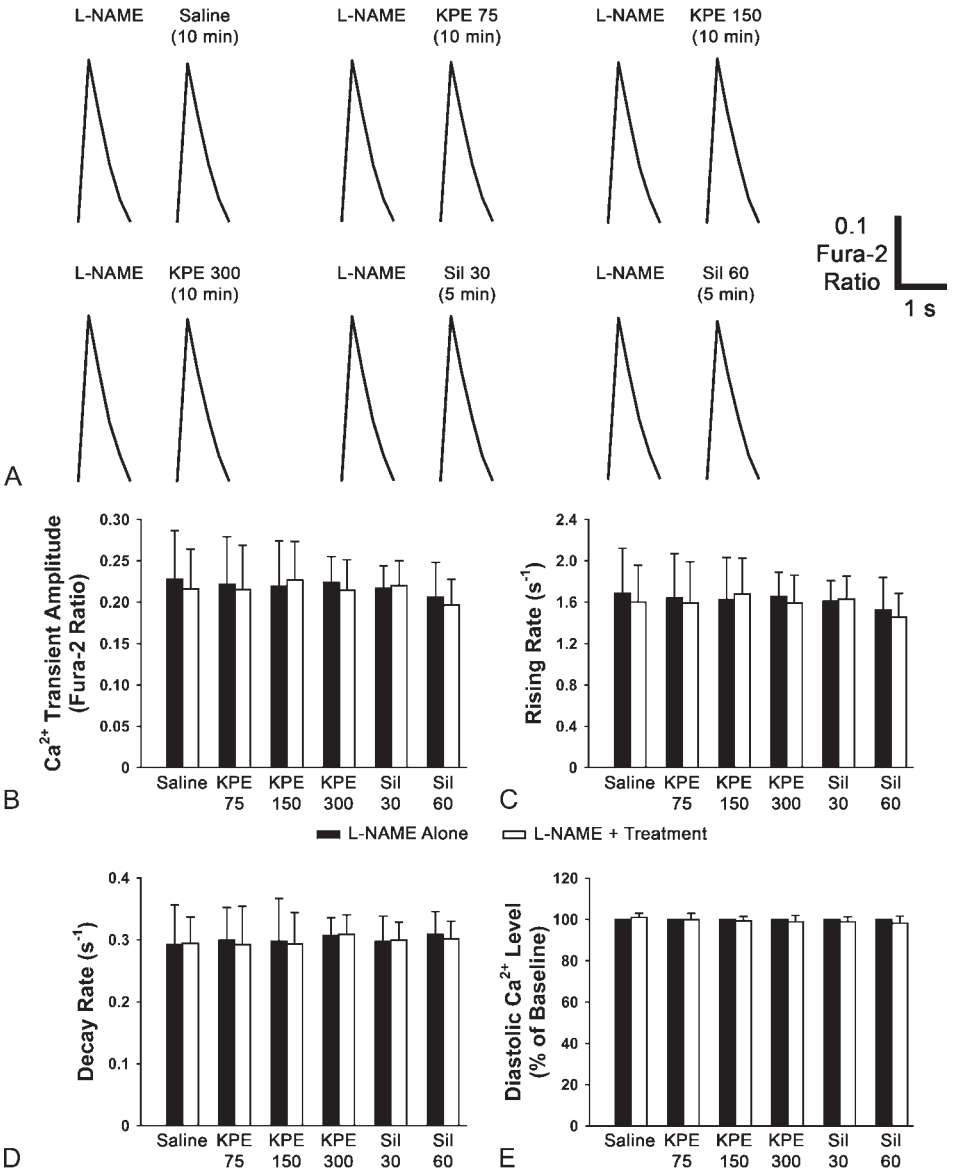

FIGURE 6. Effects of KPE at 75 (n = 9), 150 (n = 10) and 300 μg/mL (n = 8); sildenafil citrate (Sil) at 30 (n = 10) and 60 μg/mL (n = 11); and saline (n = 8) on the Ca^{2+} transient in ventricular myocytes in combination with the NOS inhibitor, L-NAME. A, the representative Ca^{2+} transient tracings; B, Ca^{2+} transient amplitude; C, Ca^{2+} transient rising rate; D, Ca^{2+} transient decay rate; E, diastolic Ca^{2+} level.

Although various studies demonstrated that KPE and its bioactive flavonoids have the positive effects on the NO signaling pathway in the vessels and endothelial cell culture,[2–6] its effect on the heart had not been investigated. Our study is the first to demonstrate that a high concentration of KPE (100 mg/kg) also affected the NO signaling pathway in rat hearts, and that its effect was similar to that of sildenafil citrate (a PDE-5 inhibitor), the positive control. In the present study, a high concentration of KPE (100 mg/kg) significantly degraded cardiac function in vivo at 30 minutes after the end of KPE infusion. This effect of KPE is possibly due to the increased cGMP level in the heart. This is supported by our findings that sildenafil citrate, the PDE-5 inhibitor that increased cGMP intracellularly and represented the positive effect of NO signaling pathway on cardiac function in our study, could decrease the cardiac function in the same manner of the high concentration of KPE. These results indicate that NO-cGMP signaling pathway could possibly explain the mechanism by which KPE modulates cardiac function. In L-NAME–treated group, the cardiac function was found to increase compared with baseline. This result suggested that the inhibition of NO signaling pathway could cause the augmentation of cardiac contractility, whereas the enhancement of this pathway causes the contrary result.

In the present study, we found that at 30 minutes after the end of KPE infusion, cGMP level in rat hearts increased, even though NOS expression in the heart was not changed. Although the study of Wattanapitayakul et al[2] in 2007 found that KPE increased the expression of eNOS mRNA and protein in human umbilical vein endothelial cells, we did not observe the change of cardiac eNOS and the other 2 types of NOS protein expressions in our study. This could be due to the different organs used, period of the treatment, animal species, and study protocol. Furthermore, we also found that

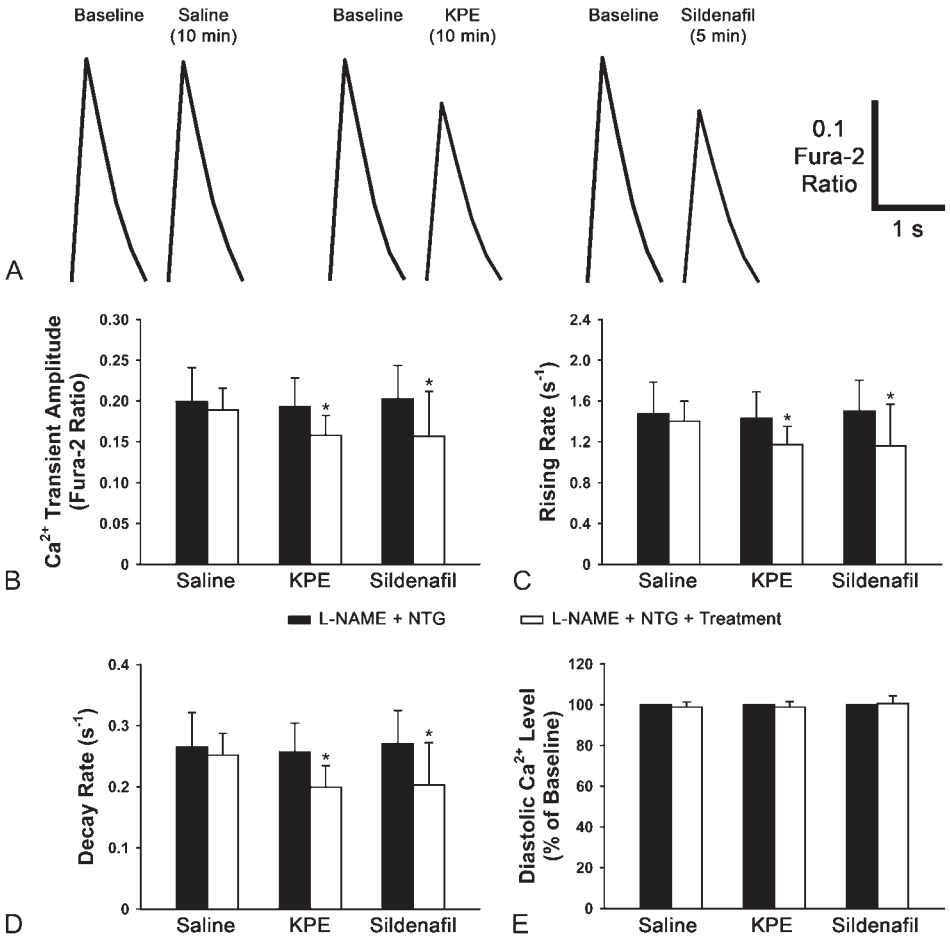

FIGURE 7. Effects of KPE (300 μg/mL, n = 10), sildenafil citrate (60 μg/mL, n = 8); and saline (n = 8) on the Ca^{2+} transient in ventricular myocytes in combination with the NOS inhibitor, L-NAME, and NO donor, NTG. A, the representative Ca^{2+} transient tracings; B, Ca^{2+} transient amplitude; C, Ca^{2+} transient rising rate; D, Ca^{2+} transient decay rate; E, diastolic Ca^{2+} level. *$P <$ 0.05 vs. baseline.

when all types of NOS were inhibited by L-NAME, cGMP level was still increased after the administration of the high concentration of KPE (ie, saline vs. KPE100 + NTG + L-NAME, Fig. 3). These results suggest that the increased cGMP level by KPE in the heart depend on neither the increasing NOS expression nor NOS activity. Because *K. parviflora* has been shown to have many kinds of flavonoids,[23–26] and previous studies demonstrated that some flavonoids and polyphenolic compounds from *K. parviflora* and other herbal plants exhibit PDE-5 inhibitory effect.[3,27–29] Therefore, we hypothesized that KPE used in the present study could have the PDE-5 inhibitory effect in the heart. Although we found that the 100-mg/kg KPE can increase cGMP level in the ventricle, it was found to be much lower than the effect of 4-mg/kg sildenafil citrate. This finding suggests that KPE could have mild PDE-5 inhibitory effects compared with that of sildenafil citrate as observed in the present study. Additionally, we found that cardiac cGMP level in the KPE-treated groups that NOS was not inhibited (ie, groups 3 and 5, Fig. 3) were higher than that of the same KPE-treated groups, and NOS was inhibited by L-NAME (ie, groups 2 and 4, Fig. 3). These findings suggest that the endogenous NO from NOS also plays a role in the difference of cGMP production in these groups.

Because KPE was found to cause vasorelaxation through the NO-cGMP signaling mechanism,[4] it is possible that KPE decreased the cardiac function through the direct effect on the heart via the modulation of excitation–contraction coupling or the indirect effect via its effect on vasculature. We investigated this hypothesis by studying the effect of KPE in isolated ventricular myocytes which could provide evidence for cardiac contractility via the Ca^{2+} induced Ca^{2+} release and excitation–contraction coupling without the interference of vascular effect of KPE. It is well recognized that the NO-cGMP signaling pathway regulates many types of ions via the modulation of ion channels and ion-handling proteins in cardiomyocytes.[14–17,30–32] Among various types of ions, Ca^{2+} is the important ion that plays a role in the regulation of electrical and mechanical function of the heart, that is the generation of action potential and excitation–contraction coupling in each cardiac cycle.[33] The NO-cGMP signaling pathway is one of the crucial pathways that attenuate the $(Ca^{2+})_i$ via the modulation of L-type Ca^{2+} current ($I_{Ca\text{-}L}$) and Ca^{2+} recycling by the sarcoplasmic reticulum.[14–17] Our results demonstrated that KPE and sildenafil citrate decreased Ca^{2+} transient amplitude, rising and decay rate, in isolated ventricular myocytes. When treated with the nonspecific NOS inhibitor L-NAME to completely inhibit the

generation of cGMP intracellularly, the effects of both KPE and sildenafil citrate were completely eliminated. These effects reappeared again when the NO donor NTG was added to activate the downstream cascade from NOS. These findings suggest that cGMP is the important mediator of KPE and sildenafil citrate in the modulation of Ca^{2+} transient in ventricular myocytes. Decreased Ca^{2+} transient amplitude and rising rate of ventricular myocytes by KPE and sildenafil citrate may result in the reduction in the cardiac contractility as shown by the decreased maximum +dP/dt, whereas the decreased Ca^{2+} transient decay rate may result in diastolic dysfunction as shown by the decreased maximum –dP/dt in our in vivo study. Although KPE and sildenafil citrate decreased Ca^{2+} transient decay rate in isolated cardiomyocytes, the baseline diastolic Ca^{2+} levels were not altered. These findings suggest that KPE not only decreased the Ca^{2+} influx but also slowed down the process of getting rid of Ca^{2+} from the cytoplasm during each cardiac cycle.

Our results also demonstrate that L-NAME alone did not change Ca^{2+} transient amplitude, rising or decay rate, and diastolic Ca^{2+} level in isolated ventricular myocytes. This result suggests that the basal level of cGMP does not alter Ca^{2+} transient of isolated ventricular myocytes. This finding is consistent with the previous study that L-NAME did not change the Ca^{2+} transient in LV-free wall of guinea pig hearts.[34] Although our cardiac function study showed that L-NAME increased cardiac contractility, this finding does not depend on the direct effect of L-NAME on intracellular Ca^{2+} regulation. In addition, the other study in isolated–perfused rabbit hearts also found that the nonspecific NOS inhibitor, L-N^G-nitroarginine, did not change cardiac contractility.[35] Because L-NAME is the drug that was used to increase the blood pressure in hypertensive animal model,[36] the increase of cardiac function after L-NAME treatment may be due to the compensatory mechanism against hypertensive effect of L-NAME (ie, Frank-Starling mechanism in response to the increased preload through the enhanced myocyte distension).[37]

CONCLUSIONS

Similar to sildenafil citrate, KPE increased cardiac cGMP level via the downstream cascade from NOS in the NO signaling pathway. KPE reduces the Ca^{2+} transient, thus attenuating LV performance in rats.

STUDY LIMITATION

The present study measured cGMP levels and NOS expression in the whole ventricles. It is possible that the cGMP level, NOS expression, and the effect of KPE vary within the heart, that is, left and right ventricle or endocardium to epicardium could be different. Also, the absolute Ca^{2+} concentration in the isolated ventricular myocytes was not known in the present study because we measured the relative change of fluorescence intensity of Fura-2 as the Ca^{2+} transient. Moreover, the effects of KPE on the contractile proteins were not investigated in the present study. Because NO-cGMP signaling pathway also modulates the excitation–contraction coupling via the desensitization mechanism of myofibril to Ca^{2+} in the heart,[38] it is possible that KPE may influence the coupling between Ca^{2+} and contractility.

REFERENCES

1. Tewtrakul S, Subhadhirasakul S, Kummee S. Anti-allergic activity of compounds from Kaempferia parviflora. *J Ethnopharmacol*. 2008;116:191–193.
2. Wattanapitayakul SK, Suwatronnakorn M, Chularojmontri L, et al. Kaempferia parviflora ethanolic extract promoted nitric oxide production in human umbilical vein endothelial cells. *J Ethnopharmacol*. 2007;110:559–562.
3. Temkitthawon P, Hinds TR, Beavo JA, et al. Kaempferia parviflora, a plant used in traditional medicine to enhance sexual performance contains large amounts of low affinity PDE5 inhibitors. *J Ethnopharmacol*. 2011;137:1437–1441.
4. Tep-areenan P, Ingkaninan K, Randall MD. Mechanisms of Kaempferia parviflora extract (KPE)-induced vasorelaxation in the rat aorta. *Asian Biomed*. 2010;4:103–111.
5. Tep-areenan P, Sawasdee P, Randall M. Possible mechanisms of vasorelaxation for 5,7-dimethoxyflavone from Kaempferia parviflora in the rat aorta. *Phytother Res*. 2010;24:1520–1525.
6. Tep-areenan P, Sawasdee P. Vasorelaxant effects of 5,7,4-trimethoxyflavone from Kaepmferia parviflora in the rat aorta. *Int J Pharmacol*. 2010;6:419–424.
7. Bruckdorfer R. The basics about nitric oxide. *Mol Aspects Med*. 2005;26:3–31.
8. Chaturapanich G, Chaiyakul S, Verawatnapakul V, et al. Effects of Kaempferia parviflora extracts on reproductive parameters and spermatic blood flow in male rats. *Reproduction*. 2008;136:515–522.
9. Wattanapitayakul SK, Chularojmontri L, Herunsalee A, et al. Vasorelaxation and antispasmodic effects of Kaempferia parviflora ethanolic extract in isolated rat organ studies. *Fitoterapia*. 2008;79:214–216.
10. Malakul W, Thirawarapan S, Ingkaninan K, et al. Effects of Kaempferia parviflora Wall. Ex Baker on endothelial dysfunction in streptozotocin-induced diabetic rats. *J Ethnopharmacol*. 2011;133:371–377.
11. Weerateerangkul P, Surinkaew S, Chattipakorn S, et al. Effects of Kaempferia parviflora Wall. Ex. Baker on electrophysiology of the swine hearts. *Indian J Med Res*. 2012. In press. AU3
12. Shinlapawittayatorn K, Sungnoon R, Chattipakorn S, et al. Effects of sildenafil citrate on defibrillation efficacy. *J Cardiovasc Electrophysiol*. 2006;17:292–295.
13. Kanlop N, Shinlapawittayatorn K, Sungnoon R, et al. Sildenafil citrate on the inducibility of ventricular fibrillation and upper limit of vulnerability in swine. *Med Sci Monit*. 2008;14:BR205–BR209.
14. Han J, Kim E, Lee SH, et al. cGMP facilitates calcium current via cGMP-dependent protein kinase in isolated rabbit ventricular myocytes. *Pflugers Arch*. 1998;435:388–393.
15. Gallo MP, Ghigo D, Bosia A, et al. Modulation of guinea-pig cardiac L-type calcium current by nitric oxide synthase inhibitors. *J Physiol*. 1998;506(pt 3):639–651.
16. Zahradníková A, Minarovic I, Venema RC, et al. Inactivation of the cardiac ryanodine receptor calcium release channel by nitric oxide. *Cell Calcium*. 1997;22:447–454.
17. Khan SA, Skaf MW, Harrison RW, et al. Nitric oxide regulation of myocardial contractility and calcium cycling: independent impact of neuronal and endothelial nitric oxide synthases. *Circ Res*. 2003;92:1322–1329.
18. Favory R, Lancel S, Tissier S, et al. Myocardial dysfunction and potential cardiac hypoxia in rats induced by carbon monoxide inhalation. *Am J Respir Crit Care Med*. 2006;174:320–325.
19. Ortiz MC, Fortepiani LA, Ruiz-Marcos FM, et al. Role of AT1 receptors in the renal papillary effects of acute and chronic nitric oxide inhibition. *Am J Physiol*. 1998;274:R760–R766.
20. Zhou ZH, Deng HW, Li YJ. Involvement of calcitonin gene-related peptide in the development of tolerance to nitroglycerin in the rat. *Eur J Pharmacol*. 2001;427:137–141.
21. Egorova MV, Afanas'ev SA, Popov SV. A simple method for isolation of cardiomyocytes from adult rat heart. *Bull Exp Biol Med*. 2005;140:370–373.

22. Xu YJ, Shao Q, Dhalla NS. Fura-2 fluorescent technique for the assessment of Ca2+ homeostasis in cardiomyocytes. *Mol Cell Biochem*. 1997; 172:149–157.
23. Jaipetch T, Reutrakul V, Tuntiwachwuttikul P, et al. Flavonoids in the black rhizomes of Boesenbergia pandurata. *Phytochemistry*. 1983;22:625–626.
24. Herunsalee A, Pancharoen O, Tuntiwachwuttikul P. Further studies of flavonoids of the black rhizomes Boesenbergia pandurata. *J Sci Soc Thailand*. 1987;13:119–122.
25. Yenjai C, Prasanphen K, Daodee S, et al. Bioactive flavonoids from Kaempferia parviflora. *Fitoterapia*. 2004;75:89–92.
26. Sutthanut K, Sripanidkulchai B, Yenjai C, et al. Simultaneous identification and quantitation of 11 flavonoid constituents in Kaempferia parviflora by gas chromatography. *J Chromatogr A*. 2007;1143:227–233.
27. Ruckstuhl M, Beretz A, Anton R, et al. Flavonoids are selective cyclic GMP phosphodiesterase inhibitors. *Biochem Pharmacol*. 1979;28:535–538.
28. Dell'Agli M, Galli GV, Bosisio E. Inhibition of cGMP-phosphodiesterase-5 by biflavones of Ginkgo biloba. *Planta Med*. 2006;72:468–470.
29. Dell'Agli M, Galli GV, Vrhovsek U, et al. In vitro inhibition of human cGMP-specific phosphodiesterase-5 by polyphenols from red grapes. *J Agric Food Chem*. 2005;53:1960–1965.
30. Ahmmed GU, Xu Y, Hong DP, et al. Nitric oxide modulates cardiac Na (+) channel via protein kinase A and protein kinase G. *Circ Res*. 2001;89: 1005–1013.
31. Bai CX, Namekata I, Kurokawa J, et al. Role of nitric oxide in Ca2+ sensitivity of the slowly activating delayed rectifier K+ current in cardiac myocytes. *Circ Res*. 2005;96:64–72.
32. Gómez R, Núñez L, Vaquero M, et al. Nitric oxide inhibits Kv4.3 and human cardiac transient outward potassium current (Ito1). *Cardiovasc Res*. 2008;80:375–384.
33. Bers DM. Calcium cycling and signaling in cardiac myocytes. *Annu Rev Physiol*. 2008;70:23–49.
34. Stowe DF, Varadarajan SG, An J, et al. Reduced cytosolic Ca(2+) loading and improved cardiac function after cardioplegic cold storage of guinea pig isolated hearts. *Circulation*. 2000;102:1172–1177.
35. Brack KE, Patel VH, Mantravardi R, et al. Direct evidence of nitric oxide release from neuronal nitric oxide synthase activation in the left ventricle as a result of cervical vagus nerve stimulation. *J Physiol*. 2009;587(pt 12):3045–3054.
36. Paulis L, Zicha J, Kunes J, et al. Regression of L-NAME-induced hypertension: the role of nitric oxide and endothelium-derived constricting factor. *Hypertens Res*. 2008;31:793–803.
37. Shiels HA, White E. The Frank-Starling mechanism in vertebrate cardiac myocytes. *J Exp Biol*. 2008;211(pt 13):2005–2013.
38. Massion PB, Feron O, Dessy C, et al. Nitric oxide and cardiac function: ten years after, and continuing. *Circ Res*. 2003;93: 388–398.

ARCHIVES OF ORAL BIOLOGY 57 (2012) 252–256

Available online at www.sciencedirect.com

SciVerse ScienceDirect

journal homepage: http://www.elsevier.com/locate/aob

Low-dose dental irradiation decreases oxidative stress in osteoblastic MC3T3-E1 cells without any changes in cell viability, cellular proliferation and cellular apoptosis

Sakarat N. Pramojanee [a,b], *Wasana Pratchayasakul* [b], *Nipon Chattipakorn* [b], *Siriporn C. Chattipakorn* [a,b,*]

[a] *Department of Oral Biology and Diagnostic Science, Faculty of Dentistry, Chiang Mai University, Thailand*
[b] *Cardiac Electrophysiology Research and Training Center, Department of Physiology, Faculty of Medicine, Chiang Mai University, Chiang Mai 50200, Thailand*

ARTICLE INFO

Article history:
Accepted 5 September 2011

Keywords:
Dental irradiation
Osteoblasts
Cyclin D1
Bax
Bcl-2

ABSTRACT

Cellular responses following low-dose irradiation have been widely debated. Several studies have revealed detrimental effects of low-dose irradiation; however, some studies have shown contrasting results. Moreover, the effects of periapical irradiation on osteoblastic cells have not yet been revealed. Therefore, in this study, we tested the hypothesis that low-dose dental irradiation of osteoblastic cells reduces reactive oxygen species (ROS) production and leads to increased cellular proliferation and high-dose dental irradiation of osteoblastic cells increases ROS production and leads to cellular apoptosis.

Methods: We irradiated MC3T3-E1 cells with various doses of periapical irradiation (0, 1, 2, 5 and 10 doses, 1.5 mGy/dose). We evaluated cell viability using MTT assay, the expression of Bax and Bcl-2, as markers for apoptosis and the expression of cyclin D1 as a marker for cell proliferation 24 h after each irradiation. We also measured ROS production 4 h following each irradiation.

Results: ROS production was significantly reduced after one dose of periapical irradiation (1.5 mGy); however, after 10 doses (15 mGy), ROS production was significantly increased ($p < 0.05$). None of the doses of dental radiation affected cell viability as determined by MTT assay, nor did they change the apoptotic marker: (the Bax/Bcl-2 ratio). However, 10 doses of dental irradiation significantly decreased the expression of cyclin D1.

Conclusions: Our findings suggest that low-dose dental radiation may help to detoxify osteoblastic cells by reducing ROS production without any changes in cell viability, cellular apoptosis or proliferation. However, high-dose dental radiation impairs osteoblastic proliferation via increase ROS production without any changes in cell viability or apoptotic responses.

1. Introduction

It is well accepted that high-dose irradiation (>1 Gy) causes a deleterious effect on cellular organisms, such as the induction of DNA damage and cell cycle arrest, in a dose-dependent manner, which lead to the impairment of cell proliferation and cell death through the apoptotic process.[1] However, the effects of low-dose irradiation (<1 Gy) on cellular responses remain

* *Corresponding author at*: Department of Oral Biology and Diagnostic Science, Faculty of Dentistry, Chiang Mai University, Chiang Mai 50200, Thailand. Tel.: +66 53 944451; fax: +66 53 9222844.
E-mail addresses: scchattipakorn@gmail.com, s.chat@chiangmai.ac.th (S.C. Chattipakorn).
0003–9969/$ – see front matter
doi:10.1016/j.archoralbio.2011.09.004

unclear. Several previous studies have revealed the detrimental effects of low-dose irradiation on cells, such as increases in reactive oxygen species (ROS) formation,[2] DNA double-strand breaks[3], chromosomal breakage[4]. However, some studies have shown contrasting results of low-dose irradiation. For example: (1) several studies have suggested that low-dose irradiation (<50 mGy) induces cell proliferation in various cell types, such as human lung fibroblasts[5], normal human diploid cells[6], Chinese hamster fibroblasts[7], neuron cells[8], and bone marrow cells[9]. (2) Ahmed and colleagues have suggested that cyclin D1 expression, an important regulator of G1 to S-phase transition in the cell cycle involving cellular proliferation, is up-regulated by low-dose ionising radiation (100 mGy) in human keratinocytes with adaptive radioresistance.[10] (3) Previous *in vitro* and *in vivo* studies have reported that low-dose irradiation (250–500 mGy) can detoxify the deleterious effects of radiation-induced ROS formation by increasing intracellular glutathione and superoxide dismutase production 3–6 h post-irradiation.[11–13]

Dental irradiation is classified as low-dose irradiation, since intraoral radiography can produce only 3.9 mGy of irradiation.[14] Low-dose irradiation may be harmful to oral tissues, particularly oral bone cells. In addition, a recent clinical study has demonstrated that extra-oral panoramic radiography can induce chromosomal damage to oral mucosal cells 10 days post-irradiation.[4] Branemark and colleagues have recommended of not performing dental irradiation procedures immediately after dental implantation due to the possibility of the detrimental effects of dental irradiation on the healing and remodelling of bone.[15] However, the effects of intra-oral radiography, particularly periapical irradiation of bone cells, have not yet been studied.

Therefore, in this study, we aimed to determine the effects of low doses of dental irradiation on osteoblastic cells by measuring cell viability, ROS production, and the apoptotic process by using an apoptotic marker (the ratio of Bax and Bcl-2) as well as cellular proliferation by using a cellular proliferative marker (cyclin D1).

2. Materials and methods

2.1. Osteoblastic cell culture

Murine osteoblastic MC3T3-E1 cells were cultured in complete Dulbecco's modified Eagles medium (DMEM), containing 10% foetal bovine serum (FBS), Penicillin G (100 U/ml), Streptomycin sulphate (100 μg/ml), Amphotericin B (25 μg/ml) and L-glutamine (2 mM) at 37 °C in 95% air/5% CO_2. When the cells reached confluence, they were subcultured using 0.025% EDTA trypsin. The cells were seeded at a density of 5000 cells/well in a 96-well plate for measurement of intracellular reactive oxygen species and cell viability, and 400,000 cells/dish in 35 mm tissue culture dishes for protein extraction. The plates were incubated at 37 °C in a CO_2 incubator for 24 h before dental irradiation.

2.2. Cell irradiation

The cultures were irradiated with 0 (the controls), 1, 5 and 10 multiples of a standard dose for a periapical film radiograph, using a portable dental X-ray machine generator (NOMAD™, Aribex, Inc., Orem, UT, USA). The radiographic parameters for one dose were 60 kVp, 2.3 mA, 0.4 s. The focal-object distance was 7.5 in. One-dose periapical irradiation was 1.5 mGy as measured by an X-ray test device (NERO mAx 8000®, Fluke Biomedical, Cleveland, OH, USA). Multiples of 1.5 mGy were delivered acutely and without any time interval between the fractions. Four hours after irradiation, the cells were collected for the intracellular reactive oxygen species analysis. Changes in cell viability and the expression of Bcl-2, Bax and cyclin D1 were determined after irradiation, as described below.

2.3. Determination of intracellular ROS

The formation of ROS was evaluated using the oxidation-sensitive dye 2,7-dichlorofluorescein diacetate (DCFH-DA). The cell cultures that had been exposed to dental radiation were treated with 5 μmol/l DCFH-DA in de-ionised (DI) water for 30 min. The fluorescence intensity was determined within 5 min thereafter using a Fluostar Optima microplate spectrofluorometer (BMG Lab Technologies, Offenburg, Germany) at 485 nm excitation and 540 nm emission.[16]

2.4. MTT assay for cell viability

The viability of the MC3T3-E1 cells was investigated by MTT conversion after aspiration of the culture supernatants. Monolayers of MC3T3-E1 cells were replenished with culture medium and 50 μl MTT reagent [5 mg/ml in phosphate buffered saline (PBS)] were added. Culture plates were then incubated for 4 h at 37 °C in a humidified atmosphere (5% CO_2/95% air), after which the cells were washed twice with PBS. After the supernatants were aspirated off again, 200 μl dimethyl sulfoxide was added, and the optical density was measured at 570 nm using an automated plate reader (Spectramax 340PC; Molecular Devices, Sunnyvale, CA, USA). All experiments were performed in triplicate.

2.5. Bcl-2, Bax, and cyclin D1 expression by western blot analysis

Cells were suspended in 200 μl lysis buffer [10 mM Tris–HCl, pH 7.4, 0.1% (SDS)] and supplemented with a protease inhibitor cocktail (Roche complete mini-tablets, Roche Molecular Biochemicals, Indianapolis, IND, USA). Samples were left on ice for 20 min and centrifuged at 14,000 × *g* for 10 min at 4 °C, and the supernatant was collected. Protein concentration was determined using a bicinchoninic acid (BCA) protein assay kit (Pierce, Rockford, IL, USA). Proteins were separated by gel electrophoresis and transferred to nitrocellulose membranes. Blots were incubated in 5% nonfat dried milk-TBS for 1 h at room temperature, followed by incubation with primary antibodies to cyclin D1(1:200), Bax(1:400), Bcl-2 (1:200) and β-actin (1:400) (Santa Cruz Biotechnology, Santa Cruz, CA, USA) overnight at 4 °C. After washing three times in TBS, the blots were incubated with horse radish peroxidase (HRP)-conjugated secondary antibodies for 1 h at room temperature. Bands were detected using the enhanced chemiluminescence kit (Amersham Biosciences, Piscataway, NJ, USA) and Kodak X-Omat Blue Film (Eastman Kodak, Rochester, NY, USA). Band

intensity was quantified by the Scion Image program and the results were shown as average signal intensity (arbitrary units).

2.6. Statistical analysis

Data were expressed as mean ± standard error (SE). The data were analysed using the Mann–Whitney *U* test to compare between all different experimental groups. Significance was assessed when $p < 0.05$. Statistical analyses were performed using the SPSS software, version 13.0 (SPSS Version 13.0, SPSS, Chicago, IL).

3. Results

3.1. Dental radiation has no effect on cell viability

Osteoblastic MC3T3-E1 cells were irradiated with 0 (0 mGy), 1 (1.5 mGy), 5 (7.5 mGy), 10 (15 mGy) multiples of a standard dose for a periapical film radiograph and cell viability was determined by MTT assay 24 h post-irradiation, since radiation-induced apoptosis begins delayed to a peak and extends to over about 24 h.[19] There were no statistically significant differences in MTT activity in irradiated osteoblastic cells between the individual doses and the non-irradiated controls, as shown in Fig. 1. These findings suggest that dental irradiation did not affect cell viability 24 h following irradiation.

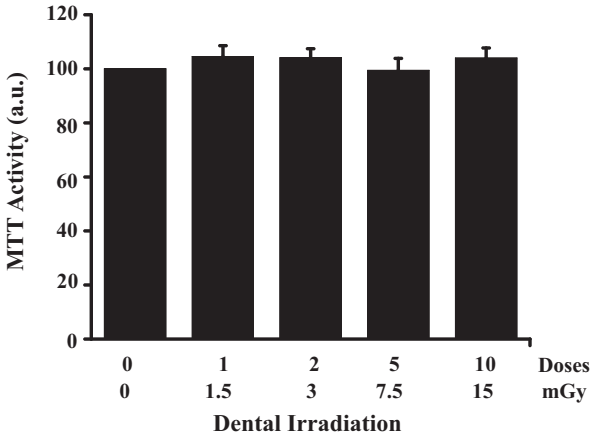

Fig. 1 – The effects of dental irradiation on cell viability. Osteoblastic cells were irradiated with 0, 1, 2, 5, 10 multiples of a standard doses of for a periapical film radiography (1.5 mGy/dose). Cell viability was assessed 24 h post-irradiation using MTT assay ($n = 5$). All doses of dental radiation did not affect the entire population of osteoblasts. Values represent the mean ± SE.

3.2. Low-dose dental irradiation reduces ROS production; however, high dose irradiation increases ROS production

Osteoblastic MC3T3-E1 cells were irradiated with 0, 1, 5, 10 multiples of a standard dose for a periapical film radiograph and intracellular ROS production was determined by a fluorescent probe, [2′,7′-dichlorofluorescein diacetate (DCFH-DA)] 4 h post-irradiation. We determined ROS production 4 h post-irradiation because it has been shown that the level of antioxidant is at maximal levels 4 h after irradiation.[20] We found that one dose (1.5 mGy) of dental irradiation significantly decreased intracellular ROS production, but, 10 doses (15 mGy) of dental radiation significantly increased ROS production 4 h following irradiation when compared with the non-irradiated controls, as shown in Fig. 2.

3.3. Dental irradiation has no effects on the apoptotic process, but possibly decreases the cellular proliferation in osteoblastic cells

We investigated the expression of proteins that are linked to cell proliferation (cyclin D1) and cellular apoptosis (Bax/Bcl-2) 24 h after dental irradiation. We found that 10 doses dental irradiation significantly decreased cyclin D1 in osteoblastic cells when compared with the non-irradiated controls, as shown in Fig. 3. However, the ratio of Bax/Bcl-2 expression from osteoblastic cells demonstrated no statistical difference between irradiated cells and the controls. The average ratio of Bax/Bcl-2 after 0, 1, 5 and 10 doses of dental irradiation were 1 ± 0.0, 1.052 ± 0.33, 0.998 ± 0.061 and 1.128 ± 0.113, respectively. These findings suggest that high doses of dental irradiation impair osteoblastic cell proliferation; however, the dental irradiation did not induce apoptotic activity in osteoblastic cells.

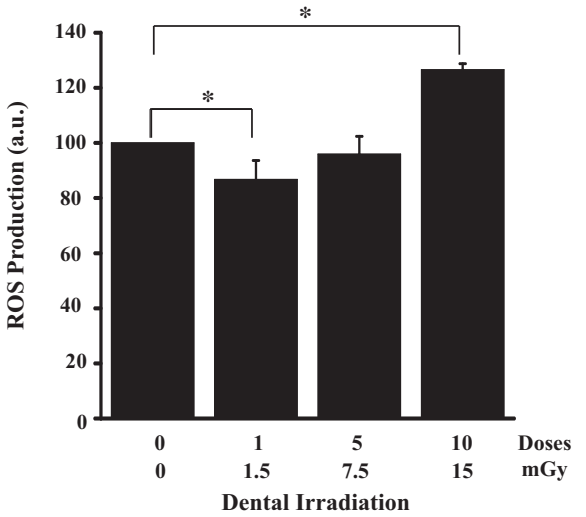

Fig. 2 – The effects of dental irradiation on intracellular ROS production. Osteoblastic cells were irradiated with 0, 1, 5, 10 multiples of a standard dose for a periapical film radiography (1.5 mGy/dose) ($n = 5$). ROS production was assessed 4 four hours post-irradiation using a fluorescent probe, 2′,7′dichlorofluorescein diacetete (DCFH-DA). The ROS production was significantly reduced after one-dose of periapical radiography. However, after 10 doses of periapical radiation ROS production was significantly increased. Values represent mean ± SE. * $p < 0.05$ compared to the controls (0 mGy).

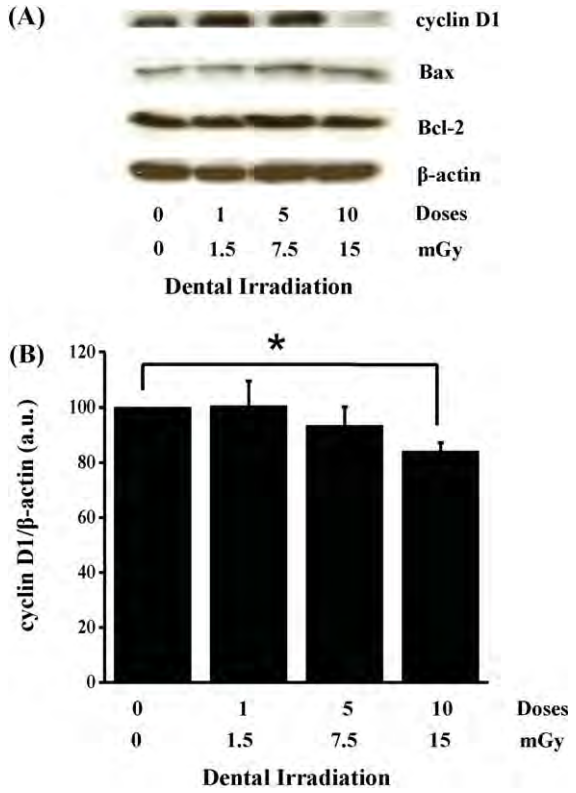

Fig. 3 – The effect of dental irradiation on cyclin D1, Bax and Bcl-2 expression. (A) A representative western blot analysis is shown. The western blot analyses were carried out on total protein lysates from cells irradiated with 0, 1, 5, 10 multiples of a standard dose for a periapical film radiography (1.5 mGy/dose) ($n = 4$). β-Actin was used as a loading control. (B) The levels of protein cyclin D1 significantly decreased when irradiated with 10 doses of periapical radiography (15 mGy) ($n = 4$). Values represent mean ± SE. $^{*}p < 0.05$ compared to the controls (0 mGy).

4. Discussion

This is the first *in vitro* study demonstrating that periapical doses of irradiation affect osteoblastic cells. A previous clinical study illustrated that panoramic radiography induces chromosomal damage in oral mucosal cells.[4] However, that finding cannot explain the various effects of dental irradiation on other types of oral cells because radiation responses depend on several factors, such as cell types, cell radiosensitivity, radiation dose and radiation dose-rate.[17]

The present study revealed that one dose of dental irradiation of about 1.5 mGy to osteoblastic cells significantly reduces ROS formation 4 h post-irradiation, but ROS production is significantly increased by 10 doses of periapical irradiation (15 mGy). Consistent with our findings, a previous study showed that after low-dose whole body irradiation (500 mGy) of mouse splenocytes, the level of glutathione, an antioxidant agent, increased and reached the maximal levels 4 h post-irradiation.[18] Therefore, a decrease in ROS production following 1.5 mGy irradiation of osteoblastic cells may be associated with an increase in the intracellular glutathione level. Several *in vitro* and *in vivo* studies have shown that low-dose irradiation can induce glutathione 3–6 h following irradiation.[11–13] In contrast to 1-dose dental irradiation, the intracellular ROS production significantly increased, accompanied by decreased cell proliferation, as determined by decreasing cyclin D1 expression, when osteoblastic cells were irradiated with 10 doses of periapical irradiation (15 mGy). Cyclin D1 plays a regulatory role in cell cycle progression, especially during the G1 to S transitional phase. It has been shown that the reduction of cyclin D1 expression is associated with induction of G1 cell cycle arrest in differentiated osteoblasts.[19] Thus, the 15 mGy irradiation may be high enough to cause arrest of the G1/S cell cycle in osteoblastic cells and to impair cellular proliferation, as shown by the reduction of cyclin D1 expression.

Radiation induced-apoptosis is one cellular response to severe DNA damage resulting from irradiation. The apoptosis occurs approximately 24 h following irradiation, as indicated by an increase in the Bax/Bcl-2 ratio.[20,21] Our findings indicate that 15 mGy of dental irradiation is not high enough to induce osteoblastic cell death through the apoptotic process 24 h post-irradiation because the ratio of Bax to Bcl-2 and the MTT activity of irradiated osteoblastic cells did not differ from that of the controls. However, irradiated cells with DNA damage may not die immediately but they may undergo several cell division cycles before reaching a critical genomic instability in an apparent dose related manner, as shown in a previous study.[22] Therefore, our study demonstrated a short term effect of dental irradiation on osteoblastic cells. The long-term effects of dental irradiation on osteoblastic cells should be further investigated.

The deleterious effects of dental irradiation on osteoblastic cells might be associated with the degree of intracellular ROS production by irradiation. Hydrogen peroxide is an important ROS produced from chemical changes in water after exposure to ionising radiation. Davies proposed that responses to ROS, particularly hydrogen peroxide, depend on its concentration.[23] Exposure to very low concentrations of hydrogen peroxide (3–15 μM) causes cellular growth stimulation. One hundred and twenty to 150 μM of hydrogen peroxide causes a temporary growth arrest in order to protect cells from excess energy use and DNA damage. A further increase to 500–1000 μM of hydrogen peroxide causes cellular apoptosis. Our findings suggest that the level of hydrogen peroxide generated from 10 doses of periapical irradiation, 15 mGy, is enough to cause cell cycle arrest in G1/S in osteoblastic cells but it is insufficient for the induction of apoptotic cell death.

We conclude that dental irradiation causes various effects in osteoblastic cells depending on the dose of irradiation. Low-dose dental irradiation, or 1.5 mGy, seems to have a radio-adaptive response by detoxifying ROS as indicated by lowering ROS formation 4 h post-irradiation, whereas high-dose dental irradiation, or 15 mGy, impairs cellular proliferation. These results provide further support for the principle of ALARA (As Low As Reasonably Achievable). However, *in vivo* findings may be similar or different from our present study since radiation intensity is normally absorbed by soft tissues (i.e. skin and gingival) before reaching the osteoblasts. Furthermore, genotypic differences can play a role in this case due to different

radiosensitivity.[21] Future studies in *in vivo* are needed to elucidate this hypothesis.

Funding

This study was supported by the grants from the Faculty of Dentistry, Chiang Mai University (SP), and the Thailand Research Fund grants BRG5480003 (SC) and RTA5280006 (NC).

Competing interest

None.

Ethical approval

Not required.

Acknowledgements

The authors thank all the staff in the Cardiac Electrophysiology Research and Training Center, Department of Physiology, Faculty of Medicine, Chiang Mai University for their technical assistance, and Prof. M. Kevin O' Carroll, Professor Emeritus, University of Mississippi School of Dentistry, USA, and Faculty Consultant, Faculty of Dentistry, Chiang Mai University, Thailand, for his editorial assistance.

REFERENCES

1. Verheij M, Bartelink H. Radiation-induced apoptosis. *Cell Tissue Res* 2000;**301**(1):133–42.
2. Sangsuwan T, Haghdoost S. The nucleotide pool, a target for low-dose gamma-ray-induced oxidative stress. *Radiat Res* 2008;**170**(6):776–83.
3. Asaithamby A, Chen DJ. Cellular responses to DNA double-strand breaks after low-dose gamma-irradiation. *Nucleic Acids Res* 2009;**37**(12):3912–23.
4. Cerqueira EM, Meireles JR, Lopes MA, Junqueira VC, Gomes-Filho IS, Trindade S, et al. Genotoxic effects of X-rays on keratinized mucosa cells during panoramic dental radiography. *Dentomaxillofac Radiol* 2008;**37**(7):398–403.
5. Kim CS, Kim JK, Nam SY, Yang KH, Jeong M, Kim HS, et al. Low-dose radiation stimulates the proliferation of normal human lung fibroblasts via a transient activation of Raf and Akt. *Mol Cells* 2007;**24**(3):424–30.
6. Suzuki K, Kodama S, Watanabe M. Extremely low-dose ionizing radiation causes activation of mitogen-activated protein kinase pathway and enhances proliferation of normal human diploid cells. *Cancer Res* 2001;**61**(14):5396–401.
7. Korystov YN, Eliseeva NA, Kublik LN, Narimanov AA. The effect of low-dose irradiation on proliferation of mammalian cells in vitro. *Radiat Res* 1996;**146**(3):329–32.
8. Kang JO, Hong SE, Kim SK, Kim CJ, Lee TH, Chang HK, et al. Adaptive responses induced by low dose radiation in dentate gyrus of rats. *J Korean Med Sci* 2006;**21**(6):1103–7.
9. Li W, Wang G, Cui J, Xue L, Cai L. Low-dose radiation (LDR) induces hematopoietic hormesis: LDR-induced mobilization of hematopoietic progenitor cells into peripheral blood circulation. *Exp Hematol* 2004;**32**(11):1088–96.
10. Ahmed KM, Fan M, Nantajit D, Cao N, Li JJ. Cyclin D1 in low-dose radiation-induced adaptive resistance. *Oncogene* 2008;**27**(53):6738–48.
11. Kawakita Y, Ikekita M, Kurozumi R, Kojima S. Increase of intracellular glutathione by low-dose gamma-ray irradiation is mediated by transcription factor AP-1 in RAW 264.7 cells. *Biol Pharm Bull* 2003;**26**(1):19–23.
12. Kojima S, Matsuki O, Kinoshita I, Gonzalez TV, Shimura N, Kubodera A. Does small-dose gamma-ray radiation induce endogenous antioxidant potential in vivo? *Biol Pharm Bull* 1997;**20**(6):601–4.
13. Kojima S, Matsuki O, Nomura T, Kubodera A, Honda Y, Honda S, et al. Induction of mRNAs for glutathione synthesis-related proteins in mouse liver by low doses of gamma-rays. *Biochim Biophys Acta* 1998;**1381**(3):312–8.
14. Napier ID. Reference doses for dental radiography. *Br Dent J* 1999;**186**(8):392–6.
15. Branemark PI, Zarb GA, Albrektsson T, editors. *Tissue-integrated prostheses: osseointegration in clinical dentistry*. Chicago: Quintessence; 1985.
16. Carini M, Aldini G, Piccone M, Facino RM. Fluorescent probes as markers of oxidative stress in keratinocyte cell lines following UVB exposure. *Farmaco* 2000;**55**(8):526–34.
17. White SC, Pharoah MJ. Biologic effects of radiation. In: White S.C.P MJ, editor. *Oral radiology: principles and interpretation*. 6th ed. New Delhi: Elsevier Inc.; 2009. p. 18–30.
18. Kojima S. Induction of glutathione and activation of immune functions by low-dose, whole-body irradiation with gamma-rays. *Yakugaku Zasshi* 2006;**126**(10):849–57.
19. Datta NS, Chen C, Berry JE, McCauley LK. PTHrP signaling targets cyclin D1 and induces osteoblastic cell growth arrest. *J Bone Miner Res* 2005;**20**(6):1051–64.
20. Borovitskaya AE, Evtushenko VI, Sabol SL. Gamma-radiation-induced cell death in the fetal rat brain possesses molecular characteristics of apoptosis and is associated with specific messenger RNA elevations. *Brain Res Mol Brain Res* 1996;**35**(1-2):19–30.
21. Williams JR, Zhang Y, Zhou H, Russell J, Gridley DS, Koch CJ, et al. Genotype-dependent radiosensitivity: clonogenic survival, apoptosis and cell-cycle redistribution. *Int J Radiat Biol* 2008;**84**(2):151–64.
22. Seymour CB, Mothersill C, Alper T. High yields of lethal mutations in somatic mammalian cells that survive ionizing radiation. *Int J Radiat Biol Relat Stud Phys Chem Med* 1986;**50**(1):167–79.
23. Davies KJ. The broad spectrum of responses to oxidants in proliferating cells: a new paradigm for oxidative stress. *IUBMB Life* 1999;**48**(1):41–7.

PPARγ Agonist Improves Neuronal Insulin Receptor Function in Hippocampus and Brain Mitochondria Function in Rats with Insulin Resistance Induced by Long Term High-Fat Diets

Noppamas Pipatpiboon, Wasana Pratchayasakul, Nipon Chattipakorn, and Siriporn C. Chattipakorn

Neuroelectrophysiology Unit, Cardiac Electrophysiology Research and Training Center (N.P., W.P., N.C., S.C.C.), Faculty of Medicine; Department of Oral Biology and Diagnostic Science (S.C.C.), Faculty of Dentistry; and Biomedical Engineering Center (N.C., S.C.C.), Chiang Mai University, Chiang Mai 50200 Thailand

We previously demonstrated that a high-fat diet (HFD) consumption can cause not only peripheral insulin resistance, but also neuronal insulin resistance. Moreover, the consumption of an HFD has been shown to cause mitochondrial dysfunction in both the skeletal muscle and liver. Rosiglitazone, a peroxizome proliferator-activated receptor-γ ligand, is a drug used to treat type 2 diabetes mellitus. Recent studies suggested that rosiglitazone can improve learning and memory in both human and animal models. However, the effects of rosiglitazone on neuronal insulin resistance and brain mitochondria after the HFD consumption have not yet been investigated. Therefore, we tested the hypothesis that rosiglitazone improves neuronal insulin resistance caused by a HFD via attenuating the dysfunction of neuronal insulin receptors and brain mitochondria. Rosiglitazone (5 mg/kg · d) was given for 14 d to rats that were fed with either a HFD or normal diet for 12 wk. After the 14th week, all animals were euthanized, and their brains were removed and examined for insulin-induced long-term depression, neuronal insulin signaling, and brain mitochondrial function. We found that rosiglitazone significantly improved peripheral insulin resistance and insulin-induced long-term depression and increased neuronal Akt/PKB-ser phosphorylation in response to insulin. Furthermore, rosiglitazone prevented brain mitochondrial conformational changes and attenuated brain mitochondrial swelling, brain mitochondrial membrane potential changes, and brain mitochondrial ROS production. Our data suggest that neuronal insulin resistance and the impairment of brain mitochondria caused by a 12-wk HFD consumption can be reversed by rosiglitazone. **(*Endocrinology* 153: 329–338, 2012)**

Insulin resistance is a pathological condition, in which target tissues cannot respond to plasma insulin at the optimal plasma insulin concentration (1). Several studies have suggested that peripheral insulin resistance is correlated with cognitive decline (2–5). In addition, a previous study by our group has shown that a 12-wk high-fat diet (HFD) consumption caused not only peripheral insulin resistance, but also neuronal insulin resistance by impairment of insulin receptor (IR) function (6).

In the central nervous system, brain mitochondria play an important role in energy-demanding neurotransmission and in controlling calcium homeostasis (7). Furthermore, mitochondria are important for ATP production via oxidative phosphorylation. Disruption of electron transport chains can lead to decreased ATP with increased reactive oxygen species (ROS) production (8, 9). Insulin resistance has been shown to dysregulate both glucose and lipid metabolisms and decrease the activity of mitochon-

ISSN Print 0013-7227 ISSN Online 1945-7170
Printed in U.S.A.

doi: 10.1210/en.2011-1502 Received July 14, 2011. Accepted October 27, 2011.
First Published Online November 22, 2011

Abbreviations: aCSF, Artificial cerebrospinal fluid; fEPSP, field excitatory postsynaptic potential; HFD, high-fat diet; HFR, HFD with rosiglitazone treatment; HFV, vehicle-treated HFD subgroup; HOMA, homeostasis model assessment; IR, insulin receptor; LTD, long-term depression; ND, normal diet; NDR, ND with rosiglitazone treatment; NDV, vehicle-treated ND subgroup; OGTT, oral glucose tolerance test; PPARγ, peroxizome proliferator-activated receptor γ; ROS, reactive oxygen species; SOD, superoxide dismutase.

drial oxidative phosphorylation (7, 10, 11). Recent studies have demonstrated that the consumption of a HFD leads to peripheral insulin resistance and also increases ROS production in adipocytes and liver (12–15). Those findings suggest that IR dysfunction may correlate with the dysfunction of mitochondria.

Rosiglitazone, a peroxizome proliferator-activated receptor γ (PPARγ) agonist, has been used for the treatment of type 2 diabetes and insulin resistance by increasing insulin sensitivity (1, 16). PPARγ is not only expressed in peripheral tissues but also in the central nervous system, including the hippocampus, an important area for learning and memory (17). Previous studies have demonstrated that rosiglitazone might improve learning and memory in both human and animal models (18–23). For example, rosiglitazone improved learning and memory as demonstrated in the Morris Water Maze test of HFD rats (22), prevented the effect of Aβ-induced neurodegeneration in Alzheimer's disease mouse models (17, 23), and promoted mitochondria biogenesis in mouse brain (24). However, the effect of rosiglitazone on neuronal insulin resistance and brain mitochondrial dysfunction induced by a HFD consumption has not yet been investigated. Therefore, in this study, we hypothesized that rosiglitazone improves not only peripheral insulin resistance but also neuronal insulin resistance via attenuating the dysfunction of neuronal IR, neuronal insulin signaling, and brain mitochondria, caused by HFD consumption.

Materials and Methods

Animals

Male Wistar rats weighing 180–200 g (n = 48) from the National Laboratory Animal Center, Salaya Campus, Mahidol University, Thailand, were used for this study. All experiments were conducted in accordance with an approved protocol from the Faculty of Medicine, Chiang Mai University Institutional Animal Care and Use Committee, in compliance with National Institutes of Health guidelines. The animals were randomized into two groups: a control group that consumed a normal diet (ND), standard laboratory chow, which had an energy content of 4.02 kcal/g, and 19.77% of total energy (%E) of the food from fat (Mouse Food no. 082, C.P. Co., Bangkok, Thailand) and a high-fat group that received an HFD, which had an energy content of 5.35 kcal/g and contained fat mostly from lard (59.28% E) for a period of 12 wk (6). The animals were given free access to the diet and drinking water. To determine the peripheral insulin resistance, the body weight of each animal was measured every other week, and blood sampling from a tail vein was performed at wk 12 and 14 after fasting for 5 h to measure glucose, cholesterol, and insulin levels. Blood samples for glucose assay were kept on ice in NaF microcentrification tubes, whereas blood samples for cholesterol and insulin assay were kept on ice in EDTA microcentrification tubes. All plasma was stored at −80 C for subsequent biochemical analysis.

After 12 wk, rats in both the ND and HFD groups (n = 24/group) were divided into two subgroups (n = 12/subgroup). Each subgroup received orally either 5 mg/kg · d of rosiglitazone (Cayman Chemical Co., Ann Arbor, MI) (dissolved in normal saline 2 ml/kg · d) for 14 consecutive days or a vehicle (normal saline, 2 ml/kg · d) for 14 consecutive days. At the end of the experimental period, the animals in each subgroup were killed to study either neuronal IR function [insulin-induced long-term depression (LTD) protocol and neuronal insulin-signaling protocol (n = 6)] or brain mitochondrial function (mitochondrial swelling, mitochondrial membrane potential ($\Delta\psi_m$), and mitochondrial ROS production) (n = 6). Before death, all animals were tested for glucose tolerance using the oral glucose tolerance test (OGTT).

Plasma analysis

Plasma glucose and cholesterol concentrations were determined using colorimetric assay, using a commercially available kit (Biotech, Bangkok, Thailand). Plasma insulin level was measured by Sandwich ELISA (LINCO Research, St. Charles, MO), with the mean intraassay variation of 1.33% and interassay variation of 6.71%.

Determination of insulin resistance [homeostasis model assessment (HOMA) index]

Insulin resistance was assessed by the HOMA index (25, 26), a mathematical model describing the degree of insulin resistance, calculated from fasting plasma insulin and fasting plasma glucose concentration. A higher HOMA index indicates a higher degree of insulin resistance. The HOMA index was determined by the following equation:

[Fasting plasma insulin (μU/ml)] × [fasting plasma glucose (mmol/liter)]/22.5

OGTT

The OGTT was performed after the rats had been fasting overnight (12 h). Then the rats received a bolus of glucose (2.0 g/kg body weight) via gavage feeding, and plasma glucose of blood samples were collected from a tail vein at 0, 30, 60, 90, and 120 min after the administration of glucose in NaF microcentrification tubes. Plasma glucose was collected and analyzed using colorimetric assay (Biotech, Bangkok, Thailand) (6).

Preparation of brain slices and insulin stimulation

Rats were killed with isoflurane and decapitated. The brains were rapidly removed. After that, the brains were immersed in ice-cold high-sucrose artificial cerebrospinal fluid (aCSF), containing (in millimolar concentration) NaCl, 85; KCl, 2.5; $MgSO_4$, 4; $CaCl_2$, 0.5; NaH_2PO_4, 1.25; $NaHCO_3$, 25; glucose, 25; sucrose, 75; kynurenic acid, 2; ascorbate, 0.5, saturated with 95% O_2/5% CO_2 (pH 7.4). That solution enhanced neuronal survival during the slicing procedure. Hippocampal slices (400 μm)were cut using a vibratome (Vibratome Co., Saint Louis, MO). After a 30-min postslice incubation in high-sucrose aCSF, the brain slices were transferred to a standard aCSF solution containing (in millimolar concentration) NaCl, 119; KCl, 2.5; $CaCl_2$, 2.5; $MgSO_4$, 1.3; NaH_2PO_4, 1; $NaHCO_3$, 26; and glucose, 10; saturated with 95% O_2/5% CO_2 (pH 7.4) for an ad-

ditional 30 min at room temperature (22–24 C). Some brain slices (n = 5–6 brain slices per animal) were used for extracellular recording. Some brain slices (n = 5–6 brain slices per animal) were used to investigate neuronal insulin signaling. In neuronal insulin-signaling protocols, brain slices with/without insulin stimulation were used by placing the brain slices into either aCSF plus insulin 500 nM (Humulin R, Eli Lilly, Giessen, Germany) or aCSF for 5 min. Then, those slices were homogenated for immunoblotting as described in a previous study (6).

Extracellular recording of hippocampal slices for insulin-induced LTD

To examine insulin-induced long term depression (LTD) as described previously, the brain slices were transferred to a submersion recording chamber and continuously perfused at 3–4 ml/min with standard aCSF warmed to 25–28 C. Field excitatory postsynaptic potentials (fEPSP) were evoked by stimulating the Schaffer collateral-commissural pathway with a bipolar tungsten electrode, whereas the fEPSP recordings were taken from the stratum radiatum of the hippocampal CA1 region with micropipettes (3 Mohm) filled with 2 M NaCl. A stimulus frequency of 0.033 Hz was used, and the stimulus intensity was adjusted to yield a fEPSP of 0.8–1.0 mV in amplitude, which produced less than 50% of the maximal monophasic response. The brain slices were perfused with aCSF (to establish a baseline condition) for 10 min, and then perfused with aCSF plus 500 nM insulin (to produce insulin-induced LTD) for an additional 10 min. Thereafter, the slices were perfused with aCSF again for a further 50 min and the fEPSP were recorded. Data were filtered at 3 kHz, digitized at 10 kHz, and stored in a computer using pClamp 9.2 software (Axon Instruments, Foster City, CA). The initial slopes of the fEPSP were measured and plotted against time, as described in a previous study (6).

Immunoblotting for neuronal insulin signaling

To investigate the expression of IR, Akt/PKB, and insulin-mediated Akt Ser473 phosphorylation, homogenated brain slices from each subgroup were boiled at 95 C, for 5 min. Then, proteins were separated by electrophoresis on 10% polyacrylamide gels (SDS-PAGE) (Bio-Rad Laboratories, Inc., Hercules, CA), and transferred into polyvinylidene difluoride membranes. After blocking with 5% nonfat milk/TBST, immunoblotting was conducted with IR, Akt, Akt Ser473 antibody, and β-actin (rabbit polyclonals, 1:2000 in TBST; Santa Cruz Biotechnology, Inc., Santa Cruz, CA) overnight. Membranes were incubated with a secondary goat antirabbit antibody, conjugated with horseradish peroxidase (1:8000 in TBST, Bio-Rad Laboratories), and the protein bands were visualized on Amersham hyperfilm ECL using the Amersham ECL Western blotting detection reagents system (GE Healthcare, Buckinghamshire, UK). Band intensity was quantified by the Scion Image program (Scion Corp., Frederick, MD), and the results were shown as average signal intensity (arbitrary units).

Preparation of brain mitochondria

Brain mitochondria were isolated according to the protocol described in a previous study (27). The whole brain was removed and put into an ice-cold MSE solution (225 mM mannitol; 75 mM sucrose; 1 mM EGTA; 5 mM HEPES; 1 mg/ml BSA, pH 7.4) to wash out the blood rapidly. Each brain was transferred to 10 ml ice-cold MSE-nagarse solution (0.05% nagarse in MSE solution) and homogenized at 600 rpm/min using a homogenizer. Next, the tissues were minced and centrifuged at 2000 $\times$ *g* for 4 min, and the supernatants were then collected and centrifuged at 12,000 $\times$ *g* for 11 min. Next, brain mitochondrial pellets were collected and resuspended in a 10-ml ice-cold MSE-digitonin solution (0.02% digitonin in MSE solution) to break down the synaptosome fraction, and the resulting brown pellets were collected. Finally, the pellets were minced with respiration buffer (150 mM KCl, 5 mM HEPES, 5 mM $K_2HPO_4.3H_2O$, 2 mM L-glutamate, 5 mM pyruvate sodium salt) (28). Mitochondrial proteins were determined by BCA assay as described in a previous study (29).

Brain mitochondrial swelling assay

Isolated mitochondrial swelling was assessed by measuring changes in the absorbance of the suspension wavelength at 540 nm using a microplate reader. Brain mitochondria (0.4 mg/ml) were incubated in 2 ml of respiration buffer (containing 150 mM KCl, 5 mM HEPES, 5 mM $K_2HPO_4.3H_2O$, 2 mM L-glutamate, 5 mM pyruvate sodium salt). Decreasing absorbance represents mitochondrial swelling.

Brain mitochondrial membrane potential ($\Delta\psi_m$) assay

The brain mitochondrial membrane potential was measured by fluorescent dye JC-1 (5,50,6,60-tetrachloro-1,10,3,30-tetraethylbenzimidazole carbocyanine iodide), which accumulates in mitochondria. JC-1 dye, a monomer form, enters mitochondria and produces a green fluorescence (emission wavelength at 530 nm) at low mitochondrial membrane potential, whereas at high mitochondrial membrane potential, JC-1 dye changes its form to be a JC-1 aggregate form, which produces a red fluorescence (emission wavelength at 590 nm). The depolarization of brain mitochondrial membrane potential is indicated by a decreased red/green fluorescence intensity ratio.

The isolated brain mitochondria (0.4 mg/ml) were strained with JC-1 dye at 37 C for 15 min, after which the fluorescence intensity was determined using a fluorescence microplate reader. JC-1 monomer form (green) fluorescence was excited at 485 nm, and the emission was detected at 530 nm. JC-1 aggregate form (red) fluorescence was excited at 485 nm, and emission fluorescence was detected at 590 nm (29).

Brain mitochondrial ROS assay

Isolated brain mitochondria were stained by 2′,7′-dichlorohydro-fluorescein diacetate that can pass through the cell membrane and is hydrolyzed by intracellular esterase. ROS oxidizes dichlorohydro-fluorescein and converts dichlorohydro-fluorescein to 2′,7′ dichlorodihydro-fluorescein diacetate, which is highly fluorescent at 485 nm, and the emission was detected at 528 nm. Therefore, ROS production causes an increase in fluorescence intensity. The isolated neuronal mitochondria (0.4 mg/ml) were stained with 2 μM 2′,7′ dichlorohydro-fluorescein diacetate and incubated at room temperature for 20 min. The fluorescence intensity was detected using a fluorescence microplate reader as described in a previous study (29).

TABLE 1. Effect of rosiglitazone on body weight, visceral fat, cholesterol, glucose, insulin, HOMA index, and OGTT AUC (area under the curve) in rats fed with ND and HFD

Parameter	NDV	NDR	HFV	HFR
Body weight (g)	431.50 ± 5.68	460.33 ± 4.13[a]	546.25 ± 12.10[a,b]	603.3 ± 9.86[a,b,c]
Visceral fat (g)	25.22 ± 1.11	32.57 ± 1.26[a]	47.94 ± 2.88[a,b]	61.90 ± 3.61[a,b,c]
Cholesterol (mg/dl)	234.78 ± 6.38	227.67 ± 6.82	301.45 ± 9.81[a,b]	251.55 ± 8.24[b,c]
Glucose (mg/dl)	130.88 ± 4.26	101.39 ± 3.25[a]	140.68 ± 3.65[b]	122.01 ± 2.14[b,c]
Insulin (ng/ml)	1.72 ± 0.13	1.84 ± 0.14	3.85 ± 0.18[a,b]	2.05 ± 0.08[c]
HOMA index	9.80 ± 0.51	8.11 ± 0.44	24.06 ± 1.26[a,b]	10.8 ± 0.56[b,c]
OGTT AUC (a.u.)	45,814 ± 789	39,875 ± 895[a]	63,020 ± 1026[a,b]	49,722 ± 935[a,b,c]

[a] $P \leq 0.05$ *vs.* NDV; [b] $P \leq 0.05$ *vs.* NDR; [c] $P \leq 0.05$ *vs.* HFR.

Data analysis

Data were recorded as mean ± SE. For all comparisons, the significant differences in body weight and peripheral biochemical parameters were calculated using one-way ANOVA followed by Fisher's least significant difference *post hoc* analysis. The percentages of insulin-induced LTD and brain mitochondrial experiments were calculated using Student's *t* test. $P < 0.05$ was considered to be statistically significant.

Results

Rosiglitazone reduced peripheral insulin resistance in HFD-fed rats

The effects of rosiglitazone on body weight, visceral fat, and biochemical parameters in plasma are shown in Table 1. The 14-wk HFD-fed rats had a significantly increased body weight, visceral fat, plasma cholesterol level, plasma insulin level, and HOMA index, compared with the ND-fed rats ($P < 0.05$). Rats from both dietary groups that were treated with rosiglitazone (5 mg/kg · d, 14 d) had significantly increased body weight and visceral fat, compared with the vehicle groups ($P < 0.05$). Rosiglitazone significantly decreased plasma cholesterol level, plasma insulin level, and HOMA index in only HFD-fed rats ($P < 0.05$), but significantly decreased plasma glucose level in both dietary groups ($P < 0.05$).

For the glucose tolerance test, the mean area under the curve of the vehicle-treated HFD subgroup (HFV) was significantly greater than that of the vehicle-treated ND subgroup (NDV) (Table 1). The administration of rosiglitazone significantly decreased the area under the curve in both dietary groups ($P < 0.05$).

Rosiglitazone improved neuronal IR function in HFD-fed rats

The characteristics of insulin-induced LTD are shown in Fig. 1A. Insulin of various concentrations (from 0 to 1000 nM) was applied onto the hippocampal slices from the NDV rats to determine the effect of insulin-induced LTD. We found that this effect was dose dependent. In this study, 500 nM insulin was used to investigate the insulin-induced LTD in the hippocampus because it has been shown previously that 500 nM insulin is the optimal dose to determine insulin-induced LTD and to measure the IR function (6, 30, 31).

In the HFV group, an HFD could attenuate insulin-induced LTD, compared with the NDV group (Fig. 1B). In both NDV and ND with rosiglitazone treatment (NDR) groups, the application of insulin led to insulin-induced LTD, and the phenomenon was stabilized at a level of 74.43% and 80.79% of preinsulin baseline, for the NDV and NDR, respectively (Fig. 1C). In the HFD groups, the insulin-induced LTD in the vehicle-treated HFD group was significantly reduced, with the mean percentage depression of insulin-induced LTD of 5.7 ± 4.6% of the preinsulin baseline (Fig. 1D). However, rosiglitazone treatment in the HFD rats could completely abolish the impairment of insulin-induced LTD caused by the HFD found in the HFD group (insulin-induced LTD: 64.3 ± 4.8% of preinsulin baseline, Fig. 1D). These findings suggest that HFD consumption could cause the neuronal IR dysfunction and ROS could prevent this undesired effect.

To confirm whether rosiglitazone can reverse or enhance neuronal insulin signaling of neuronal insulin resistance after HFD, the Ser473 phosphorylation of Akt/PKB between both dietary groups, either with or without rosiglitazone treatment, was investigated. The serine 473 phosphorylation of Akt/PKB was used as a marker for the neuronal IR signaling activity, because we previously showed that neuronal insulin resistance after HFD consumption led to the reduction of serine 473 phosphorylation of Akt/PKB (6). In this study, we found that, without insulin stimulation, the protein levels of IR, Akt/PKB and the serine phosphorylation of Akt/PKB in all treated subgroups, *i.e.* ND with vehicle treatment (NDV), ND with rosiglitazone treatment (NDR), HFV, and HFD with rosiglitazone treatment (HFR), were not significantly different (Fig. 2, A, B, and C, respectively). However, with insulin stimulation the serine phosphorylation of Akt/PKB in the HFV subgroup was significantly decreased, com-

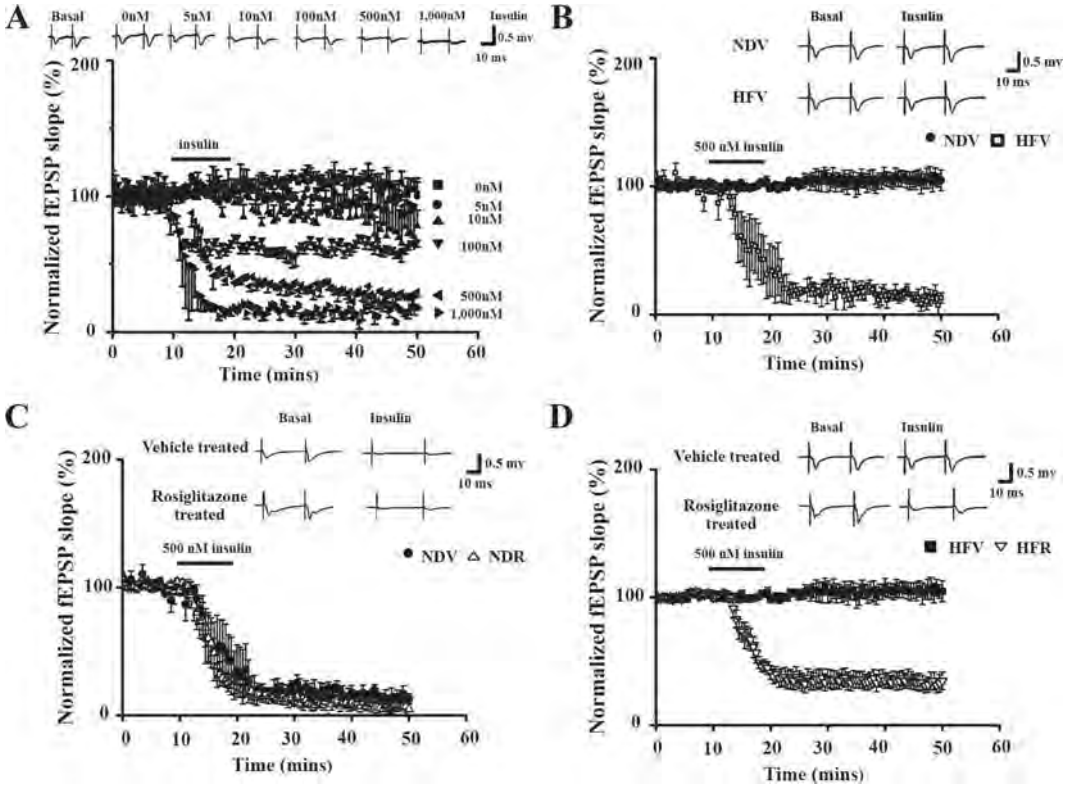

FIG. 1. HFD feeding significantly diminished the ability of insulin to induce LTD in the CA1 hippocampus. Rosiglitazone, 14 d after 12-wk HFD, significantly improved the ability of insulin to induce LTD in the CA1 hippocampus. A, The phenomenon of insulin-induced LTD in NDV animals (n = 3/dose). B, Insulin-induced LTD in the brain slices from NDV and HFV subgroup, confirming the impairment of insulin-induced LTD in CA1 hippocampus after HFD feeding. C, Insulin-induced LTD in the brain slices from NDV and NDR subgroup. D, Insulin-induced LTD in the brain slices from HFV and HFR subgroup. *Inset* in each panel shows examples of averages of 20 consecutive traces taken from a slice treated with aCSF (basal) and with 500 nM (insulin). A–D, A summary of averages of normalized fEPSP (fEPSPt/fEPSPo with fEPSP being points at which fEPSP slopes stabilized) from NDV (n = 6–8 independent slices), NDR (n = 6–8 independent slices) brain slices, HFV(n = 6–8 independent slices), and HFR (n = 6–8 independent slices) brain slices. There were no differences between the insulin-induced LTD in NDV and NDR subgroups. However, the HFR subgroup showed a significant increase in insulin-induced LTD compared with the HFV subgroup.

pared with the NDV subgroup ($P < 0.05$, Fig. 2D). The administration of rosiglitazone significantly increased Akt/PKB phosphorylation with insulin stimulation in only the HFD group ($P < 0.05$, Fig. 2D). All of these findings indicate that rosiglitazone could attenuate the neuronal insulin resistance induced by HFD consumption by preserving both neuronal IR function and neuronal IR signaling.

Rosiglitazone reduced brain mitochondrial dysfunction from HFD consumption

In addition to the effect of rosiglitazone on improving the neuronal insulin resistance induced by HFD consumption, we further investigated whether rosiglitazone can improve brain mitochondrial dysfunction after HFD consumption. We investigated the dysfunction of brain mitochondria by measuring brain mitochondrial swelling, brain ROS production, and brain mitochondrial membrane potentials ($\Delta\psi_m$). We found that brain mitochondrial morphology in the HFV subgroup was changed, with the mitochondria unfolding and swelling, whereas rosiglitazone treatment did not change the brain mitochondrial morphology in the HFD subgroup (Fig. 3A).

To investigate the brain mitochondrial swelling, we measured the absorbance of brain mitochondria in all four treatment subgroups (NDV, NDR, HFV, HFR). The absorbance of brain mitochondria in the HFV subgroup was decreased compared with that in the NDV subgroup, indicating that brain mitochondria in the HFV subgroup were swollen (Fig. 3B). In HFD rats, we found that the absorbance of brain mitochondria in the rosiglitazone-treated (HFR) subgroup was significantly increased, compared with that in the vehicle-treated (HFV) subgroup (Fig. 3B). These findings suggest that rosiglitazone can attenuate brain mitochondrial swelling after HFD consumption. We also demonstrated that the HFV subgroup had significantly increased ROS levels after H_2O_2 application, compared with the NDV subgroup (Fig. 4A). Rosiglitazone treatment significantly reduced brain mitochondrial ROS levels in both dietary groups during oxidative stress stimulation (Fig. 4A).

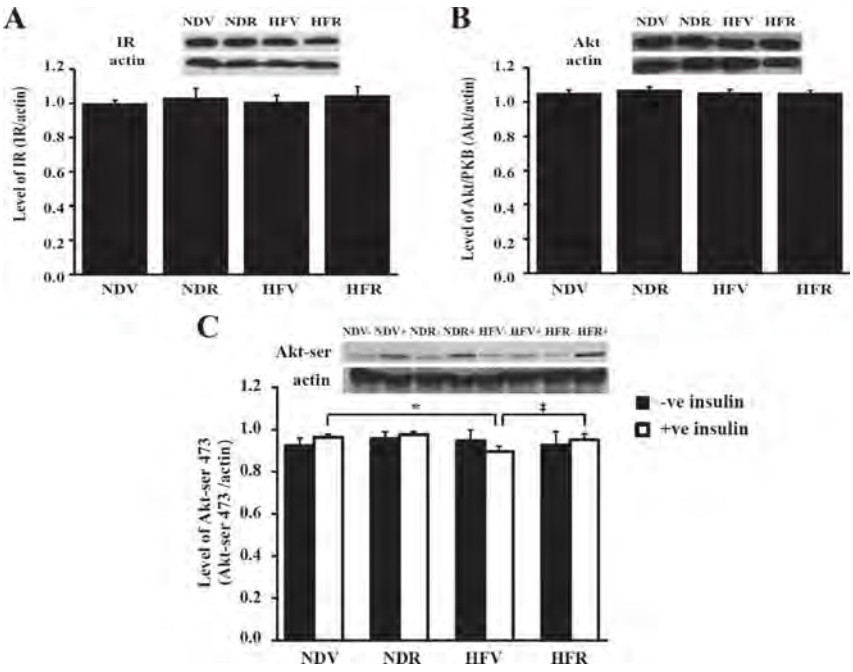

FIG. 2. A and B, There was no change in the protein levels of IR (A) and Akt/PKB (B) in any group. All immunoblot lanes were loaded with the same amount of protein (30 μg/lane). C, The Ser473 phosphorylation did not change in any group without insulin stimulation. Rosiglitazone significantly improved insulin-induced phosphorylation of Akt/PKB at Ser473 residue in HFD consumption. Insulin-induced phosphorylation of Akt/PKB at Ser473 residue was significantly weakened in HFV group ($P < 0.05$). However, insulin-induced phosphorylation of Akt/PKB at Ser473 of the HFR subgroup significantly increased compared with the HFV subgroup ($P < 0.05$). All immunoblotting lanes were loaded with the same amount of protein (60 μg/lane). *, $P < 0.05$ *vs.* NDV; ‡, $P < 0.05$ *vs.* HFV.

For brain mitochondrial membrane potential change, we found that the rate of $\Delta\psi_m$ changes in the HFV subgroup was greater than that in the NDV subgroup after H_2O_2 application (Fig. 4B). Rosiglitazone treatment decreased the rate of $\Delta\psi_m$ changes in both dietary groups (Fig. 4B). These findings suggest that brain mitochondria in the HFV subgroup were more depolarized than in the NDV subgroup during oxidative stress stimulation, and that rosiglitazone can attenuate the mitochondrial membrane depolarization caused by HFD consumption. All of these mitochondrial findings suggest that HFD consumption can lead to brain mitochondrial dysfunction and that rosiglitazone can attenuate the brain mitochondrial dysfunction caused by HFD.

Discussion

The major findings of our study are as follows: 1) rosiglitazone prevents the impairment of neuronal insulin-induced LTD in neuronal insulin-resistant rats caused by HFD consumption; 2) rosiglitazone improves IR signaling dysfunction by increasing ser 473 Akt/PKB phosphorylation in neuronal insulin-resistant rats caused by HFD consumption; 3) HFD consumption can cause brain mitochondrial dysfunction; and 4) rosiglitazone reverses the brain mitochondrial dysfunction by preventing mitochondrial swelling, decreasing ROS production, and attenuating brain mitochondrial membrane potential changes, particularly during oxidative stress stimulation.

Consistent with our previous study (6), we also found that 14-wk HFD-fed rats (59.28% energy of fat) exhibited not only peripheral insulin resistance, as indicated by excessive body weight gain and visceral fat, hypercholesterolemia, hyperinsulinemia, increased HOMA index, and the impairment of OGTT, but also neuronal insulin resistance indicated by decreased insulin-induced LTD. Previous studies have shown that HFD consumption can impair neuronal function, such as the impairment of spatial learning in both radial arm maze and Morris Water Maze tests in rats (22, 32), the reduction of hippocampal dendritic spines (4), the reduction of long-term potentiation (4), increased brain malondialdehyde (33), and decreased brain-derived neurotrophic factor (4). In this study, we have demonstrated, for the first time, that 14-wk HFD consumption can cause brain mitochondrial dysfunction. Consumption of HFD has been shown to increase ROS production in kidney, liver, and skeletal muscle (34, 35), decrease mitochondrial sizes and numbers in liver and muscle (36), and reduce mitochondrial membrane potential in the liver (13, 37). In our study, HFD consumption disturbs brain mitochondrial functions, as indicated by mitochondrial morphological changes, increased swelling, increased ROS production, and mitochondrial depolarization.

Brain mitochondria are important organelles for maintaining intracellular Ca^{2+} levels and play an important role in synaptic transmission (38). The dysfunction of brain mitochondria has been shown to cause the impairment of synaptic plasticity (38). In our study, the brain mitochondrial dysfunction may be responsible for the impairment of insulin-induced LTD in rats fed with HFD. Increased brain mitochondrial ROS production caused by HFD consumption may cause the opening of mitochondrial permeability transition, leading to brain mitochondrial swelling and the depolarization of mitochondrial membrane potential (29, 39). These ROS-mediated mitochondrial changes can induce Akt dephosphorylation

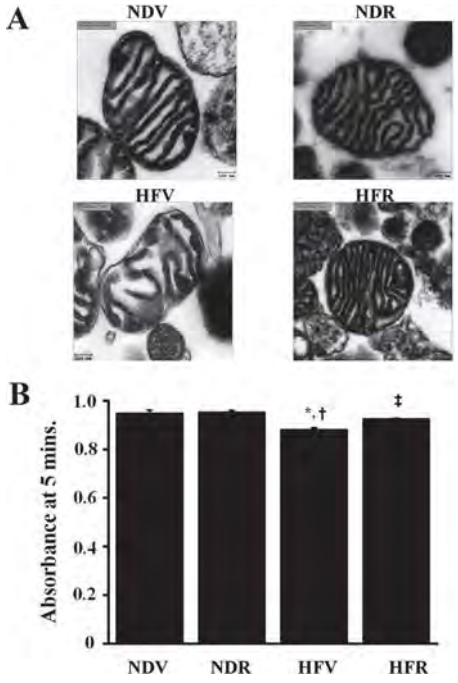

FIG. 3. A, Transmission electron microscopy (original magnification, ×25,000) shows the ultrastructure of brain mitochondria in NDV, NDR, HFV, and HFR. Rosiglitazone prevented the morphology change after HFD consumption. *Scale bar*, 1:100 nm. B, HFD consumption induced mitochondrial swelling as measured by absorbance at 540 nm. Rosiglitazone significantly decreased mitochondrial swelling in both dietary groups. *, $P < 0.05$ *vs.* NDV; †, $P < 0.05$ *vs.* NDR; ‡, $P < 0.05$ *vs.* HFV.

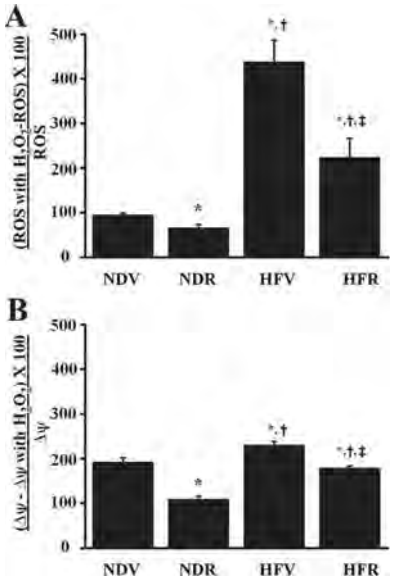

FIG. 4. A, Brain mitochondrial ROS production was measured by fluorescent dye during 2 mM H_2O_2 application onto brain mitochondria. Rosiglitazone significantly reduced ROS production after H_2O_2 application in both ND and HFD consumption. B, HFD consumption induced an increase in mitochondrial membrane potential change ($\Delta\psi_m$) during 2 mM H_2O_2 application to brain mitochondria, measured by fluorescent dye. Rosiglitazone significantly decreased brain mitochondrial membrane potential change ($\Delta\psi_m$) after H_2O_2 application in both ND and HFD consumption. *, $P < 0.05$ *vs.* NDV; †, $P < 0.05$ *vs.* NDR; ‡, $P < 0.05$ *vs.* HFV.

at Ser-473 (40), indicating the disruption of downstream insulin signaling. Therefore, neuronal insulin resistance induced by HFD consumption might be developed from the brain mitochondrial dysfunction.

Rosiglitazone has been shown to increase the expression of IR and stimulate tyrosine phosphorylation of IR in the brown adipocytes of fetal rats (41). In our study, rosiglitazone increased Akt/PKB ser-473 phosphorylation in the HFD subgroup and also tended to increase that in the NDV subgroup. An increase in the phosphorylation of Akt/PKB may be responsible for the improvement of insulin-induced LTD in rosiglitazone-treated HFD rats, because increased Akt/PKB phosphorylation can lead to increased intracellular Ca^{2+} levels, thus restoring the insulin-induced LTD in the brain (31).

Because rosiglitazone can cross the blood-brain barrier rapidly after ip administration (42), the effect of rosiglitazone on brain function may be the result of direct interaction of rosiglitazone with neurons. Several studies support the direct effects of rosiglitazone on neurons. First, the administration of rosiglitazone to HFD rats can improve learning and memory, as demonstrated in the Morris Water Maze test (21, 22). Second, rosiglitazone can increase dendritic spine density in neuronal culture models (43). Third, in the Tg2576 mouse model for Alzheimer's disease, rosiglitazone can reduce amyloid peptide 42 in the brain (21). Those previous reports and the findings in this study suggest that rosiglitazone passes the blood-brain barrier and may act directly in the brain to improve neuronal IR function as well as improve peripheral insulin sensitivity.

This study has also shown that rosiglitazone protects brain mitochondrial dysfunction caused by HFD by preserving conformational changes, preventing mitochondrial swelling, attenuating ROS production, and decreasing mitochondrial membrane potential dissipation. Rosiglitazone has been shown to have neuroprotective effects (44) and has beneficial effects on brain mitochondria (45–47). Rosiglitazone increases the production of at least two antioxidant agents, Cu/Zn-superoxide dismutase (SOD) and Mn-SOD, in traumatic brain injury, leading to decreased ROS production (48). It also increases SOD activity and decreases lipid peroxidation production (49), resulting in decreased ROS production. Furthermore, rosiglitazone, in a dose-dependent manner, increase mitochondrial activity by regulating ATP production and transcription of mitochondrial structural proteins and cellular antioxidant enzymes, thus attenuating ROS level (50). Moreover, rosiglitazone prevents the depolarization of mitochondrial membrane potential in brain oxygen-glucose deprivation followed by reoxygenation (51, 52).

Rosiglitazone protects hippocampal and dorsal root ganglion neurons against Aβ-induced mitochondrial damage and nerve growth factor deprivation-induced apoptosis by up-regulation of Bcl-2 (46). Those previous findings suggest that the role of PPARγ agonists is to help in mitochondrial biogenesis and the repair of mitochondria during cellular injury or cell death. Consistent with those previous studies, our study showed that rosiglitazone can reduce brain mitochondrial dysfunction caused by 12-wk HFD consumption by reducing ROS production and decreasing mitochondrial membrane depolarization. It has also been shown that the reduction of ROS production can prevent the dissipation of mitochondrial membrane potential (48). In addition, keeping ROS production at a low level has been shown to improve insulin signaling (53). Therefore, the effects of rosiglitazone in reducing brain mitochondrial dysfunction may be one of the reasons that rosiglitazone improves neuronal insulin sensitivity in the brain. In addition, the improvement of brain mitochondrial dysfunction found in the rosiglitazone-treated group could also improve other metabolic control in the brain such as the hypothalamic insulin signaling, which plays an important role in maintaining normal glucose homeostasis (54).

In conclusion, our findings suggest that rosiglitazone improves not only peripheral insulin resistance but also neuronal insulin resistance in hippocampal regions caused by HFD consumption. The improvement of neuronal insulin sensitivity may occur via the effect of rosiglitazone on attenuating brain mitochondrial dysfunction. Therefore, PPARγ agonists may be a useful medicine to ameliorate neuronal insulin resistance.

Limitation of this study

Although the direct evidence whether rosiglitazone acted directly on the brain to attenuate the neuronal insulin resistance and brain mitochondrial dysfunction induced by HFD consumption was not provided in this study, it has been clearly shown previously that rosiglitazone could pass the blood-brain barrier (42). In that study, they determined the brain concentration of rosiglitazone in normal male gerbils receiving ip injection of rosiglitazone at a dose of 3 mg/kg. They found that the mean concentration of rosiglitazone in the brain increased during the first 15 min and reached a plateau at 90–120 min, suggesting that rosiglitazone could pass blood-brain barrier even in a normal condition. Nevertheless, it is possible that rosiglitazone could also improve the peripheral insulin resistance and other systemic effects, subsequently resulting in improvement of neuronal insulin resistance caused by a HFD consumption. Furthermore, the change in the PPARγ target gene in the brain was not investigated in the present study. Finally, because the function of IR and the phosphorylation of Akt in response to insulin were analyzed in the hippocampal slices, the effects on other neuronal populations could be similar or different according to their anatomical areas.

Acknowledgments

We thank Professor M. Kevin O Carroll (Professor Emeritus, University of Mississippi, Oxford, MI, and Faculty Consultant, Chiang Mai University, Thailand), for his editorial assistance.

Address all correspondence and requests for reprints to: Siriporn Chattipakorn, D.D.S., Ph.D., Department of Oral Biology and Diagnostic Science, Faculty of Dentistry, Chiang Mai University, Chiang Mai, 50200, Thailand. E-mail: s.chat@chiangmai.ac.th.

This work was supported by grants from the Thailand Research Fund BRG 5480003 (to S.C.), RTA 5280006 (to N.C.), CHE-Ph.D.-SW Scholarship (to N.P., S.C.), Royal Golden Jubilee PhD. program (to W.P., S.C.) under Office of the Higher Education Commission, Ministry of Education, Thailand and Faculty of Dentistry, Chiang Mai University (to S.C.).

Disclosure Summary: The authors have nothing to disclose.

References

1. **Guo L, Tabrizchi R** 2006 Peroxisome proliferator-activated receptor γ as a drug target in the pathogenesis of insulin resistance. Pharmacol Ther 111:145–173
2. **Craft S** 2005 Insulin resistance syndrome and Alzheimer's disease: age- and obesity-related effects on memory, amyloid, and inflammation. Neurobiol Aging 26(Suppl 1):65–69
3. **Craft S** 2007 Insulin resistance and Alzheimer's disease pathogenesis: potential mechanisms and implications for treatment. Curr Alzheimer Res 4:147–152
4. **Stranahan AM, Norman ED, Lee K, Cutler RG, Telljohann RS, Egan JM, Mattson MP** 2008 Diet-induced insulin resistance impairs hippocampal synaptic plasticity and cognition in middle-aged rats. Hippocampus 18:1085–1088
5. **Greenwood CE, Winocur G** 2005 High-fat diets, insulin resistance and declining cognitive function. Neurobiol Aging 26(Suppl 1): 42–45
6. **Pratchayasakul W, Kerdphoo S, Petsophonsakul P, Pongchaidecha A, Chattipakorn N, Chattipakorn SC** 2011 Effects of high-fat diet on insulin receptor function in rat hippocampus and the level of neuronal corticosterone. Life Sci 88:619–627
7. **Wang CH, Wang CC, Wei YH** 2010 Mitochondrial dysfunction in insulin insensitivity: implication of mitochondrial role in type 2 diabetes. Ann N Y Acad Sci 1201:157–165
8. **Johannsen DL, Ravussin E** 2009 The role of mitochondria in health and disease. Curr Opin Pharmacol 9:780–786
9. **Rabøl R, Boushel R, Dela F** 2006 Mitochondrial oxidative function and type 2 diabetes. Appl Physiol Nutr Metab 31:675–683
10. **Möhlig M, Isken F, Ristow M** 2004 Impaired mitochondrial activity and insulin-resistant offspring of patients with type 2 diabetes. N Engl J Med 350:2419–2421
11. **Befroy DE, Petersen KF, Dufour S, Mason GF, de Graaf RA, Rothman DL, Shulman GI** 2007 Impaired mitochondrial substrate oxi-

dation in muscle of insulin-resistant offspring of type 2 diabetic patients. Diabetes 56:1376–1381
12. **Bournat JC, Brown CW** 2010 Mitochondrial dysfunction in obesity. Curr Opin Endocrinol Diabetes Obes 17:446–452
13. **Vial G, Dubouchaud H, Couturier K, Cottet-Rousselle C, Taleux N, Athias A, Galinier A, Casteilla L, Leverve XM** 2011 Effects of a high-fat diet on energy metabolism and ROS production in rat liver. J Hepatol 54:348–356
14. **Lin Y, Berg AH, Iyengar P, Lam TK, Giacca A, Combs TP, Rajala MW, Du X, Rollman B, Li W, Hawkins M, Barzilai N, Rhodes CJ, Fantus IG, Brownlee M, Scherer PE** 2005 The hyperglycemia-induced inflammatory response in adipocytes: the role of reactive oxygen species. J Biol Chem 280:4617–4626
15. **Talior I, Yarkoni M, Bashan N, Eldar-Finkelman H** 2003 Increased glucose uptake promotes oxidative stress and PKC-δ activation in adipocytes of obese, insulin-resistant mice. Am J Physiol Endocrinol Metab 285:E295–E302
16. **Handschin C, Spiegelman BM** 2006 Peroxisome proliferator-activated receptor gamma coactivator 1 coactivators, energy homeostasis, and metabolism. Endocr Rev 27:728–735
17. **Inestrosa NC, Godoy JA, Quintanilla RA, Koenig CS, Bronfman M** 2005 Peroxisome proliferator-activated receptor γ is expressed in hippocampal neurons and its activation prevents β-amyloid neurodegeneration: role of Wnt signaling. Exp Cell Res 304:91–104
18. **Abbatecola AM, Lattanzio F, Molinari AM, Cioffi M, Mansi L, Rambaldi P, DiCioccio L, Cacciapuoti F, Canonico R, Paolisso G** 2010 Rosiglitazone and cognitive stability in older individuals with type 2 diabetes and mild cognitive impairment. Diabetes Care 33: 1706–1711
19. **Gold M, Alderton C, Zvartau-Hind M, Egginton S, Saunders AM, Irizarry M, Craft S, Landreth G, Linnamägi U, Sawchak S** 2010 Rosiglitazone monotherapy in mild-to-moderate Alzheimer's disease: results from a randomized, double-blind, placebo-controlled phase III study. Dement Geriatr Cogn Disord 30:131–146
20. **Rodriguez-Rivera J, Denner L, Dineley KT** 2011 Rosiglitazone reversal of Tg2576 cognitive deficits is independent of peripheral gluco-regulatory status. Behav Brain Res 216:255–261
21. **Pedersen WA, McMillan PJ, Kulstad JJ, Leverenz JB, Craft S, Haynatzki GR** 2006 Rosiglitazone attenuates learning and memory deficits in Tg2576 Alzheimer mice. Exp Neurol 199:265–273
22. **Pathan AR, Gaikwad AB, Viswanad B, Ramarao P** 2008 Rosiglitazone attenuates the cognitive deficits induced by high fat diet feeding in rats. Eur J Pharmacol 589:176–179
23. **Escribano L, Simón AM, Pérez-Mediavilla A, Salazar-Colocho P, Del Río J, Frechilla D** 2009 Rosiglitazone reverses memory decline and hippocampal glucocorticoid receptor down-regulation in an Alzheimer's disease mouse model. Biochem Biophys Res Commun 379:406–410
24. **Strum JC, Shehee R, Virley D, Richardson J, Mattie M, Selley P, Ghosh S, Nock C, Saunders A, Roses A** 2007 Rosiglitazone induces mitochondrial biogenesis in mouse brain. J Alzheimers Dis 11: 45–51
25. **Haffner SM, Miettinen H, Stern MP** 1997 The homeostasis model in the San Antonio Heart Study. Diabetes Care 20:1087–1092
26. **Appleton DJ, Rand JS, Sunvold GD** 2005 Basal plasma insulin and homeostasis model assessment (HOMA) are indicators of insulin sensitivity in cats. J Feline Med Surg 7:183–193
27. **Kulawiak B, Kudin AP, Szewczyk A, Kunz WS** 2008 BK channel openers inhibit ROS production of isolated rat brain mitochondria. Exp Neurol 212:543–547
28. **Du H, Guo L, Zhang W, Rydzewska M, Yan S** 2011 Cyclophilin D deficiency improves mitochondrial function and learning/memory in aging Alzheimer disease mouse model. Neurobiol Aging 32:398–406
29. **Thummasorn S, Kumfu S, Chattipakorn S, Chattipakorn N** 2011 Granulocyte-colony stimulating factor attenuates mitochondrial dysfunction induced by oxidative stress in cardiac mitochondria. Mitochondrion 11:457–466
30. **Mielke JG, Taghibiglou C, Liu L, Zhang Y, Jia Z, Adeli K, Wang YT** 2005 A biochemical and functional characterization of diet-induced brain insulin resistance. J Neurochem 93:1568–1578
31. **Huang CC, You JL, Lee CC, Hsu KS** 2003 Insulin induces a novel form of postsynaptic mossy fiber long-term depression in the hippocampus. Mol Cell Neurosci 24:831–841
32. **Valladolid-Acebes I, Stucchi P, Cano V, Fernández-Alfonso MS, Merino B, Gil-Ortega M, Fole A, Morales L, Ruiz-Gayo M, Del Olmo N** 2011 High-fat diets impair spatial learning in the radial-arm maze in mice. Neurobiol Learn Mem 95:80–85
33. **Park HR, Park M, Choi J, Park KY, Chung HY, Lee J** 2010 A high-fat diet impairs neurogenesis: involvement of lipid peroxidation and brain-derived neurotrophic factor. Neurosci Lett 482:235–239
34. **Ruggiero C, Ehrenshaft M, Cleland E, Stadler K** 2011 High fat diet induces an initial adaptation of mitochondrial bioenergetics in the kidney despite evident oxidative stress and mitochondrial ROS production. Am J Physiol Endocrinol Metab 300:E1047–E1058
35. **Bonnard C, Durand A, Peyrol S, Chanseaume E, Chauvin MA, Morio B, Vidal H, Rieusset J** 2008 Mitochondrial dysfunction results from oxidative stress in the skeletal muscle of diet-induced insulin-resistant mice. J Clin Invest 118:789–800
36. **Mao G, Kraus GA, Kim I, Spurlock ME, Bailey TB, Beitz DC** 2011 Effect of a mitochondria-targeted vitamin E derivative on mitochondrial alteration and systemic oxidative stress in mice. Br J Nutr 106:87–95
37. **Han JW, Zhan XR, Li XY, Xia B, Wang YY, Zhang J, Li BX** 2010 Impaired PI3K/Akt signal pathway and hepatocellular injury in high-fat fed rats. World J Gastroenterol 16:6111–6118
38. **Levy M, Faas GC, Saggau P, Craigen WJ, Sweatt JD** 2003 Mitochondrial regulation of synaptic plasticity in the hippocampus. J Biol Chem 278:17727–17734
39. **Sedlic F, Sepac A, Pravdic D, Camara AK, Bienengraeber M, Brzezinska AK, Wakatsuki T, Bosnjak ZJ** 2010 Mitochondrial depolarization underlies delay in permeability transition by preconditioning with isoflurane: roles of ROS and Ca^{2+}. Am J Physiol Cell Physiol 299:C506–C515
40. **Cao J, Xu D, Wang D, Wu R, Zhang L, Zhu H, He Q, Yang B** 2009 ROS-driven Akt dephosphorylation at Ser-473 is involved in 4-HPR-mediated apoptosis in NB4 cells. Free Radic Biol Med 47: 536–547
41. **Hernandez R, Teruel T, Lorenzo M** 2003 Rosiglitazone produces insulin sensitisation by increasing expression of the insulin receptor and its tyrosine kinase activity in brown adipocytes. Diabetologia 46:1618–1628
42. **Sheu WH, Chuang HC, Cheng SM, Lee MR, Chou CC, Cheng FC** 2011 Microdialysis combined blood sampling technique for the determination of rosiglitazone and glucose in brain and blood of gerbils subjected to cerebral ischemia. J Pharm Biomed Anal 54:759–764
43. **Brodbeck J, Balestra ME, Saunders AM, Roses AD, Mahley RW, Huang Y** 2008 Rosiglitazone increases dendritic spine density and rescues spine loss caused by apolipoprotein E4 in primary cortical neurons. Proc Natl Acad Sci USA 105:1343–1346
44. **Kapadia R, Yi JH, Vemuganti R** 2008 Mechanisms of anti-inflammatory and neuroprotective actions of PPAR-γ agonists. Front Biosci 13:1813–1826
45. **Dello Russo C, Gavrilyuk V, Weinberg G, Almeida A, Bolanos JP, Palmer J, Pelligrino D, Galea E, Feinstein DL** 2003 Peroxisome proliferator-activated receptor γ thiazolidinedione agonists increase glucose metabolism in astrocytes. J Biol Chem 278:5828–5836
46. **Fuenzalida K, Quintanilla R, Ramos P, Piderit D, Fuentealba RA, Martinez G, Inestrosa NC, Bronfman M** 2007 Peroxisome proliferator-activated receptor γ up-regulates the Bcl-2 anti-apoptotic protein in neurons and induces mitochondrial stabilization and pro-

tection against oxidative stress and apoptosis. J Biol Chem 282: 37006–37015
47. **Jung TW, Lee JY, Shim WS, Kang ES, Kim SK, Ahn CW, Lee HC, Cha BS** 2007 Rosiglitazone protects human neuroblastoma SH-SY5Y cells against MPP+ induced cytotoxicity via inhibition of mitochondrial dysfunction and ROS production. J Neurol Sci 253: 53–60
48. **Yi JH, Park SW, Brooks N, Lang BT, Vemuganti R** 2008 PPARγ agonist rosiglitazone is neuroprotective after traumatic brain injury via anti-inflammatory and anti-oxidative mechanisms. Brain Res 1244:164–172
49. **Potenza MA, Gagliardi S, De Benedictis L, Zigrino A, Tiravanti E, Colantuono G, Federici A, Lorusso L, Benagiano V, Quon MJ, Montagnani M** 2009 Treatment of spontaneously hypertensive rats with rosiglitazone ameliorates cardiovascular pathophysiology via antioxidant mechanisms in the vasculature. Am J Physiol Endocrinol Metab 297:E685–E694
50. **Rong JX, Qiu Y, Hansen MK, Zhu L, Zhang V, Xie M, Okamoto Y, Mattie MD, Higashiyama H, Asano S, Strum JC, Ryan TE** 2007 Adipose mitochondrial biogenesis is suppressed in db/db and high-fat diet-fed mice and improved by rosiglitazone. Diabetes 56:1751–1760
51. **Wu JS, Lin TN, Wu KK** 2009 Rosiglitazone and PPAR-γ overexpression protect mitochondrial membrane potential and prevent apoptosis by upregulating anti-apoptotic Bcl-2 family proteins. J Cell Physiol 220:58–71
52. **Miglio G, Rosa AC, Rattazzi L, Collino M, Lombardi G, Fantozzi R** 2009 PPARγ stimulation promotes mitochondrial biogenesis and prevents glucose deprivation-induced neuronal cell loss. Neurochem Int 55:496–504
53. **Loh K, Deng H, Fukushima A, Cai X, Boivin B, Galic S, Bruce C, Shields BJ, Skiba B, Ooms LM, Stepto N, Wu B, Mitchell CA, Tonks NK, Watt MJ, Febbraio MA, Crack PJ, Andrikopoulos S, Tiganis T** 2009 Reactive oxygen species enhance insulin sensitivity. Cell Metab 10:260–272
54. **Marino JS, Xu Y, Hill JW** 2011 Central insulin and leptin-mediated autonomic control of glucose homeostasis. Trends Endocrinol Metab 22:275–285

Pediatr Cardiol (2011) 32:1158–1163
DOI 10.1007/s00246-011-0040-7

ORIGINAL ARTICLE

Heart Rate Variability and Exercise Capacity of Patients With Repaired Tetralogy of Fallot

Suchaya Silvilairat · Jatuporn Wongsathikun · Rekwan Sittiwangkul · Yupada Pongprot · Nipon Chattipakorn

Received: 15 February 2011 / Accepted: 16 June 2011 / Published online: 8 July 2011

Abstract Heart rate variability (HRV) has been used as a reliable method to detect cardiac autonomic nervous system activity. Peak oxygen uptake (VO_2 peak) has been a predictor of death for adults with repaired tetralogy of Fallot (TOF). This study investigated the correlation between HRV and exercise capacity in 30 patients with TOF after surgery for total correction. The median age of the patients was 14 years (range, 9–25 years), and the median follow-up period was 11.6 months (range, 5.3–20.2 months). Low- and high-frequency-domain HRV significantly correlated with VO_2 peak ($r = 0.56$, $P = 0.001$ and $r = 0.44$, $P = 0.02$, respectively). After the 1-year follow-up evaluation, VO_2 peak and HRV analysis did not differ from those at entry to the study. However, low- and high-frequency-domain HRV still correlated significantly with VO_2 peak ($r = 0.43$, $P = 0.03$ and $r = 0.52$, $P = 0.007$, respectively). Left ventricular early diastolic myocardial velocity was most closely correlated with the VO_2 peak ($r = 0.51, P = 0.005$). Impaired cardiovascular autonomic control and left ventricular diastolic dysfunction may be responsible for exercise intolerance in patients with repaired TOF. Long-term follow-up evaluation with exercise testing and 24-h Holter monitoring are warranted.

Keywords Exercise capacity · Heart rate variability · Repaired tetralogy of Fallot

S. Silvilairat (✉) · R. Sittiwangkul · Y. Pongprot
Division of Pediatric Cardiology, Department of Pediatrics, Faculty of Medicine, Chiang Mai University, Chiang Mai 50200, Thailand
e-mail: ssamana@med.cmu.ac.th

J. Wongsathikun
Department of Physical Therapy, Faculty of Associated Medical Sciences, Chiang Mai University, Chiang Mai 50200, Thailand

N. Chattipakorn
Cardiac Electrophysiology Research and Training Center, Chiang Mai University, Chiang Mai 50200, Thailand

The surgical repair of tetralogy of Fallot (TOF) can be performed with a low mortality rate and an excellent long-term outcome [1, 3, 6, 8, 15, 16, 19, 22, 25, 26]. However, some hemodynamic abnormalities may be found after surgery including pulmonary stenosis, pulmonary regurgitation, and myocardial dysfunction. The majority of patients have no symptoms resulting from these abnormalities. However, evaluation of exercise capacity shows cardiopulmonary compromise in some patients with repaired TOF [5, 17, 24, 27–30, 32].

Peak oxygen uptake (VO_2 peak) has been an independent predictor of death for adults with repaired TOF [13]. Heart rate variability (HRV) has been used as a reliable method to detect autonomic nervous system activity [31]. Ventricular tachycardia, progressive heart failure, and sudden cardiac death have been the late complications in the long term [12, 14, 23]. Reduced HRV is a predictor of sudden cardiac death after myocardial infraction and chronic heart failure [18, 20]. Previous studies have demonstrated that patients with TOF after complete repair have a reduction of HRV [4, 9, 10, 21].

To our knowledge, no previous studies of HRV have been correlated with exercise capacity in pediatric and adolescent patients with repaired TOF. The early recognition of patients at greater risk for exercise intolerance and

increased morbidity is of clinical relevance for refinement in management. Therefore, in the current study, echocardiography, exercise testing, and a 24-h Holter electrocardiography (ECG) were evaluated among patients with repaired TOF. We hypothesized that heart rate variability is correlated with exercise intolerance in patients with TOF after surgical repair.

Methods

Study Patients

We prospectively studied 30 patients with TOF who underwent total surgical correction at Chiang Mai University Hospital. Electrocardiography, echocardiography, exercise testing, and a 24-h Holter ECG were performed at entry to the study and at the 1 year follow-up examination. The relationship between HRV analysis and exercise capacity was evaluated during the 1-year follow-up exam. The study protocol was reviewed and approved by the Chiang Mai University Review Board. All the patients or their parents consented to research participation.

HRV Analysis

A 24-h ECG was recorded for HRV analysis. The recordings were reviewed before the HRV was determined by the analysis software. The HRV analysis included frequency domain and time domain. The frequency-domain HRV parameters were low-frequency power (LF), high-frequency power (HF), and the LF/HF ratio. The time-domain HRV parameters included the standard deviation of all the normal sinus R-R intervals in the entire 24-h recording (SDNN) and the standard deviation of all the average normal sinus R-R intervals for all the 5-min segments in the 24-h recordings (SDANN).

Exercise Test

An exercise test was performed using an electric cycle ergometer (Corival, Lode, Groningen, Netherlands). All patients performed a maximal exercise test with a 2-min incremental bicycle protocol with a workload increment of 20 W for females and 25 W for males. The electrocardiogram, oxygen saturation, and blood pressure were monitored. The VO_2 peak, carbon dioxide production (VCO_2), minute ventilation (V_E), and respiratory exchange ratio (RER) were determined by using the breath-by-breath technique (Ultima CPX, Medgraphics, St. Paul, MN, USA). The test was terminated according to American College of Sports Medicine (ACSM) guidelines [2].

Doppler Echocardiography

Doppler echocardiographic examinations were performed using Philips Sonos 7500 (Philips Medical Systems, Bothell, WA). Echocardiographic data included left ventricular fractional shortening, pulse-wave Doppler assessment of the tricuspid valve and mitral valve, and tissue Doppler imaging. A tissue Doppler imaging signal was obtained from an apical four-chamber view at the right ventricular free wall, the ventricular septum, and the left ventricular free wall. The tissue Doppler imaging variables included systolic myocardial velocity (Sm), early diastolic myocardial velocity (Em), and late diastolic myocardial velocity (Am). The myocardial performance index was calculated by the atrioventricular valve closing-to-opening time minus the ventricular ejection time divided by the ejection time.

Statistical Analysis

All statistical calculations were assessed using commercially available software (SPSS Version 16, SPSS Inc., Chicago, IL, USA). Linear regression analysis was used to assess the correlation between the HRV and the VO_2 peak. Comparison of parameters between those at study entry and those at the 1-year follow-up assessment was performed using the Wilcoxon rank sum. Multiple linear regression analysis was used for the predictive model of VO_2. A P value less than 0.05 was considered statistically significant.

Results

The study enrolled 30 patients (11 females [37%] and 19 males; median age, 14 years; range, 9–25 years) with repaired TOF. The median follow-up period was 11.6 months (range, 5.3–20.2 months). The baseline characteristics are reported in Table 1. The median time from surgical repair for tetralogy of Fallot to exercise testing was 9 years (range, 2–16 years). Six patients had a previously modified Blalock-Taussig shunt. Right ventricular outflow tract reconstruction with a transannular patch was performed for 14 patients (47%). Echocardiography, exercise testing, and HRV analysis at study entry and at the 1-year follow-up assessment are compared in Table 2. Echocardiographic parameters, VO_2 peak, and HRV analysis did not differ during the 1-year follow-up period.

Relationship of Heart Rate Variability to VO_2 Peak

The results for the relationship between the HRV and the VO_2 peak are graphically displayed in Fig. 1. Low- and high-frequency-domain HRV significantly correlated with

Table 1 Demographic and baseline characteristics of patients with repaired tetralogy of Fallot (TOF) ($n = 30$)

	TOF patients at entry (mean ± SD)
Age (years)	15.8 ± 4.4
Age at operation (years)	6.3 ± 3.0
Follow-up time from operation (years)	9.5 ± 3.0
Female: *n* (%)	11 (37)
BSA (m^2)	1.3 ± 0.2
Heart rate at rest (beats/min)	78 ± 11
Systolic BP (mmHg)	106 ± 13
Diastolic BP (mmHg)	65 ± 12
Previous Blalock-Taussig shunt: *n* (%)	6 (20)
Transannular patch: *n* (%)	14 (47)
QRS duration (ms)	138 ± 25
Pro-BNP (pg/ml)	198 ± 178

SD standard deviation, *BSA* body surface area, *BP* blood pressure, *BNP* brain natriuretic peptide

Table 2 Echocardiography, exercise test, and heart rate variability at entry to the study and at the 1-year follow-up assessment for patients with repaired tetralogy of Fallot (TOF)

Parameter	At the entry	At the 1 year	*P* value
Echocardiography			
LVEF (%)	57 ± 9	60 ± 8	NS
LVSm (m/s)	0.06 ± 0.01	0.07 ± 0.01	NS
LVEm (m/s)	0.13 ± 0.03	0.14 ± 0.03	NS
LVAm (m/s)	0.04 ± 0.01	0.04 ± 0.01	NS
RVFAC (%)	51 ± 7	53 ± 5	NS
RVSm (m/s)	0.08 ± 0.02	0.08 ± 0.02	NS
RVEm (m/s)	0.11 ± 0.03	0.12 ± 0.04	NS
RVAm (m/s)	0.04 ± 0.01	0.08 ± 0.18	NS
Exercise test (peak)			
Heart rate (bpm)	162 ± 14	160 ± 12	NS
VO_2 peak (ml/kg/min)	33 ± 9	31 ± 10	NS
Minute ventilation (l/min)	44 ± 14	43 ± 11	NS
V_E/CO_2	29 ± 5	29 ± 5	NS
Gas exchange ratio	1.14 ± 0.13	1.13 ± 0.16	NS
Time domain			
SDNN (ms)	132 ± 30	139 ± 46	NS
SDANN (ms)	122 ± 31	128 ± 49	NS
Frequency domain			
Low frequency (ms^2)	20 ± 7	21 ± 8	NS
High frequency (ms^2)	14 ± 6	16 ± 7	NS
LF/HF ratio	1.6 ± 0.4	1.4 ± 0.4	NS

LVEF left ventricular ejection fraction, *NS* not significant, *LVSm* left ventricular systolic myocardial velocity, *LVEm* left ventricular early diastolic myocardial velocity, *LVAm* left ventricular late diastolic myocardial velocity, *RVFAC* right ventricular fractional area change, *RVSm* right ventricular systolic myocardial velocity, *RVEm* ventricular early diastolic myocardial velocity, *RVAm* right ventricular late diastolic myocardial velocity, *VO_2 peak* peak oxygen uptake, *V_E/CO_2* minute ventilation and carbon dioxide production ratio, *SDNN* standard deviation of all normal sinus R-R intervals in the entire 24-h recording, *SDANN* standard deviation of all average normal sinus R-R intervals for all 5-min segments in the 24-h recording, *LF* low-frequency power, *HF* high-frequency power

VO_2 peak ($r = 0.56$, $P = 0.001$ and $r = 0.44$, $P = 0.02$, respectively). After the 1 year follow-up period, VO_2 peak and HRV analysis did not differ from those at entry to the study. However, low- and high-frequency-domain HRV still correlated significantly with the VO_2 peak at the 1-year follow-up assessment ($r = 0.43$, $P = 0.03$ and $r = 0.52$, $P = 0.007$, respectively).

Relationship of Pulse Wave Doppler and Tissue Doppler Data to VO_2 Peak

Left ventricular early diastolic myocardial velocity was most closely correlated with the VO_2 peak ($r = 0.51$, $P = 0.005$). The ratio of peak early ventricular filling velocity to early diastolic myocardial velocity (E/Em) significantly correlated with VO_2 peak ($r = -0.50$, $P = 0.006$).

Predictors for VO_2 Peak

Using multiple regression analysis, female, reduced heart rate variability and the ratio of increased peak early ventricular filling velocity to early diastolic myocardial velocity were associated with a decreased VO_2 peak ($R^2 = 0.61$).

Discussion

The current study supports our hypothesis that HRV is correlated with exercise intolerance in patients with repaired TOF. Low- and high-frequency-domain HRV significantly correlated with VO_2 peak ($r = 0.56$, $P = 0.001$ and $r = 0.44$, $P = 0.02$, respectively). The low- and high-frequency-domain HRV still significantly correlated with VO_2 peak at the 1-year follow-up assessment ($r = 0.43$, $P = 0.03$ and $r = 0.52$, $P = 0.007$, respectively). Furthermore, left ventricular early diastolic myocardial velocity was most closely correlated with the VO_2 peak ($r = 0.51$, $P = 0.005$). The ratio of peak early ventricular filling velocity to early diastolic myocardial velocity significantly correlated with VO_2 peak ($r = -0.50$, $P = 0.006$). In fact, a decreased early diastolic myocardial velocity and an increased ratio of early ventricular filling velocity to early diastolic myocardial velocity are characteristics of left ventricular diastolic dysfunction. In the females, a reduced HRV and an

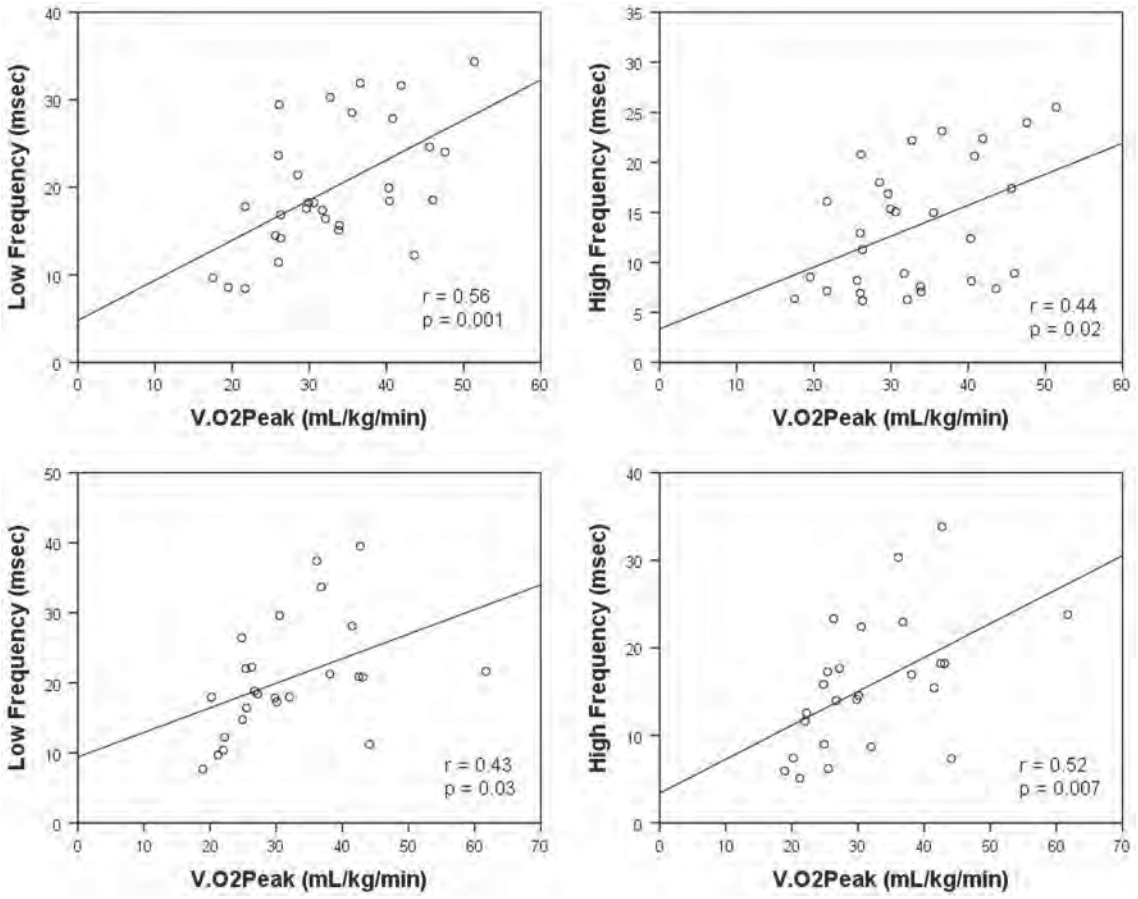

Fig. 1 Linear regression analysis of the correlation between heart rate variability and peak oxygen uptake (VO_2 peak) at study entry (*upper*) and at the 1-year follow-up evaluation (*lower*) in patients with repaired tetralogy of Fallot. VO_2 peak, peak oxygen uptake

increased ratio of peak early ventricular filling velocity to early diastolic myocardial velocity were associated with a decreased VO_2 peak.

Several studies have reported that adolescent and adult patients with repaired TOF had reduced HRV [4, 9, 10, 21]. Reduced HRV is a predictor of sudden cardiac death after myocardial infraction and chronic heart failure [18, 20]. To our knowledge, no previous studies of HRV have correlated with exercise capacity in pediatric and adolescent patients with repaired TOF. Peak oxygen uptake has been an independent predictor of death for adults with repaired TOF [13]. The current study found that low- and high-frequency-domain HRV significantly correlated with VO_2 peak at entry to the study and at the 1-year follow-up assessment.

McLeod et al. [21], and Davos et al. [9] reported that reduced HRV was associated with widening of the QRS complex, which had been identified as a risk factor for sustained ventricular tachycardia and sudden death [11]. Folino et al. [10], and Butera et al. [4] reported that patients with ventricular tachycardia had reduced HRV. The current study did not find an association between the HRV and the QRS duration in pediatric and adolescent patients with repaired TOF. No ventricular tachycardia was found in the 24-h Holter monitoring because the patients in the current study were younger than those in previous studies.

Cheung et al. [7] reported that the impaired global left ventricular deformation due to right ventricular dilation was an independent predictor of VO_2 peak in patients with repaired TOF. The current study supported this finding that left ventricular diastolic dysfunction was correlated with VO_2 peak. Therefore, reduced HRV and left ventricular diastolic dysfunction may be responsible for exercise intolerance in patients with repaired tetralogy of Fallot.

Conclusions

Heart rate variability had a significant correlation with VO_2 peak at entry to the study and at the 1-year follow-up

assessment. Left ventricular early diastolic myocardial velocity was correlated with the VO_2 peak. Impaired cardiovascular autonomic control and left ventricular diastolic dysfunction may be responsible for exercise intolerance in patients with repaired tetralogy of Fallot. Long-term follow-up exercise testing, echocardiography, and a 24-h Holter monitoring are warranted.

Acknowledgments This work was supported by Thailand Research Fund grants MRG5180103 (SS) and RTA5280006 (NC).

References

1. Alexiou C, Mahmoud H, Al-Khaddour A, Gnanapragasam J, Salmon AP, Keeton BR, Monro JL (2001) Outcome after repair of tetralogy of Fallot in the first year of life. Ann Thorac Surg 71:494–500
2. American College of Sports Medicine (ed) (2006) ACSM's guidelines for exercise testing and prescription, 7th edn. Lippincott Williams & Wilkins, Baltimore, p 106
3. Bacha EA, Scheule AM, Zurakowski D, Erickson LC, Hung J, Lang P, Mayer JE Jr, del Nido PJ, Jonas RA (2001) Long-term results after early primary repair of tetralogy of Fallot. J Thorac Cardiovasc Surg 122:154–161
4. Butera G, Bonnet D, Sidi D, Kachaner J, Chessa M, Bossone E, Carminati M, Villain E (2004) Patients operated for tetralogy of Fallot and with nonsustained ventricular tachycardia have reduced heart rate variability. Herz 29:304–309
5. Carvalho JS, Shinebourne EA, Busst C, Rigby ML, Redington AN (1992) Exercise capacity after complete repair of tetralogy of Fallot: deleterious effects of residual pulmonary regurgitation. Br Heart J 67:470–473
6. Caspi J, Zalstein E, Zucker N, Applebaum A, Harrison LH Jr, Munfakh NA, Heck HA Jr, Ferguson TB Jr, Stopa A, White M, Fontenot EE (1999) Surgical management of tetralogy of Fallot in the first year of life. Ann Thorac Surg 68:1344–1348
7. Cheung EW, Liang XC, Lam WW, Cheung YF (2009) Impact of right ventricular dilation on left ventricular myocardial deformation in patients after surgical repair of tetralogy of Fallot. Am J Cardiol 104:1264–1270
8. Cobanoglu A, Schultz JM (2002) Total correction of tetralogy of Fallot in the first year of life: late results. Ann Thorac Surg 74:133–138
9. Davos CH, Davlouros PA, Wensel R, Francis D, Davies LC, Kilner PJ, Coats AJ, Piepoli M, Gatzoulis MA (2002) Global impairment of cardiac autonomic nervous activity late after repair of tetralogy of Fallot. Circulation 106:I69–I75
10. Folino AF, Russo G, Bauce B, Mazzotti E, Daliento L (2004) Autonomic profile and arrhythmic risk stratification after surgical repair of tetralogy of Fallot. Am Heart J 148:985–989
11. Gatzoulis MA, Till JA, Somerville J, Redington AN (1995) Mechanoelectrical interaction in tetralogy of Fallot: QRS prolongation relates to right ventricular size and predicts malignant ventricular arrhythmias and sudden death. Circulation 92: 231–237
12. Gatzoulis MA, Balaji S, Webber SA, Siu SC, Hokanson JS, Poile C, Rosenthal M, Nakazawa M, Moller JH, Gillette PC, Webb GD, Redington AN (2000) Risk factors for arrhythmia and sudden cardiac death late after repair of tetralogy of Fallot: a multicentre study. Lancet 356:975–981
13. Giardini A, Specchia S, Tacy TA, Coutsoumbas G, Gargiulo G, Donti A, Formigari R, Bonvicini M, Picchio FM (2007) Usefulness of cardiopulmonary exercise to predict long-term prognosis in adults with repaired tetralogy of Fallot. Am J Cardiol 99:1462–1467
14. Harrison DA, Harris L, Siu SC, MacLoghlin CJ, Connelly MS, Webb GD, Downar E, McLaughlin PR, Williams WG (1997) Sustained ventricular tachycardia in adult patients late after repair of tetralogy of Fallot. J Am Coll Cardiol 30:1368–1373
15. Hirsch JC, Mosca RS, Bove EL (2000) Complete repair of tetralogy of Fallot in the neonate: results in the modern era. Ann Thorac Surg 232:508–514
16. Horneffer PJ, Zahka KG, Rowe SA, Manolio TA, Gott VL, Reitz BA, Gardner TJ (1990) Long-term results of total repair of tetralogy of Fallot in childhood. Ann Thorac Surg 50:179–183
17. Jonsson H, Ivert T, Jonasson R, Holmgren A, Bjork VO (1995) Work capacity and central hemodynamics thirteen to twenty-six years after repair of tetralogy of Fallot. J Thorac Cardiovasc Surg 110:416–426
18. Kleiger RE, Miller JP, Bigger JT Jr, Moss AJ (1987) Decreased heart rate variability and its association with increased mortality after acute myocardial infarction. Am J Cardiol 59:256–262
19. Knott-Craig CJ, Elkins RC, Lane MM, Holz J, McCue C, Ward KE (1998) A 26-year experience with surgical management of tetralogy of Fallot: risk analysis for mortality or late reintervention. Ann Thorac Surg 66:506–511
20. La Rovere MT, Pinna GD, Maestri R, Mortara A, Capomolla S, Febo O, Ferrari R, Franchini M, Gnemmi M, Opasich C, Riccardi PG, Traversi E, Cobelli F (2003) Short-term heart rate variability strongly predicts sudden cardiac death in chronic heart failure patients. Circulation 107:565–570
21. McLeod KA, Hillis WS, Houston AB, Wilson N, Trainer A, Neilson J, Doig WB (1999) Reduced heart rate variability following repair of tetralogy of Fallot. Heart 81:656–660
22. Murphy JG, Gersh BJ, Mair DD, Fuster V, McGoon MD, Ilstrup DM, McGoon DC, Kirklin JW, Danielson GK (1993) Long-term outcome in patients undergoing surgical repair of tetralogy of Fallot. N Engl J Med 329:593–599
23. Nollert G, Fischlein T, Bouterwek S, Böhmer C, Klinner W, Reichart B (1997) Long-term survival in patients with repair of tetralogy of Fallot: 36-year follow-up of 490 survivors of the first year after surgical repair. J Am Coll Cardiol 30:1374–1383
24. Norgard G, Bjorkhaug A, Vik-Mo H (1992) Effects of impaired lung function and pulmonary regurgitation on maximal exercise capacity in patients with repaired tetralogy of Fallot. Eur Heart J 13:1380–1386
25. Pigula FA, Khalil PN, Mayer JE, del Nido PJ, Jonas RA (1999) Repair of tetralogy of Fallot in neonates and young infants. Circulation 100:II157–II161
26. Reddy VM, Liddicoat JR, McElhinney DB, Brook MM, Stanger P, Hanley FL (1995) Routine primary repair of tetralogy of Fallot in neonates and infants less than three months of age. Ann Thorac Surg 60:S592–S596
27. Rhodes J, Dave A, Pulling MC, Geggel RL, Marx GR, Fulton DR, Hijazi ZM (1998) Effect of pulmonary artery stenoses on the cardiopulmonary response to exercise following repair of tetralogy of Fallot. Am J Cardiol 81:1217–1219
28. Rowe SA, Zahka KG, Manolio TA, Horneffer PJ, Kidd L (1991) Lung function and pulmonary regurgitation limit exercise capacity in postoperative tetralogy of Fallot. J Am Coll Cardiol 17:461–466
29. Sarubbi B, Pacileo G, Pisacane C, Ducceschi V, Iacono C, Russo MG, Iacono A, Calabrò R (2000) Exercise capacity in young patients after total repair of tetralogy of Fallot. Pediatr Cardiol 21:211–215
30. Strieder DJ, Aziz K, Zaver AG, Fellows KE (1975) Exercise tolerance after repair of tetralogy of Fallot. Ann Thorac Surg 19:397–405

31. Task Force of the European Society of Cardiology and the North American Society of Pacing and Electrophysiology (1996) Heart rate variability: standards of measurement, physiological interpretation, and clinical use. Eur Heart J 17:354–381

32. Wessel HU, Cunningham WJ, Paul MH, Bastanier CK, Muster AJ, Idriss FS (1980) Exercise performance in tetralogy of Fallot after intracardiac repair. J Thorac Cardiovasc Surg 80:582–593

Asian Biomedicine Vol. 5 No. 6 December 2011; 735-746 DOI: 10.5372/1905-7415.0506.100

Review article

Expression of sodium channels in dental pulp

Amornrat Suwanchai[a], Ubonwan Theerapiboon[a], Nipon Chattipakorn[b], Siriporn C. Chattipakorn[b, c]
[a]Division of Pediatric Dentistry, Department of Orthodontics and Pediatric Dentistry, Faculty of Dentistry, [b]Cardiac Electrophysiology Research and Training Center, Department of Physiology, Faculty of Medicine, [c]Department of Oral Biology and Diagnostic Science, Faculty of Dentistry, Chiang Mai University, Chiang Mai 50200, Thailand

***Background*:** Several isoforms of voltage-gated sodium channels (VGSCs) found in peripheral nerves is associated in the pathogenesis of neuropathic and inflammatory pain. Until now, there are few studies of the distribution of VGSCs in dental pulp and its relationship to dental pain.
***Objective*:** Perform literature review to provide update information of VGSCs in dental pulp.
Methods: We reviewed and discussed seventy-eight articles listed in MEDLINE (PubMed) database using keywords including "sodium channels" and "dental pain". They are articles published in English from 1978 to 2010.
***Results*:** Although several VGSCs isoforms are distributed in dental pulp, only $Na_V1.7$, $Na_V1.8$, and $Na_V1.9$ have been found to be upregulated in painful pulpitis.
***Conclusion*:** $Na_V1.7$, $Na_V1.8$, and $Na_V1.9$ seem to have key roles in inflammatory dental pain. As a result, they might be the targets to treat dental pulp inflammation.

Keywords: Dental pulp, expression, inflammation, sodium channels

List of abbreviations

CGRP	Calcitonin gene related peptide
CNS	Central nervous system
DRG	Dorsal root ganglion
ENaC	Epithelial sodium channel
NKA	Neurokinin A
PGP9.5	Protein gene product 9.5
PNS	Peripheral nervous system
SP	Substance P
TTX	Tetrodotoxin
TTX-R	Tetrodotoxin-resistant voltage-gated sodium channel
TTX-S	Tetrodotoxin-sensitive sodium channel
VGSCs	Voltage-gated sodium channels

Our review aims to focus on recent information regarding sodium channels, which are related to dental pain from both primary and permanent teeth, information which has not yet been thoroughly reviewed. We also include information on a variety of fields of the pulpodentin complex, particularly the field of neural reaction to pulpal injury. Therefore, our review is divided into three parts as follows,

1. The pulpodentin complex
   - 1.1 Innervation in permanent and primary tooth pulp
   - 1.2 Sensory neuropeptides in dental pulp
   - 1.3 Neural reactions to pulpal injuries
2. The expression of sodium channels in dental pulp
3. The expression of sodium channels related to dental pain

1. The pulpodentin complex

The dental pulp is surrounded by the dental hard tissues, which form a physical barrier against pathogens and injury. The dental pulp and dentin are often discussed together as one functional unit, the pulpodentin complex. Dental pulp is responsible for dentin formation. The permeable properties of dentin regulate the diffusion rate of irritants that can initiate pulpal inflammation. Dental pulp contains a dense vascularity and nerve supply. The blood vessels in pulpal tissue are for nutrient supply and cellular recruitment, while the nerves in pulpal tissue are for

Correspondence to: Siriporn Chattipakorn, DDS, PhD, Department of Oral Biology and Diagnostic Science, Faculty of Dentistry, Chiang Mai University, Chiang Mai 50200, Thailand. E-mail: s.chat@chiangmai.ac.th

dental sensitivity and defense response following pulpal injury, from either dental caries or trauma. The dental pulp has a low capacity for defense or repair responses because of the lack of an adequate blood supply and cellular recruitment following dental injury [1]. Several studies have shown that pulpal innervation plays an important role in both defense and repair responses [2-4]. Therefore, this review article focuses on pulpal innervation in the response to pulpal injury.

1.1 Normal innervation in primary and permanent tooth pulp

The pulpodentin complex in both primary and permanent teeth is extremely rich in innervation [5], and the innervation influences the defense reactions in the connective tissue of the dental pulp. This innervation consists of sensory, sympathetic, and parasympathetic nerve fibers.

The sensory nerve fibers are the major innervation in the dental pulp of both primary and permanent teeth. They originate from the trigeminal ganglion, and peripherally pass through the apical foramen to innervate the coronal pulp. Into the coronal pulp, they diverge, branch, and terminate as free nerve endings in the odontoblast layers, sub-odontoblastic plexus, predentin, in the inner 0.1 mm of dentin, or along blood vessels, as shown in Byers's study [6]. After stimulation, sensory nerve fibers transmit signals back via the trigeminal nerves to the trigeminal ganglion. The signals from trigeminal ganglion provide input through the spinal trigeminal tract to the spinal trigeminal nucleus and then, these signals pass through the spinothalamic tract to terminate in the somatosensory cortex of brain. There are three subgroups of sensory nerve fibers in dental pulp. They are based on size, conduction velocity, and function. First, the A-β nerve fibers are medium-sized myelinated fibers. They comprise the smallest population of sensory nerve fibers and are sensitive to mechanical stimuli such as hydrodynamic, percussion, and movement force. Second, it is the small myelinated A-□ nerve fibers. Finally, the largest population is the unmyelinated, slow conducting C fibers. Both A-□ and C fibers are classified as nociceptive, which respond to noxious stimuli. The sensory nerve fibers are also involved in dentinal fluid dynamics, vasoregulation, and protective reflexes against dental injuries [7-9]. They provide the vitality of the dental pulp by interacting with other pulpal components, such as odontoblasts, immunocompetent cells, and blood vessels. A previous study in the rat model indicated that the sensory nerve fibers in dental pulp play an important role in the survival of pulpal tissue. In that study, the authors demonstrated that teeth with sensory denervation had greater loss of pulpal tissue than those with innervation [4].

Sympathetic nerve fibers are sparse in the dental pulp of both primary and permanent teeth. They originate in the superior cervical ganglion, are located along the blood vessels in the deeper pulp, and are involved in vasoconstriction.

The parasympathetic nerve fibers play roles in the regulation of pulpal blood flow but are much less important than either the sensory or the sympathetic fibers [10].

During maturation and aging in permanent teeth, dental pulp chamber becomes narrower with the deposition of tertiary dentin and dead tracts, which are normally not innervated. With increasing loss of primary dentin, tooth innervation decreases, as shown by the reduction in expression of neuropeptides and their receptors in the dental pulp [9, 11]. Several studies have shown the distribution of nerve fibers in dental pulp by using the expression of protein gene product 9.5 (PGP9.5), a soluble protein isolated from brains, as a marker of nerve fibers. PGP9.5 staining appears to be reliable in reacting with nerve fibers, in several studies using different techniques: immunohistochemistry [12], immunoblotting [13], immunocytochemistry [14-16], and immunofluorescence [5, 16, 17].

The sensory innervation of permanent teeth is greater than that of primary teeth [5, 14, 18]. Due to the prominent function of sensory nerve fibers in pain transmission, several investigators have hypothesized that the primary teeth have less sensitivity than the permanent teeth. This is because the primary teeth have less sensory innervation. However, another study revealed different results in sensory innervation between primary and permanent teeth [19]. In that study, the sensory nerve supply in human primary teeth differs from that in permanent teeth in two ways. First, the distribution of the innervation within the crowns of primary teeth was highest cervically, while the permanent teeth were densely supplied in the pulpal horn. Second, the primary teeth were particularly innervated at the cervical ends of the roots, but the roots of permanent dentin were virtually uninnervated. In addition, physiologic root resorption does not affect the histological structure [20] or overall innervation [21] of primary teeth.

1.2 Sensory neuropeptides in dental pulp

The sensory nerve fibers in dental pulp are afferent fibers involved predominantly in dental pain perception. The terminals of sensory nerve fibers contain neuropeptides, synthesized neurotransmitter proteins from neurons. These peptidergic neurons are associated with neurogenic inflammation, caused by extreme stimuli, such as dental caries, drilling, probing of the exposed dentin, or percussion of the teeth, in order to maintain the vitality of dental pulp [22]. Dynamic changes in peptidergic neurons occur during inflammation by extensive nerve fiber sprouting. These sprouting result in an increased number of potential sites of neuropeptide-containing fibers and, consequently, an increased quantity of neuropeptide release [3, 14, 15, 23-25]. Neuropeptides cannot cross cell membranes, so they trigger biological effects by activating their receptors located on the plasma membrane of the target cells and they are rapidly degraded by the enzymes in pulpal tissue after exerting the effects [26]. The functions of sensory neuropeptides are multiple and varied. They can act as neurotransmitters, growth factors, hormones, vasoregulators, and immune system signaling molecules. It is known that neuropeptides contribute to promoting neurogenic inflammation to the control of pulpal blood flow and to the pain mechanisms of the pulpodentin complex [10]. Several studies demonstrated that neuropeptides could modulate vascular smooth muscles, increase vascular permeability, and modulate the immune system [8, 10, 27]. The sensory neuropeptides in primary and permanent tooth pulp consist of calcitonin gene-related peptides (CGRP), substance P (SP) and neurokinin A (NKA) [10, 28]. The origin, localization, stimulation, and biological effects of sensory neuropeptides in dental pulp are summarized in **Table 1**.

Table 1. Summary of sensory neuropeptides, receptors, and their functions (modified from [26])

Neuropeptide	Origin	Localization	Stimulus for release	Biologic effect
Calcitonin gene-related peptide	Trigeminal ganglion	C and Aδ fibers	- Thermal - Mechanical - Chemical - Electrical - Caries - Capsaicin - Inflammatory mediators - Bradykinin - Prostaglandins	- Vasodilation - Plasma extravasation - Chemotaxis - T lymphocyte suppression - Hard tissue formation - Repair - Mitogen for odontoblasts - Pain - Resorption control
Substance P	Trigeminal ganglion	C and A fibers	- Thermal - Mechanical - Chemical - Electrical - Caries - Capsaicin - Inflammatory mediators - Bradykinin - Prostaglandins	- Vasodilation - Plasma extravasation - Immune system stimulation - Chemotaxis - Enhances macrophages activity - Hard tissue formation - Tissue reparation - Mitogen for T lymphocyte
Neurokinin A	Trigeminal ganglion	C and A fibers	- Thermal - Mechanical - Chemical - Electrical - Caries - Capsaicin - Inflammatory mediators - Bradykinin - Prostaglandins	- Vasodilation - Plasma extravasation - Chemotaxis - Pain

1.3 Neural reactions to pulpal injuries

When dental pulp is injured, the injury activates nerve fibers to induce neurogenic inflammation. That is a process of stimuli-induced neuropeptide release, change in vascular permeability, and the recruitment of immunocompetent cells. The neurogenic inflammation can lead to the healing process [10, 29]. Several studies have demonstrated the neurogenic inflammation occurring in the dental pulp following dental injury. For example, sensory [14, 30, 31] and sympathetic [2] nerve fiber sprouting were found in inflamed dental pulp. Byers and colleagues [32] demonstrated that the variable degrees of sensory nerve fiber sprouting is correlated with various degrees of pulpal injury in the rat model. In their study, a mild injury, e.g. shallow cavities, caused an increase in CGRP-immunoreactive fibers, and those sprouting CGRP-nerve fibers subsided within 21 days. The deeper cavities caused more injury to the dental pulp and led to microabscess formation, with more numerous branches of sensory nerve fibers sprouting underneath. The sprouting fibers took a longer time to subside and reparative dentin was substituted in the microabscesses. When the dental pulp was exposed, three defensive reactions could be found, pulp polyps, coagulation necrosis and liquefying necrosis. In those severe pulpal injuries, the CGRP-immunoreactive fibers were found sprouting adjacent to the borders of defensive reactions and the axons were found to assemble in the core of surviving pulp. As we have mentioned before, due to the increased number of potential sites of neuropeptide release and the role of sensory neuropeptides in pain transmission, the sprouting of sensory nerve fibers following inflammation may alter cytochemical reactions in the dental pulp and contribute to the altered efficacy of local anesthesia.

2. The expression of sodium channels in dental pulp

Voltage-gated sodium channels (VGSCs) are complex transmembrane pores that are responsible for depolarization of the membrane potential, or the rising phase of the action potential in the membrane. They are found in excitable cells, such as neurons, myocytes [33], and some types of glial cells [34]. VGSCs open within a millisecond in response to electrical change across the membrane to allow sodium ion influx. This causes the increased neuronal membrane potential. Then, they terminate very fast to occlude the sodium ion flow. The neurons enter a repolarization stage by the allowance of potassium ion influx at the neuronal membrane. After closing, VGSCs return to the resting state and are available to reopen in response to new waves of electrical change. Therefore, VGSCs contribute to the determination of neuronal excitability and play a role in the propagation of nerve impulses. During injuries or inflammation, VGSCs in primary sensory neurons are continuously activated and the continuous activation of VGSCs gives rise to an unprovoked, spontaneous action potential, that finally causes continuous pain [35].

The sodium channel is a selective filter composed of one large, continuous protein, the β-subunit, and one or two smaller proteins, the β-subunits. The β-subunit, a 220-260 kD polypeptide, is a functional part of the sodium ion channel, and contains a voltage sensor, an ion pore, and activation and inactivation gates. The β-subunits modulate the functions of the α-subunits and stabilize them to the plasma membrane. In mammals, nine genes have been identified to encode VGSC β-s ubunits into nine isoforms, depending on amino acid sequence homology and genetic location. These isoforms include $Na_V1.1$, $Na_V1.2$, $Na_V1.3$, $Na_V1.4$, $Na_V1.5$, $Na_V1.6$, $Na_V1.7$, $Na_V1.8$, and $Na_V1.9$. Each isoform differs in function, such as tissue distribution, electrophysiological properties, pharmacological properties, and response to nerve injury and inflammation. Moreover, different isoforms aggregate to form a variety of macromolecules and to regulate the excitability of nociceptors. Therefore, there are diversified processes of nerve impulse propagation such as variation in opening thresholds, opening time length, amount of inactivation time, rate of isoform transition from the closed inactivated state to the resting, or closed state, depending on the presence of sodium channel α-subunit isoforms [36].

VGSCs can be functionally classified depending on the criteria used, as shown in **Table 2**, and the properties of each VGSC α-subunit isoform are summarized in **Table 3**.

In physiological, rather than pathological, conditions, the sensory neurons in the dorsal root ganglion (DRG) and trigeminal ganglion express both TTX-sensitive (TTX-S) and TTX-resistant (TTX-R) sodium channels. The population of sensory neurons is primarily mechanoreceptive, expressing rapidly-inactivating TTX-S sodium channels, with a small proportion being nociceptive, expressing a mixture of

Table 2. Classification of VGSCs depending on function [36]

Criteria	Classification of VGSCs
Threshold of activation	- Low threshold - High threshold
Rate of activation	- Fast activation - Slow activation
Rate of inactivation	- Fast inactivation - Slow inactivation
Sensitivity to tetrodotoxin (TTX), which is a toxin found in the liver of puffer fish	- TTX-sensitive (TTX-S) - TTX-resistant (TTX-R)

Table 3. Voltage-gated sodium channel -subunit isoforms and their properties [35, 36]

α-subunit isoform	Site of expression	Inactivation rate	Sensitivity to blockade by TTX
$Na_V1.1$	CNS and DRG sensory neurons	Fast	Sensitive
$Na_V1.2$	CNS neurons	Fast	Sensitive
$Na_V1.3$	Immature neurons	Fast	Sensitive
$Na_V1.4$	Skeletal muscle	Fast	Sensitive
$Na_V1.5$	Cardiac muscle	Slow	Intermediately sensitive
$Na_V1.6$	CNS and DRG sensory neurons	Fast	Sensitive
$Na_V1.7$	DRG sensory neurons and sympathetic ganglia	Fast	Sensitive
$Na_V1.8$	DRG sensory neurons	Slow	Resistant
$Na_V1.9$	Small DRG sensory neurons and trigeminal ganglia	Very slow (persistent)	Resistant

rapidly-inactivating TTX-S and slowly-inactivating TTX-R sodium channels. Details of studies of the expression of sodium channels in normal dental pulp are described in **Table 4**.

During the inflammatory process, inflammatory mediators can lower the threshold of activation and increase the excitability of TTX-R in primary sensory neurons, contributing to neuronal hyperexcitability [37]. Moreover, several studies have shown the alteration in the expression of both TTX-S and TTX-R VGSCs in inflamed peripheral tissues [36, 38]. These changes may lead to increased pain states.

The rapidly inactivating, TTX-S sodium currents have been detected in cultured human dental pulp cells [39]. Davidson suggested that the main source of these sodium currents is neuronal satellite cells, not odontogenic cells, because the odontoblastic processes firmly embed the odontoblasts to the dentin and do not allow these cells to be explanted. On the other hand, an *in vitro* study of Allard and colleagues [40] found that odontoblasts expressed voltage-gated TTX-S currents which have the ability to generate action potential, but TTX-R sodium currents have not been detected.

Henry and colleagues [41] found no change in overall sodium channel expression in painful human dental pulp. However, they found that the quantity of atypical nodal sites and the expression of sodium channels at such sites were increased but the quantity of typical nodal sites and the accumulating sodium channels at those sites were decreased. That study showed that inflammation caused the demyelinating process and the remodeling of the pattern of sodium channel accumulation. Several studies supported the study of Henry and colleagues [41], revealing, for example, an increase in the expression of $Na_V1.7$ [17], $Na_V1.8$ [12, 13] and $Na_V1.9$ [42] in permanent human dental pulp with irreversible pulpitis compared to permanent dental pulp of non-painful teeth. $Na_V1.6$ has also been found in the dental pulp of both humans and rats [43], but its function in pulpal inflammation remains unclear. The expression of multiple VGSC

isoforms in inflamed dental pulp suggests the collaborative roles of various VGSC isoforms in generating spontaneous action potential, leading to pulpal pain.

$Na_V1.1$, $Na_V1.2$, $Na_V1.3$, $Na_V1.4$, and $Na_V1.5$ have not been evidenced in dental pulp. $Na_V1.1$ and $Na_V1.2$ are predominantly expressed in adult central nervous system (CNS) neurons, in combination with $Na_V1.6$. In contrast, the expression of $Na_V1.3$ is particular in immature neurons. $Na_V1.4$ has been seen in skeletal muscle, while $Na_V1.5$ has been remarkably found in cardiac muscle [35]. Not only VGSCs isoforms, but also epithelial sodium channels, which are non-VGSCs, have been found in dental pulp [44]. The expression of each sodium channel isoform in permanent dental pulp is shown in **Table 4**.

3. The expression of sodium channels related to dental pain

$Na_V1.6$ is a TTX-sensitive VGSC isoform, remarkably expressed at the nodes of Ranvier within the myelinated PNS and CNS neurons [45] and also expressed along unmyelinated neurons of the PNS [46] and CNS [45]. Its function has been suggested to be an electrical conduction in both myelinated and unmyelinated axons [45, 46] but the role in nociception is obscure. The expression of $Na_V1.6$ in human permanent tooth pulp has been reported in the study of Luo and colleagues [47] using immunocytochemistry, in which there was no significant difference in the expression of $Na_V1.6$ in normal and painful pulp, despite an increase in the proportion of atypical nodes of Ranvier and a decrease in typical nodal sites in painful pulp. Another study of $Na_V1.6$ in dental pulp, a study in rats, using immunohistochemistry and double immuno-fluorescence [43], found that $Na_V1.6$ was expressed in non-neuronal cells, such as pulpal immune cells, dendritic pulpal cells, and odontoblasts. That finding suggests that $Na_V1.6$ play a role in those cells. Furthermore, it might be implicated in neuro-immune interactions. In contrast to the study of Luo and colleagues [47], pulpal tissue of injured rat teeth in Byers and colleagues' study [43] showed an increase in $Na_V1.6$ immunoreactive cells, predominantly around the injured pulpal tissue and dilated blood vessels. The increased expression of $Na_V1.6$ in non-neuronal dental pulp cells of injured rats [47], despite the unchanged expression of $Na_V1.6$ at the nodes of Ranvier in human inflammatory pulp [43], may reflect the different

Table 4. Sodium channel expression in normal dental pulp

In vitro/In vivo	**Models**	**Major findings**	**References**
In vitro Whole-cell, patch-clamp methods	Human dental pulp cells	Detection of TTX-S current in human dental pulp cells	Davidson, 1994 [39]
In vitro Immunohistochemistry	Human dental pulp	Expression of NaV1.8 immunoreactive nerve fibers in the sub-odontoblastic layers of dental pulp	Renton, et al 2005 [11]
In vitro Immunocytochemistry	Human dental pulp	Expression of NaV1.8 in 16.5% of nodes of Ranvier in radicular tooth pulp	Henry, et al 2005 [61]
In vitro Immuno-electron microscopic methods	Rat dental pulp	Expression of and ENaC in mechanoreceptive myelinated nerve fibers	Ichikawa, et al 2005 [44]
In vitro Immunohistochemistry	Rat dental pulp	Expression of NaV1.9 in unmyelinated nerve fibers and suggested role of NaV1.9 in thermal pain stimuli	Padilla, et al 2007 [62]
In vitro immunohistochemistry	Rat dental pulp	Expression of NaV1.6 in dental pulp cells and odontoblasts	Byers et al, 2009 [43]
In vitro immunocytochemistry	Human dental pulp	Prominent expression of NaV1.6 at nodes of Ranvier, particularly at typical nodal sites	Luo et al, 2010 [47]

function of $Na_V1.6$ in different cell types. However, the difference in the expression and response mechanism of $Na_V1.6$ in various species and different types of pulpal tissue damage should not be ignored.

$Na_V1.7$ is a TTX-sensitive VGSC isoform that has been widely studied. It has been identified in the sympathetic neurons and small and medium sized sensory neurons of the DRG, including nociceptive neurons. $Na_V1.7$ is rapidly activated, rapidly inactivated and slowly recovers from fast activation, so it plays an important role in setting the threshold for the generation of action potentials in peripheral nociceptive neurons [35]. $Na_V1.7$ is markedly involved in perceiving pain sensations, as evidenced in patients with the loss-of-function mutation in the SCN9A gene, a gene that encodes $Na_V1.7$, or meaning that those who have loss of $Na_V1.7$ function are unable to experience pain [48, 49]. In addition, patients with congenital pain syndrome, who have an alteration in $Na_V1.7$ function, have increased pain sensitivity associated with edema, redness, and warmth, suggesting the role of $Na_V1.7$ in chronic inflammatory pain [50]. In the dental pulp of human permanent teeth, the upregulation of $Na_V1.7$ expression has also been reported in painful pulpitis studied using either immunohistochemistry [51], or immunocytochemistry [17], demonstrating the increased expression of the $Na_V1.7$ isoform at both typical and atypical nodal sites.

The VGSC α-subunit isoform 1.8 ($Na_V1.8$) and VGSC α-subunit isoform 1.9 ($Na_V1.9$), the slower TTX-R components, are remarkably found in small unmyelinated sensory neurons that have been identified as nociceptive neurons [36]. $Na_V1.8$ has a high activation threshold, slow inactivation kinetics and contributes to the electrogenesis of an action potential in C-type peripheral neurons of mice [52]. $Na_V1.9$ is activated at potentials near resting membrane potential and generates relatively persistent current [53]. Both TTX-R isoforms, $Na_V1.8$ and $Na_V1.9$, are believed to be involved in the prolonged duration of the action potential in response to painful stimuli and have been found to upregulate during inflammatory pain in rat [38, 54] and mouse [55] models. Therefore, both sodium channel isoforms might be new targets for treatment of inflammatory pain. The different properties of $Na_V1.8$ and $Na_V1.9$ are as follows. $Na_V1.8$ currents have a slow activation and inactivation rate. The slower inactivation rate of $Na_V1.8$ compared to those of other isoforms prolongs the action potential of neurons and may cause chronic pain. The steady-state voltage dependence of inactivation contributes to generating an action potential even in the depolarized state. $Na_V1.9$ currents are unique. They can be activated at voltages near the resting membrane potential. Furthermore, they can generate persistent currents. $Na_V1.9$ can be easily activated. It can contribute to the setting of the threshold of activation. Finally, it can remain opening for a longer time than $Na_V1.8$ [36, 56]. Previous studies in rats, using oligodeoxynucleotides as antisense for $Na_V1.8$ [55, 57] and a study in $Na_V1.8$-null mice have shown that $Na_V1.8$ plays a role in inflammatory pain and neuropathic pain [58]. $Na_V1.9$ channels also have a role in inflammatory pain, but not in neuropathic pain [59, 60].

Localization of $Na_V1.8$ in human teeth with painful pulpitis has been investigated using immunohistochemistry [12]. It has been found that $Na_V1.8$-immunoreactive nerve fibers were localized in the sub-odontoblastic layer of both healthy and inflamed pulp tissue. However, the detection of $Na_V1.8$-immunoreactive fibers was much greater in the inflamed dental pulp. Moreover, the upregulation of $Na_V1.8$ has been reported using the immmunoblotting method in inflamed human permanent tooth pulp compared to healthy pulp [13]. An immunocytochemical study has revealed that not only the predominant $Na_V1.6$, but also $Na_V1.8$ has presented at the nodes of Ranvier in the radicular part of healthy human permanent tooth pulp [61]. This finding suggests the coexistence of multiple sodium channel isoforms in those areas where the levels of expression may change during the inflammatory period and may contribute to an increased pain status.

For $Na_V1.9$, an investigation in rats has revealed the innervation of $Na_V1.9$-immunoreactive fibers in the lip skin and in the dental pulp of non-painful teeth, suggesting the role of this VGSC isoform in orofacial pain [62]. As well as the other sodium channel mentioned above, the immunocytochemical method has reported the increased expression of $Na_V1.9$ in the axons of symptomatic pulpitis of human permanent teeth [42].

Epithelial sodium channel (ENaC) protein is a member of the degenerins family (DEG), which is a large protein family of diverse functions, such as sodium ion transport, acid sensation, proprioception, and mechanosensation [63]. Differing from VGSCs, which consist of α- and β- subunits, ENaC consists of four subunits: α, β, γ and □ subunits [64]. Only

α, β and γ subunits of ENaC have been indicated in mechanoreceptors in the trigeminal ganglion of rat models with a possible function in mechanotransduction [65]. βENaC has been identified in the terminal Schwann cells associated with the periodontal Ruffini endings in the periodontal ligament of rat incisors and is believed to be a key molecule for mechanosensation in mastication [66]. ENaC has also been found in rat dental pulp tissue, by using immunohistochemistry [44]. In that study, the βENaC and γENaC-immunoreactive fibers have appeared in trigeminal ganglion neurons, periodontal ligament, and deep layer of oral mucosa, inferior alveolar nerve fibers, radicular pulp, and sub-odontoblastic plexus of rat molars pulp tissue. γENaC in dental pulp was mostly around myelinated nerve fibers, which are sensitive to mechanical stimuli, whereas it was mostly absent around unmyelinated nociceptive axons.

Those studies of changes in sodium channel expression within painful dental pulp are summarized in **Table 5**.

There have been attempts to discover new substances to act as sodium channel blockers for the treatment of both neuropathic and inflammatory pain. Lidocaine, a commonly used anesthetic, is a sodium channel blocker with a non-specific blocking property that can block TTX-R and TTX-S channels. Scholz and colleagues reported that TTX-R channels are more resistant to lidocaine than are TTX-S channels in A- and C type neurons from the dorsal root ganglion of rats [67]. In contrast, other studies reported that TTX-R channels are more sensitive to lidocaine than are TTX-S sodium channels in rat models [68] and in the mammalian dorsal root ganglion neuroblastoma hybridoma cell line0 [69]. The differences in the results of these studies may be the result of several factors. First, the ability of lidocaine to bind sodium channels depends on the status of the sodium channels. TTX-R currents were found to be blocked by lidocaine in the inactivated state more than in the resting state [67]. It was also found that TTX-S and TTX-R currents were equally sensitive to lidocaine in the

Table 5. Sodium channel expression related to dental pain

In vitro/In vivo	Models	Major findings	References
In vitro Immunohistochemistry	Inflamed human permanent tooth pulp	Significant increase in $Na_V1.8$ immunoreactive nerve fibers in painful pulpitis	Renton, et al 2005 [11]
In vitro immunocytochemistry	Inflamed human permanent tooth pulp	Increase expression of $Na_V1.9$ in axons of painful pulp	Wells et al, 2007 [42]
In vitro immunocytochemistry	Inflamed human permanent tooth pulp	Increased expression of $Na_V1.7$ at both intact and remodeling nodal sites within the painful human dental pulp	Luo et al, 2008 [16]
In vitro Western blot	Inflamed human permanent tooth pulp	Increase in $Na_V1.8$ density in inflamed dental pulp	Warren, et al 2008 [12]
In vitro immunohistochemistry	Injured rat dental pulp	Increased expression of $Na_V1.6$ near dilated blood vessels beneath the injured site and nearly affected pulp	Byers et al, 2009 [43]
In vitro immunocytochemistry	Inflamed human dental pulp	1. Increased expression of NaCh at atypical nodal sites, but decreased expression at typical nodal sites within painful pulpitis 2. Decrease in density of NaCh expression in painful pulp but no significant difference when compared to normal pulp 3. Accumulation of NaCh at atypical nodal sites within A- fibers	Henry, et al 2009 [41]
In vitro immunocytochemistry	Inflamed human dental pulp	No difference in $Na_V1.6$ expression at nodal sites of painful and non-painful pulp	Luo et al, 2010 [47]
In vitro immunohistochemistry	Inflamed human dental pulp	Increase in $Na_V1.7$ immunoreactive area within sub-odontoblastic plexus of painful dental pulp	Beneng et al, 2010 [51]

resting state, while in the activated or opened state, TTX-S currents were more sensitive to lidocaine [69]. Another reason for different findings in the sensitivity of sodium channels to lidocaine may be the blocking methods used in the studies. Drug-bound TTX-R channels have a slower recovery period than do TTX-S channels [69]. Then, the use of frequency-dependent and tonic blockade of the channels by lidocaine leads to dissimilar results in comparing the sensitivity of TTX-S and TTX-R. Until now, the specific VGSC isoforms that are the problems in anesthetic failure are still controversial. The use of a combination of permanently charged lidocaine (N-ethyl-lidocaine) and capsaicin, an agonist for the transient receptor potential vanilloid 1 (TRPV1), in injured rats has been reported in the study of Kim and colleagues [70]. Those authors claimed that the advantage of that regimen over the use of plain local anesthetic agents is that it does not cause a deficit in motor and autonomic nerve function, but the authors claimed that it requires further study for clinical application. Isoflurane, an inhalation anesthetic agent, was also proved to block TTX-S and $Na_V1.8$ currents in rats [71]. Eugenol, a widely used agent in dentistry, has an ability to inhibit both TTX-R and TTX-S sodium ion currents in rats and has effect on nociceptive, as well as non-nociceptive, fibers [72, 73]. Therefore, eugenol may be another good choice to be an analgesic and anesthetic agent in dental treatment. In addition to the sodium channel blockers mentioned above, the sodium channel blocking efficacy of variety opioid derivatives has been studied and it has been found that tramadol, fentanyl and sufentanil have sodium channel blocking ability, especially in slow-activation sodium channel isoforms, while morphine does not [74]. The specific sodium channel blockers have been improved but they are limited to specific $Na_V1.8$ blockers, such as O-conotoxin MrVIB from *Conus Marmoreus* [75], a small molecule antisense oligonucleotide (A-803467) [76, 77] and 5-Aryl-2-furfuramides [78]. Unfortunately, despite much research on sodium channel blockers, none of the sodium channel blocking agents is considered to be effective and safe enough to use in humans. Further studies on the new generation of pain treatments, particularly in the field of dentistry, are still needed.

Conclusions

Dental pain is a significant health problem. Although several voltage-gated sodium channel isoforms, as well as an epithelial sodium channel, have been identified in dental pulp with different location and function, only $Na_V1.7$, $Na_V1.8$, and $Na_V1.9$ play a key role in inflamed pulp. These sodium channel isoforms are suggested as potential targets for novel treatments of pain from pulpal inflammation and as options for novel anesthetics in the treatment of painful pulpitis.

Acknowledgements

This work was supported by the Thailand Research Fund (RTA5280006, NC), Thailand Research Fund (BRG5480003, SC), Chiang Mai University Fund (UT), Faculty of Dentistry, Chiang Mai University (UT, SC). The authors wish to thank Dr. M. Kevin O Carroll, Professor Emeritus of the University of Mississippi School of Dentistry, USA and Faculty Consultant at Faculty of Dentistry, Chiang Mai University, Thailand, for his assistance in the preparation of the manuscript.

The authors have no conflict of interest to report.

References

1. Okiji T. Pulp As a Connective Tissue. In: Bywaters LC, ed. Seltzer and Bender's Dental Pulp. 3rd ed. IL: Quintessence Publishing; 2002. p. 95-121.
2. Haug SR, Heyeraas KJ. Modulation of dental inflammation by the sympathetic nervous system. J Dent Res. 2006; 85:488-95.
3. Khayat BG, Byers MR, Taylor PE, Mecifi K, Kimberly CL. Responses of nerve fibers to pulpal inflammation and periapical lesions in rat molars demonstrated by calcitonin gene-related peptide immunocytochemistry. J Endod. 1988; 14:577-87.
4. Byers MR, Taylor PE. Effect of sensory denervation on the response of rat molar pulp to exposure injury. J Dent Res. 1993; 72:613-8.
5. Rodd HD, Boissonade FM. Innervation of human tooth pulp in relation to caries and dentition type. J Dent Res. 2001; 80:389-93.
6. Byers MR. Dynamic plasticity of dental sensory nerve structure and cytochemistry. Arch Oral Biol. 1994; 39 Suppl:S13-S21.
7. Kim S. Neurovascular interactions in the dental pulp in health and inflammation. J Endod. 1990; 16:48-53.
8. Rodd HD, Boissonade FM. Immunocytochemical investigation of neurovascular relationships in human tooth pulp. J Anat. 2003; 202:195-203.
9. Pashley DH. Dynamics of the pulpo-dentin complex.

Crit Rev Oral Biol Med. 1996; 7:104-33.
10. Caviedes-Bucheli J, Munoz HR, Azuero-Holguin MM, Ulate E. Neuropeptides in dental pulp: the silent protagonists. J Endod. 2008; 34:773-88.
11. Byers MR, Schatteman GC, Bothwell M. Multiple functions for NGF receptor in developing, aging and injured rat teeth are suggested by epithelial, mesenchymal and neural immunoreactivity. Development. 1990; 109:461-71.
12. Renton T, Yiangou Y, Plumpton C, Tate S, Bountra C, Anand P. Sodium channel Nav1.8 immunoreactivity in painful human dental pulp. BMC Oral Health. 2005; 5:5.
13. Warren CA, Mok L, Gordon S, Fouad AF, Gold MS. Quantification of neural protein in extirpated tooth pulp. J Endod. 2008; 34:7-10.
14. Rodd HD, Boissonade FM. Comparative immunohistochemical analysis of the peptidergic innervation of human primary and permanent tooth pulp. Arch Oral Biol. 2002; 47:375-85.
15. Rodd HD, Boissonade FM. Substance P expression in human tooth pulp in relation to caries and pain experience. Eur J Oral Sci. 2000; 108:467-74.
16. Wells JE, Rose ET, Rowland KC, Hatton JF. Kv1.4 subunit expression is decreased in neurons of painful human pulp. J Endod. 2007; 33:827-9.
17. Luo S, Perry GM, Levinson SR, Henry MA. Nav1.7 expression is increased in painful human dental pulp. Mol Pain. 2008; 4:16.
18. Johnsen D, Johns S. Quantitation of nerve fibres in the primary and permanent canine and incisor teeth in man. Arch Oral Biol. 1978; 23:825-9.
19. Egan CA, Bishop MA, Hector MP. An immunohistochemical study of the pulpal nerve supply in primary human teeth: evidence for the innervation of deciduous dentine. J Anat. 1996; 188:623-31.
20. Sari S, Aras S, Gunhan O. The effect of physiological root resorption on the histological structure of primary tooth pulp. J Clin Pediatr Dent. 1999 Spring; 23:221-5.
21. Monteiro J, Day P, Duggal M, Morgan C, Rodd H. Pulpal status of human primary teeth with physiological root resorption. Int J Paediatr Dent. 2009; 19:16-25.
22. Byers MR, Narhi MVO. Nerves Supply of the Pulpodentin Complex and Responses to Injury In: Bywaters LC, ed. Seltzer and Bender's Dental Pulp. 3rd ed. IL: Quintessence Publishing; 2002. p. 151-80.
23. Caviedes-Bucheli J, Camargo-Beltran C, Gomez-la-Rotta AM, Moreno SC, Abello GC, Gonzalez-Escobar JM. Expression of calcitonin gene-related peptide (CGRP) in irreversible acute pulpitis. J Endod. 2004; 30 :201-4.
24. Awawdeh L, Lundy FT, Shaw C, Lamey PJ, Linden GJ, Kennedy JG. Quantitative analysis of substance P, neurokinin A and calcitonin gene-related peptide in pulp tissue from painful and healthy human teeth. Int Endod J. 2002; 35:30-6.
25. Okiji T, Jontell M, Belichenko P, Dahlgren U, Bergenholtz G, Dahlstrom A. Structural and functional association between substance P- and calcitonin gene-related peptide-immunoreactive nerves and accessory cells in the rat dental pulp. J Dent Res. 1997; 76: 1818-24.
26. Gazelius B, Brodin E, Olgart L. Depletion of substance P-like immunoreactivity in the cat dental pulp by antidromic nerve stimulation. Acta Physiol Scand. 1981; 111:319-27.
27. Olgart L, Kerezoudis NP. Nerve-pulp interactions. Arch Oral Biol. 1994; 39 Suppl:S47-S54.
28. Wakisaka S. Neuropeptides in the dental pulp: distribution, origins, and correlation. J Endod. 1990; 16:67-9.
29. Byers MR, Narhi MV. Dental injury models: experimental tools for understanding neuroinflammatory interactions and polymodal nociceptor functions. Crit Rev Oral Biol Med. 1999; 10:4-39.
30. Taylor PE, Byers MR, Redd PE. Sprouting of CGRP nerve fibers in response to dentin injury in rat molars. Brain Res. 1988; 461:371-6.
31. Byers MR, Suzuki H, Maeda T. Dental neuroplasticity, neuro-pulpal interactions, and nerve regeneration. Microsc Res Tech. 2003; 60:503-15.
32. Byers MR, Taylor PE, Khayat BG, Kimberly CL. Effects of injury and inflammation on pulpal and periapical nerves. J Endod. 1990; 16:78-84.
33. Goodman BE. Channels active in the excitability of nerves and skeletal muscles across the neuromuscular junction: basic function and pathophysiology. Adv Physiol Educ. 2008; 32:127-35.
34. Eder C. Regulation of microglial behavior by ion channel activity. J Neurosci Res. 2005; 81:314-21.
35. Cummins TR, Sheets PL, Waxman SG. The roles of sodium channels in nociception: Implications for mechanisms of pain. Pain. 2007; 131:243-57.
36. Amir R, Argoff CE, Bennett GJ, Cummins TR, Durieux ME, Gerner P, et al. The role of sodium channels in chronic inflammatory and neuropathic pain. J Pain. 2006; 7:S1-S29.
37. Maingret F, Coste B, Padilla F, Clerc N, Crest M, Korogod SM, et al. Inflammatory mediators increase

Nav1.9 current and excitability in nociceptors through a coincident detection mechanism. J Gen Physiol. 2008; 131:211-25.
38. Strickland IT, Martindale JC, Woodhams PL, Reeve AJ, Chessell IP, McQueen DS. Changes in the expression of NaV1.7, NaV1.8 and NaV1.9 in a distinct population of dorsal root ganglia innervating the rat knee joint in a model of chronic inflammatory joint pain. Eur J Pain. 2008; 12:564-72.
39. Davidson RM. Neural form of voltage-dependent sodium current in human cultured dental pulp cells. Arch Oral Biol. 1994; 39:613-20.
40. Allard B, Magloire H, Couble ML, Maurin JC, Bleicher F. Voltage-gated sodium channels confer excitability to human odontoblasts: possible role in tooth pain transmission. J Biol Chem. 2006; 281:29002-10.
41. Henry MA, Luo S, Foley BD, Rzasa RS, Johnson LR, Levinson SR. Sodium channel expression and localization at demyelinated sites in painful human dental pulp. J Pain. 2009; 10:750-8.
42. Wells JE, Bingham V, Rowland KC, Hatton J. Expression of Nav1.9 channels in human dental pulp and trigeminal ganglion. J Endod. 2007; 33:1172-6.
43. Byers MR, Rafie MM, Westenbroek RE. Dexamethasone effects on Na(v)1.6 in tooth pulp, dental nerves, and alveolar osteoclasts of adult rats. Cell Tissue Res. 2009; 338:217-26.
44. Ichikawa H, Fukuda T, Terayama R, Yamaai T, Kuboki T, Sugimoto T. Immunohistochemical localization of gamma and beta subunits of epithelial Na+ channel in the rat molar tooth pulp. Brain Res. 2005; 1065: 138-41.
45. Caldwell JH, Schaller KL, Lasher RS, Peles E, Levinson SR. Sodium channel Na(v)1.6 is localized at nodes of ranvier, dendrites, and synapses. Proc Natl Acad Sci U S A. 2000; 97:5616-20.
46. Black JA, Renganathan M, Waxman SG. Sodium channel Na(v)1.6 is expressed along nonmyelinated axons and it contributes to conduction. Brain Res Mol Brain Res. 2002; 105:19-28.
47. Luo S, Perry GM, Levinson SR, Henry MA. Pulpitis increases the proportion of atypical nodes of Ranvier in human dental pulp axons without a change in Na v 1.6 sodium channel expression. Neuroscience. 2010; 169:1881-7.
48. Staud R, Price DD, Janicke D, Andrade E, Hadjipanayis AG, Eaton WT, et al. Two novel mutations of SCN9A (Nav1.7) are associated with partial congenital insensitivity to pain. Eur J Pain [Internet]. 2010. Available from: doi:10.1016/j.ejpain.2010.07.003.
49. Nilsen KB, Nicholas AK, Woods CG, Mellgren SI, Nebuchennykh M, Aasly J. Two novel SCN9A mutations causing insensitivity to pain. Pain. 2009; 143:155-8.
50. Nassar MA, Stirling LC, Forlani G, Baker MD, Matthews EA, Dickenson AH, et al. Nociceptor-specific gene deletion reveals a major role for Nav1.7 (PN1) in acute and inflammatory pain. Proc Natl Acad Sci U S A. 2004; 101:12706-11.
51. Beneng K, Renton T, Yilmaz Z, Yiangou Y, Anand P. Sodium channel Na v 1.7 immunoreactivity in painful human dental pulp and burning mouth syndrome. BMC Neurosci. 2010; 11:71.
52. Renganathan M, Cummins TR, Waxman SG. Contribution of Na(v)1.8 sodium channels to action potential electrogenesis in DRG neurons. J Neurophysiol. 2001; 86:629-40.
53. Dib-Hajj S, Black JA, Cummins TR, Waxman SG. NaN/Nav1.9: a sodium channel with unique properties. Trends Neurosci. 2002; 25:253-9.
54. Amaya F, Wang H, Costigan M, Allchorne AJ, Hatcher JP, Egerton J, et al. The voltage-gated sodium channel Na(v)1.9 is an effector of peripheral inflammatory pain hypersensitivity. J Neurosci. 2006; 26:12852-60.
55. Joshi SK, Mikusa JP, Hernandez G, Baker S, Shieh CC, Neelands T, et al. Involvement of the TTX-resistant sodium channel Nav 1.8 in inflammatory and neuropathic, but not post-operative, pain states. Pain. 2006; 123:75-82.
56. Devor M. Sodium channels and mechanisms of neuropathic pain. J Pain. 2006; 7:S3-S12.
57. Khasar SG, Gold MS, Levine JD. A tetrodotoxin-resistant sodium current mediates inflammatory pain in the rat. Neurosci Lett. 1998; 256:17-20.
58. Akopian AN, Souslova V, England S, Okuse K, Ogata N, Ure J, et al. The tetrodotoxin-resistant sodium channel SNS has a specialized function in pain pathways. Nat Neurosci. 1999; 2:541-8.
59. Tate S, Benn S, Hick C, Trezise D, John V, Mannion RJ, et al. Two sodium channels contribute to the TTX-R sodium current in primary sensory neurons. Nat Neurosci. 1998; 1:653-5.
60. Dib-Hajj SD, Tyrrell L, Black JA, Waxman SG. NaN, a novel voltage-gated Na channel, is expressed preferentially in peripheral sensory neurons and down-regulated after axotomy. Proc Natl Acad Sci U S A. 1998; 95:8963-8.
61. Henry MA, Sorensen HJ, Johnson LR, Levinson SR. Localization of the Nav1.8 sodium channel isoform at

nodes of Ranvier in normal human radicular tooth pulp. Neurosci Lett. 2005; 380:32-6.
62. Padilla F, Couble ML, Coste B, Maingret F, Clerc N, Crest M, et al. Expression and localization of the Nav1. 9 sodium channel in enteric neurons and in trigeminal sensory endings: implication for intestinal reflex function and orofacial pain. Mol Cell Neurosci. 2007; 35:138-52.
63. Drummond HA, Grifoni SC, Jernigan NL. A new trick for an old dogma: ENaC proteins as mechanotransducers in vascular smooth muscle. Physiology (Bethesda). 2008; 23:23-31.
64. Kellenberger S, Schild L. Epithelial sodium channel/ degenerin family of ion channels: a variety of functions for a shared structure. Physiol Rev. 2002; 82:735-67.
65. Fricke B, Lints R, Stewart G, Drummond H, Dodt G, Driscoll M, et al. Epithelial Na+ channels and stomatin are expressed in rat trigeminal mechanosensory neurons. Cell Tissue Res. 2000; 299:327-34.
66. Hitomi Y, Suzuki A, Kawano Y, Nozawa-Inoue K, Inoue M, Maeda T. Immunohistochemical detection of ENaCbeta in the terminal Schwann cells associated with the periodontal Ruffini endings of the rat incisor. Biomed Res. 2009; 30:113-9.
67. Scholz A, Kuboyama N, Hempelmann G, Vogel W. Complex blockade of TTX-resistant Na+ currents by lidocaine and bupivacaine reduce firing frequency in DRG neurons. J Neurophysiol. 1998; 79:1746-54.
68. Chevrier P, Vijayaragavan K, Chahine M. Differential modulation of Nav1.7 and Nav1.8 peripheral nerve sodium channels by the local anesthetic lidocaine. Br J Pharmacol. 2004; 142:576-84.
69. Leffler A, Reiprich A, Mohapatra DP, Nau C. Use-dependent block by lidocaine but not amitriptyline is more pronounced in tetrodotoxin (TTX)-Resistant Nav1.8 than in TTX-sensitive Na+ channels. J Pharmacol Exp Ther. 2007; 320:354-64.
70. Kim HY, Kim K, Li HY, Chung G, Park CK, Kim JS, et al. Selectively targeting pain in the trigeminal system. Pain. 2010; 150:29-40.
71. Herold KF, Nau C, Ouyang W, Hemmings HC, Jr. Isoflurane inhibits the tetrodotoxin-resistant voltage-gated sodium channel Nav1.8. Anesthesiology. 2009; 111:591-9.
72. Park CK, Li HY, Yeon KY, Jung SJ, Choi SY, Lee SJ, et al. Eugenol inhibits sodium currents in dental afferent neurons. J Dent Res. 2006; 85:900-4.
73. Park CK, Kim K, Jung SJ, Kim MJ, Ahn DK, Hong SD, et al. Molecular mechanism for local anesthetic action of eugenol in the rat trigeminal system. Pain. 2009; 144:84-94.
74. Haeseler G, Foadi N, Ahrens J, Dengler R, Hecker H, Leuwer M. Tramadol, fentanyl and sufentanil but not morphine block voltage-operated sodium channels. Pain. 2006; 126:234-44.
75. Ekberg J, Jayamanne A, Vaughan CW, Aslan S, Thomas L, Mould J, et al. muO-conotoxin MrVIB selectively blocks Nav1.8 sensory neuron specific sodium channels and chronic pain behavior without motor deficits. Proc Natl Acad Sci U S A. 2006; 103: 17030-5.
76. Jarvis MF, Honore P, Shieh CC, Chapman M, Joshi S, Zhang XF, et al. A-803467, a potent and selective Nav1.8 sodium channel blocker, attenuates neuropathic and inflammatory pain in the rat. Proc Natl Acad Sci U S A. 2007; 104:8520-5.
77. Krafte DS, Chapman M, Marron B, Atkinson R, Liu Y, Ye F, et al. Block of Nav1.8 by small molecules. Channels (Austin). 2007; 1:152-3.
78. Kort ME, Drizin I, Gregg RJ, Scanio MJ, Shi L, Gross MF, et al. Discovery and biological evaluation of 5-aryl-2-furfuramides, potent and selective blockers of the Nav1.8 sodium channel with efficacy in models of neuropathic and inflammatory pain. J Med Chem. 2008; 51:407-16.

Life Sciences 89 (2011) 702–707

Contents lists available at SciVerse ScienceDirect

Life Sciences

journal homepage: www.elsevier.com/locate/lifescie

Effects of estrogen in preventing neuronal insulin resistance in hippocampus of obese rats are different between genders

Wasana Pratchayasakul [a], Nipon Chattipakorn [a], Siriporn C. Chattipakorn [a,b,*]

[a] Cardiac Electrophysiology Research and Training Center, Department of Physiology, Faculty of Medicine, Chiang Mai University, Chiang Mai 50200, Thailand
[b] Department of Oral Biology and Diagnostic Science, Faculty of Dentistry, Chiang Mai University, Chiang Mai 50200, Thailand

ARTICLE INFO

Article history:
Received 15 March 2011
Accepted 9 August 2011

Keywords:
Estradiol
Insulin resistance
Hippocampus
Insulin-induced LTD
High-fat diet
Genders

ABSTRACT

Aim: The effects of estrogen on the prevention of impaired insulin-induced long-term depression in the hippocampus and neuronal insulin signaling caused by high-fat diet (HF) were studied in male and female rats.
Main methods: Both male and female rats were fed with a normal diet (ND; 19.7% energy from fat) or a high-fat diet (HF; 59.3% energy from fat) for 12 weeks. Then, rats were divided into four subgroups: ND, ND + E, HF and HF + E. The subgroups with + E were given 50 μg/kg estrogen subcutaneously once a day for 30 days. At the end of the experimental period, blood and brain samples were collected to determine the peripheral insulin resistance and neuronal insulin resistance, respectively.
Key findings: Both male and female rats fed with HF developed peripheral insulin resistance as indicated by increased body weight, visceral fat, plasma insulin and HOMA index. Estrogen administration decreased those parameters, indicating improved peripheral insulin sensitivity, in both male and female HF rats. HF diet consumption also caused impaired insulin-induced long-term depression in hippocampus and impaired neuronal insulin receptor function and signaling, indicating neuronal insulin resistance, in both male and female rats. Estrogen treatment could attenuate these neuronal impairments only in HF female rats.
Significance: The activation of the estrogen pathway could preserve insulin sensitivity in the peripheral tissue in both male and female rats. In neuronal tissue, however, the benefit of estrogen could be found only in female rats.

Introduction

Several studies demonstrated that high-fat (HF) feeding in animal models could cause obesity and insulin resistance in peripheral tissues, which are features of the metabolic syndrome (Cani et al., 2007; Shoelson, 2006). Our previous study has shown that a 12-week HF diet consumption in male rats could lead not only to peripheral insulin resistance but also to neuronal insulin resistance, indicating an important role of diet on neuronal insulin sensitivity (Pratchayasakul et al., 2011). In addition, it is known that the loss of ovarian hormones, such as estrogen, can cause a significant increase in visceral fat deposition and insulin resistance, which can then easily develop into type 2 diabetes (Alonso and Gonzalez, 2008; Asthana et al., 2001; Asthana et al., 1999; Gonzalez et al., 2008). Estrogen has been shown to contribute to glucose homeostasis (Louet et al., 2004). The beneficial effect of estrogen on insulin activity has been found to be greater in women before menopause than in aged-matched men (Desrocher and Rovet, 2004; Nuutila et al., 1995). A number of studies have also demonstrated several beneficial effects of estrogen replacement on the insulin resistance model, such as the improvement of peripheral insulin sensitivity, the increase in the rate of IRS-1 and Akt phosphorylation of insulin receptors in skeletal muscle, the reduction of central body fat, the lowering of lipid and cholesterol levels, and the reduced risk of the development of type 2 diabetes (Alonso and Gonzalez, 2008; Godsland, 2005; Palin et al., 2001). Nevertheless, only two studies have demonstrated those beneficial effects of estrogen on improving insulin sensitivity in peripheral tissues induced by HF consumption (Bryzgalova et al., 2008; Riant et al., 2009). Both studies showed that the estrogen treatment exerted anti-diabetic and anti-obesity effects in rats which received a HF diet. Their findings suggest that the pathway of estrogen acts as an effective target to protect against HF-induced metabolic imbalance.

Previous studies also demonstrated the beneficial effects of estrogen on improving memory function in human and animal models (Daniel et al., 1997; Luine et al., 1998; Sherwin, 2005). We have shown previously that a significant modification of important neuronal insulin receptor signaling can be induced by a fat-enriched diet in male rats (Pratchayasakul et al., 2011). Being fed the HF diet for 12 weeks, clearly induces neuronal insulin resistance, which is identified as a significant reduction in the ability of insulin to induce long-

* Corresponding author at: Department of Oral Biology and Diagnostic Science, Faculty of Dentistry, Chiang Mai University, Chiang Mai 50200, Thailand. Tel.: +66 53 944 451; fax: +66 53 222 844.
E-mail address: s.chat@chiangmai.ac.th (S.C. Chattipakorn).

0024-3205/$ – see front matter © 2011 Elsevier Inc. All rights reserved.
doi:10.1016/j.lfs.2011.08.011

term depression (LTD), and a reduction in the stimulated phosphotyrosine activity of IR, IRS-1 and Akt/PKB in brain slices (Pratchayasakul et al., 2011). Those findings indicated that the impairment of neuronal insulin resistance was induced by a HF diet. Nevertheless, the effects of estrogen administration on neuronal insulin signaling in HF-fed rats have never been investigated. In the present study, we tested the hypothesis that the administration of estrogen in both male and female rats can reverse the impairment of both insulin-induced LTD in the hippocampus and neuronal insulin signaling caused by a 12-week HF diet consumption.

Materials and methods

Animals and dietary protocols

All experiments were conducted in accordance with an approved protocol from the Faculty of Medicine, Chiang Mai University Institutional Animal Care and Use Committee, in compliance with NIH guidelines. Male (n = 40) and female (n = 40) Wistar rats weighing ~ 180–200 g were obtained from the National Animal Center, Salaya Campus, Mahidol University, Thailand. All animals were individually housed in a temperature-controlled environment with a 12:12 light–dark cycle. One week after arrival, all rats were randomly assigned to one of the two dietary groups (n = 40 in a HF diet group, 20 male:20 female and n = 40 in a normal diet group, 20 male:20 female). The normal-diet (ND) group received a standard laboratory chow, in which 19.7% of total energy (%E) was from fat, with energy content calculated at 4.02 kcal/g (Mouse Feed Food No. 082, C.P. Company, Bangkok, Thailand). The HF group consumed a fat-enriched diet, containing fat, mostly from lard (59.3% E), with energy content calculated at 5.35 kcal/g, for 12 weeks. The animals were maintained in individual cages with unrestricted access to food and water. Body weight and food intake were recorded daily. Blood samples were collected from the tail at weeks 0 and 12 after fasting for at least 5 h and kept at −80 °C for subsequent biochemical analyses, such as plasma glucose, triglyceride, and insulin assay. After 12 weeks, each dietary group was divided into two subgroups and each subgroup was given either vehicle (90% sesame oil + 10% ethanol) or 17-β estradiol (50 μg/kg) subcutaneously for 30 days (Bryzgalova et al., 2008). This dose and duration were chosen since it has been shown to improve the peripheral insulin resistant condition (Bryzgalova et al., 2008). At the end of the experimental periods, animals were deeply anesthetized with isoflurane after fasting for at least 5 h and decapitated. The brain was rapidly removed for brain slice preparation. Visceral fat was removed and weighed. Plasma collected from animals was stored at −80 °C for further biochemical analysis.

Analytical procedure

Fasting plasma glucose and triglyceride were determined by colorimetric assay using commercially available kits (Biotech, Bangkok, Thailand). Fasting plasma insulin level and plasma estrogen were measured by Sandwich ELISA kits (LINCO Research, St. Charles, Missouri, USA).

Determination of insulin resistance (HOMA index)

Insulin resistance was assessed by Homeostasis Model Assessment (HOMA) (Appleton et al., 2005; Haffner et al., 1997) as a mathematical model describing the degree of insulin resistance, calculated from fasting plasma insulin and fasting plasma glucose concentration.

Brain slice preparation

After decapitation, the brain was removed and immersed in ice-cold "high sucrose" aCSF containing (mM): NaCl 85; KCl 2.5; $MgSO_4$ 4; $CaCl_2$ 0.5; NaH_2PO_4 1.25; $NaHCO_3$ 25; glucose 25; sucrose 75; kynurenic acid 2; ascorbate 0.5, saturated with 95%O_2/5%CO_2 (pH 7.4). This solution enhanced neuronal survival during the slicing procedure (Chattipakorn and McMahon, 2002). Hippocampal slices were cut using a vibratome (Vibratome Company, St. Louis, Missouri, USA). Following a 30-minute post-slice incubation in high sucrose aCSF, slices were transferred to a standard aCSF solution containing (mM): NaCl 119; KCl 2.5; $CaCl_2$ 2.5; $MgSO_4$ 1.3; NaH_2PO_4 1; $NaHCO_3$ 26; and glucose 10, saturated with 95% O_2/5%CO_2 (pH 7.4) for an additional 30 min, before being used for the extracellular recordings and immunoblotting.

Extracellular recording of hippocampal slices

To investigate insulin-induced LTD, the hippocampal slices were transferred to a submersion recording chamber and continuously perfused at 3–4 ml/min with standard aCSF warmed to 25–28 °C. Field excitatory postsynaptic potentials (fEPSPs) were evoked by stimulating the Schaffer collateral–commissural pathway with a bipolar tungsten electrode, while recordings were gathered from the stratum radiatum of the hippocampal CA1 region with micropipettes (3 Mohm) filled with 2 M NaCl. Stimulus frequency was 0.033 Hz. Stimulus intensity was adjusted to yield a fEPSP of 0.8–1.0 mV in amplitude. Hippocampal slices were perfused with aCSF (as baseline condition) for 10 min and then perfused with aCSF plus 500 nM insulin (as insulin stimulation) for 10 min, after which the hippocampal slices were perfused with aCSF again (wash out) and fEPSPs were recorded for the next 30 min.

All data were filtered at 3 kHz, digitized at 10 kHz, and stored on a computer using pClamp 9.2 software (Axon Instruments, Foster City, California, USA). The initial slope of the fEPSPs was measured and plotted versus time using Origin 8.0 software.

Preparation of brain homogenates for immunoprecipitation, immunoblotting, and neuronal estrogen levels

To examine the alteration of neuronal insulin-mediated phosphorylation of the Akt/PKB following vehicle and estrogen treatment of two dietary regimens, six brain slices per animal were placed into either aCSF or aCSF plus 500 nM insulin (Humulin R, Eli Lilly, Giessen, Germany) for 5 min. Then, three brain slices in each conditioned group were homogenized in 500 μl of ice-cold brain slice lysis buffer [1 mM EDTA, 1 mM EGTA, 1% NP-40, 1% Triton X-100 and supplemented with a protease inhibitor cocktail, Roche complete mini-tablets, (Roche Molecular Biochemicals, Indianapolis, Indiana, USA)]. Next, the homogenates were centrifuged at 9000 *g* for 30 min at 4 °C and the protein concentration was measured using the Bio-Rad DC Protein assay kit (Bio-Rad Laboratories, Hercules, California, USA). These homogenates were then stored at −80 °C for further biochemical analysis of neuronal estrogen levels and the western blot analysis of the serine phosphorylation of Akt/PKB.

To determine the level of Akt/PKB protein expression in the brain, another set of three brain slices in aCSF was homogenized over ice in non-ionizing lysis buffer containing: 100 mM NaCl, 25 mM EDTA, 10 mM Tris, 1% Triton X-100, 1% NP-40 supplemented with a protease inhibitor cocktail (Roche Molecular Biochemicals).

Immunoprecipitation and immunoblotting

Akt/PKB at serine 473 kinases phosphorylation was electrophoresed and immunoblotted with rabbit antibodies for Akt/PKB at serine 473. Examination of the levels of Akt/PKB protein was conducted with

homogenates prepared from another set of three brain slices. Both proteins were resolved by the immunoprecipitation and immunoblot assay conducted with rabbit anti-Akt/PKB (1:1000 in TBST, Santa Cruz Biotechnology, Santa Cruz, California, USA). For loading control, immunoblotting for each membrane was incubated with anti-β-actin (1:400; rabbit polyclonal; Sigma, St. Louis, Missouri, USA).

All membranes for visualizing the phosphorylation and the protein levels of Akt/PKB were incubated with secondary goat anti-rabbit antibody conjugated with horseradish peroxidase (1:8000 in TBST, Bio-Rad Laboratories). The protein bands were visualized on Amersham hyperfilm ECL (GE Healthcare, Buckinghamshire, UK) using Amersham ECL western blotting detection reagents (GE Healthcare). Band intensities were quantified by Scion Image and the results were shown in average signal intensity (arbitrary) units.

Statistical analysis

Data were presented as means ± SE. All statistical analyses were performed using the program SPSS (version 16; SPSS, Chicago, Ill., USA). The significance of the difference between the means was calculated by two way ANOVA and posthoc analysis with Fisher's test with $p<0.05$ for the level of phosphorylated Akt/PKB at serine 473 site in all animals. Pearson's correlation analysis was used to determine the relationship among the plasma parameters, liver triglyceride content, visceral fat, body weight, HOMA index, plasma estrogen and brain estrogen in all animals.

Results

β-Estradiol (E2) administration improved peripheral insulin sensitivity in both male and female HF-fed rats

After 12-weeks of HF feeding, both male and female rats demonstrated the characteristics of peripheral insulin resistance, such as increased body weight, visceral fat, liver triglyceride, fasting plasma insulin and HOMA index (Table 1). After 1 month of E2 administration, these parameters were significantly decreased in both male and female HF-fed rats, compared to the vehicle-treated group. These parameters were not altered in ND-fed rats (Table 1). Furthermore, the circulating estrogen level in the vehicle-treated female HF-fed rats was also significantly reduced, compared to the vehicle-treated female ND rats. This finding is consistent with a previous study demonstrating that high body fat in female rats was associated with decreased estradiol levels (Ziomkiewicz et al., 2008). In contrast; the circulating estrogen levels were not significantly changed between the HF and ND groups that received E2 in either gender (Table 1).

E2 administration prevented neuronal insulin resistance in female HF-fed rats

The neuronal insulin receptor function or insulin-induced LTD was impaired following HF consumption in both male and female rats as indicated by the disappearance of insulin-induced LTD in the hippocampus of HF-fed rats (Fig. 1A). E2 administration could significantly prevent the impairment of insulin-induced LTD only in female HF rats (Fig. 1B). In E2-treated female HF-fed rats, the percentage depression of fEPSPs after insulin administration was 31.18 ± 9.93%, compared to 2.37 ± 3.18% from E2-treated male HF-fed rats. These findings indicated that administration of E2 decreased the occurrence of HF-induced neuronal insulin resistance in female HF-fed rats, but not in male HF-fed rats. The body weight, fasting insulin level and HOMA index were also decreased by E2 treatment in both male and female rats fed with HF ($p<0.05$, Table 1).

E2 administration improved neuronal insulin signaling in female HF-FED rats

To study the mechanism of E2 on neuronal insulin resistance, we determined whether the E2 improves insulin signaling, particularly Akt/PKB in the brain. As shown in our previous study (Pratchayasakul et al., 2011), 12-week HF consumption led to deleterious effects on insulin receptor signaling, such as phosphorylated IR, phosphorylated IRS-1 and phosphorylated Akt/PKB. In the present study, the impairment of neuronal insulin signaling was examined using immunoblot Akt/PKB phosphorylation. We also investigated whether estrogen can improve neuronal insulin signaling, particularly Akt/PKB phosphorylation to investigate the mechanism of E2 in neuronal insulin signaling in both male and female rats. Our results demonstrated that the level of Akt/PKB protein was not different in both male and female rats receiving either ND or HF diet. Furthermore, E2 administration did not alter Akt/PKB protein concentration in the brain of both male and female rats of either dietary group (Fig. 2A). However, the amounts of the phosphorylated form of Akt/PKB at the serine 473 site were significantly decreased in both vehicle-treated male and female rats in the HF group, compared to the vehicle-treated rats in the ND group (Fig. 2B). However, the amounts of the

Table 1
The effects of estrogen on peripheral insulin sensitivity parameters in rats fed with normal and high-fat diet.

Parameters	Vehicle-treated				Estrogen-treated			
	Normal diet		High-fat diet		Normal diet		High-fat diet	
	Male	Female	Male	Female	Male	Female	Male	Female
Body weight (g)	482.50 ± 12.50	282.50 ± 10.31[a]	595.00 ± 47.[*]	380.00 ± 4.[*,a]	407.50 ± 14.93[*]	254.00 ± 6.00[a]	514.00 ± 6.00[*,#,a]	340.00 ± 17.03[*,#,a]
Visceral fat (g)	22.41 ± 2.72	10.16 ± 0.42[a]	43.81 ± 7.95[*]	37.71 ± 2.02[*]	17.69 ± 2.20	13.33 ± 0.83	40.99 ± 3.76[*]	29.93 ± 2.09[*,#]
Glucose (mg%)	121.70 ± 4.70	119.78 ± 2.54	134.36 ± 12.72	130.75 ± 19.11	99.43 ± 4.89	102.28 ± 5.86	118.52 ± 9.07	108.58 ± 9.57
Triglyceride (mg%)	86.99 ± 20.58	47.12 ± 1.29	77.16 ± 17.71	128.18 ± 3.18[*,a]	126.50 ± 24.11	53.75 ± 11.43[a]	79.89 ± 7.19	61.25 ± 8.11[#]
Free fatty acid (mM)	0.44 ± 0.17	0.47 ± 0.07	0.42 ± 0.07	0.46 ± 0.04	0.57 ± 0.13	0.53 ± 0.05	0.55 ± 0.10	0.38 ± 0.01
Insulin (ng/ml)	1.61 ± 0.48	1.32 ± 0.23	4.88 ± 0.34[*]	3.40 ± 0.25[*,a]	0.93 ± 0.15	1.29 ± 0.13	2.50 ± 0.46[#]	2.43 ± 0.42[*,#]
Liver triglyceride (mg/g tissue)	39.31 ± 4.39	24.21 ± 1.80	103.00 ± 3.56[*]	109.28 ± 8.42[*]	24.37 ± 3.91	23.43 ± 3.53	61.61 ± 6.52[*,#]	75.69 ± 6.69[*,#,a]
HOMA index	11.57 ± 2.87	9.35 ± 1.64	40.04 ± 4.76[*]	26.41 ± 4.15[*,a]	5.51 ± 0.92	7.69 ± 0.55	16.72 ± 2.69[*,#]	14.89 ± 1.99[*,#]
Plasma estrogen (pg/ml)	56.66 ± 4.60	133.38 ± 10.32[a]	44.80 ± 6.85	112.91 ± 24.43[a]	240.23 ± 27.91[#]	266.89 ± 37.87[#]	247.74 ± 23.61[#]	260.01 ± 12.36[#]
Brain estrogen (pg/mg protein)	64.87 ± 14.17	75.33 ± 7.32	65.11 ± 7.74	82.03 ± 15.44	74.25 ± 6.81	149.06 ± 16.78[#,a]	68.80 ± 9.20	128.54 ± 22.99[#,a]

[a] $p<0.05$ from male.
[*] $p<0.05$ from diet.
[#] $p<0.05$ from vehicle.

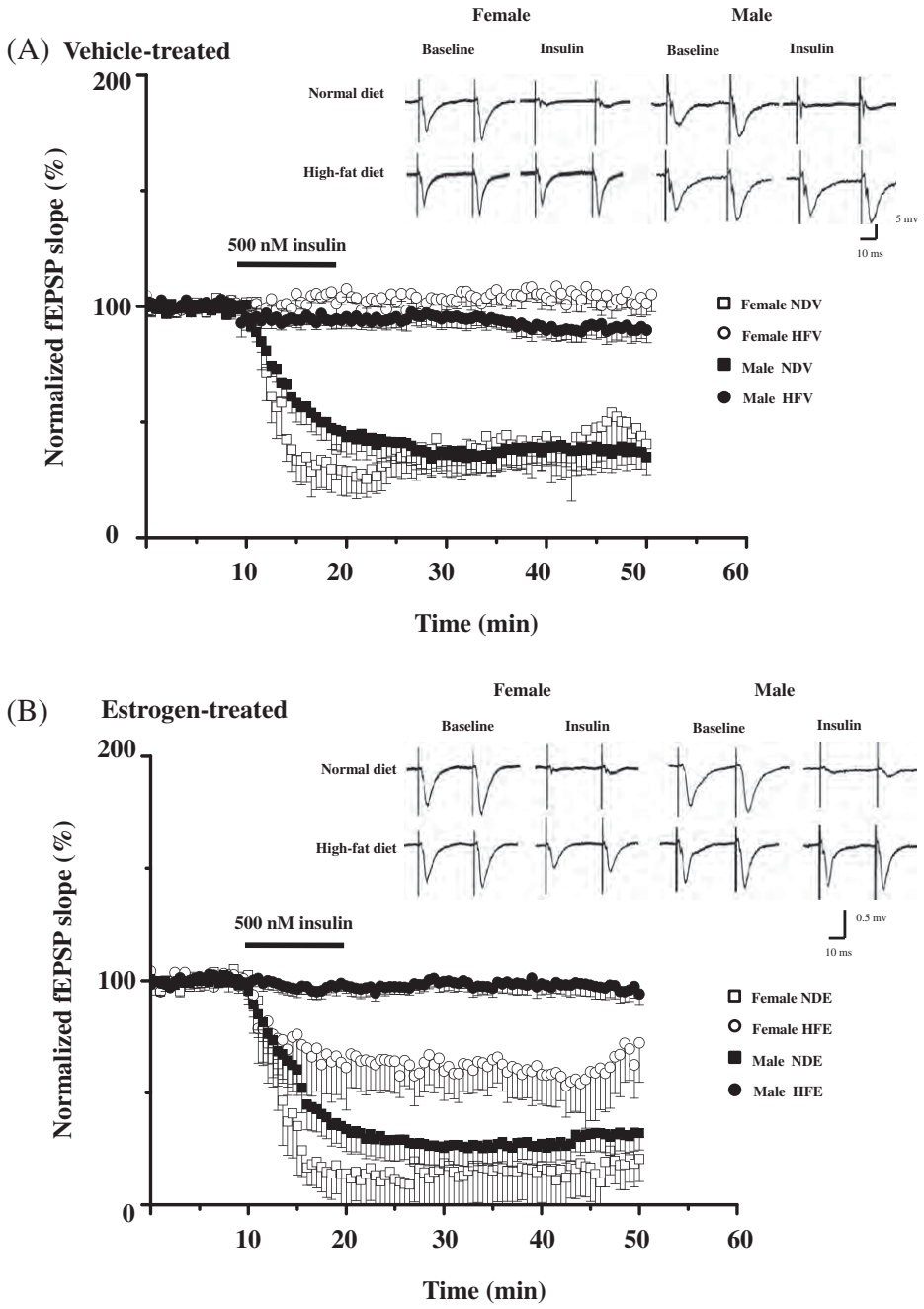

Fig. 1. E2 administration for 30 days significantly improved the impairment of insulin-mediated long term depression (LTD) in the CA1 hippocampus following HF consumption in female rats. *Panel A*: A summary of average normalized fEPSPs (fEPSPt/fEPSPo with fEPSPs being points at which fEPSP slopes stabilized) from NDV male and female rats (n = 8–9 independent slices, n = 4–5 animals/group) and HFV male and female rats (n = 8–9 independent slices, n = 4–5 animals/group) brain slices. It shows that bath application of 500 nM insulin for 10 min produced a depression of fEPSPs in male and female NDV brain slices and the fEPSPs did not fully recover after washout of insulin. However, 500 nM insulin-mediated LTD was significantly attenuated in both male and female HFV rats. *Panel B*: summary of average normalized fEPSPs from estrogen-treated ND (NDE) male and female rats (n = 8–9 independent slices, n = 4–5 animals/group) and estrogen-treated HF(HFE) male and female rats (n = 8–9 independent slices, n = 4–5 animals/group) brain slices. NDV = normal diet group with vehicle treatment, HFV = high-fat diet group with vehicle treatment, NDE = normal diet group with E2 treatment, HFE = high-fat diet group with E2 treatment.

phosphorylated form of Akt/PKB at the serine 473 site were significantly increased in the brains of E2-treated female rats compared to the vehicle-treated female rats in the HF group, suggesting that E2 could protect neuronal insulin signaling from the deleterious effect of HF feeding in female rats (Fig. 2B). In male brains, the phosphorylated form of Akt/PKB at the serine 473 site was still decreased after E2 treatment (Fig. 2B). Furthermore, in the E2 treatment group, the amount of the phosphorylated form of Akt/PKB at the serine 473 site in the ND and HF-fed groups was not different in female rats. However, in male rats that received E2 treatment, the level of phosphorylated Akt/PKB at the serine 473 site of the HF group was significantly reduced compared to that in the ND group (Fig. 2B).

Discussion

Our study demonstrated that a 30-day administration of estrogen reduces the occurrence of HF-induced peripheral insulin resistance in male and female rats. Our findings confirmed the therapeutic effect of exogenous estrogen on peripheral insulin resistance induced by HF consumption as shown in previous studies (Kumagai et al., 1993;

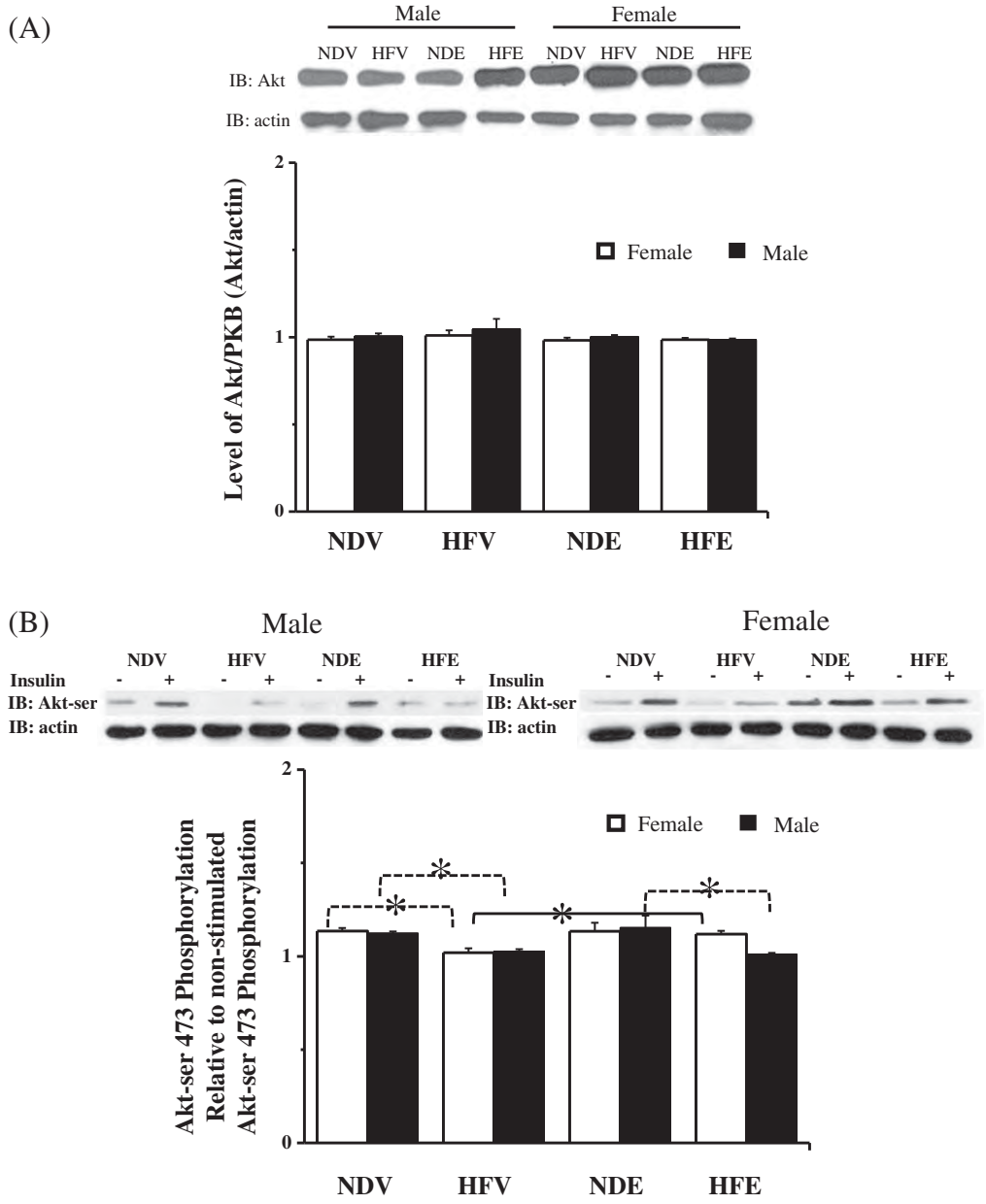

Fig. 2. Insulin-induced serine phosphorylation of neuronal Akt/PKB was decreased in both male and female HFV groups. *Panel A*: Representative blots of protein level of AKt/PKB in brain slices harvested from the NDV, NDE, HFV and HFV groups (n = 4–5/group) compared between male and female. The densitometric quantitation of blots from all groups was not different. *Panel B*: Representative blots of serine 473 kinase of Akt/PKB phosphorylation in brain slices harvested from the NDV, NDE, HFV and HFV groups compared between male and female rats. Densitometric quantitation of blots from insulin-stimulated Akt/PKB in the female HFE group was significantly greater than in the female HFV group. All immunoblotting lanes were loaded with equal amounts of protein (40 μg/lane). *, $p<0.05$; NDV = normal diet group with vehicle treatment, HFV = high-fat diet group with vehicle treatment, DE = normal diet group with E2 treatment, HFE = high-fat diet group with E2 treatment; −, no insulin stimulation; +, insulin stimulation.

Riant et al., 2009). Furthermore, the present study was the first to demonstrate the beneficial effect of exogenous estrogen on neuronal insulin resistance in ND- and HF-fed rats. Our results demonstrated that estrogen treatment could attenuate the impairment of neuronal insulin receptors and neuronal insulin signaling dysfunction, particularly the Akt/PKB phosphorylation, caused by HF diet consumption only in female rats. These findings support the hypothesis that estrogen could exert its beneficial effect on neuronal insulin receptor function via improved downstream neuronal insulin receptor signaling. Our findings also indicated that estrogen could enhance Akt/PKB phosphorylation in insulin-stimulated neuronal tissues, suggesting that estrogen is directly involved in the insulin signaling pathway in neuronal-sensitive tissues. Moreover, the present study also demonstrated an important role of estrogen receptor activation in the central nervous system which could play an important role in the metabolic effect of insulin signaling in the brain.

Estrogen has been shown to play an important role in regulating neuronal structure and function. Previous studies have demonstrated that estrogen can either prevent or improve the cognitive deficits of Alzheimer's disease (AD) (Shang et al., 2010; Simpkins et al., 1997) that regulate synaptic density in hippocampal regions (Woolley et al., 1996). In addition, chronic estradiol (90 days) treatment in female rats has been shown to induce the activation of the insulin receptor substrate-1 signaling pathway in the cerebral cortex and diencephalon of the brain (Alonso and Gonzalez, 2008). Our findings demonstrated that estrogen could improve the impairment of Akt/PKB phosphorylation. All of these beneficial effects of estrogen help explain the